THE ROLE OF NRF2 IN PREVENTING OXIDATIVE/ELECTROPHILIC STRESS-INDUCED LIVER INJURY

By

Kai Connie Wu

B.S., Wuhan University, 2007

Submitted to the Graduate Degree Program in Pharmacology, Toxicology, and Therapeutics and the Graduate Faculty of the University of Kansas in partial fulfillment of the requirements for the degree of Doctor of Philosophy

Dissertation Committee

Curtis Klaassen, Ph.D. (Chair) _____

Steven Weinman, M.D., Ph.D _____

Thomas Pazdernik, Ph.D. _____

Partha Kasturi, Ph.D. _____

Bruno Hagenbuch, Ph.D. _____

Date defended: _____06-15-2012_____

The Dissertation Committee for Kai Connie Wu certifies that this is the approved version of the following dissertation:

THE ROLE OF NRF2 IN PREVENTING OXIDATIVE/ELECTROPHILIC STRESS-INDUCED LIVER INJURY

Curtis Klaassen, Ph.D. (Chair) _____

Date approved: _____07-05-2012_____

ABSTRACT

Redox maintenance is critical for all biological species. Prolonged electrophilic or oxidative events shorten life and induce tissue pathogenesis. Amplification of mechanisms that reduces oxidative/electrophilic stress promotes health and extends life.

Nuclear factor, erythroid derived 2, like 2 (Nrf2) is a master regulator of biochemical mechanisms that respond to oxidative/electrophilic stress. Under basal conditions, Nrf2 is held in an inactive state in the cytoplasm by binding to the cytoskeletal anchoring protein Kelch-like ECH-associated protein 1 (Keap1). Upon generation of oxidative/electrophilic stress, Nrf2 is released from Keap1 and translocates to the nucleus, where it promotes transcription of a battery of cytoprotective genes.

The antioxidative role of Nrf2 has been extensively studied for more than ten years, but the global Nrf2 target genes in liver still remain unknown. The present dissertation utilizes a Nrf2 "gene dose-response" model to genetically modulate the levels of Nrf2 in mouse liver, where the transcription profiles in livers of mice with graded Nrf2 activation is correlated with activation of Nrf2-target genes. Thus, the Nrf2-target genes in mouse liver were investigated systematically. Pathway analyses indicate that genes induced by Nrf2 are involved in glutathione synthesis, oxidation/reduction using NADPH as the co-factor, and xenobiotic metabolism. Moreover, mRNA of genes involved in the pentose phosphate pathway and malic enzyme levels had a clear dose-dependent correlation to active levels of Nrf2, indicating that Nrf2 promotes NADPH generation. The use of these genetic mice with graded Nrf2 activation identified 115

genes that are induced and 80 genes that are suppressed with increasing levels of Nrf2. Among genes suppressed by Nrf2, the majority are involved in lipid synthesis and fatty-acid desaturation. Thus, Nrf2 promotes generation of NADPH, and reduces fatty acid synthesis and desaturation, contributing factors towards protecting liver against environmental oxidative/electrophilic stress.

In addition to oxidative stress scavenging and reduction, Nrf2 also plays a role in xenobiotic detoxification. The mRNA abundance of 124 drug processing genes in the Nrf2 "gene dose-response" model was determined in this dissertation. Nrf2 has a minimal effect on the mRNA of uptake transporters and cytochrome P450 phase-I enzymes. However, Nrf2 does increase mRNA of many non P-450 phase-I enzymes, such as aldo-keto reductases, carbonyl reductases, and aldehyde dehydrogenase 1. Many genes involved in phase-II drug metabolism are induced by Nrf2, including most isoforms of the Gst gene family. In contrast to uptake transporters, a number of efflux transporters, such as Mrps, Bcrp (Abcg2), as well as Abcg5 and Abcg8 were induced by Nrf2. Nrf2 also facilitates electrophile detoxification through inducing non P-450 phase-I enzymes that reduce electrophiles, Gsts that conjugate electrophiles, and efflux transporters that excretes electrophile-GSH conjugates out of cells.

In addition to the assessment of the effect of Nrf2 on the global gene transcription profiles in mouse liver, the function of Nrf2 in vivo was examined by testing whether Nrf2 activation protects against chemical-induced oxidative stress and subsequent liver injury in mice. Diquat is a contact herbicide that undergoes oxidation/reduction cycling, resulting in the generation of superoxide. Nrf2 activation prevents diquat-induced lethality, alveolar collapse in lungs, and necrosis in livers of

mice. Nrf2 activation also prevents glutathione depletion in mouse lung and liver tissues, and increased ROS staining in primary hepatocytes. Oxidative stress and lipid accumulation play important roles in ethanol-induced liver injury. Ethanol increased serum ALT and LDH activities in Nrf2-null mice and wild-type mice, but not in Nrf2-enhanced mice, indicating that Nrf2-enhanced mice are more resistant to ethanol toxicity. After ethanol exposure, ROS were increased in livers and primary hepatoctyes in Nrf2-null mice but not in Nrf2-enhanced mice. Ethanol increased free fatty acids in livers of Nrf2-null mice, and this increase was blunted in Nrf2-enhanced mice. Mechanistic studies show that Nrf2 prevents ethanol-induced oxidative stress through inducing cytoprotective genes including Nqo1 and Gclc, and prevents accumulation of free fatty acids in liver by suppressing the Srebp1 pathway. Oxidative stress also plays an important role in cadmium-induced liver injury. Nrf2-null mice are more susceptible, whereas Nrf2-enhanced mice are more resistant to cadmium-induced acute livery injury. Gclc, Gpx2, and Srxn-1, genes that involved in GSH synthesis and reducing oxidative stress, were only induced in Nrf2-enhanced mice, but not in Nrf2-null mice, indicating that Nrf2 protects against cadmium induced oxidative stress and acute liver injury, at least partially, through the induction of these cytoprotective genes. Surprisingly, metallothioneins (Mt-1 and Mt-2), cysteine-rich proteins that scavenge cadmium to prevent toxicity, were induced markedly in both Nrf2-null and Nrf2-enhanced mice. Thus, there are at least two distinct pathways to protect cadmium-induced toxicity: Nrf2-dependent induction of antioxidative genes and Nrf2-independent induction of metallothioneins.

These findings suggest potential therapeutic applications of the Keap1-Nrf2 pathway, and thus Nrf2 activators are promising drug candidates for the treatment of oxidative/electrophilic stress-induced diseases. To develop effective and potent Nrf2 activators, a library of synthetic and natural existing compounds was screened to test their efficacy and potency to activate Nrf2. After screening 47,000 compounds, 238 compounds (0.5%) had comparable or better efficacy to activate Nrf2 than tertiary butylhydroquinone (tBHQ), the prototypical Nrf2 activator. Among these 238 compounds, 19 produce more induction of Nrf2 than 2-cyano-3,12-dioxooleana-1,9-dien-28-imidazolide (CDDO-Im), the most effective and potent Nrf2 activator known. However, none of the tested compounds were more potent in activating Nrf2 than CDDO-Im. In addition, chemical structural relationship analysis of these 238 compounds showed enrichment of four chemical scaffolds (diaryl amides and diaryl ureas, oxazoles and thiazoles, pyranones and thiapyranones, and pyridinones and pyridazinones). The top 30 compounds were screened in Hepa1c1c7 cells to increase Nqo1 mRNA, the prototypical Nrf2 target gene. The results indicate that 17 of the 30 most active hits also increased Nqo1 mRNA in the cell line in a concentration-dependent manner.

In addition to synthetic compounds, a number of natural compounds are known to be antioxidants, and some of these natural compounds have been shown to exhibit antioxidant effects through activating the Nrf2 pathway. Utilizing the same screening system (AREc32 cells), 54 natural existing compounds were tested. Andrographolide had the highest efficacy, followed by trans-chalcone, sulforaphane, curcumin, flavone, kahweol, and carnosol, which were all more potent and effective than tBHQ. None of the natural compounds were more potent than CDDO-Im.

In conclusion, Nrf2-target genes are involved in NADPH generation, NADPH-facilitated oxidative stress reduction, and detoxification and excretion of electrophiles. Nrf2 activation protects against ethanol-, cadmium-, and diquat-induced liver oxidative stress and liver injury in mice. Lastly, a few synthetic and natural existing compounds were shown to be effective in activating the Keap1-Nrf2-ARE pathway.

ACKNOWLEDGMENTS

I would like to acknowledge my dissertation committee, Drs. Curtis Klaassen, Steven Weinman, Thomas Pazdernik, Partha Kasturi, and Qi Chen for serving on my thesis committee and guidance through my Ph.D. training.

I am very grateful to my mentor Dr. Curtis Klaassen, who gave me the opportunity to conduct biomedical research, inspired me to have my own ideas and hypotheses, and supports my research projects with his full capability. He opened a window so I can see how fascinating science could be, he always has a positive attitude so I have the courage to overcome the difficulties, and he works as hard as he can so I learned how good science should be done.

I would like to acknowledge all the faculty members of the Department of Pharmacology, Toxicology, and Therapeutics for their help and discussion. I would like to especially thank Drs. Xiaochao Ma and Wenxing Ding for their technical support. They are always available to help me with the experiments, and give me valuable suggestions on experimental design and data interpretation. I would like to thank Dr. James Luyendyk, a previous member on my dissertation committee, for his constructive criticisms and discussion.

I would like to acknowledge my peer graduate students and labmates, especially Dr. Yue Cui, Dr. Youcai Zhang, Dr. Pan Wang, Zidong Fu, and Lai Peng for their friendship during the past five years.

TABLE OF CONTENTS

LIST OF ABBREVIATIONS

Abbreviation	Full name
Abcg	ATP-binding cassette g
Aldh	aldehyde dehydrogenase
ALT	alanine aminotransferase
Akr	aldo-keto reductase
Aldoa	fructose-bisphosphate
ANIT	alpha-naphthylisothiocyanate
Aox	aldehyde oxidase
ARE	antioxidant response element
Bcrp	breast cancer resistance protein
bDNA	branched DNA amplification
Blvrd	biliverdin reductase
CAPE	caffeic acid phenethyl ester
CAR	constitutive androstane receptor
Cbr	carbonyl reductase
CDDO-Im	2-cyano-3,12-dioxooleana-1,9-diene-28-imidazolide
Ces	carboxylesterase
Cd	cadmium
Cyp	cytochrome P450 enzyme
DAVID	the database for annotation, visualization and integrated discovery
Dera	putative deoxyribose phosphate aldolase
Ephx1	epoxide hydrolase 1
Fads	fatty acid desaturase
Fasn	fatty acid synthase
Fech	ferrochelatase
Fmo	flavin monooxygenase
Fth	ferritin heavy chain
Ftl	ferritin light chain
G6pd	glucose 6-phosphate dehydrogenase
Gclc	glutamate-cysteine ligase, catalytic subunit
Glrx	glutaredoxin
Gpx	glutathione peroxidase
GSH	glutathione
Gsr	glutathione reductase
Gss	glutathione synthase
H_2DCFDA	2′,7′-dichlorodihydrofluoresein diacetate
HPLC-UV	high performance liquid chromatography-ultraviolet absorbance
IPA	ingenuity pathway analysis
Keap1	kelch-like ECH associating protein 1
Keap1-KD	kelch-like ECH associating protein 1-knock down
Keap1-HKO	kelch-like ECH associating protein 1-hepatocyte knockout
LDH	lactate dehydrogenase

Abbreviation	Full name (Con'd)
Me1	malic enzyme
Mrp	multidrug resistance-associated protein
MT	metallothionein
NADPH	nicotinamide adenine dinucleotide phosphate reduced form
Nrf2	nuclear factor E2 p45-related factor 2
Ntcp	sodium taurocholate cotransporting polypeptide
Oat	organic anion transporter
Oatp	organic anion transporting polypeptide
Pgd	6-phosphogluconate dehydrogenase
PPARα	peroxisome proliferator activated receptor α
Prdx	peroxiredoxin
Prps1	phosphoribosyl pyrophosphate synthetase 1
PXR	pregnane X receptor
ROS	reactive oxygen species
RNS	reactive nitrogen species
RXR	retinoid X receptor
Scd1	stearoyl-CoA desaturase
Srxn	sulfiredoxin
Taldo1	transaldolase 1
tBHQ	*tert*-butylhydroquinone
TBP	TATA-box binding protein
TFBS	transcription factor binding site
Tkt	transketolase
TSS	transcription start site
Txnrd	thioredoxin reductase
Ugt	UDP-glucuronosyltransferase
UPLC-MS/MS	ultra high performance liquid chromatography-tandem mass spectrometry
Xdh	xanthine dehydrogenase

LIST OF TABLES

LIST OF FIGURES

Chapter 1 : INTRODUCTION AND BACKGROUND

Free radicals and oxidative stress

One of the major challenges in a biological system is to maintain cellular redox homeostasis through balancing the rate and magnitude of oxidant generation and oxidant detoxification. An imbalanced ratio between reactive oxygen species (ROS) production and adaptive antioxidant capacity will result in oxidative stress, a pathogenic stage that serves as both cause and consequence of numerous acute toxicities and chronic diseases.

ROS refers to oxygen-containing free radicals with one or more unpaired electrons, which make them highly reactive. Most common cellular oxidative stress is generated from oxygen metabolism, resulting in generation of superoxide radical ($O^{\cdot-}$). In the presence of superoxide dismutase (SOD), superoxide radical is catalyzed into hydrogen peroxide (H_2O_2). In fact, the cellular concentration of SOD is so high (10 μM versus 1-10 pM of superoxide radical), that the majority of superoxide radicals are rapidly catalyzed into hydrogen peroxide. In the presence of transient metal ions, such as Fe^{2+}, Cu^+, and Mn^{2+}, hydrogen peroxide undergoes a Fenton-like reaction and generates hydroxyl free radicals ($HO^{\cdot}$). Hydroxyl free radicals react with almost every type of molecule found in living cells, including sugars, amino acids, phospholipids, and nucleotides, with extremely high rate-constants (10^5-10^{10} $M^{-1}S^{-1}$) (Anbar and Neta, 1967). Thus, the hydroxyl free radical is especially difficult to detoxify. Hydrogen peroxide can also be used to oxidize chloride to produce hypochlorous acid through myeloperoxidase (Winterbourn and Kettle, 2004). In addition, superoxide radical can bind to nitric oxide (NO) to generate peroxynitrite radical ($ONOO^{\cdot}$), and subsequently

nitrogen dioxide ($NO_2^{\bullet}$) as well as carbonate radical ($CO_2^{\bullet-}$). Examples of ROS and

reactive nitrogen species (RNS) are illustrated in figure 1.1.
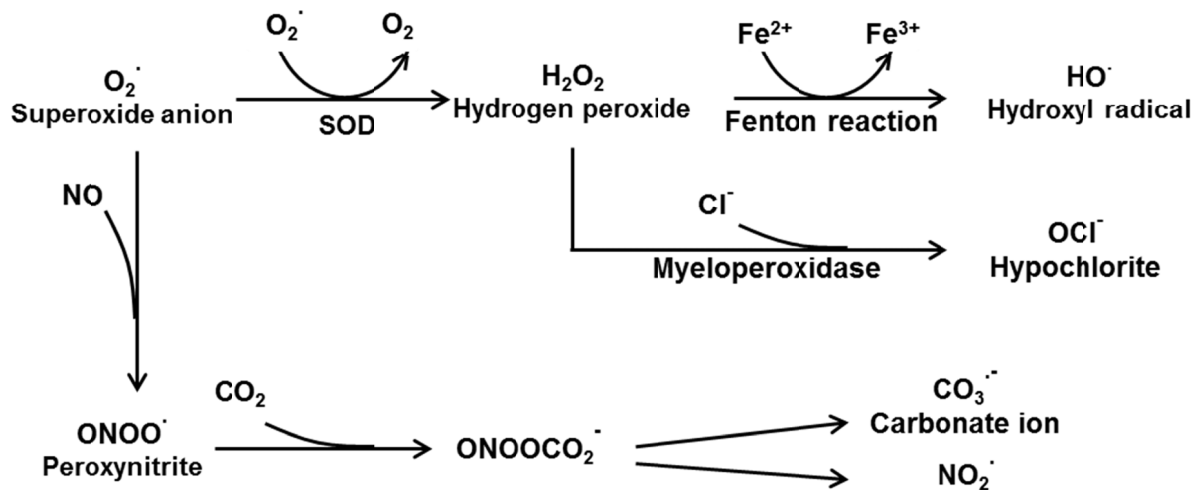
Figure 1.1. Illustration of reactive oxygen species and reactive nitrogen species.

Reactive oxygen species are represented in the top portion and reactive nitrogen species are represented on the bottom portion of the figure. Superoxide radical ($O_2^.$) is catalyzed into hydrogen peroxide (H_2O_2) by SOD. Hydrogen peroxide generates hydroxyl free radical ($HO^.$) through a Fenton-like reaction, and produces hypochlorous acid through myeloperoxidase. Superoxide radical can bind to nitric oxide (NO) to generate peroxynitrite radical ($ONOO^.$), and subsequently nitrogen dioxide ($NO_2^.$), as well as carbonate radical ($CO_2^.$).

Superoxide radicals are generated during normal physiological processes, xenobiotic metabolism, as well as pathological responses. Among numerous sources of superoxide radical generation, the electron transport chain in mitochondria is the primary and the most important source. Under ideal conditions, one oxygen molecule should receive two hydrogen molecules to generate water, but even under physiological conditions, 2% of the oxygen receive one electron to become superoxide radical. Thus, the hydrogen peroxide concentration in mitochondria is always 5-fold higher than the cytosol (Mari et al., 2009).

Cellular oxidases serve as another important source to generate ROS, and oxidases are widely distributed in tissues and various cell types that generate superoxide radical as a product. For example, NADPH oxidases (Nox) represent a class of enzymes whose primary function is the generation of ROS. Seven isoforms of Nox have been identified, each with a distinct cell and tissue distribution (Manea, 2010). Nox1 is predominantly found in the colon, Nox2 is the NADPH oxidase in phagocytes, Nox3 is almost exclusively expressed in the inner ear, and Nox4 is the most abundant Nox and widely expressed in kidney, vascular cells, osteoclasts, etc. Nox5 is predominantly expressed in lymphoid tissues and testis. Duox1(dual oxidase 1) is expressed in the thyroid and in respiratory epithelia, whereas Duox2 is expressed in the thyroid and in gastrointestinal glandular epithelia (Krause, 2004). In addition to the Nox enzyme family, superoxide radical is also the product of other oxidase catalyzed reactions, such as xanthine oxidase, glucose oxidase, and amino acid oxidases.

In addition to cellular oxidases, the cytochrome P-450 (Cyps) enzyme family generates superoxide radicals. Cyp2e1 oxidizes a variety of small, hydrophobic

substrates and drugs using oxygen. When Cyp2e1 uses oxygen to metabolize its substrates, reactive oxygen species (ROS) can be generated by a chain of uncoupled reactions (Comporti et al., 2010). Various toxicants, including ethanol, carbon tetrachloride, acetaminophen, benzene, halothane, and many other halogenated substrates, have been reported to generate oxidative stress, at least partially through this mechanism (Lu and Cederbaum, 2008). Certain xenobiotics, including paraquat, diquat, doxorubicin, and nitrofurantoin can receive one electron from NADPH through cytochrome P450 reductase, and donate this electron to molecular oxygen to generate superoxide radical. Through this cytochrome P450 reductase-mediated redox cycling, small amounts of these xenobiotics are able to produce excessive amounts of superoxide radicals.

The immediate outcome of oxidative stress includes lipid peroxidation, protein oxidation, and DNA damage. Some of the products of oxidative stress are detectable and can serve as biomarkers. For example, lipid peroxidation is initiated by an attack of hydroxyl radicals on polyunsaturated fatty acids that begins a chain reaction to generate lipid hydroperoxides. A single initiating event can trigger the peroxidation of a large number of target molecules. Biological membranes contain large amounts of polyunsaturated fatty acids, which make them highly vulnerable to oxidative stress. Lipid peroxidation of membranes results in a decrease of fluidity, increase in permeability, and abnormal activity of membrane bound enzymes. ROS can also attack thiol groups on cysteine residues of proteins to form disulfide bonds, leading to structural changes of the proteins. Carbon-carbon double bonds in amino acid residues, such as tryptophan, can react with ROS, resulting in the formation of protein carbonyl. RNS (peroxynitrite)

can react with tyrosine residues and generate nitrotyrosine as protein adducts. Finally, DNA is also an important cellular target for attack by oxidative stress. The attack of hydroxyl radicals on DNA produces a wide range of chemical changes. These include conversion of thymine residues into thymine glycol and 5-hydroxy-methyluracil. These damaged thymine residues undergo base excision repair and are secreted into urine. It has been reported that normal humans excrete 10 nanomoles of thymidine glycol and hydroxymethyluracil every day (Loft and Poulsen, 1998).

ROS also have important roles in diverse physiological and pathological processes, and the hypothetical model showing the role of ROS in different biological process is illustrated in Fig. 1.2. Low levels of ROS play important roles in regulating vascular tone (Gutterman et al., 2005), cell adhesion (Chiarugi et al., 2003; Huo et al., 2009), immune responses (Grisham, 2004), and growth factor actions (Hensley et al., 2000). Intermediate levels of oxidative stress induce an adaptive protective signal pathway (i.e. Keap1-Nrf2 signal pathway) to induce the antioxidant response. The ROS-induced Keap1-Nrf2 pathway will be discussed later. Higher amounts of ROS can trigger an inflammatory response through activation of NFκB and Ap-1. In T cells, ROS induces the phosphorylation of Tyr42 on IκBα through activating spleen tyrosine kinase (Syk), or phosphorylation of Ser32 and 36 on IκBα through inhibition of kappaB kinase (IKK). In epithelial cells, ROS triggers IKK complex activation through the Src-PKD pathway (Gloire et al., 2006). High levels of oxidative stress can trigger apoptosis-mediated cell death through activating apoptosis signal-regulating kinase 1 (Ask1). Ask1 is one of MAP3Ks identified in the JNK and p38 pathways (Ichijo et al., 1997), and activation of Ask1 induces death of various cells through mitochondria-dependent
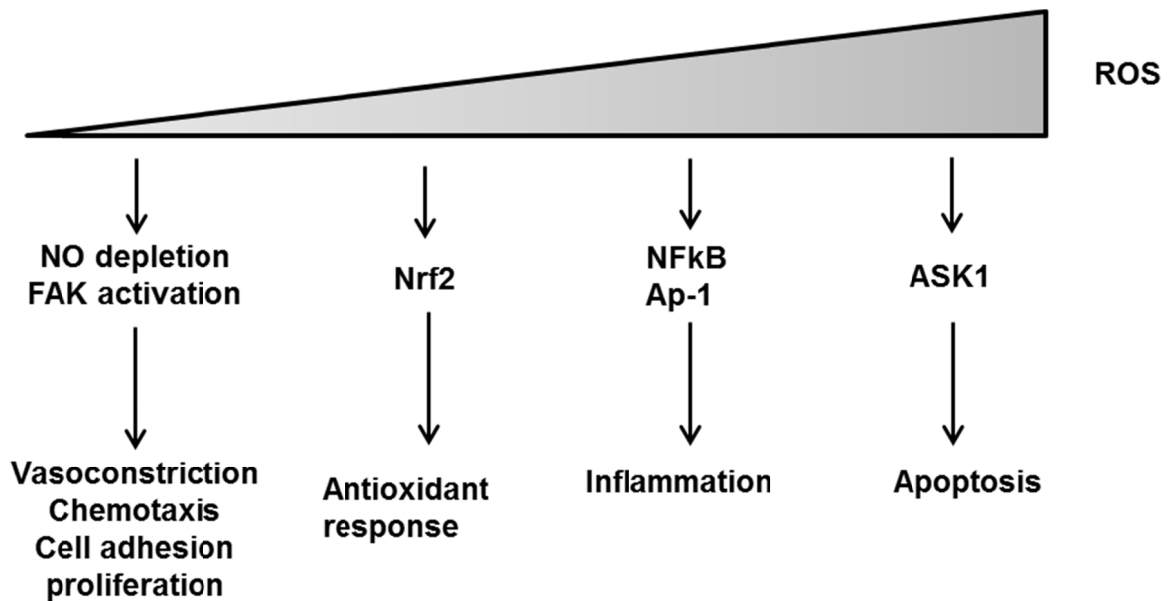
Figure 1.2. Hypothetical model of hierachical role of oxidative stress. Low oxidative stress mediates physiological functions including vasoconstriction, chemotaxis, cell adhesion, and proliferation. An intermediate amount of oxidative stress induces adaptive antioxidant response through Nrf2. A higher amount of oxidative stress can trigger an inflammatory response through activation of NFκB and Ap-1. A high amount of oxidative stress can induce activation of Ask1 and subsequent apoptosis. Modified from (Gloire et al., 2006).

caspase activation. Under basal conditions, Ask1 is inactivated by thioredoxin (Trx) by direct binding to the N-terminal region of Ask1. Under oxidative stress conditions, Trx is oxidized, dissociates from Ask1, and thereby activates Ask1-mediated apoptosis (Takeda et al., 2008).

Given the toxic effects of high levels of ROS, it is not surprising that oxidative stress has been implicated in ageing-related diseases (Lee and Wei, 2007), atherosclerosis (Stocker and Keaney, 2004), neurodegenerative diseases (Knight, 1997), tumor progression (Storz, 2005), obesity, and diabetes (Martinez, 2006). Thus, cellular antioxidant defense systems are crucial for cell survival and prevention of oxidative stress-induced diseases.

In general, there are three cellular antioxidant defense systems to fight against oxidative stress: low-molecular-weight antioxidants, enzymatic-antioxidant pathways, and free-ion sequestration. The major endogenous low-molecular-weight antioxidants are ascorbic acid (vitamin C), tocopherol (vitamin E), glutathione (GSH), and bilirubin. Ascorbic acid is a water soluble compound which reacts rapidly with the superoxide radical and even more rapidly with the hydroxyl free radical. It also scavenges singlet oxygen and hypochlorous acid. Oxidation of ascorbic acid gives the semidehydroascorbate radical, which is further oxidized to dehydroascorbate. Dehydroascrobate is unstable and breaks down rapidly to produce oxalic and L-threonic acids. Given the reducing properties of ascorbic acid, several studies have shown the beneficial effects of ascorbic acid in prevention and treatment of cancer (Mamede et al., 2011). Plants and most animals can synthesize ascorbic acid from glucose, but humans rely on ascorbic acid (vitamin C) from the diet (Puertollano et al., 2011). In contrast to

vitamin C, vitamin E is a lipid soluble antioxidant. Dietary vitamin E is absorbed with lipids, bound to α-tocopherol transfer protein in the liver, and distributed throughout the body (Brigelius-Flohe and Traber, 1999). Vitamin E is localized in the membranes of the cell, where it primarily serves as a chain-breaking antioxidant to prevent lipid peroxidation. GSH serves as the most abundant cellular thiol resource, and provides a buffer system to maintain cellular redox status. GSH reduces hydrogen peroxide through glutathione peroxidase (Gpx), and is also oxidized to its disulfide form (GSSG). GSSG is returned to GSH through glutathione reductase using NADPH as the co-factor. Multiple studies have shown that the Gpx-GSH pathway is also a major intracellular antioxidative mechanism that repairs lipid peroxidation (Imai and Nakagawa, 2003), DNA fragmentation (Higuchi, 2004), and protein adduction (Filippin et al., 2008). Bilirubin, which is formed by biliverdin reductase, is the major degradation product of heme catabolism. Bilirubin reduces oxidative stress and becomes oxidized to biliverdin once again. Biliverdin reductase, together with biliverdin and bilirubin, are important players in cellular signal transduction pathways, gene expression, and oxidative responses (Florczyk et al., 2008).

The enzymatic antioxidant pathways include catalase, peroxiredoxin pathway, and glutathione peroxidase pathway. Catalase reduces two molecules of hydrogen peroxide into water, producing one molecule of singlet oxygen. Catalase is localized in peroxisomes, and is found in every organ, with particularly high concentrations in liver. Glutathione peroxidase (GPX) reduces hydrogen peroxide to water and spontaneously oxidizes GSH into GSSG. GSH can be either synthesized from glutamate-cysteine ligase (Gcl) and GSH synthase (Gss), or recovered from GSSG via GSH reductase

(Gsr). However, the enzyme activity of GPX is about one-tenth of catalase in multiple organs (i.e., liver, kidney, spleen, and lung) (Marklund et al., 1982), indicating a minor role of GPX in detoxifying ROS. In addition, hydrogen peroxide can be reduced by peroxiredoxin (Prdx), resulting in oxidation of Prdx from the reduced form (Prdx-SH) to the oxidized form (Prdx-S-S-Prdx). Prdx-S-S-Prdx can be reduced to Prdx-SH through thioredoxin (Txn) and thioredoxin reductase (Txnrd). If Prdx is further oxidized into the sulfinic acid form (Prdx-SOOH), it can be reduced by sulfiredoxin. The gene names, tissue distribution, and cellular localization of the genes involved in enzymatic antioxidant pathways are summarized in table 1.1.

Table 1.1. **Genes involved in enzymatic antioxidant pathways. Gene names, tissue distribution, and cellular localization of genes involved in enzymatic antioxidant pathways.**

Gene	Tissue distribution	Subcellular localization	Reference
Txnrd1	Lung, liver, kidney, heart, muscle, and brain	Cytosol	(Deroo et al., 2004) (Kiermayer et al., 2007)
Txnrd2	Lung, liver, kidney, heart, muscle, and brain	Mitochondria	(Deroo et al., 2004)
Txnrd3	Testis	Endoplasmic reticulum	(Deroo et al., 2004) (Soerensen et al., 2008)
Txn1	Ubiquitous	Cytosol and nucleus	(Deroo et al., 2004) (Hoshino et al., 2007)
Txn2	Metabolically active tissues such as heart, brain, and liver	Mitochondria	(Perez et al., 2008)
Prdx1	Ubiquitous, especially abundant in liver	Cytosol	(Ishii et al., 1993)
Prdx2	Brain, testis, and spleen	Cytosol	(Chiba et al., 2008)
Prdx3	Ubiquitous	Mitochondria	(Deroo et al., 2004) (Chae et al., 1999)
Prdx4	Pancreas and testis	Extracellular space	(Okado-Matsumoto et al., 2000)
Prdx5	Ubiquitous	Mitochondria	(Kropotov et al., 2007)
Prdx6	Ubiquitous, especially abundant in liver and lung	Cytosol	(Eismann et al., 2009)
Grx1	Ubiquitous	Cytosol	(Jurado et al., 2003)
Grx2	Testis	Mitochondria	(Jurado et al., 2003)
Srx1	NA	NA	
Gpx1	Ubiquitous	Cytosol and mitochondria	(Takebe et al., 2002)
Gpx2	Gastrointestinal tract	Cytosol	(Takebe et al., 2002)
Gpx3	Mainly expressed by the kidneys from where it is released into the blood	Extracellular space	(Takebe et al., 2002)
Gpx4	Ubiquitous	Cell membrane	(Takebe et al., 2002)
Catalase	Ubiquitous	Peroxisome	(Lenzen et al., 1996)
SOD1	Ubiquitous	Cytosol	(Lenzen et al., 1996)
SOD2	Ubiquitous	Mitochondria	(Lenzen et al., 1996)
SOD3	Ubiquitous	Extracellular	(Lenzen et al., 1996)

As discussed above, transient metal ions (especially Fe^{2+} and Cu^+), facilitate generation of hydroxyl free radicals from hydrogen peroxide through the Fenton-like reaction. Thus, free ion binding proteins are important in preventing oxidative stress. Ferritin is a high-molecular-weight protein (450 KDa) consisting of 24 subunits. In vertebrates, these subunits consist of light (L) and heavy (H) chains with molecular weights of 19 kDa and 21 kDa, respectively. Ferritin serves to store, deposit, and transfer iron in a non-toxic form (Arosio and Levi, 2010). Some heavy metals, including cadmium and mercury, readily bind to thiol groups of proteins, leading to disruption of redox homeostasis and protein damage. Metallothioneins are a family of low-molecular-weight (6 kDa), cysteine-rich (22%-33%) proteins that bind endogenous and exdogenous heavy metals. Metallothioneins are highly inducible upon heavy ion overload, and metallothionein-bound metals are generally considered as non-toixic (Klaassen et al., 1999). Collectively, the functions of low-molecular-weight antioxidants, enzymatic antioxidant pathways, and free-ion sequestration are illustrated in Fig. 1.3.
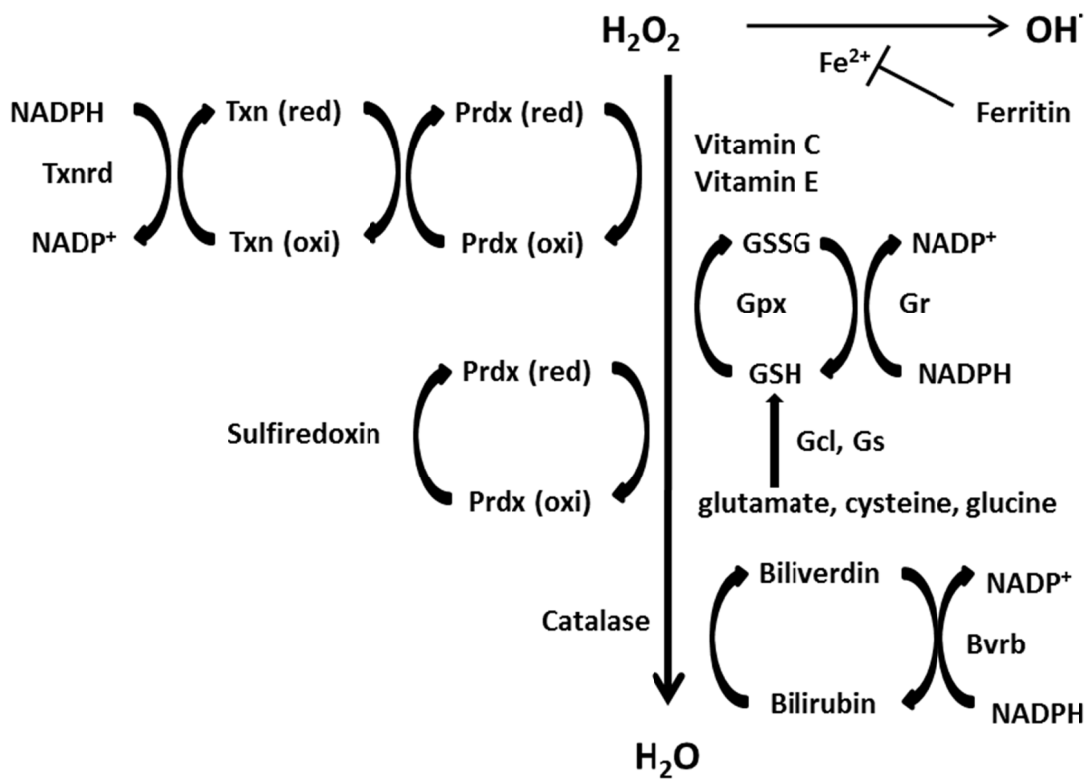
Figure 1.3. Illustration of low-molecular-weight antioxidants, enzymatic-antioxidant pathways, and free-ion sequestration. Hydrogen peroxide can be non-enzymatically reduced by vitamin C, vitamin E, GSH, and bilirubin. In addition, hydrogen peroxide can be reduced enzymatically through Prdx-Txn pathway, Prdx-Sxn pathway, and GSH-Gpx pathway. Finally, ion-binding proteins store free ions in a non-toxic form, preventing ROS production through a Fenton-like reaction.

Nrf2 and Keap1 Signaling Pathway

Nrf2 was first cloned as one of the proteins that activates transcription by binding to the NF-E2/AP-1 motif of the hypersensitive site-2 in the β-globin locus control region, and belongs to a subset of basic leucine-zipper (bZip) genes highly homologous to that of NF-E2 (Moi et al., 1994). Early studies on Nrf2 showed that it is not essential for murine erythropoiesis and development (Chan et al., 1996), however, evidence from the past 10 years points to Nrf2 as a key regulator of the cellular response to oxidative stress in multiple tissues and cell types. Under basal conditions, Nrf2 is sequestered by the cytoskeletal anchoring protein Kelch-like ECH-associated protein 1 (Keap1) through extensive hydrogen bonds in the cytoplasm (Fig. 1.4). Upon stimuli of oxidative stress or antioxidants, Nrf2 is released from Keap1 and translocates into the nucleus (Itoh et al., 1999). Once in the nucleus, Nrf2 heterodimerizes with a variety of transcriptional regulatory proteins, including members of the activator protein-1 family (such as Jun and Fos) or the small Maf family of transcription factors (Itoh et al., 1997; Jeyapaul and Jaiswal, 2000; Zhu and Fahl, 2001). These protein complexes then bind to antioxidant response elements (ARE) located in the upstream promoter regions of a battery of genes to drive transcription of these genes (Rushmore et al., 1991).

Nrf2 target genes

Genomic analyses indicate that a number of gene families are affected by Nrf2: (*a*) provide direct antioxidants or encode enzymes that inactivate oxidants, (*b*) increase levels of glutathione synthesis and regeneration, *(c)* conjugate xenobiotics with glutathione or glucuronic acid to make them more water soluble, *(d)* increase multidrug
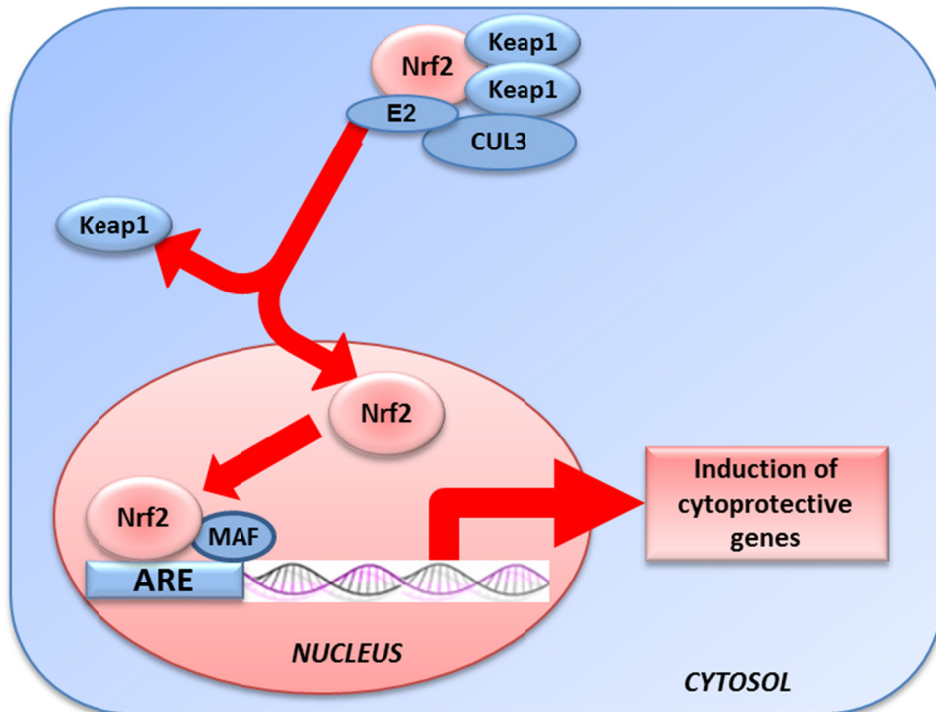
Figure 1.4. Illustration of the Keap1-Nrf2 pathway. Under basal conditions, Nrf2 is sequestered by the cytoskeletal anchoring protein Keap1. Upon stimuli of oxidative stress or electrophiles, Nrf2 is released from Keap1 and translocates into the nucleus. Once in the nucleus, Nrf2 heterodimerizes with the activator protein-1 family (such as Jun and Fos) or the small Maf family, and then binds to AREs located in the upstream promoter regions of a battery of genes to drive their transcription.

Table 1.2. Typical Nrf2 target genes reported in the literature.

Gene	Function	Reference
Anti-oxidative enzymes and proteins		
Heme oxygenase-1(Ho-1)	Catalyzes pro-oxidant heme into bilirubin	(Primiano et al., 1996)
NAD(P)H quinone oxidoreductase 1 (Nqo1)	Reduces highly reactive quinones	(Dhakshinamoorthy and Jaiswal, 2000)
Glutathione peroxidase (Gpx)	Reduces hydrogen peroxide	(Thimmulappa et al., 2002)
Ferritin (Ftn)	Ion sequester	(Primiano et al., 1996)
Thioredoxin-1 (Txn1)	Reduces oxidized protein to restore enzyme activity	(Kim et al., 2003)
Thioredoxin reductase-1 (Txnrd1)	Reduces oxidized thioredoxin	(Kim et al., 2003)
Glutathione homeostasis		
Glutamate-cysteine ligase (Gcl, Gclc and Gclm)	Catalyzes rate-limiting step in GSH synthesis	(Moinova and Mulcahy, 1999)
Glutathione reductase (Gr)	Reduces GSSG into GSH to restore GSH concentration	(Moinova and Mulcahy, 1999)
Conjugation		
Glutathione-*S*-transferases (GSTs)	Conjugates GSH to electrophiles for detoxification	(Thimmulappa et al., 2002)
Glucuronosyltransferases (UGTs)	Conjugates glucuronic acid to xenobiotics to increase excretion	(Thimmulappa et al., 2002)
Transporters		
Multidrug resistance-associated proteins (Mrps)	Effluxes conjugates from liver to bile or blood for excretion	(Maher et al., 2007)
NADPH regenerating system		
Glucose 6-phosphate dehydrogenase, 6-phosphogluconate dehydrogenase	Regenerate NADPH from NADP	(Thimmulappa et al., 2002)

response transporters and enhance chemical export, and *(e)* stimulate NADPH synthesis (Table 1.2).

Recently, our laboratory characterized the gene expression profile in liver of Nrf2-null mice and mice with decreased Keap1 protein throughout the body, and identified a pattern of genes with low expression in Nrf2-null mice, and high expression in Keap1-knock down mice (Table 1.3). In this way, biological effects of increased Nrf2 function were studied in vivo, and Nrf2 target genes were investigated systematically (Reisman et al., 2009e).

Table 1.3. Characterization of gene expression profile in liver of wild-type, Nrf2-null, and Keap1-KD mice. Percent change from wild-type mice in Nrf2-null and Keap1-KD mice are presented.

Gene	Function	Nrf2-null % change	Keap1-KD % change
Gstp2	Conjugation enzyme	-40	586
Gsta1	Conjugation enzyme	-84	448
Gstm3	Conjugation enzyme	-81	336
Nqo1	Phase-I metabolizing enzyme	-88	222
Gstm1	Conjugation enzyme	-74	140
Mrp3	Efflux transporter	-85	111
Gstm4	Conjugation enzyme	-67	102
Ugdh	Co-substrate synthesis	-50	75
Gstm2	Conjugation enzyme	-57	65
Gclc	Glutathione synthesis	-37	63
Ces1e1	Phase I metabolizing enzyme	-94	59
Mrp4	Efflux transporter	-3	55
Gsta4	Conjugation enzyme	-53	45
Abcg5	Transporter	-29	45
Abcg8	Transporter	-20	40
Ces2a6	Phase-I metabolizing enzyme	-85	28
Ugt2b35	Conjugation enzyme	-79	32
Mrp2	Efflux transporter	-17	24
Ugt1a6	Conjugation enzyme	-46	23
Txnrd1	Anti-oxidative enzyme	-41	23
Gclm	Glutathione synthesis	-16	22
Gsr	Glutathione homeostasis	-23	17
Bcrp	Transporter	-27	16

Mechanism of induction of Keap-Nrf2 signal pathway and Nrf2 activators

Studies using functional ARE reporter assays together with Keap1 and Nrf2 expression vectors revealed that coexpression of Keap1 with Nrf2 in cells repressed the transcription of Nrf2 target genes compared with expressing Nrf2 alone (Kobayashi et al., 2002). Inducer treatment of cells with dual expression of Keap1 and Nrf2 abrogated the repressing activity of Keap1. Exaggerated Nrf2 activation in Keap1-disrupted mice provided additional evidence that Keap1 is a negative regulator of Nrf2, and the key process of Nrf2 activation is releasing Nrf2 from Keap1 binding.

The interaction between Keap1 and Nrf2 is through the C-terminal Kelch domain, which contains six copies of the evolutionarily conserved Kelch repeat sequence motif (Kobayashi et al., 2004). The structure of the Kelch domain from human Keap1 has been determined by x-ray crystallography (Li et al., 2004). The Kelch domain forms a 6-bladed β-propeller structure, with residues at the C terminus forming the first strand in the first blade. Key structural roles have been identified for the highly conserved glycine, tyrosine, and tryptophan residues that define the Kelch repeat sequence motif. The crystal structure of the C-terminal Kelch domain of Keap1 provides structure basis to design Nrf2 activators.
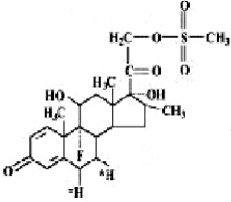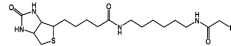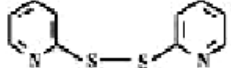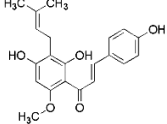
The high cysteine content of Keap1 suggested that cysteine residues would be an excellent candidate as the sensor for inducers. Keap1 has 27 highly-reactive cysteine residues that have the potential to sense electrophilic Nrf2 activators by forming covalent adducts with them. Yamamoto and coworkers have therefore proposed the model that Nrf2-activating compounds directly modify the sulfhydryl groups of Keap1

cysteines by oxidation, reduction, or alkylation, which alters the conformation of Keap1 and ceases the ubiquitination of Nrf2 (Kobayashi and Yamamoto, 2006). Consistent with this hypothesis, a number of Nrf2 activators have been reported to react with different cysteine residues in Keap1 (Table 1.4).

A variety of synthetic and natural compounds have been identified as Nrf2 activators with various potency and selectivity. The doses used in animal studies and concentrations used in cell studies that were able to either induce transcription of Nrf2 target genes or protect against injury models were shown in table 1.5. Only a few compounds are potent enough to activate Nrf2 at low concentrations (Table 1.5)

Table 1.4. Nrf2 activators with chemical structure and response Keap1 cysteine residues.

Nrf2 activator	Structure	Keap1 cysteine residues	Reference
Dexamethasone 21-mesylate		257, 273, 288, 297, and 613 (human)	(Dinkova-Kostova et al., 2002)
Iodoacetyl-*N*-biotinylhexylenediamine		196, 226, 241, 257, 288, and 319 (mouse)	(Hong et al., 2005a)
Sulforaphane		77, 226, 249, 257, 489, 513, 518 (human)	(Hong et al., 2005a)
Xanthohumol		151, 319, and 613 (human)	(Luo et al., 2007)

Table 1.5. Known Nrf2 activators.

Chemical	Dose/Conc.	Animal/cell line	Reference
Oltipraz	50 mg/kg i.p. once daily for 2 days	Mice	(Tanaka et al., 2009)
	50 µM	Human hepatocytes	(Jigorel et al., 2006)
*t*BHQ *tert*-Butylhydroquinone	10 µM	ARE-reporter cell line (AREc32)	(Wang et al., 2007)
	20 µM	Mouse cortical neuronal cells	(Shah et al., 2007)
	40 mg/kg i.p. single dose	Mice	(Yueh and Tukey, 2007)
BHA Butylated hydroxyanisole	350 mg/kg i.p. single dose	Mice	(Buckley and Klaassen, 2009)
	100 and 250 µM	Human hepatocellular carcinoma cells	(Yuan et al., 2006)
CDDO-Im 1[2-Cyano-3,12-dioxooleana-1,9(11)-dien-28-oyl]imidazole	1 mg/kg, i.p.	Mice	(Reisman et al., 2009b)
	20 n*M*	Human peripheral blood mononuclear cells and neutrophils	(Thimmulappa et al., 2007)
CDDO	300 nM	Human leukemia cells	(Liby et al., 2005)
Curcumin	50 mg/kg or 100 mg/kg, ip	Rats	(Yang et al., 2009)
	15 µM	Porcine renal epithelial proximal tubule cells	(Balogun et al., 2003)
Genistein	25 and 50 µM	EA.hy926 cells (endothelial cell line)	(Hernandez-Montes et al., 2006)
	2 g/kg in diet for 3 weeks	Rats	(Wiegand et al., 2009)
Resveratrol	5 µM	Human bronchial epithelial cell line (HBE1 cell)	(Zhang et al., 2009)
Caffeic acid phenethyl ester	15 µM	Porcine renal epithelial proximal tubule cells	(Balogun et al., 2003)
Oleanolic acid	90 mg/kg, i.p. once daily for 3 days	Mice	(Reisman et al., 2009a)

Chapter 2 : STATEMENT OF PURPOSE

Oxidative stress plays key roles in the pathogenesis of liver diseases. Nrf2 is a transcription factor that promotes transcription of a battery of genes involved in reducing reactive oxygen species (ROS) and oxidized protein, glutathione synthesis, as well as conjugation and excretion of electrophiles. The antioxidative properties of Nrf2 target genes make Nrf2 a promising target in therapies of liver diseases. However, there still is limited knowledge in alterations about gene expression after Nrf2 activation in liver. The critical role of Nrf2 in protection against oxidative stress-induced liver injury is unclear. Therefore, the present dissertation is poised to fill this critical knowledge gap. The central hypothesis of the present dissertation is that Nrf2 is essential in liver protection through its multifaceted roles in antioxidative defense and xenobiotic metabolism in the liver. The goal of this dissertation is to determine the gene regulation by Nrf2 activation, and determine the protective role of Nrf2 against oxidative stress-involved liver diseases using various research models, and develop activators of the Keap1-Nrf2 signaling pathway through high-throughput screening.

Specific aim 1 was designed to investigate the role of Nrf2 on global gene expression in liver. Nrf2 is a transcription factor that has great therapeutic potential. It is important to study the role of Nrf2 for genomic gene expression if one wants to develop Nrf2 activators as drug candidates. Gene transcription profiles of Nrf2 target genes have been studied in mouse macrophages, lung tissue, and embryonic fibroblasts, but there is a significant gap in our understanding of the role Nrf2 plays on genomic gene expression in liver. Liver is the primary organ in regard to multiple vital functions, including protein synthesis (e.g., albumin and clotting factors), glucose homeostasis, and lipid metabolism. Liver also plays the major role in detoxication of environmental

chemicals, drugs, and endogenous toxicants. Thus, studying the function of Nrf2 in liver is of great importance. In the present study, I have utilized a "gene dose-response" approach including Nrf2-null mice lacking any functional Nrf2, wild-type mice having normal Nrf2 activation, Keap1-KD mice having enhanced Nrf2 activation, and Keap1-HKO mice having the highest Nrf2 activation in liver. Global gene expression profiles were performed by microarray analysis in this gene dose-response approach.

Specific aim 2 was designed to investigate the protective role of Nrf2 against chemical-induced liver injury. Information has been obtained on the consequence of Nrf2 deficiency by studying Nrf2-null mice, indicating the importance of Nrf2 in preventing the development of liver injury. For example, compared with wild-type mice, Nrf2-null mice are more susceptible to liver injury by acetaminophen, ethanol, pentachlorophenol, and a high-fat diet. However, it is more important to know whether Nrf2 activation protects against chemical-induced liver injury. Diquat, ethanol, and cadmium produce oxidative stress and liver injury through diverse mechanisms. For example, diquat generates superoxide free radicals through redox cycling, ethanol generates reactive oxygen species through its metabolism, and cadmium generates oxidative stress through binding to the sulfhydryls of glutathione and proteins. Specific aim 2 utilized the gene dose-response model with Nrf2-null, wild-type, Keap1-KD, and Keap1-HKO mice to investigate whether Nrf2 deficiency will aggravate, whereas Nrf2 enhancement will protect against diquat, ethanol, and cadmium induced oxidative stress and subsequent liver injury.

Specific aim 3 was designed to develop novel Nrf2 activators by high-throughput screening. A library of 47,000 synthetic and natural existing compounds was screened

in AREc32 cells, a stably transfected MCF7 cell line that contains a luciferase gene construct under the control of ARE. Pharmacological activation of Nrf2 was monitored by quantifying luminescent intensity as an indicator of activation of ARE. The active compounds identified from the primary screening were validated with a range of eleven concentrations using the same screening system. The validated hits were further confirmed and prioritized by secondary screening in Hepa1c1c7 cells by monitoring induction of Nrf2 target genes. The lead compounds provide a starting point for chemical optimization and further development. Chemical structures of lead compounds also provide important information on structure-activity-relationship to activate the Keap1-Nrf2 signal pathway.

In summary, utilizing a gene dose-response model and high-throughput techniques, the present dissertation has investigated the role of Nrf2 on genomic gene expression in liver, the protective effect of Nrf2 against chemical-induced oxidative stress and subsequent liver injury, and found multiple compounds that are highly effective in activating the Keap1-Nrf2 pathway. The data generated from these studies will provide fundamental knowledge to further understand the Keap1-Nrf2 pathway, and identify the Keap1-Nrf2 pathway as an important target in therapy of liver diseases.

Chapter 3 : EXPERIMENTAL MATERIALS AND METHODS

Reagents

Nrf2 antibody was purchased from Santa Cruz Biotechnology (sc-30915, Santa Cruz, CA). TATA-box binding protein (TBP) antibody was purchased from Abcam (ab51841, Cambrdige, MA). Nqo1 and β-actin antibodies were purchased from Abcam (Ab2346, Ab8227, respectively, Cambridge, MA), Srebp1 antibody was purchased from Santa Cruz Biotechnology (sc-367, Santa Cruz, CA), and histone 3 antibody was purchased from Millipore (DAM170816, Billerica, MA). Gclc antibody was a gift from Dr. Terry Kavanagh (University of Washington, Seattle, WA). 2-Cyano-3,12-dioxooleana-1,9-diene-28-imidazolide (CDDO-Im) was a generous gift from Dr. Michael Sporn (Dartmouth College, Hanover, New Hampshire). All other chemicals, unless otherwise specified, were purchased from Sigma-Aldrich (St Louis, MO).

Animals and husbandry

Eight-week-old male mice were used for this study. C57BL/6 mice were purchased from Charles River Laboratories, Inc. (Wilmington, MA). Nrf2-null mice were obtained from Dr Jefferson Chan (University of California, Irvine, CA) (Chan et al., 1996). Keap1-KD mice were supplied by Dr Masayuki Yamamoto (Tohoku University, Sendai, Japan). In an attempt to make a hepatocyte-specific Keap1-null mouse, utilizing a loxP, Alb-Cre system, a Keap1-Flox mouse, in which Keap1 was decreased throughout the body (Keap1-kncokdown, Keap1-KD mice), was engineered (Okada et al., 2008). Nrf2-null and Keap1-KD mice were backcrossed into the C57BL/6 background, and > 99% congenicity was confirmed by Jackson Laboratories (Bar Harbor, ME). Keap1-HKO mice were generated by crossing Keap1-KD mice and AlbCre[+] mice, which express Cre only in hepatocytes. All the mice used in the study were bred at University of Kansas

Medical Center and housed in a temperature-, light-, and humidity-controlled environment and had access to Teklad Rodent Diet #8604 (Harlan Laboratories, Madison, WI) and water *ad libitum*. The housing facility at the University of Kansas Medical Center is accredited by the Association for Assessment and Accreditation of Laboratory Animal Care. All the mice were euthanized in the morning (8:00-10:00am) under the fed state. All procedures were pre-approved in accordance with Institutional Animal Care and Use Committee guidelines.

A modified "binge drinking" model was used to study ethanol-induced hepatic alterations (Bergheim *et al.*, 2006). Nrf2-null mice, wild-type mice, Keap1-KD mice, and Keap1-HKO mice were treated with either ethanol (5 g/kg, oral gavage) or an isocaloric glucose solution. Six h after ethanol administration, blood and liver samples were collected and stored at -80°C for further analysis. Food and tap water were allowed *ad libitum* during the experimentation.

To investigate whether Nrf2 protects against cadmium-induced toxicity, Nrf2-null mice, wild-type mice, Keap1-KD mice, and Keap1-HKO mice were treated with either cadmium chloride (3.5 mg Cd/kg, i.p.) or saline (10 mL/kg, i.p.). Eight h after administration of $CdCl_2$, blood and liver samples were collected. Portions of liver were fixed in 10% zinc formalin for histological analysis, and other portions were frozen in liquid nitrogen and stored at -80℃.

To investigate whether Nrf2 protects against diquat-induced toxicity, Nrf2-null, wild-type, and Keap1-KD mice were dosed with either saline (5 mL/kg, i.p.) or diquat dibromide (125 mg/kg, i.p.). Blood, livers, and lungs were collected at 1, 2, 4, and 6 h after diquat

treatment or 3 h after saline treatment. Upon removal, livers and lungs were weighed immediately. Portions of livers and lungs were fixed in 10% zinc formalin for histological analysis, and the remainder was frozen in liquid nitrogen and stored at -80℃.

Nrf2 protein expression in hepatic nuclear extracts

Nuclear extracts were prepared with the NE-PER nuclear extraction kit according to the manufacturer's protocol (Pierce Biotechnology, Rockford, IL). Protein concentrations were determined with a BCA Assay Kit from Pierce Biotechnology. Nuclear proteins (40 μg protein per lane) were electrophoretically resolved using polyacrylamide gels (4% stacking and 10% resolving). Gels were transblotted overnight at 4°C onto polyvinylidene fluoride membranes. Membranes were then washed with PBS-buffered saline containing 0.05% Tween-20 (PBS-T). Membranes were blocked for 1 h at room temperature with 5% nonfat milk in PBS-T. Blots were then incubated with primary antibody (1:1000 dilution in 2% nonfat milk in PBS-T) for 3 h at room temperature. Blots were washed in PBS-T and incubated with species-appropriate secondary antibody conjugated with horseradish peroxidase (1:2000 dilution) in 2% nonfat milk in PBS-T buffer for 1 h at room temperature. Blots were then washed with PBS-T. Protein-antibody complexes were detected using an ECL chemiluminescent kit (Pierce Biotechnology, Rockford, IL) and exposed to X-ray film (Denville Scientific, Metuchen, NJ). Equal protein loading was confirmed by TATA-box binding protein (TBP). Nrf2 and TBP proteins migrated the same distance as proteins of approximately 110 and 37 kDa, respectively. Intensity of protein bands was quantified by Discovery Series Quantity One 1-D Analysis Software (Bio-Rad Laboratories, Hercules, CA). Individual blot densities were normalized to that of wild-type mice.

Gclc, Nqo1, and Srebp1 protein expression in hepatic cytosolic fraction

Livers were homogenized in sucrose-Tris buffer (0.25 mol/L sucrose, 10 mmol/L Tris–HCl, pH 7.4) and centrifuged at 100,000 x g for 60 min at 4°C. The resulting supernatant, that is the cytosolic fraction, was used to assay Gclc and Nqo1 protein. Nuclear extracts were prepared with the NE-PER nuclear extraction kit, according to the manufacturer's directions (Pierce Biotechnology, Rockford, IL). Nuclear extracts were used for Srebp1 immunoblotting.

Cytosolic and nuclear proteins (40 µg protein/lane) were electrophoretically resolved using polyacrylamide gels. Gels were transblotted overnight at 4°C onto a nitrocellulose membrane. Membranes were then washed with PBS-buffered saline containing 0.05% Tween-20 (PBS-T). Membranes were blocked for 1 h at room temperature with 5% non-fat milk in PBS-T. Blots were then incubated with primary antibody (1:2000 dilution for Gclc, Nqo1, and histone 3, and 1:200 for Srebp1, in 1% non-fat milk in PBS-T) for 1 h at room temperature. Blots were then washed in PBS-T and incubated with secondary antibody conjugated with horseradish peroxidase (1:2000) in 2% non-fat milk in PBS-T buffer for 1 h at room temperature. Blots were then washed with PBS-T. Protein-antibody complexes were detected using an enhanced chemiluminescent kit (Pierce Biotechnology, Rockford, IL) and exposed to X-ray film (Denville Scientific, Metuchen, NJ). Intensity of protein bands was quantified using the Discovery Series Quantity One 1-D Analysis software (Bio-Rad Laboratories, Hercules, CA). Intensity values were normalized to β-actin or histone 3 and expressed as relative protein concentrations.

GSH quantification

GSH concentrations were quantified by UPLC-MS/MS according to a previous method with small modifications (Guan et al., 2003; New and Chan, 2008). Briefly, frozen liver tissue (50 mg) was diced, added to 200 µl of ice-cold KCl (1.15%) and homogenized over ice for 2 min. Tissue homogenates (50 µL) were transferred to a 1.5 ml snapcap conical-bottom centrifuge vial with glutathione ethyl ester (0.01 mg/ml, 20 µL) added as the internal standard (IS). Ellman's reagent (10 mM, 100 µl) was added to the homogenate and vortexed, followed by addition of 30 µl of 5-sulfosalicylic acid (20%). After centrifuging at 11,600 g for 15 min, the supernatant was collected for LC/MS analysis. A Waters Acquity ultra performance LC system (Waters, Milford, MA) was used and all chromatographic separations were performed using an Acquity UPLC BEH C18 column (1.7 µm, 100 x 2.1 mm I.D.). The mass spectrometer was a Waters Quattro Premier XE triple quadrupole instrument with an ESI source (Waters, Milford, MA). The multiple reaction monitoring (MRM) transitions under ESI positive mode are as follows: m/z 504.8>272.9 for GSH-Ellman, 532.88>204.9 for IS-Ellman.

Total RNA isolation

Total RNA was isolated using RNAzol B reagent (Tel Test, Inc., Friendswood, TX) according to the manufacturer's protocol. The concentration of total RNA in each sample was quantified spectrophotometrically at 260 nm. The integrity of each RNA sample was evaluated by formaldehyde-agarose gel electrophoresis before analysis.

Quantification of mRNA expression by RT-PCR assay

Total RNA in mouse livers was reverse-transcribed into cDNA by High Capacity cDNA Archive Kit (Applied Biosystems, Foster City, CA), and the resulting cDNA was used for real-time PCR analysis using SYBR® Green PCR Master Mix in 7900HT Fast Real-Time PCR System (Applied Biosystems, Foster City, CA). Oligonucleotide primers specific to mouse β-actin, Gclc, Nqo1, Me1, G6pdx, Pgd, Scd1, Srebp1, MT-1, MT-2, Gpx2, Prdx1, Txnrd1, Srxn1, and Txn1 are described in table 3.1.

Microarray and data analysis

Gene expression in livers of Nrf2-null, WT, Keap1-KD, and Keap1-HKO mice was determined by the Affymetrix Mouse 430.20 arrays at the KUMC Microarray Core Facility. Biological replicates (n = 3) of each genotype were hybridized to individual arrays. Raw data CEL files were pre-processed using R in the Bioconducter by "affy" and Robust Multichip Averaging (gcRMA) packages (Irizarry et al., 2003). The mean probe intensities higher than $\log_2 100$ in at least one group were selected for further analysis. Gene annotations were obtained using the mouse 4302 and "annaffy" packages. Differential gene expression analysis was performed across all genotypes (P-value < 0.05) by the Linear Models for Microarray Data (Limma) package. Probes that were shown to be differentially expressed were included in a Venn diagram which identifies the common and exclusively expressed genes of each genotype (Nrf2-null, WT, Keap1-KD, and Keap1-HKO). Two-way hierarchical clustering of pathway specific gene expression was conducted using JMP 8.0 software (SAS Institute, Cary, NC) using agglomerative clustering for hierarchical clustering. The method starts with each point (gene) as its own cluster. At each step, the two clusters that are closest together are combined into a single cluster. This process continues until there is only one cluster

containing all the points (genes). This kind of clustering is good for smaller data sets (a few hundred observations). The distance between two genes was calculated by the Ward method.

Pathway analysis

Functional and pathway analysis of differentially expressed probe sets was performed using the Ingenuity Pathway Analysis (IPA, Ingenuity Systems, www.ingenuity.com), and Database for Annotation, Visualization and Integrated Discovery (DAVID) (http://david.abcc.ncifcrf.gov) database. Pathway enrichment was determined by P value ≤ 0.05 and a minimum of 4 probes in the pathway. False-discovery rates (FDRs) are also reported.

Motif analyses and transcription factor-binding site over-representation

The core sequence of Antioxidant Response Element (ARE, TGACnnnGC) was searched for in the 5' region (up to 10kb upstream of transcription start site) of each gene using Genamics Expression DNA Sequence Analyses Software (GENAMICS, Hamilton, New Zealand). Over-represented conserved transcription factor binding sites in genes induced by Nrf2 activation were searched for by the oPOSSUM system (http://opossum.cisreg.ca/oPOSSUM3). The over-representation was calculated on a conserved region (from 5kb upstream to 2kb downstream) around the transcription start site (TSS) of the drug processing genes that were induced by Nrf2, and the over-representation was calculated by comparing with the same region in a battery of drug processing genes that were not altered by Nrf2 as a background.

Serum lactate dehydrogenase (LDH) and alanine aminotransferase (ALT) activities

Serum LDH activities were determined as a biochemical indicator of hepacellular necrosis using a LDH-L Reagent Set (Thermo Fisher Scientific Inc., Fair Lawn, NJ). Serum ALT concentrations were determined using a Pointe Scientific Liquid ALT Reagent Set (Canton, MI) according to the manufacturer's protocol.

Lipid peroxidation in serum

Lipid peroxidation in serum was monitored by quantifying thiobarbituric acid reactive substances (TBARS) using a TBARS assay kit (Thermo Fisher Scientific Inc., Fair Lawn, NJ).

Isolation and purification of mitochondria

Mitochondria were isolated as previously described with minor modifications (Chavan *et al*., 2011). Liver samples (50 mg) were homogenized in 400 µL of isolation buffer (250 mM sucrose, 1 mM EDTA , 10 mM Tris-HCl [pH 7.4]) containing 1× protease inhibitor cocktail (Roche Applied Science, Indianapolis, IN) on ice. The liver homogenates were centrifuged at 960 x g for 15 min at 4°C to remove large debris and nuclei. The resultant supernatants were centrifuged at 8,600 x g for 15 min at 4°C. The pellets (crude mitochondria) were stored in mitochondria stock buffer (210 mM mannitol, 70 mM sucrose, 5 mM Tris-HCl, [pH 7.5], and 1 mM EDTA) at -80°C before use.

Primary hepatocyte isolation and treatment

Primary hepatocytes from Nrf2-null, wild-type, Keap1-KD, and Keap1-HKO mice were isolated as described previously (Ding *et al.*, 2010). After isolation, cells were plated in 12-well plates (1×10^5 cells per well) and cultured in Williams' Medium E (Invitrogen Corporation, Carlsbad, CA) containing 10% fetal bovine serum, 100 U/mL penicillin/streptomycin, and 2 mM glutamate. The plates were placed in a humidified, 5% CO_2 and 95% air incubator at 37°C. After 3 h, cells were washed with PBS and adherent hepatocytes were allowed to acclimate to culture conditions overnight. Cells were then cultured with fresh medium containing 0, 30, 100, or 300 mM ethanol, or 0, 10, 30, or 100 μM cadmium, or 0, 10, 30, or 100 μM diquat for 0, 3, 6, or 24 h.

Measurement of ROS Production

For general oxidative stress detection, cells were loaded with 2′,7′-dichlorodihydrofluoresein diacetate (H₂DCFDA; Invitrogen Corporation, Carlsbad, CA) for 30 min, and then washed with PBS, and incubated with Hanks′ Balanced Salt Solution (HBSS, with calcium and magnesium) for another 30 min. Images were taken using an Olympus B×41 microscope (Olympus Optical, Tokyo, Japan). Images were captured using an Olympus DP70 camera (×40) with DP Controller software. For quantification, cells were scraped and lysed using a lysis buffer (25 mM HEPES, 5 mM EDTA, and 0.1% CHAPS), and the fluorescence intensity of the DCF formed was determined with a Synergy 2 Multi-Detection Microplate Reader interfaced with a Gen5 Reader Control and Data Analysis Software (Biotek, Winoosky, VT) at excitation and emission wavelengths of 480 nm and 530 nm, respectively.

Triglyceride and free fatty acid concentrations in liver and serum

Liver lipids were extracted as previously described (Zhang *et al.*, 2010). Triglyceride concentrations were determined using the L-Type TG M test kit (Wako Chemicals Inc., Richmond, VA), and free fatty acids using the HR Series NEFA-HR(2) test kit (Wako Chemicals Inc., Richmond, VA) following the manufacturer's instructions.

Protein concentration assay

Protein concentrations from mitochondria extracts and cell lysis were determined by a BCA Protein Assay following the manufacturer's instructions (Pierce Biotechnology, Rockford, IL).

Histopathology

Liver and lung samples were fixed in 10% formalin prior to routine processing and paraffin embedding. Liver and lung sections (5 µm in thickness) were stained with hematoxylin and eosin and evaluated for hepatocellular necrosis.

Statistical analysis

Data were analyzed using a one-way ANOVA followed by Duncan's multiple range test ($p \leq 0.05$) utilizing SigmaStat Software (Systat Software Inc., San Jose, CA). Values are expressed as mean ± SEM.

Table 3.1. Oligonucleotide sequences for primers for RT-PCR analysis.

Gene	Forward	Reverse
β-actin	tgaccgagcgtggctacag	gggcaacatagcacagcttct
Nqo1	tatccttccgagtcatctctagca	tctgcagcttccagcttcttg
Gclc	tggccactatctgcccaatt	gtctgacacgtagcctcggtaa
G6pdx	agtgggtgaaccctcacaag	agctgggtttactggtggtg
Me1	gggattgctcacttggttgt	gttcatgggcaaacacctct
Pgd	gggcactttgtgaagatggt	aacagctctttgccgtcagt
Srebp1	gtgagcctgacaagcaatca	ggtgcctacagagcaagagg
Scd1	gcgatacactctggtgctca	cccagggaaaccaggatatt
MT-1	ctccgtagctccagcttcac	aggagcagcagctcttcttg
MT-2	ccgatctctcgtcgatcttc	aggagcagcagcttttcttg
Ho-1	cctcactggcaggaaatcatc	cctcgtggagacgctttacata
Trxn1	gccaaaatggtgaagctgat	tgatcattttgcaaggtcca
Gpx2	cagcttccagaccatcaaca	cactgagccctgaggaagac
Srxn1	cccactggaccaacttctgt	gtggctagctcagaccaagg
Prdx1	cacccaagaaacaaggagga	aaaaaggcccctgaaagaga
Txnrd1	gcagaccaatgtgccttacat	acggcttttcttcagagagg

Cell growth and maintenance

The AREc32 cell line was obtained from CRX biosciences (Dundee, Scotland). The AREc32 are a stable cell line derived from human MCF7 breast carcinoma cells. AREc32 cells were constructed by a luciferase gene construct that under the control of eight copies of rat Gsta2 AREs in the promoter region (Wang et al., 2006). AREc32 cells were maintained at University of Kansas High Throughput Center in Dulbecco's Modified Eagle's medium (DMEM) containing glutamax supplemented with 10% fetal calf serum and the antibiotic G418 (Life Technologies Corporation, Carlsbad, CA). The cell line was grown at 37ºC in the presence of 5% CO_2.

AREc32 cells were seeded into 384-well plates (flat-bottom white, opaque, sterile, with lids). Cells were seeded at a density of 3,500 cells/well using a Wellmate bulk dispenser (Thermo Fisher Scientific, Waltham, MA) in 50µL complete media per well. Cell plates were incubated at room temperature for 30 min following seeding to allow for even cell settling. Cell plates were then incubated at 37ºC, 5% CO_2 in a 95% humidified incubator for 20 hrs.

Murine hepatoma Hepa1c1c7 cells were obtained from ATCC (Manassas, VA) and maintained in DMEM with glutamate, supplemented with 10% (v/v) heat-inactivated FBS, penicillin (100 units/mL), and streptomycin (100 µg/ml). The cell line was grown at 37ºC in the presence of 5% CO_2.

Compound Libraries and preparation

Four libraries of compounds were screened for Nrf2 activation in the present study: MicroSource Discovery Systems (www.msdiscovery.com/spectrum.html)

containing 2000 compounds, Prestwick Chemical Library (Prestwick Chemical, Washington, DC) containing 1120 compounds, 1920 compounds from the University of Kansas Center of Excellence in Chemical Methodologies & Library Development (KU-CMLD) containing, and ChemBridge Small Molecule Library (ChemBridge Corporation, San Diego, CA) containing 41,888 compounds. The chemical names, CAS-numbers, and sources of all the natural chemicals are summarized in Table 3.2.

The four libraries of compounds were stored at 2859 μM in 100% DMSO, and 175 nL from each compound well was transferred to the 50 μL cell culture medium in the receiving well. Chembridge library compounds were dispensed by the Matrix PlateMate Plus automated nanoliter capacity liquid handler (Thermo Fisher Scientific, Waltham, MA), followed by three gentle mixings. Compounds from MicroSource, Prestwick, and CMLD libraries, as well as the compounds for the concentration-response validation, were dispensed by Labcyte Echo 550 Compound Reformatter (Labcyte Inc., Sunnyvale, CA), which allows the accurate transfer of small volumes of liquid. The final concentration of each chemical in the full library screen was 10.0 μM, with a DMSO content of 0.35%.

Table 3.2. Chemical names, CAS-numbers and sources of all the test natural chemicals.

Compound	CAS	Source
CDDO-Im	NA	Sporn [a]
tBHQ	1948-33-0	Sigma [b]
Andrographolide	5508-58-7	Sigma
Trans-chalcone	614-47-1	Acros [c]
Sulforaphane	4478-93-7	Sigma
Curcumin	458-37-7	Acros
Flavone	525-82-6	Sigma
Kahweol	6894-43-5	LKT [d]
Cafestol	469-83-0	LKT
Carnosol	5957-80-2	Cayman [e]
Caffeic acid	331-39-5	Cayman
Caffeic acid phenethyl ester	104594-70-9	Sigma
Chlorogenic acid	327-97-9	LKT
Allyl disulfide	2179-57-9	Sigma
Chrysin	480-40-0	Sigma
Caffeic acid phenethyl ester	104594-70-9	Sigma
Myricetin	529-44-2	Sigma
Apigenin	520-36-5	Sigma
(s,s)-(+)-Tetrandrine	518-34-3	Sigma
Quercetin	117-39-5	Sigma
Luteolin	491-70-3	Cayman
Berberine	2086-83-1	Sigma
Fisetin	528-48-3	Sigma
Resveratrol	501-36-0	Sigma
Baicalin	21967-41-9	Sigma
Kaempferol	520-18-3	Sigma
Galangin	548-83-4	Sigma
(-)-Epicatechin	490-46-0	Sigma
Hesperetin	520-33-2	Sigma
Genistein	446-72-0	Acros
Indole-3-carbinol	700-06-1	Acros
Chlorophyllin	15611-43-5	Sigma
Daidzein	486-66-8	Sigma
Lupeol	545-47-1	Sigma
Glycitein	40957-83-3	LKT
Daidzin	552-66-9	Cayman
Evodiamine	5956-87-6	Sigma
Quercitrin	522-12-3	Sigma
Zebularine	3690-10-6	Sigma
Naringenin	480-41-1	LKT
Silymarin	65666-07-1	LKT
Matrine	519-02-8	INDOFINE [f]
Oleanolic acid	508-02-1	Quality [g]
Sennoside B	128-57-4	Quality
Crocin	42553-65-1	Sigma
Morin	480-16-0	Sigma
Oxymatrine	16837-52-8	INDOFINE
Chrysophanic acid	481-74-3	Sigma
Icariin	489-32-7	Sigma
Silibinin	22888-70-6	Sigma
Glycyrrhetinic acid	471-53-4	Acros
Synephrine	94-07-5	Quality
Rutin	153-18-4	Sigma
Epigallocatechin 3-gallate	989-51-5	Sigma
Naringin	10236-47-2	Sigma
(+)-Catechin	7295-85-4	Sigma

[a]: generous gift from Dr. Michael Sporn (Dartmouth College, Hanover, New Hampshire)

[b]: Sigma-Aldrich (St. Louis, MO)

[c]: Acros Organics (Geel, Belgium)

[d]: LKT Laboratories (St. Paul, MN)

[e]: Cayman Chemicals (Ann Arbor, MI)

[f]: INDOFINE Chemical Company (Hillsborough, NJ).

[g]: Quality Phytochemicals, LLC (Edison, NJ)

Quantification of ARE activation by Promega Steady-Glo luciferase assay system.

The AREc32 cell line was exposed to library compounds for 24 hrs at 37°C, 5% CO_2 in a 95% humidified incubator, then the plates were removed from the incubator and left at room temperature for 20 min to equilibrate the plate and its contents to room temperature. The Matrix Wellmate dispensed Steady-Glo luciferase assay reagent (Promega, Madison, WI) to all cells, 10 μL per well, and plates were shaken for 1 min at 1600 rpm. The luminescence intensities were read 30 min later on a Tecan Safire2 microplate reader (Männedorf, Switzerland). The Steady-Glo reagent produces cell lysis and generation of a luminescent signal, which is proportional to ARE activation, through the luciferase reporter in the AREc32 cell line.

Four controls were used on each plate of cells: (1) cells treated with tBHQ, a known ARE activator (positive control), (2) cells treated with CDDO-Im, a very potent activator of Nrf2/ARE (positive control), (3) cells in media containing 0.35% DMSO (vehicle control), and (4) cells in media containing no DMSO (fully healthy cells) to measure background luminescence.

Z' factor for Pass/Fail Criterion

The positive and negative controls were required to assure uniformity from plate to plate, and from screening batch to batch. The controls were used to calculate a Z' factor value for each plate, a measure of assay robustness and variability popularly used for high throughput screening. The Z' factor compares the baseline background (minimum ARE signal) from the DMSO vehicle control, and the maximum signal of response of the positive controls tBHQ and CDDO-Im (Zhang et al., 1999; Iversen et al.,

2006).The Z' factor formula relies on the standard deviation and mean of the maximum

signal and the minimum baseline:

$$Z'_{factor} = 1- \frac{3\left(SD_{max\ signal} + SD_{min\ signal}\right)}{|mean_{max\ signal} - mean_{min\ signal}|}$$

In this assay, screening plates were expected to have a Z' of equal to or greater

than 0.6. Plates with Z' values below 0.4 were individually investigated, and rejected or

repeated on a plate by plate basis.

Quantification of Nqo1 mRNA in Hepa1c1c7 cells

The top 30 hits from the primary screen were further validated by quantifying the

mRNA of Nqo1, a prototypical Nrf2 target gene, in Hepa1c1c7 cells by real time-PCR.

Cells were grown in 24-well plates at a density of 30,000 cells per well for 12 hrs, and

subsequently incubated with test compounds at 6 concentrations (0.1- 3 µM) for 24 hrs.

After incubation, the medium was decanted and total RNA was isolated using RNAzol B

reagent (Tel Test, Inc., Friendswood, TX). cDNA was synthesized with a High Capacity

cDNA Archive Kit (Applied Biosystems, Foster City, CA) from total RNA, and the

resulting cDNA was used for real-time PCR to quantify Nqo1 mRNA, with β-actin used

as the internal control.

Compound structure clustering analysis

Preliminary hit clustering was based on EC_{50} values from the concentration-

response curves of the top 240 compounds, and accomplished via the Selector program

from Tripos via the Jarvis Patrick routine, using default parameters. From each

preliminary cluster, the largest conserved substructure present in at least half of the

cluster members was identified. Each cluster was then manually edited to remove

compounds that did not contain the largest conserved substructure identified in the

previous step. Compounds that had not originally been selected to a given cluster but containing the cluster's characteristic conserved substructure were then added to the cluster.

Chapter 4 : BENEFICIAL ROLE OF NRF2 IN REGULATING NADPH GENERATION

AND CONSUMPTION

Abstract

Nrf2 (nuclear factor erythroid 2-related factor 2) is a transcription factor that promotes the transcription of cytoprotective genes in response to oxidative and electrophilic stresses. Most functions of Nrf2 were identified by studying biological models with Nrf2 deficiency, however, little is known about the effects of graded Nrf2 activation. In the present study, genomic gene expression profiles by microarray analysis were characterized with a 'gene dose-response' model in livers of Nrf2-null mice, wild-type mice, Keap1-knockdown (Keap1-KD) mice with enhanced Nrf2 activation, and Keap1-hepatocyte knockout (Keap1-HKO) mice with maximum hepatic Nrf2 activation. Hepatic nuclear Nrf2 protein, glutathione concentrations, and known Nrf2 target genes were increased in a dose-dependent manner. In total, 115 genes were identified to be constitutively induced and 80 genes suppressed with graded Nrf2 activation. Messenger RNA of genes encoding enzymes in the pentose phosphate pathway and enzyme were low with Nrf2 deficiency and high with Nrf2 activation, indicating that Nrf2 is important for NADPH production. NADPH is the major reducing resource to scavenge oxidative stress, including regenerating glutathione and thioredoxin, and is also used for anabolic pathways including lipid synthesis. HPLC-UV analysis confirmed that hepatic NADPH concentration was lowest in Nrf2-null mice and highest in Keap1-HKO mice. In addition, genes involved in fatty acid synthesis and desaturation were down-regulated with graded Nrf2 activation. In conclusion, the present study suggests that Nrf2 protects against environmental insults by promoting the generation of NADPH, which is preferentially consumed by aiding scavenging of oxidative stress rather than fatty acid synthesis and desaturation.

Introduction

Nuclear factor erythroid 2-related factor 2 (Nrf2) is a transcription factor that induces a battery of cytoprotective genes in response to oxidative/electrophilic insults. Under physiological conditions, Nrf2 is bound to its repressor, Kelch-like ECH associating protein 1 (Keap1), in the cytosol. Keap1 functions as an adapter protein that retains Nrf2 in the cytoplasm by interacting with the cytoskeleton, and it facilitates degradation of Nrf2 by binding with Cullin 3-based E3 ligase, a protein-protein complex that ubiquitinates Nrf2 protein (Cullinan et al., 2004). With the negative regulatory system of Keap1, Nrf2 protein has a very rapid turnover, with a half-life less than 20 min (Kobayashi et al., 2004), and thus Nrf2 protein is minimally detectable in unstressed conditions. There are numerous cysteine residues in Keap1 protein: murine and rat Keap1 have 25 cysteine residues, and human Keap1 has 27 cysteine residues. The high cysteine content of Keap1 makes it an excellent sensor for oxidative/electrophilic stress. Yamamoto and coworkers, therefore, proposed that Nrf2-activating compounds directly modify the sulfhydryl groups of cysteines in Keap1 by oxidation, reduction, or alkylation, which would alter the conformation of Keap1 and cease the ubiquitination of Nrf2 (Kobayashi and Yamamoto, 2006). Once released from Keap1, Nrf2 translocates into the nucleus, heterodimerizes with a small musculo-aponeurotic fibrosarcoma (Maf) protein, and promotes transcription of its target genes (Itoh et al., 1997). Consistent with this hypothesis, a number of Nrf2 activators have been reported to react with different cysteine residues of Keap1 (Hong et al., 2005b; Luo et al., 2007).

After the Keap1-Nrf2 signal pathway was discovered, a number of natural and synthetic compounds were shown to activate Nrf2, and protect against oxidative stress-

induced toxicity through Nrf2 activation. Potential therapeutic applications of Keap1-Nrf2 pathway have therefore been investigated. For example, curcumin was shown to protect against focal ischemia of cerebrum through upregulation of Nrf2, indicating Nrf2 may be suitable target for therapy of cerebral ischemia (Yang et al., 2009). Resveratrol was shown to increase transcription of GSH synthesis enzymes through activating Nrf2 (Zhang et al., 2009). Oltipraz was shown to protect against Alpha-naphthylisothiocyanate (ANIT)-induced cholestasis through Nrf2 activation, which indicated that pharmacological activation of Nrf2 may represent a therapeutic option for intrahepatic cholestasis (Tanaka et al., 2009). 2-Cyano-3,12-dioxooleana-1,9-dien-28-oic imidazolide (CDDO-Im), a synthetic triterpenoid, was shown to activate Nrf2 and protect against acetaminophen-induced liver injury (Reisman et al., 2009b). However, pharmacological activation of Nrf2 by chemicals is problematic, for they often have many off-target effects. For example, curcumin also activates AP-1, a transcription factor that promotes cell proliferation (Anand et al., 2008); Resveratrol also activates SIRT-1 (Baur, 2010); oltipraz activates CAR, and induces Cyp2b10 through CAR activation (Merrell et al., 2008); CDDO-Im activates Smad and ERK, and induces cell differentiation (Ji et al., 2006).

Nrf2-null mice have served as a valuable model to examine the Keap1-Nrf2 pathway. Compared to wild-type mice, Nrf2-null mice are more susceptible to liver injury by oxidative and electrophilic stress (Aleksunes and Manautou, 2007), acetaminophen (Enomoto et al., 2001), ethanol (Lamle et al., 2008), pentachlorophenol (Umemura et al., 2006), and high-fat diet (Tanaka et al., 2008). To investigate the effect of increased Nrf2 activation, Keap1-null mice were engineered. However, Keap1-null mice died at about

20 days of age (Wakabayashi et al., 2003), and thus a Keap1-hepatocyte knockout mouse (Keap1-HKO mouse) was engineered, utilizing the albumin-Cre loxP system. The Keap1-HKO mice have maximal activation of Nrf2 and Nrf2-target genes in liver, and are more resistant to acetaminophen hepatotoxicity (Okawa et al., 2006). Later it was discovered that mice homozygous for Keap1 loxP sites (no Albumin-Cre transgene) have decreased or a "knockdown" of Keap1 (Keap1-KD), resulting in an intermediate activation of Nrf2 in multiple organs(Okada et al., 2008). Taking advantage of the fact that floxed Keap1 allele is hypomorphic, an animal of graded reduction of Keap1 expression in adult mice was generated (Taguchi et al., 2010).

Gene transcription profiles have been performed on the effect of Nrf2 in mouse macrophages (Woods et al., 2009), lung tissue (Blake et al., 2010), and embryonic fibroblasts (Malhotra et al., 2010), but there is a significant gap in our understanding of Nrf2 on genomic gene expression in liver. Liver is the primary organ for the detoxification of environmental chemicals, drugs, and endogenous toxicants. Thus, studying the function of Nrf2 in liver is of great importance. In the present study, we have utilized a "gene dose-response" approach including Nrf2-null mice lacking any functional Nrf2, wild-type mice having normal Nrf2 activation, Keap1-KD mice having enhanced Nrf2 activation, and Keap1-HKO mice having the highest Nrf2 activation in liver. Hepatic phenotypes as well as genomic gene expression profile were analyzed in this "gene dose-response" approach.

Results

Characterization of "gene dose-response" model for Nrf2 activation

To confirm differential Nrf2 activation of the "gene dose-response" model, nuclear Nrf2 concentration, relative liver weight, hepatic GSH concentration, as well as mRNA expression of known Nrf2-target genes were characterized in livers of Nrf2-null, wild-type, Keap1-KD, and Keap1-HKO mice. Nuclear Nrf2 protein was undetectable in Nrf2-null mice, 1.4-fold higher in Keap1-KD mice, and 2.3-fold higher in Keap1-HKO mice than wild-type mice (Fig. 4.1A). The relative liver weight in Nrf2-null mice tended to be lower than wild-type mice but not statistically significant. The relative liver weight in Keap1-KD and Keap1-HKO mice was 11% and 24% higher than in wild-type mice, respectively (Fig.4.1B). GSH concentrations in livers of Nrf2-null mice were 18% lower than in wild-type mice. In livers of Keap1-KD and Keap1-HKO mice, GSH concentrations were 7% and 14% higher than wild-type mice, respectively (Fig.4.1C). Compared to wild-type mice, mRNA expression of Nqo1, a prototypical Nrf2 target gene, was 88% lower in Nrf2-null mice, and 167% and 1262% higher in Keap1-KD and Keap1-HKO mice, respectively (Fig.4.1D, upper panel). Compared to wild-type mice, mRNA of Gclc, another known Nrf2 target gene, was 36% lower in Nrf2-null mice, and 49% and 138% higher in Keap1-KD and Keap1-HKO mice, respectively (Fig.4.1.D, lower panel). In summary, Nrf2 activation was low in Nrf2-null mice, normal in wild-type mice, enhanced in Keap1-KD mice, and greatest in Keap1-HKO mice.
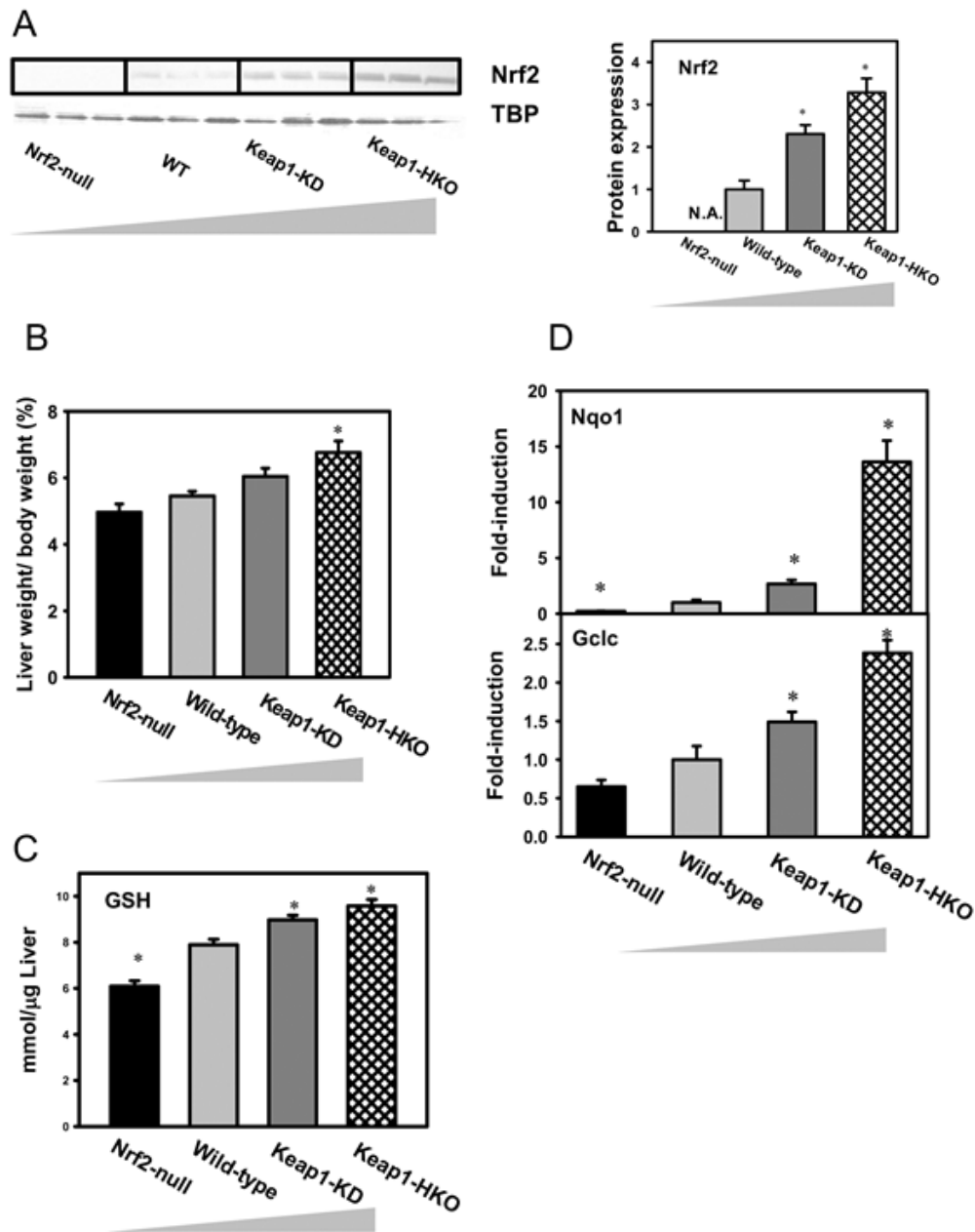
Figure 4.1. Characterization of "gene dose-response" model. (A) Nuclear Nrf2 protein levels by western blot analysis, (B) relative liver weight, (C) hepatic GSH concentrations by UPLC-MS/MS analysis, and (D) mRNA concentrations of known Nrf2 target genes by RT-PCR analysis in livers of Nrf2-null, wild-type, Keap1-KD, and Keap1-HKO mice. Data are presented as Mean ± S.E.M of 3 animals per group for Fig 1A, and 5 animals per group for Fig 1B, 1C and 1D. Asterisks (*) indicate statistically significant differences from wild-type mice ($p < 0.05$).

Transcriptional profiling of "gene dose-response" model

To investigate the effect of Nrf2 on gene transcription profiles in livers of mice, genomic mRNA expression was characterized by microarray. With approximately 45101 probes, 8021 were detected with signal intensity higher than the threshold and were selected for further analysis. In the pool of 8021 probe sets, 1519 probes were identified to be differentially expressed among the "gene-dose response" groups based on LIMMA. Specifically, 310 probe sets were expressed higher in wild-type mice than in Nrf2-null mice, 294 were higher in Keap1-KD mice than in wild-type mice, and 550 were higher in Keap1-HKO mice than Keap1-KD mice. Focusing on the intersection of the three sets, 115 probes were identified to have dose-response behavior and were constitutively induced by Nrf2. In contrast, the signal intensity of 362 probe sets were lower in wild-type mice than in Nrf2-null mice, 263 were lower in Keap1-KD mice than in wild-type mice, and 612 were lower in Keap1-HKO mice than Keap1-KD mice. Focusing on the intersection of the three sets, 80 probe sets were identified to have dose-response behavior and were constitutively suppressed by Nrf2 (Fig.4.2).

Pathway analysis of genes constitutively induced or suppressed with Nrf2 activation

To categorize the functions of genes induced or suppressed by Nrf2, constitutively up-regulated and down-regulated probes sets were submitted separately to Ingenuity Pathway Analysis (IPA) and the Database for Annotation, Visualization, and Integrated Discovery (DAVID). From the list of probe sets that were up-regulated by Nrf2, core analysis using IPA revealed enrichment of Nrf2-mediated oxidative stress
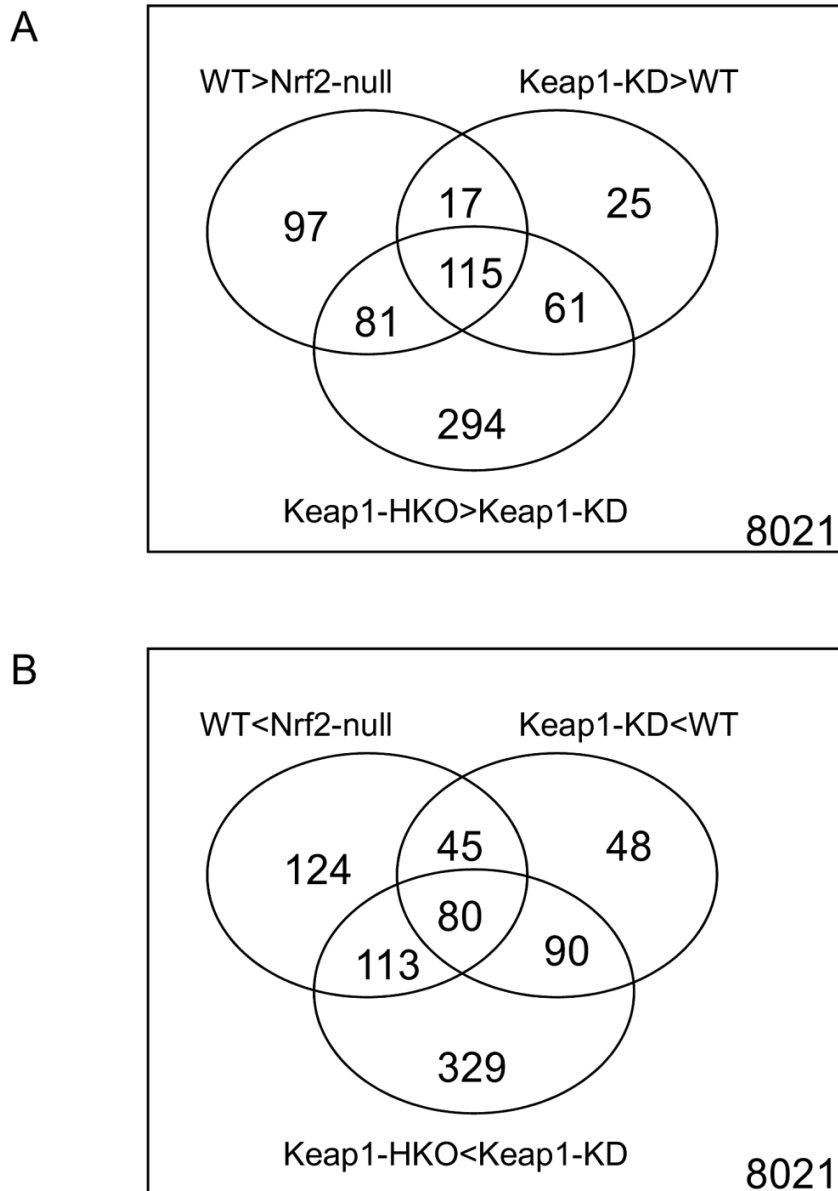
Figure 4.2. Transcriptional profiling of "gene dose-response" model to reveal Nrf2-dependent transcriptional targets. (A) Venn diagram of probe sets that had higher expression in wild-type mice than in Nrf2-null mice (WT>Nrf2-null), in Keap1-KD mice than in wild-type mice (Keap1-KD>WT), and in Keap1-HKO mice than in Keap1-KD mice (Keap1-HKO>Keap1-KD). (B) Venn diagram of probe sets that had lower expression in wild-type mice than in Nrf2-null mice (WT<Nrf2-null), in Keap1-KD mice than in wild-type mice (Keap1-KD<WT), and in Keap1-HKO mice than in Keap1-KD mice (Keap1-HKO<Keap1-KD).

Category	Count	%*	P-Value
Clusters of genes induced through Nrf2 activation			
Nrf2-mediated oxidative stress response	14	7.7	5.84E-12
Glutathione metabolism	10	10	2.78E-11
Xenobiotic metabolism signaling	15	5.2	6.58E-10
Clusters of genes suppressed through Nrf2 activation			
PPAR α /RXR α activation	4	2.2	5.05E-03

Table 4.1. Functional clustering of genes constitutively induced or suppressed with Nrf2 activation using Ingenuity Pathway Analysis. A canonical pathway–based analysis was conducted using the IPA (Ingenuity Systems, www.ingenuity.com) to identify the pathways enriched in genes constitutively induced or suppressed with Nrf2 activation.

 *: The ratio of the number of genes that were differentially regulated by Nrf2 and map to the pathway (for example, 14 genes induced by Nrf2 were mapped to "Nrf2-mediated oxidative stress response pathway"), divided by the total number of genes that map to the same pathway (for example, 182 genes were mapped to "Nrf2-mediated oxidative stress response pathway" in total), was calculated(14/182=7.7%) Fisher's exact test was used to calculate the p value determining that the probability of the association between the genes differentially regulated by Nrf2 and the canonical pathway was random.

Term	Enrichment Score	Gene Symbols
Top annotation cluster for the set of genes induced through Nrf2 activation		
Glutathione transferase and glutathione metabolism	8.2	Gstm1, Gss, Gsta2, Gstm2, Gsta3, Gstm3, Gclc, Gstm4, Gsta4, Gpx4, Gstm6
Oxidation reduction and NADPH bind enzymes	6.0	Cyp2g1, Xdh, Ptgr1, Htatip2, Ugdh, Coq7, Fth1, Akr1c13, Akr1a4, Cryl1, Fmo1, Gpx4, Aox1, Cyp2a5, Txnrd1, Nqo1, Srxn1
Carboxylesterase	3.9	Ces2, Ces1, BC015286, Ces5
Chemical and iron homeostasis	3.2	Xdh, Ftl1, Gclc, Fech, Ftl2, Hexa, Hexb, Bnip3, Afg3l2, Fth1, Abcg8, Anxa7
Cofactor biosynthetic process	2.4	Gss, Fech, Gclc, Coq7, Gch1
Top annotation cluster for the set of genes suppressed through Nrf2 activation		
Response to nutrient and extracellular stimulus	2.3	Avpr1a, Adipor2, Cp, Apom, Cbs

Table 4.2. Annotation clustering of genes constitutively induced or suppressed with Nrf2 activation using DAVID analysis. Database for Annotation, Visualization and Integrated Discovery (DAVID) (http://david.abcc.ncifcrf.gov) database was used to identify the pathways enriched in genes constitutively induced or suppressed with Nrf2 activation. Pathway enrichment was determined by the enrichment score > 2.

response, glutathione metabolism, and xenobiotic metabolism pathways (Table 4.1, upper panel). Down-regulated pathways included PPARα/RXRα activation (Table 4.1, lower panel). Annotation clustering using DAVID analysis revealed enrichment of glutathione transferases, NADPH mediated oxidation reduction, carboxylesterase, chemical and iron homeostasis, and cofactor biosynthesis in genes induced by Nrf2. The only annotation cluster enriched in genes suppressed by Nrf2 was involved in response to extracellular stimulus and nutrient (Table 4.2).

Regulation of antioxidant system genes by Nrf2

Figure 4.3 summarizes the antioxidant-associated enzymes that were significantly increased in the "gene dose-response" model. As shown in Fig.4.3A, Nrf2 activation increased transcription of genes involved in GSH biosynthesis (glutamate-cysteine ligase, Gclc; and glutathione synthase, Gss) as well as GSH regeneration (glutathione reductase, Gsr). Compared to wild-type mice, mRNA of Gclc was induced 58% in Keap1-KD mice and 210% in Keap1-HKO mice, and mRNA of Gss was induced 18% in Keap1-KD mice and 91% in Keap1-HKO mice. mRNA of Gsr increased 110% in Keap1-HKO mice over wild-type mice. Figure 4.3B indicates that Nrf2 activation increased the mRNA of genes involved in reduction of superoxide using GSH (glutathione peroxidase: Gpx2 and Gpx4) as well as using NADPH (peroxiredoxin, Prdx6). Especially, mRNA of Gpx2 and Gpx4 were increased in Keap1-HKO mice by 2260% and 105%, respectively. Figure 4.3C shows that Nrf2 activation increased transcription of genes involved in reduction of disulfide bonds between protein and GSH (glutaredoxin: Glrx1 and Glrx5), disulfide bonds with oxidized protein (sulfiredoxin:

Srxn1), and disulfide bonds in oxidized thioredoxin (thioredoxin reductase: Txnrd1). The

mRNA of Srxn1 increased 743% and Txnrd1 221% in Keap1-HKO mice. Figure 4.3D

shows that Nrf2 activation increased transcription of genes involved in heme

metabolism (biliverdin reductase B: Blvrb; and ferrochelatase: Fech) and free ion

storage (ferritin heavy chain: Fth1; and ferritin light chain: Ftl1 and Ftl2). In particular,

the mRNA of Blvrb was increased in Keap1-HKO mice by 270% and Ftl2 171%.

Regulation of NADPH production genes by Nrf2

Figure 4.4 summarizes the effect of Nrf2 in producing NADPH in the Nrf2 "gene

dose-response" model. The pentose phosphate pathway produces NADPH, and

generates 90% of the NADPH in the body. Figure 4A shows hierarchical clustering of

genes involved in the pentose phosphate pathway. Of the 16 genes examined, 12 were

highly expressed in Keap1-HKO mice, and only one gene was highly expressed in Nrf2-

null mice. In addition, the expression of the gene that encodes malic enzyme (Me1) was

low in Nrf2-null mice, and high in wild-type, Keap1-KD, and Keap1-HKO mice (Fig.4B).

To validate the role of Nrf2 in increasing NADPH production, hepatic NADPH

concentrations were determined by HPLC-UV analysis. As shown in Figure 4C, NADPH

concentrations tended to be lower in livers of Nrf2-null mice and were 24% higher in

Keap1-HKO mice than wild-type mice.
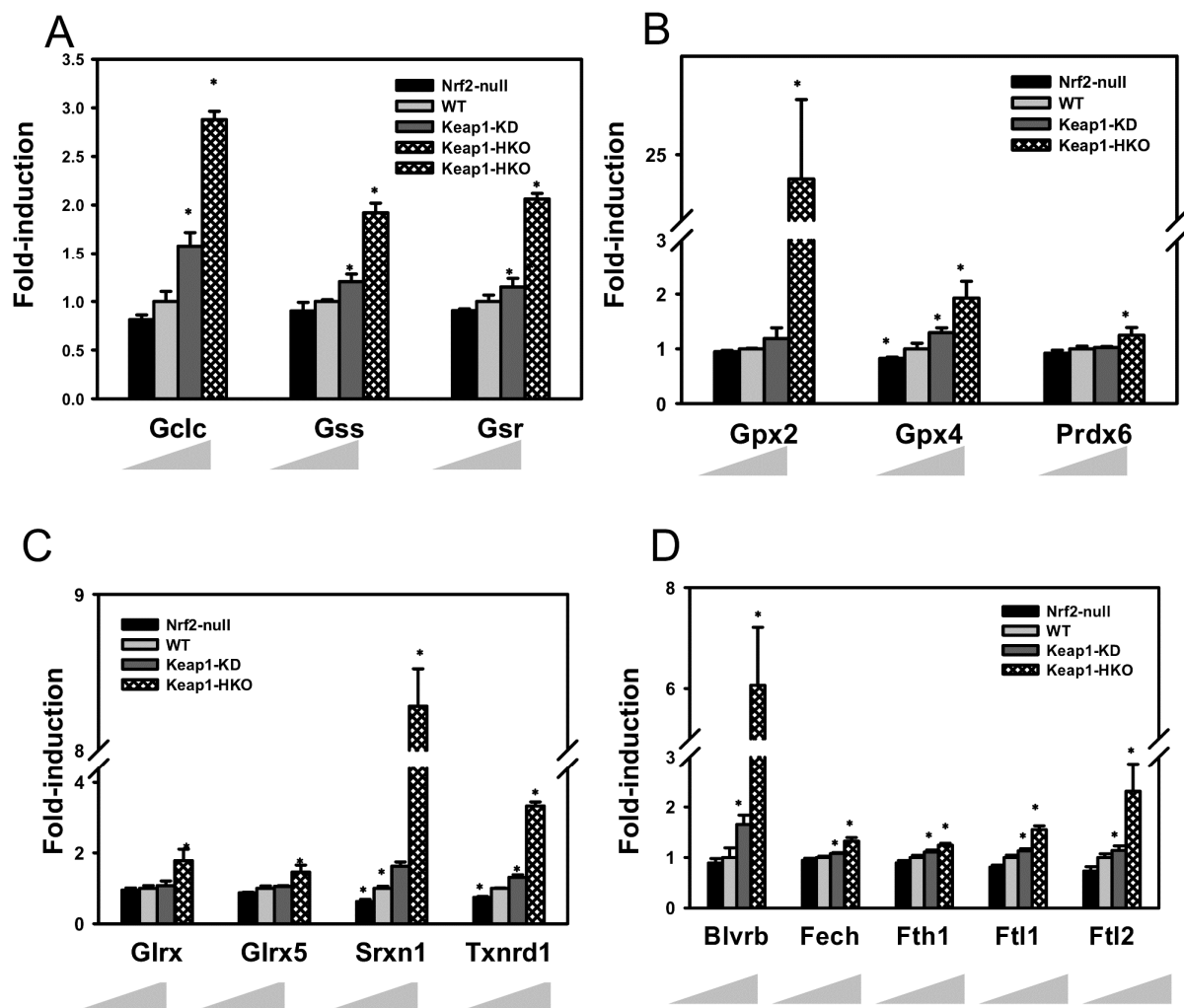
Figure 4.3. Antioxidant genes that were induced in "gene dose-response" model. Messenger RNA expression of genes involve in (A) GSH synthesis and regeneration, (B) reduction of protein disulfide bond, (C) reduction of hydrogen peroxide, and (D) bilirubin synthesis and ion storage in "gene dose-response" model. Data are presented as Mean ± S.E.M of 3 animals per group. Asterisks (*) indicate statistically significant differences from wild-type mice ($p < 0.05$).
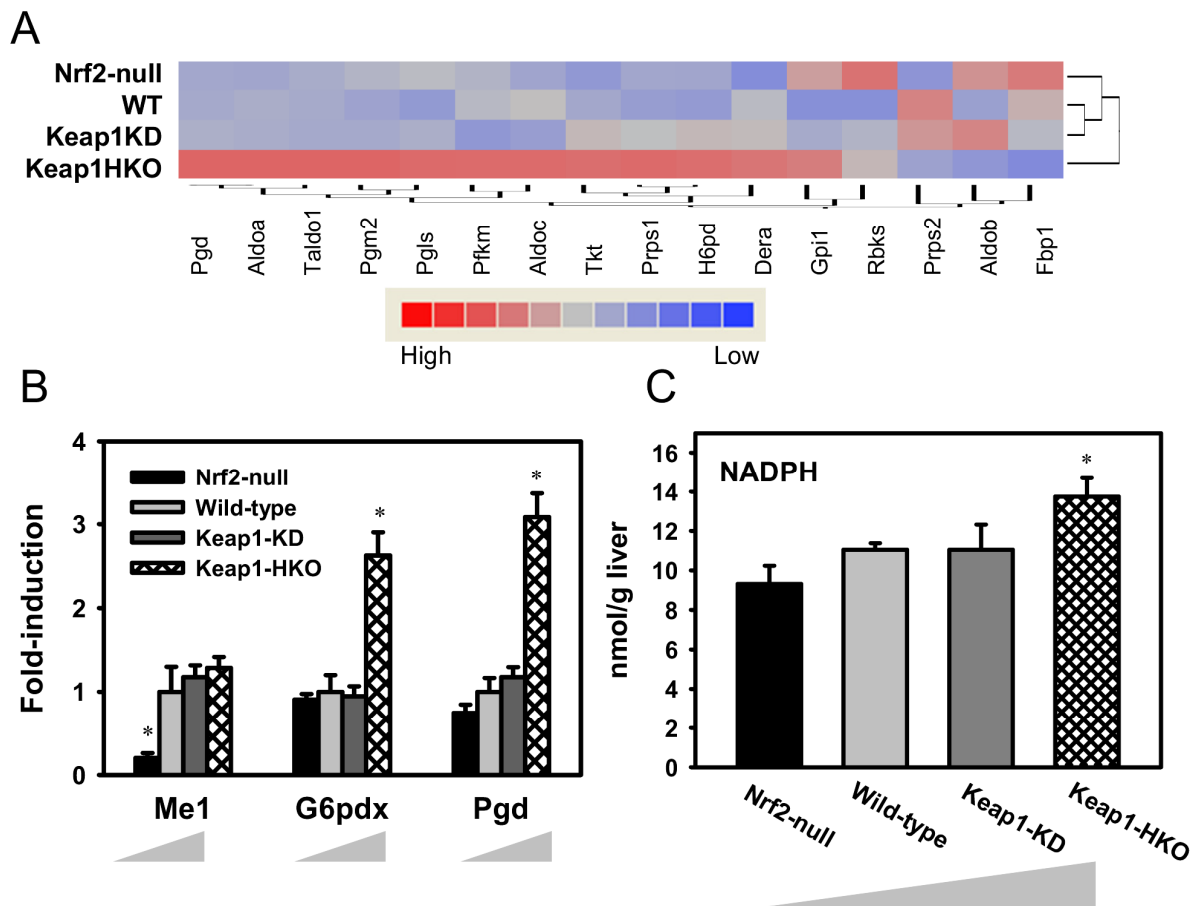
Figure 4.4. NADPH production was induced in "gene dose-response" model. (A) Hierarchical clustering of genes involved in pentose phosphate pathway. Shading is based on the fold-induction of mRNA of each gene compared to the wild-type mice. Genes involved in pentose phosphate pathway were selected according to KEGG category (KEGG: 00030). (B) Messenger RNA expression of Me1, G6pdx, and Pgd by RT-PCR analysis and (C) hepatic NADPH concentration by HPLC-UV analysis in "gene dose-response" model. Data are presented as Mean ± S.E.M 3 animals per group for Fig 4A, and 5 animals per group for Fig 4B and 4C. Asterisks (*) indicate statistically significant differences from wild-type mice ($p < 0.05$).

Regulation of lipid biosynthesis genes by Nrf2

Figure 5A indicates hierarchical clustering of genes involved in lipid biosynthesis. Of 52 genes examined, 36 genes were expressed at higher levels in Nrf2-null mice and at lower levels in Keap1-HKO mice. In contrast, 7 genes were expressed at higher levels in Keap1-HKO mice and lower levels in Nrf2-null mice. Specifically, Figure 5B shows hierarchical clustering of genes involved in fatty acid synthesis. Of 21 genes examined, 14 genes were expressed at higher levels in Nrf2-null mice and lower levels in Keap1-HKO mice. In contrast, only one gene was expressed at lower level in Nrf2-null mice and at higher level in Keap1-HKO mice. Figure 5C shows that genes involved in fatty acid desaturation were suppressed with Nrf2 activation. Fatty acid desaturase (Fads1 and Fads2) and Stearoyl-CoA desaturase (Scd1) are desaturases that catalyze the addition of a double bond utilizing NADPH as the cofactor. The abundance of Fads1 mRNA was 54% higher in Nrf2-null mice and 46% lower in Keap1-HKO mice than wild-type mice. Similarly, the abundance of Fads2 mRNA was 52% higher in Nrf2-null mice and 30% lower in Keap1-HKO mice than wild-type mice, and the abundance of Scd1 mRNA was 81% higher in Nrf2-null mice and 73% lower in Keap1-HKO mice than wild-type mice.
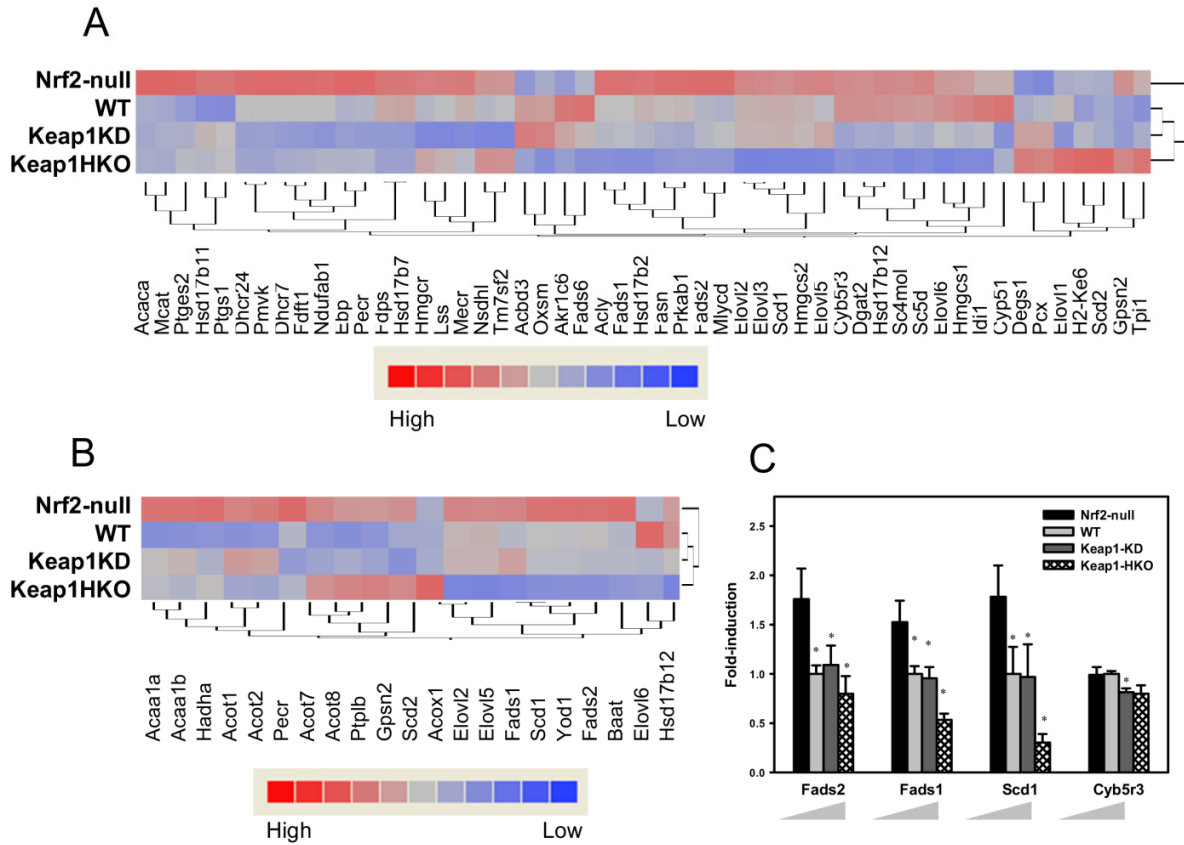
Figure 4.5.Lipid biosynthesis and fatty acid desaturation were suppressed in gene dose-response" model. (A) Hierarchical clustering of genes involved in lipid biosynthesis. Genes were selected according to Gene Ontology category (GO:0008610). (B) Hierarchical clustering of genes involved in fatty acid biosynthesis. Shading is based on the fold-induction of mRNA of each gene compared to the wild-type mice. Genes were selected according to Gene Ontology category (GO:0006633). (C) Messenger RNA expression of genes involved in fatty acid desaturation. Data are presented as Mean ± S.E.M of 3 animals per group. Asterisks (*) indicate statistically significant differences from wild-type mice ($p < 0.05$).

Discussion

Liver is an organ in responsible for multiple vital functions, including protein synthesis (e.g., albumin and clotting factors), glucose homeostasis, and lipid metabolism. Liver also plays the major role in detoxication of environmental chemicals, drugs, and endogenous toxicants. Nrf2 is the central regulator for increasing expression of genes that protect against oxidative and electrophilic stress. Thus, studying the function of Nrf2 in liver is of great importance. The present study used a "gene dose-response" model characterized by graded Nrf2 activation in livers of mice to systematically study the functions of Nrf2 in liver.

Continuous efforts have been made to identify Nrf2 target genes and thus the function of Nrf2. However, varied conclusions have been drawn using different models. For example, by comparing transcription profiles of the prostate of control mice and mice treated with soy isoflavones, which are natural Nrf2 inducers, Nrf2 was shown to be primarily involved in induction of phase-I and phase-II drug metabolism genes (Barve et al., 2008). By comparing transcription profiles of lung tissues in wild-type mice and Clara-cell specific Keap1-KO mice, Nrf2 was shown to be important in induction of antioxidant genes (Blake et al., 2010). Chromatin-immunoprecipitation (ChIP-seq) of Nrf2 binding sites utilizing parallel sequencing of mouse embryonic fibroblasts of Nrf2-null mice and wild-type mice showed that Nrf2 is essential for basal expression of genes involved in cell proliferation (Malhotra et al., 2010). In the same study, by comparing mouse embryonic fibroblasts of wild-type mice and Keap1-null mice, genes induced by Nrf2 were enriched in anti-oxidative stress pathways. A proteomic expression profile of livers of Nrf2-null mice and wild-type mice, found that the most profound changes were

observed in proteins involved in lipid catabolism (Kitteringham et al., 2010). In the present study, by comparing genomic gene transcription profile in livers utilizing a "gene dose-response" model, it was determined that Nrf2-inducible genes are most enriched in protection against oxidative stress, glutathione metabolism, and xenobiotic metabolism. The observations in these various studies may result from different biological samples used for comparison (cell lines versus animal tissues), or different models to modulate Nrf2 activation (pharmacological versus genetic).

With few exceptions, previously identified Nrf2-target genes involved in protection against oxidative stress were identified to be inducible in the "gene dose-reponse" model. GSH is a tripeptide that serves as the predominant cellular thiol resource, and protects against oxidative and electrophilic stress by either directly scavenging reactive oxygen species or conjugating with electrophiles. It is well-documented that Nrf2 activation can increase GSH content in both cell line models (Gao et al., 2010) and animal models (Reisman et al., 2009a). Consistent with the previous study, hepatic GSH concentrations increased in the "gene dose-response" model in a dose-dependent manner (Fig.4.1C). GSH is mainly synthesized in liver, by a two-step reaction. The first and rate-limiting step is catalyzed by glutamate-cysteine ligase (Gcl), which is made up of a catalytic and a modifier subunit (Gclc and Gclm), that combine glutamate and cysteine into a dipeptide. The second step is catalyzed by glutathione synthase (Gss), which adds a glycine to the glutamate-cysteine dipeptide. In addition to de novo biosynthesis, GSH can be regenerated from GSSG by GSH reductase (Gsr). It is known that Gclc, Gss, and Gsr are Nrf2 target genes (Chan et al., 2001; Li et al., 2009), and the present study also shows that these genes were induced by Nrf2 in the "gene dose-

response" model (Fig.3A). Once hydrogen peroxide is formed, it can be detoxified through peroxiredoxin (Prdx), or reduced by GSH through GSH peroxidase (Gpx). In the present study, Prdx6, Gpx2, and Gpx4 were increased with Nrf2 activation (Fig.3B). Similarly, induction of Gpx2 and Prdx6 are reported to be induced by Nrf2 in lung (Blake et al., 2010), and inorganic arsenic activated Nrf2 and increased Gpx4 expression in mouse embryonic stem cells (Chan et al., 2001). Failure to scavenge reactive oxygen species leads to oxidation of proteins and abnormal enzyme activity. Oxidized thiol groups in proteins can be reduced by glutaredoxin (Glrx) and thioredoxin. Oxidized thioredoxin can be regenerated by thioredoxin reductase (Txnrd), and oxidized peroxireduction can be regenerated by sulfiredoxin (Srxn). In the present study, Glrx1, Glrx5, Srxn1, and Txnrd1 were induced with Nrf2 activation, whereas only mRNA of Srxn1 and Txnrd1 were decreased in the absence of Nrf2 (Fig.4.3C).

Bilirubin is another endogenous antioxidant, and has been shown to efficiently scavenge peroxyl radicals (Stocker et al., 1987). Heme degradation generates biliverdin, and bilverdin reductase (Blvrb) converts the pro-oxidant biliverdin to the antioxidant bilirubin. Ferrochelatase (Fech) catalyzes the final step of heme biosynthesis. Both Blvrb and Fech are induced in the "gene dose-response model" (Fig.4.3D), suggesting a role for Nrf2 in bilirubin metabolism. Ferritin is an iron-sequestering protein that prevents uncontrolled surges in the free intracellular concentration of ferric iron (Goven et al., 2010). The reduction of ferric ion by superoxide can generate reactive hydroxyl radicals via the Fenton reaction. Ferritin is composed of ferritin heavy chains (Fth) and ferritin light chains (Ftl). Fth1, Ftl1, and Ftl2 are induced by Nrf2 (Fig.4.4), indicating an important role of Nrf2 in ferric ion scavenging.

The central role of Nrf2 in inducing genes encoding enzymes that directly synthesize GSH and scavenge oxidative stress is well recognized, however, its role in promoting NADPH production has received less attention. NADPH serves as the major reducing resource in the body, and many oxido-reduction reactions, including reducing oxidized GSH and thioredoxin, are performed by oxidizing NADPH into $NADP^+$. Most of the cellular NADPH is generated by the pentose phosphate pathway, and small amounts of NADPH are generated by malic enzyme. In an earlier study, microarray analysis comparing intestinal gene expression profile between control mice and mice treated with sulforaphane identified glucose 6-phosphate dehydrogenase (G6pd), 6-phosphogluconate dehydrogenase (Pgd), and malic enzyme (Me1) as Nrf2 target genes, and linked NADPH production to the Nrf2 signal pathway (Kirby et al., 2005). The effect of Nrf2 on these NADPH generating enzymes was later confirmed in mouse lung (Goven et al., 2010) and liver (Reisman et al., 2009e). Consistent with these observations, Pgd and Me1 were induced in mouse liver with Nrf2 activation in the present study. More importantly, the present study shows that the majority of genes encoding enzymes involved in the pentose phosphate pathway are induced by Nrf2. The induction of the mRNA of multiple genes, including Aldoa (aldolase A, fructose-bisphosphate), Taldo1 (transaldolase 1), Tkt (transketolase), Prps1 (phosphoribosyl pyrophosphate synthetase 1), and Dera (putative deoxyribose phosphate aldolase) strongly correlated with Nrf2 activation in the "gene dose-response" model (Fig.4A), indicating these genes are novel Nrf2 target genes. To further confirm the role of Nrf2 in promoting NADPH production, hepatic NADPH concentrations were quantified in the "gene dose-response" model. Nrf2-null mice have less, whereas Keap1-HKO mice have

more hepatic NADPH than wild-type mice (Fig.4.4C). Higher NADPH concentrations in the Keap1-HKO mouse increase the availability of the cellular reducing resource. In contrast, lower NADPH concentrations render Nrf2-null mice less capable of reducing oxidative stress.

In contrast to the role of Nrf2 in reducing oxidative stress, conflicting data have been reported on the role of Nrf2 in lipid metabolism. One study reported that pharmacological activation of Nrf2 by CDDO-Im effectively prevented high-fat diet-induced increases in body weight, adipose mass, and hepatic lipid accumulation in wild-type mice but not in Nrf2-disrupted mice, indicating that the Nrf2 pathway is a novel target for the prevention of obesity (Shin et al., 2009). In contrast, another study showed that Nrf2-null mice have lower adipose tissue mass, greater formation of small adipocytes, and protects against weight gain and obesity by a high fat diet (Pi et al., 2010), indicating that intact Nrf2 signaling facilitates obesity. Proteomic analysis comparing livers of wild-type mice and Nrf2-null mice showed that the majority of proteins up-regulated in Nrf2-null mice are primarily involved in lipid metabolism with particular respect to lipogenesis (Kitteringham et al., 2010). Consistent with this, the present study shows that most genes involved in lipid biosynthesis were induced in Nrf2-null mice, and suppressed in Nrf2 activated mice, suggesting that Nrf2 negatively regulates lipogenesis (Fig. 4.5A). In addition, the mRNA expression of most genes involved in fatty acid synthesis and desaturation are much higher in Nrf2-null mice than the other 3 genotypes of mice, indicating that Nrf2 strongly suppresses the basal level of fatty acid synthesis and desaturation. It should be noted that NADPH, the major reducing power in the body, is used to reduce oxidative stress, and also provides the

reducing equivalents for biosynthetic reactions, including lipid synthesis and fatty acid desaturation (Kuhajda et al., 1994; Shimomura et al., 1998). Specifically, expression of Fasn (fatty acid synthase) and Scd1 (stearoyl-CoA desaturase), which encode enzymes that use NADPH as the cofactor (Ntambi et al., 1988; Kuhajda et al., 1994), are suppressed by Nrf2 in a dose-dependent manner. Thus, Nrf2 regulation favors the use of NADPH to reduce oxidative stress rather than the biosynthesis of lipids (Fig.4.6).

In conclusion, the present study shows that Nrf2 induces expression of genes involved in antioxidant defense as well as NADPH generation. In addition, the absence of Nrf2 results in decreased expression of genes involved in lipid synthesis and fatty acid desaturation. Thus, Nrf2 activation increases the availability of NADPH for reducing oxidative stress decrease NADPH consumption for lipid biosynthesis.
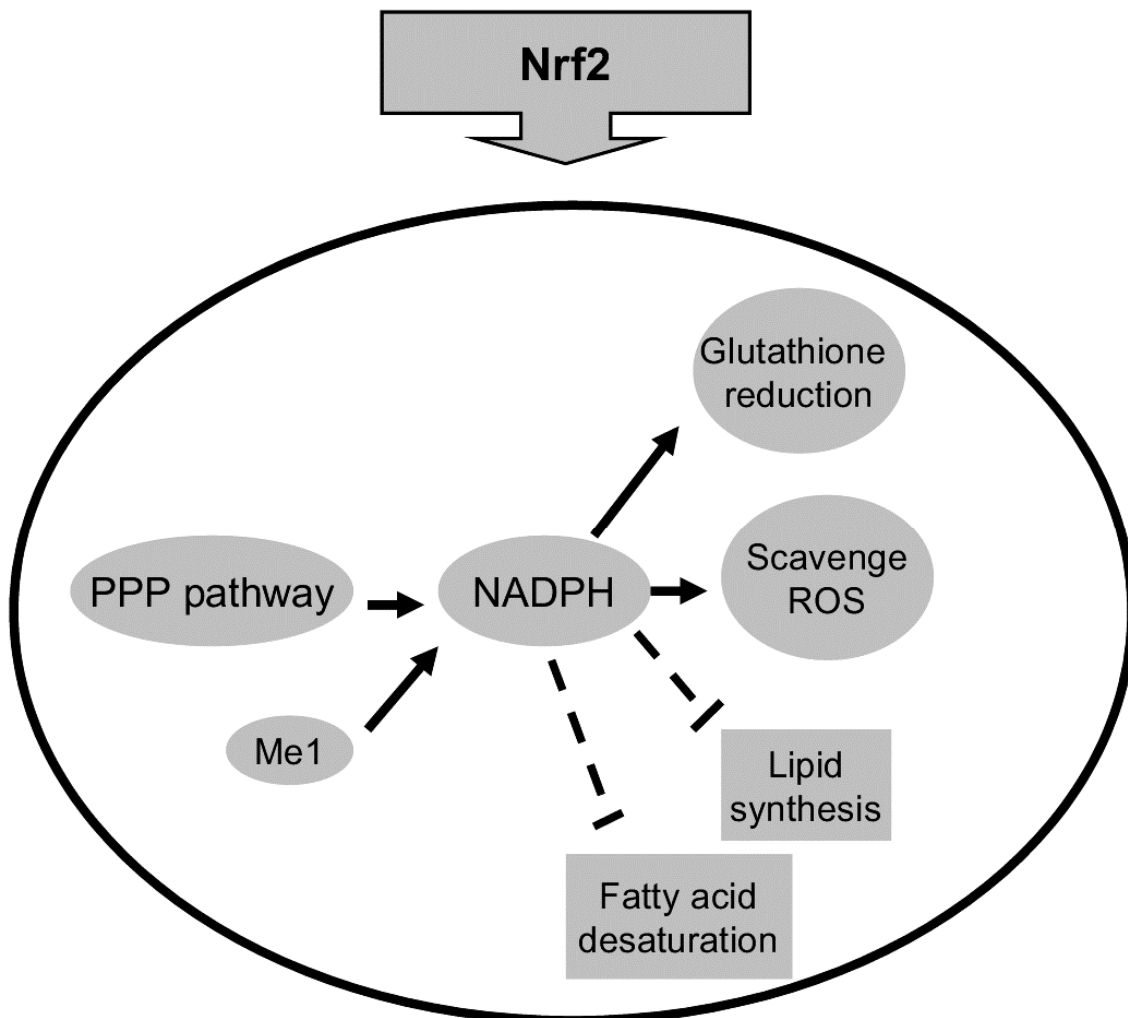
Figure 4.6. Proposed regulatory model for the role of Nrf2 in NADPH production and consumption. In Nrf2 activated cells, NADPH generation was promoted through pentose phosphate pathway and malic enzyme. Genes involved in antioxidant defense by using NADPH were induced, and genes involved in lipid biosynthesis by using NADPH were suppressed.

Chapter 5 : EFFECT OF GRADED NRF2 ACTIVATION ON PAHSE-I AND –II DRUG

METABOLIZING ENZYMES AND TRANSPORTERS

Abstract

Nuclear factor erythroid 2-related factor 2 (Nrf2) is a transcription factor that induces a battery of cytoprotective genes in response to oxidative/electrophilic stress. Kelch-like ECH associating protein 1 (Keap1) sequesters Nrf2 in the cytosol. The purpose of this study was to investigate the role of Nrf2 in regulating the mRNA of genes encoding drug metabolizing enzymes and xenobiotic transporters. Microarray analysis was performed in livers of Nrf2-null, wild-type, Keap1-knockdown mice with increased Nrf2 activation, and Keap1-hepatocyte knockout mice with maximum Nrf2 activation. In general, Nrf2 did not have a marked effect on uptake transporters, but the mRNAs of organic anion transporting polypeptide 1a1, sodium taurocholate cotransporting polypeptide, and organic anion transporter 2 were decreased with Nrf2 activation. The effect of Nrf2 on cytochrome P450 (Cyp) genes was minimal, with only Cyp2a5, Cyp2c50, Cyp2c54, and Cyp2g1 increased, and Cyp2u1 decreased with enhanced Nrf2 activation. However, Nrf2 increased mRNA of many other phase-I enzymes, such as aldo-keto reductases, carbonyl reductases, and aldehyde dehydrogenase 1. Many genes involved in phase-II drug metabolism were induced by Nrf2, including glutathione *S*-transferases, UDP- glucuronosyltransferases, and UDP-glucuronic acid synthesis enzymes. Efflux transporters, such as multidrug resistance-associated proteins, breast cancer resistant protein, as well as ATP-binding cassette g5 and g8 were induced by Nrf2. In conclusion, Nrf2 markedly alters hepatic mRNA of a large number of drug metabolizing enzymes and xenobiotic transporters, and thus Nrf2 plays a central role in xenobiotic metabolism and detoxification.

Introduction

Nuclear factor erythroid 2-related factor 2 (Nrf2) is a transcription factor that induces a battery of cytoprotective genes in response to oxidative/electrophilic stress. The role of Nrf2 in protecting against oxidative and electrophilic stress has been well established, and the majority of genes involved in antioxidant defense have been identified as Nrf2 target genes in various models. For example, genes that are involved in direct reduction of reactive oxygen species (ROS), including superoxide dismutase, catalase, and glutathione peroxidases are induced by Nrf2 (Kensler et al., 2007). Genes involved in reduction of oxidized proteins, such as thioredoxin-1, thioredoxin reductase-1, and sulfuredoxin, are also Nrf2-target genes (Wu et al., 2011a). Genes encoding enzymes that synthesize glutathione (GSH), the most abundant cellular thiol resource, namely γ-glutamate-cysteine ligase catalyze subunit (Gclc) and the modifier subunit (Gclm), as well as glutathione synthase (Gss), are known to be Nrf2 target genes. In addition, genes involved in generation of NADPH, the co-substrate to reduce oxidized GSH, such as glucose-6-phosphate dehydrogenase (G6pd) and malic enzyme (Me1), are induced upon Nrf2 activation (Klaassen and Reisman, 2010; Wu et al., 2011a).

There is increasing recognition of the role of Nrf2 in regulating drug metabolizing enzymes as well as uptake and efflux transporters, which alter the kinetics and disposition of xenobiotics (Cheng et al., 2011). For example, Nrf2 has been shown to increase the mRNA of phase-I drug-metabolizing genes, such as NAD(P)H quinone oxidoreductase 1 (Nqo1) and Cyp2a5 (Lamsa et al., 2010), as well as phase-II drug-metabolizing enzymes, such as glutathione *S*-transferase and UDP-glucuronosyltransferase (Kwak et al., 2004). In addition, efflux transporters, such as

Mrp3 and Mrp4, can be induced by Nrf2 (Maher et al., 2007). Nrf2 deficiency results in decreased, whereas Nrf2 activation results in increased elimination of acetaminophen from the liver (Reisman et al., 2009c), and Nrf2 activation increased biliary excretion of sulfobromophthalein by inducing glutathione-*S*-transferase activity (Reisman et al., 2009d).

Liver is the primary organ in the metabolism and detoxification of drugs and environmental toxicants. Whereas Nrf2 is known to regulate a few drug metabolizing enzymes and xenobiotic transporters, there has not been a systematic study to determine the role of Nrf2 in regulating all drug metabolizing enzymes and xenobiotic transporters in liver. In the present study, a "gene dose-response" model with graded hepatic Nrf2 activation was generated by using Nrf2-null, wild-type, Keap1-knockdown (Keap1-KD) mice with enhanced Nrf2 activation in all tissues, and Keap1-hepatocyte knockout (Keap1-HKO) mice with maximum Nrf2 activation in liver. Microarray analyses of livers of the "gene dose-response" model were performed to obtain genomic gene expression profiles to determine the role of Nrf2 in regulating each individual drug metabolizing enzyme and xenobiotic transporter.

Results

Uptake transporters

Maximum activation of Nrf2 in Keap1-HKO mice resulted in a marked decrease in mRNA of organic anion-transporting polypeptide 1 (Oatp1a1) and organic anion transporter 2 (Oat2), and a slight decrease in the mRNA of sodium taurocholate cotransporting polypeptide (Ntcp) (Fig. 5.1). The mRNA of other uptake transporters,

namely Oatp1a4, Oatp1b2, organic cation transporter 1 (Oct1), and organic

cation/carnitine transporter 2 (Octn2) were not changed with graded Nrf2 activation.

Cytochrome P450 phase-I drug-metabolizing enzymes

Cyp1, Cyp2, and Cyp3 gene families are the major cytochrome P450 enzymes

that catalyze phase-I drug metabolism in humans. Compared to wild-type mice, mRNA

of Cyp2a5 was 76% lower in Nrf2-null mice, 139% higher in Keap1-KD mice, and 969%

higher in Keap1-HKO mice (Fig. 5.2). The mRNA of Cyp2c50 and Cyp2c54 in Nrf2-null

mice was 45 and 65% lower than in wild-type mice, respectively, but in Keap1-KD and

Keap1-HKO mice the mRNA of Cyp2c50 and Cyp2c54 tended to be higher than in wild-

type mice, although this was not statistically significant. Compared to wild-type mice, the

mRNA of Cyp2g1 was 36% lower in Nrf2-null mice, moderately higher with a 91%

increase in Keap1-KD mice, and markedly higher with a 850% increase in Keap1-HKO

mice. In contrast, Cyp2u1 mRNA decreased with increased Nrf2 activation. More

specifically, mRNA of Cyp2u1 was 81% higher in Nrf2-null mice and 48% lower in

Keap1-HKO mice. The mRNA of the other 22 genes encoding cytochrome P450

enzymes of the 1-4 families, including Cyp1a2, Cyp2b10, Cyp2c29, Cyp3a11, and

Cyp3a13, were not altered with various expression of Nrf2.
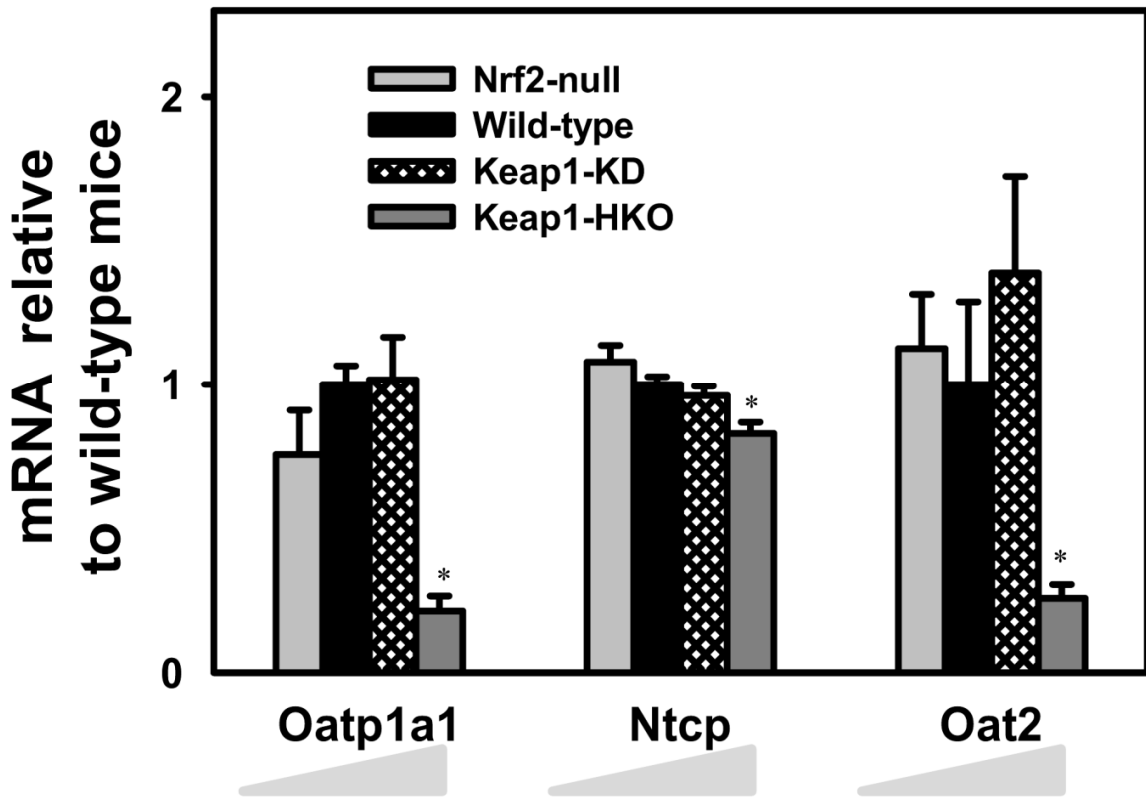
Figure 5.1. Messenger RNA expression of uptake transporters in a "gene dose-response" model. Data of Nrf2-null, Keap1-KD, and Keap1-HKO mice are normalized by the value of wild-type mice and presented as Mean ± S.E.M. Asterisks (*) indicate statistically significant differences from wild-type mice (p < 0.05).
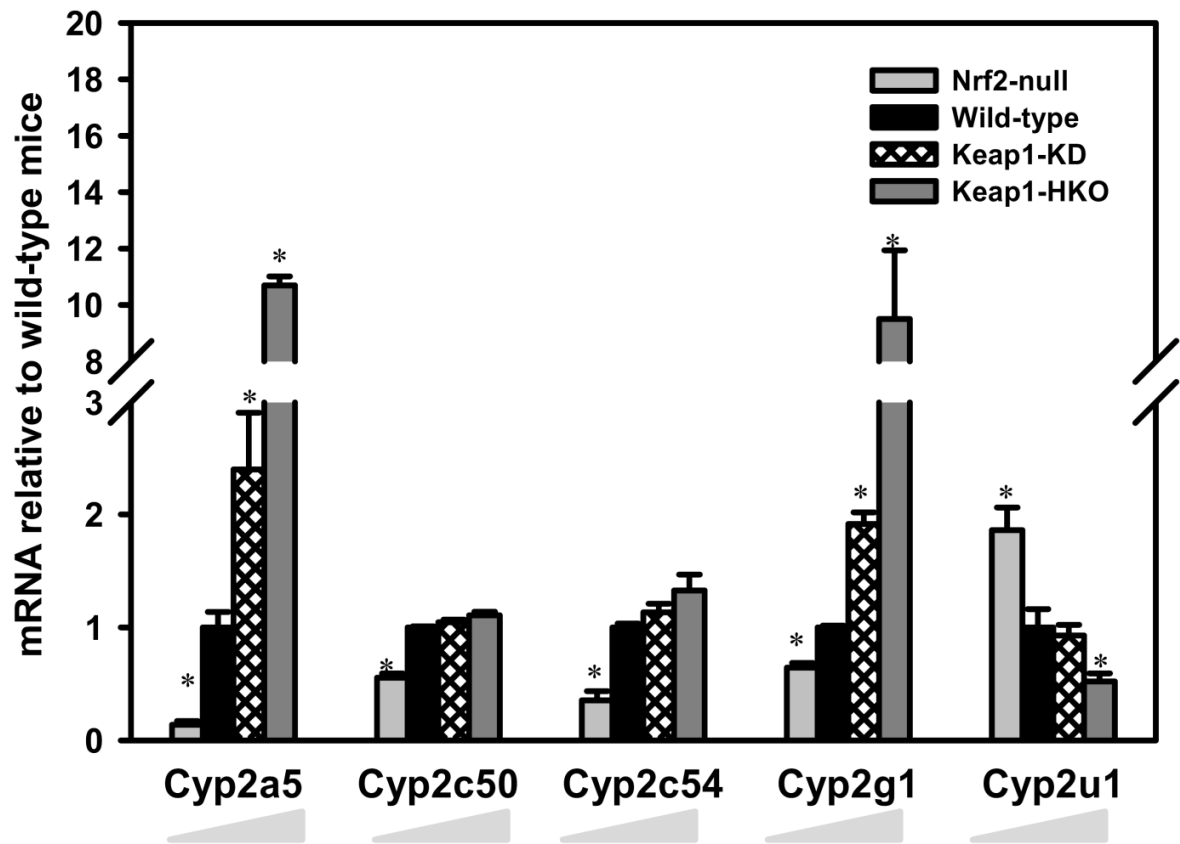
Figure 5.2. Messenger RNA expression of Cytochrome P450 phase-I drug metabolism enzymes in a "gene dose-response" model. Data of Nrf2-null, Keap1-KD, and Keap1-HKO mice are normalized by the value of wild-type mice and presented as Mean ± S.E.M. Asterisks (*) indicate statistically significant differences from wild-type mice (p < 0.05).

Non-p450 phase-I drug-metabolizing enzymes

Aldo-keto reductases (gene name: Akr) catalyze NADPH-dependent reduction of endogenous and xenobiotic substrates. Figure 5.3 illustrates the mRNA expression of the aldo-keto reductases that were significantly increased in the "gene dose-response" model. Compared to wild-type mice, mRNA of Akr1a4 was 29% lower in Nrf2-null mice, 14% higher in Keap1-KD mice, and 43% higher in Keap1-HKO mice. Messenger RNA of Akr1c13 was 22% lower in Nrf2-null mice and 39% higher in Keap1-HKO mice. Akr1b3 and Akr1c19 mRNA were increased 75 and 142% in Keap1-HKO mice over wild-type mice, respectively. The mRNA of Akr7a5 tended to be lower in Nrf2-null mice, higher in Keap1-KD mice, and highest in Keap1-HKO mice, but these alterations were not statistically significant. Other genes in the Akr gene family, namely Akr1c6, Akr1c12, Akr1c14, Akr1d1, and Akr1e1, were not altered with graded Nrf2 activation.

Carbonyl reductase 1 (Cbr1) was induced in Keap1-KD and Keap1-HKO mice 76 and 1,110%, respectively. Similarly, Cbr3 was induced 430% in Keap1-KD mice and 1318-fold in Keap1-HKO mice (Fig. 5.4A). Cbr4 mRNA was not changed with graded Nrf2 activation. Carboxylesterase 1 (Ces1) and Ces2 mRNAs were lower in Nrf2-null mice, higher in Keap1-KD mice (71 and 61% higher, respectively), and highest in Keap1-HKO mice (216 and 219% higher, respectively). Although Ces5 mRNA tended to be lower in Nrf2-null mice, higher in Keap1-KD mice, and highest in Keap1-HKO mice, these changes were not statistically significant (Fig. 5.4B). Ces3 and Ces6 mRNA were not changed with graded Nrf2 activation.

Of the 13 mRNA of aldehyde dehydrogenases (Aldh1a1, Aldh1a7, Aldh1b1, Aldh1l1, Aldh2, Aldh3a2, Aldh5a1, Aldh6a1, Aldh7a1, Aldh8a1, Aldh9a1, and Aldh16a1) detected in the microarray, only Aldh1a1 mRNA was altered in the "gene dose-response" model, with Nrf2-null lower and Keap1-HKO higher than wild-type mice. The mRNA of aldehyde oxidase (gene name: Aox1) was 85% lower in Nrf2-null mice, and 63% higher in Keap1-KD mice, and 191% higher in Keap1-HKO mice (Fig. 5.4C). Compared to wild-type mice, mRNA of epoxide hydrolase 1 (Ephx1) was 64% lower in Nrf2-null mice, 73% higher in Keap1-KD mice, and 218% higher in Keap1-HKO mice than wild-type mice. The mRNA of Ephx2 was not changed with graded Nrf2 activation. The mRNA of Nqo1 was 52% lower in Nrf2-null mice, 335% higher in Keap1-KD mice, and 3860% higher in Keap1-HKO mice than wild-type mice. The mRNA of Nqo2 was not changed with graded Nrf2 activation. The mRNA of Fmo1 and Xdh was slightly increased in Keap1-HKO mice over that in wild-type mice (Fig. 5.4D), whereas the mRNA of Fmo5 was not altered with graded Nrf2 activation.

Figure 5.3. Messenger RNA expression of aldo-keto reductase in a "gene dose-response" model. Data of Nrf2-null, Keap1-KD, and Keap1-HKO mice are normalized by the value of wild-type mice and presented as Mean ± S.E.M. Asterisks (*) indicate statistically significant differences from wild-type mice ($p < 0.05$).
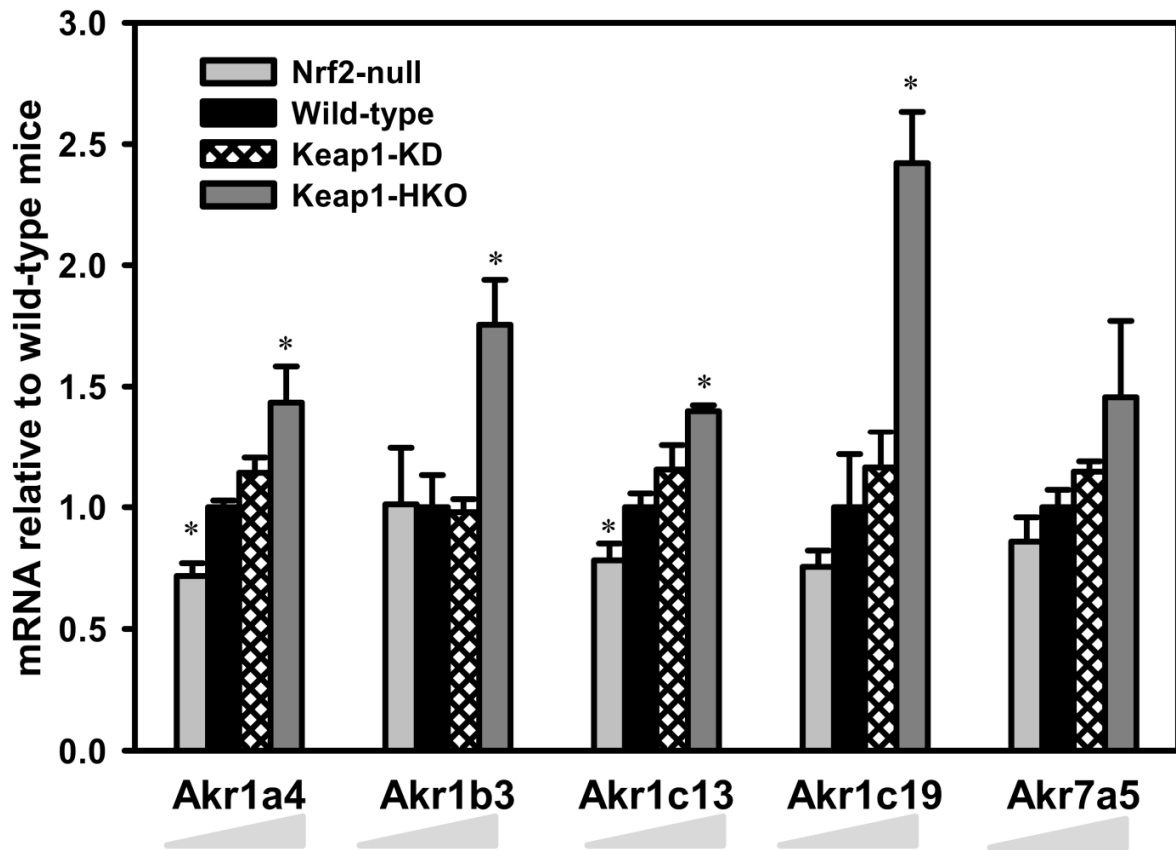
Figure 5.4. Messenger RNA expression of (A) Carbonyl reductase; (B) Carboxylesterase; (C) Aldehyde dehydrogenase and aldehyde oxidase; (D) Other non-P450 phase-I drug metabolism enzymes in "gene dose-response" model. Data of Nrf2-null, Keap1-KD, and Keap1-HKO mice are normalized by the value of wild-type mice and presented as Mean ± S.E.M. Asterisks (*) indicate statistically significant differences from wild-type mice (p < 0.05).
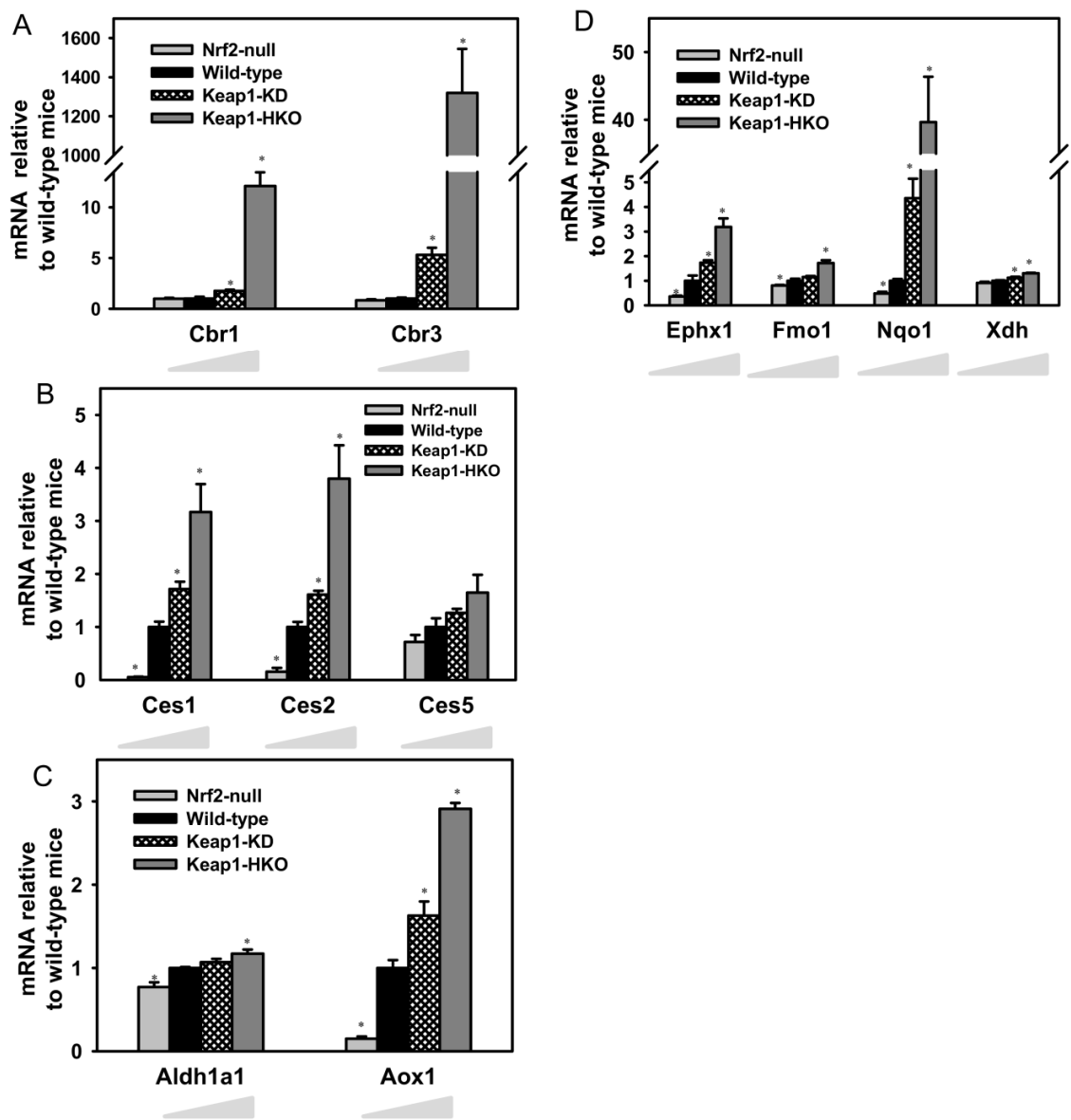
Phase-II drug metabolizing enzymes and transporters

Of the 25 mouse glutathione *S*-transferases (Gst), 18 Gsts were detected in the microarray, and 11 of them were decreased in the absence of Nrf2, and/or induced with Nrf2 activation (Fig. 5.5A). The most marked changes in Nrf2-null mice were the 87% decrease in Gsta2, 76% decrease in Gstm1, and 81% decrease in Gstm3. In comparison to wild-type mice, the most marked inductions of Gsts were the 890% increase of Gsta2, 3,000% increase of Gstm3, and 820% increase of Gstm4 in Keap1-HKO mice. Graded Nrf2 activation had no effect on the other 7 Gsts, namely Gstk1, Gstm5, Gstm7, Gsto1, Gstt1, Gstt2, Gstz1.

Graded Nrf2 activation had less of an effect on mRNA profile of UDP-glucuronosyltransferases (Ugt). Of the 21 mouse Ugts, 13 Ugts were detected in the microarray, and 6 were lower without Nrf2, and/or increased with Nrf2 activation (Fig. 5.5B). The most marked changes in the Ugts in Nrf2-null mice were the 80% lower expression of Ugt2b35, 51% lower Ugt2b36, and 55% lower Ugt2b5 than in the wild-type mice. The most marked increase was 87% of Ugt2b35 in Keap1-HKO mice. UDP-glucose pyrophosphorylase 2 (Ugp2) and UDP-glucose dehydrogenase (Ugdh) are the two enzymes that synthesize UDP-glucuronic acid from glucose. Although Ugp2 mRNA tended to be lower in Nrf2-null mice, higher in Keap1-KD mice, and highest in Keap1-HKO mice, the changes were not statistically significant. In contrast, Ugdh mRNA was significantly lower in Nrf2-null mice (56%), higher in Keap1-KD mice (48%), and highest in Keap1-HKO mice (214%). The solute carrier family 35 member D1 (Slc35d1) is the transporter that imports UDP-glucuronic acid into the endoplasmic reticulum for

Figure 5.5. Messenger RNA expression of genes encoding (A) Glutathione *S*-transferase; (B) UDP- glucuronosyltransferase and related enzymes and transproters; (C) Sulfotransferases in a "gene dose-response" model. Data of Nrf2-null, Keap1-KD, and Keap1-HKO mice are normalized by the value of wild-type mice and presented as Mean ± S.E.M. Asterisks (*) indicate statistically significant differences from wild-type mice (p < 0.05).
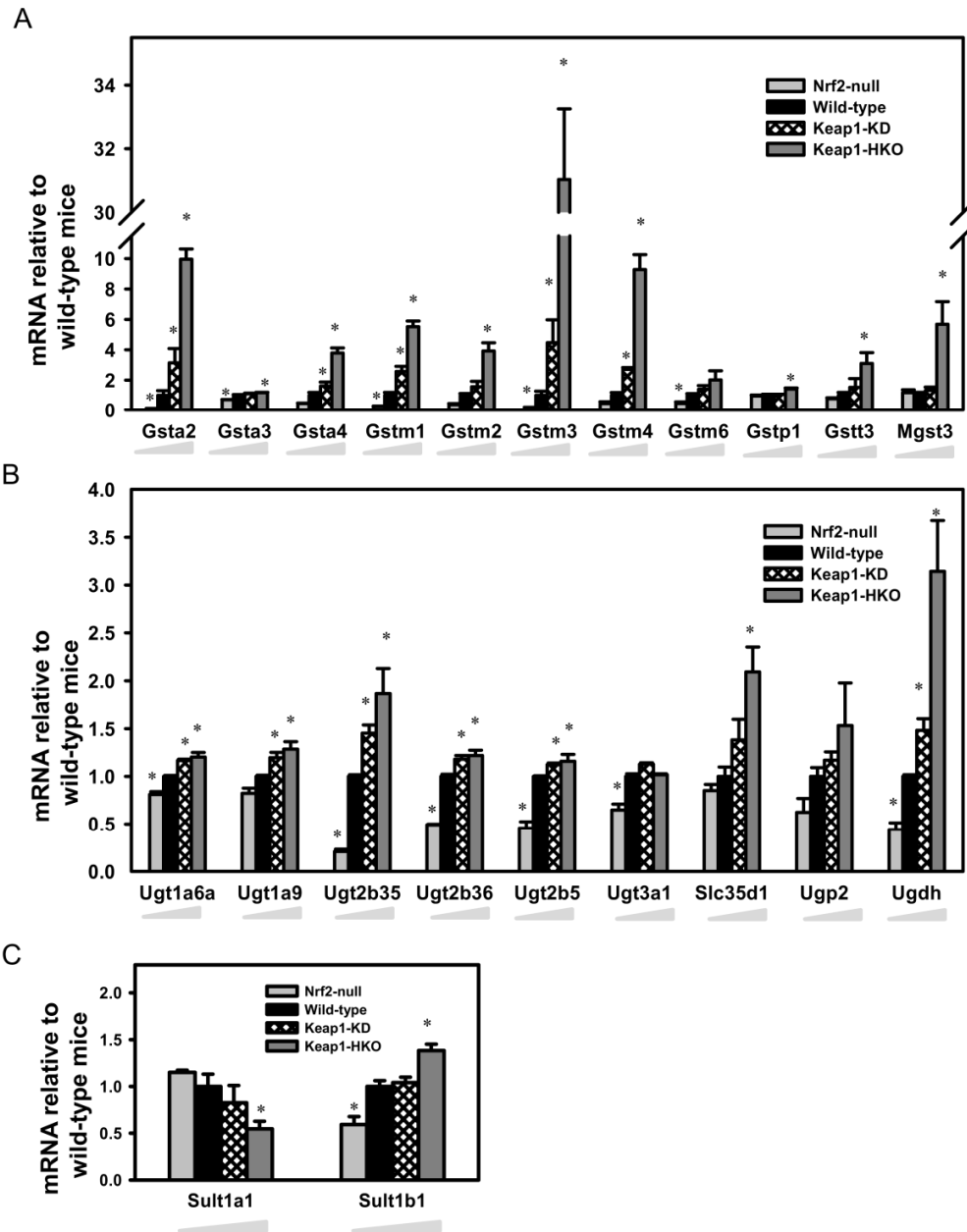
glucuronidation of substrates. Slc35d1 mRNA was 110% higher in Keap1-HKO mice than in wild-type mice. For the sulfotransferases (Sults), Sult1b1 was higher, whereas Sult1a1 was lower with graded Nrf2 activation (Fig. 5.5C). Messenger RNA of Sult1d1 and Sult5a1 did not change with graded Nrf2 activation.

Efflux transporters

For efflux transporters, Nrf2 activation increased 5 out of 6 ATP-binding cassette sub-family C (Mrp, Abcc) members detected by microarray. The most marked changes were the 108- and 21-fold higher Mrp4 and Mrp9 mRNA in Keap1-HKO mice, respectively. The mRNA of Breast cancer resistance protein (Bcrp, Abcg2) was 19% lower in Nrf2-null mice, 40% higher in Keap1-KD mice, and 63% higher in Keap1-HKO mice than in wild-type mice. Similarly, Abcg5 and Abcg8 were constitutively higher with graded Nrf2 activation (Fig. 5.6). Other efflux transporters, namely Mrp6, multiple drug resistant 1a (Mdr1a/Abcb1a), Mdr2, bile salt export pump (Bsep/Abcb11), and multidrug and toxin extrusion 1 (Mate1/Slc47a1) remained unchanged with graded Nrf2 activation.

Expression of chemical-sensing xenobiotic transcription factors

Compared to wild-type mice, constitutive androstane receptor (CAR, Nr1i3) mRNA was 64% lower in Nrf2-null mice, 41% higher in Keap1-KD mice, and 166% higher in Keap1-HKO mice (Fig. 5.7). Other genes encoding transcription factors that are involved in drug metabolism, namely pregnane X receptor (PXR, Nr1i2), liver X receptor (LXR, Nr1h3), farnesoid X activated receptor (FXR, Nr1h4), aryl-hydrocarbon receptor (AhR), and hepatic nuclear factor 4, alpha (HNF4α) remained unchanged with graded Nrf2 activation.
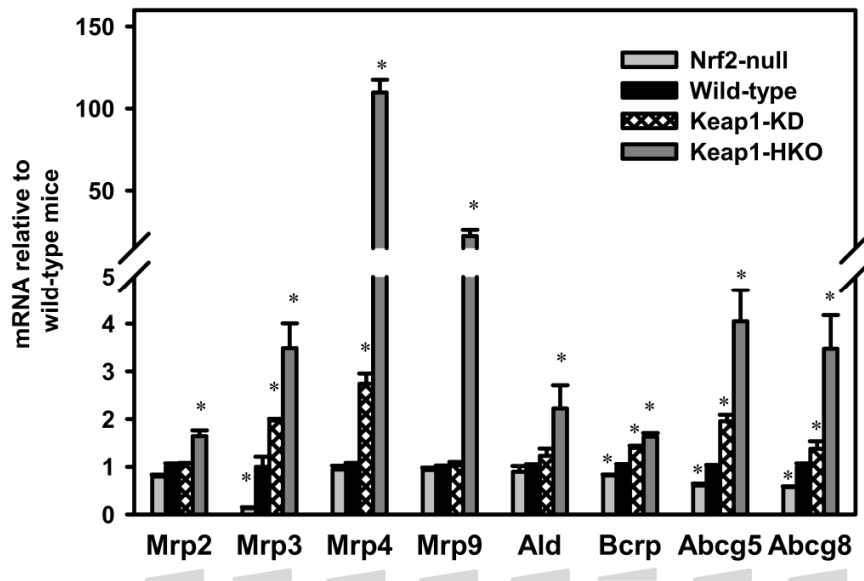
Figure 5.6. Messenger RNA of efflux transporters in a "gene dose-response" model. Data of Nrf2-null, Keap1-KD, and Keap1-HKO mice are normalized by the value of wild-type mice and presented as Mean ± S.E.M. Asterisks (*) indicate statistically significant differences from wild-type mice (p < 0.05).
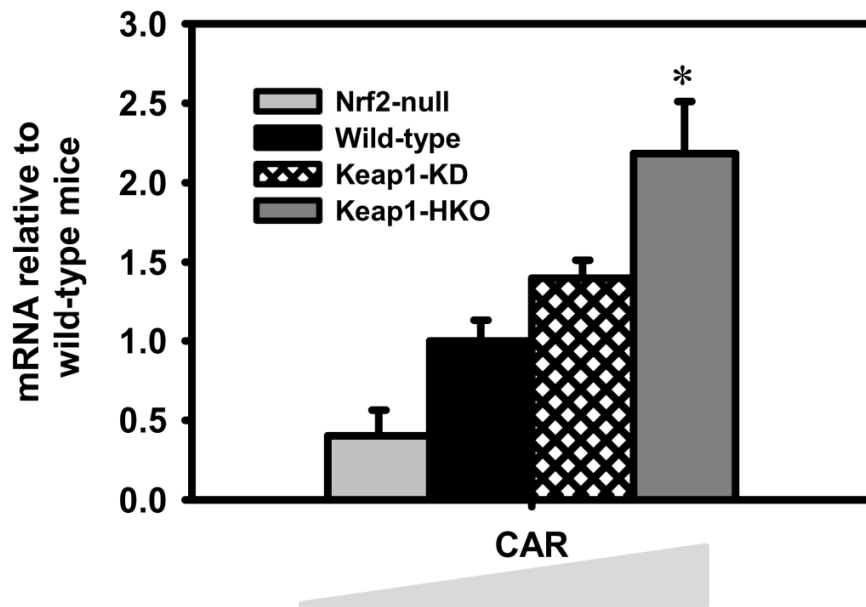
Figure 5.7. Messenger RNA of CAR in "gene dose-response" model. Data of Nrf2-null, Keap1-KD, and Keap1-HKO mice are normalized by the value of wild-type mice and presented as Mean ± S.E.M. Asterisks (*) indicate statistically significant differences from wild-type mice (p < 0.05).

Motif analyses of the 5' region of drug processing genes

The 5' region (up to 10kb upstream of TSS) of drug processing genes that are induced (47 genes), not changed (72 genes), and suppressed (5 genes) with graded Nrf2 activation were searched for the core sequence of ARE (TGACnnnGC) as putative Nrf2 binding sites. In the 5' region up to 2kb upstream from the TSS, 47 AREs were found in 62% of the genes (29 genes) that were induced with Nrf2 activation, 43 AREs were in 47% of the genes (34 genes) that were not changed with Nrf2 activation, and one ARE was found in 20% of the genes (one gene) suppressed with Nrf2 activation (Table 5.1). In the 5' region up to 10kb upstream from the TSS, 163 AREs were found in 94% of the genes (44 genes) that were induced with Nrf2 activation, 201 AREs were in 86% of the genes (62 genes) that were not changed with Nrf2 activation, and 11 AREs were in the five genes suppressed with Nrf2 activation.

Transcription factor-binding site over-representation

The transcription factor binding site enrichment profile was investigated around the transcription start site of the drug processing genes that were induced by Nrf2. As shown in Table 2, the putative binding site of Nrf2 was greatly enriched in genes that were induced with graded Nrf2 activation. In addition, the putative binding sites for other transcription factors, namely C/EBPα, CTCF, NFATC2, Max, NFkB, USF1, Arnt, PPARγ, and Lhx3, were also enriched in genes that were induced with graded Nrf2 activation.

Table 5.1. Summary of total number of AREs in the 5' region of drug processing genes that were induced, not changed, and suppressed in the Nrf2 "gene dose-response" model. The core sequence of ARE (TGACnnnGC) was searched for using Genamics Expression DNA Sequence Analyses Software.

Gene category	Number of genes	Number of AREs up to 2kb upstream of TSS	Number of genes that contain at least one ARE up to 2kb upstream of TSS	Number of AREs up to 10kb upstream of TSS	Number of genes that contain at least one ARE up to 10kb upstream of TSS
Induced	47	47	29 (62%)	163	44 (94%)
No change	72	43	34 (47%)	201	62 (86%)
Suppressed	5	1	1 (20%)	11	5 (100%)

Table 5.2. Putative binding sites of transcription factors in drug processing genes induced by Nrf2 using the oPOSSUM system.

TF	TF Class	Target gene hits	Background gene hits	Target TFBS nucleotide rate[1]	Background TFBS nucleotide rate[2]	Z-score	Fisher score
Nrf2	Zipper-Type	17	4	0.0134	0.003	37.007	5.173
C/EBPα	Zipper-Type	32	18	0.0431	0.024	21.456	3.129
CTCF	Zinc-coordinating	8	1	0.00489	0.001	19.468	3.432
Nfatc2	Ig-fold	32	22	0.0493	0.031	18.409	1.477
Max	Zipper-Type	17	8	0.0129	0.005	17.872	2.309
Nfkb1	Ig-fold	11	2	0.00495	0.001	17.531	3.94
Usf1	Zipper-Type	21	10	0.0169	0.008	16.307	2.76
Arnt	Zipper-Type	24	11	0.0158	0.008	15.637	3.43
PPARγ:: RXRα	Zinc-coordinating	21	8	0.0227	0.014	13.93	3.959
Lhx3	Helix-Turn-Helix	15	9	0.0155	0.009	13.089	1.285

[1]The rate of occurrence of this transcription factor binding sites (TFBS) within the searched regions of the genes induced by Nrf2.

[2]The rate of occurrence of this TFBS within the searched regions of the set of background genes (genes not induced by Nrf2).

Discussion

The present data indicate that Nrf2 plays a critical role in regulating mRNA of numerous phase-I and phase-II drug-metabolizing genes as well as a number of efflux transporters that are important for the hepatic disposition of xenobiotics (Fig. 5.8). Although the role of Nrf2 in regulating some of the drug metabolizing genes were investigated previously through comparing wild-type mice with Nrf2-null or Keap1-HKO mice (Reisman et al., 2009e; Cheng et al., 2011), the present study is among the first reports to make a systematic comparison in four lines of mice with a Nrf2 "gene dose-response". Taking advantage of microarray analysis, which determines global gene transcription profiles, the present study also systematically compared the importance of Nrf2 in basal and inducible expression of each individual gene involved in drug metabolism and disposition. For example, the present study compared fold-induction of glutathione S-transferase (Gst) gene family by Nrf2 and showed that the mRNA of Gsta3 was increased 20%, whereas the mRNA of Gstm3 was increased 3000% in Keap1-HKO mice. In addition, we also report the mRNA of the drug metabolizing genes that are expressed in liver and not changed with absence of Nrf2 or with Nrf2 activation. For example, although the majority of the Gsts are induced by Nrf2, we report seven Gsts (Gstk1, Gstm5, Gstm7, Gsto1, Gstp1, Gstt1, Gstt2) are not changed with graded Nrf2 activation, indicating that Nrf2 is not qualitatively or quantitatively equally important in induction of this family of enzymes. It is also interesting to note that the mRNA of some genes, such as Fmo1, Xdh, and Aldh1a1, decreased slightly (less than 20%) with the absence of Nrf2, and increased slightly (less than 20%) with maximum Nrf2 activation. However, the mRNA of another battery of genes, including Cyp2a5, Ces1, Ces2, and Gstm3, was almost absent with no Nrf2 in the Nrf2-null mice, and markedly

increased (more than 30-fold) with maximum Nrf2 activation in Keap1-HKO mice. This observation suggests that Nrf2 is critical in both the basal and inducible expression of these genes.

In contrast to the minor impact of Nrf2 on mRNA of uptake transporters, Nrf2 has a major effect on the abundance of mRNAs of efflux transporters, with most Mrps, Bcrp, and Abcg5/Abcg8 induced in Nrf2 activated mice (Fig. 5.6). Mrp2 transports GSH and GSH-conjugated xenobiotics from hepatocytes into bile, whereas Mrp3 and Mrp4 transport glucuronated and GSH conjugates, bile acids, and nucleoside analogues from hepatocytes into blood (Klaassen and Lu, 2008; Klaassen and Aleksunes, 2010). Bcrp is an efflux transporter that mediates the biliary excretion of sulfate metabolites as well as glucuronated conjugates (Zamek-Gliszczynski et al., 2006). Abcg5 and Abcg8 function as a heterodimer and transport cholesterol as well as dietary plant sterols into bile (Jansen et al., 2006). Taken together, the increase of multiple Mrp isoforms, Bcrp, and Abcg5/Abcg8 probably results in enhanced elimination of xenobiotics from hepatocytes by increased transport into bile and blood.

Nrf2 has a minor role in regulating cytochrome P450s drug metabolizing genes, with only Cyp2a5 and Cyp2g1 induced with Nrf2 activation. The human ortholog of mouse Cyp2a5 is CYP2A6, which is the major CYP that catalyzes the initial metabolism of nicotine, and is also involved in the metabolism of drugs (e.g. valproic acid and pilocarpine) as well as environmental toxicants (e.g. nitrosamines and aflatoxin B1). The present study as well as previous reports show that both human CYP2A6 (Yokota et al., 2010) and mouse Cyp2a5 (Abu-Bakar et al., 2007) are induced by Nrf2, indicating Nrf2

may play a role in nicotine metabolism. Cyp2g1 metabolizes exogenous compounds including coumarin and acetaminophen *in vitro* (Gu et al., 1998), and there is little information about the regulation of Cyp2g1. The present study shows that Cyp2g1 mRNA was lower in the absence of Nrf2 and markedly higher with Nrf2 activation, indicating the novel role of Nrf2 in activating Cyp2g1 transcription.

In contrast to the minor role of Nrf2 in regulating cytochrome P450s, most isoforms of aldo-keto reductases (AKR), including Akr1a4, Akr1b3, Akr1c13, and Akr1c19, were induced with Nrf2 activation (Fig. 5.3), indicating these genes are novel Nrf2 target genes. Akr1a4 (human ortholog: AKR1A1) plays a key role in ascorbic acid synthesis (Gabbay et al., 2010), reduction of trans-muconaldehyde, a cytotoxic metabolite of benzene (Short et al., 2006), and scavenges free radicals (Singh et al., 2010). The human ortholog of mouse Akr1b3 is AKR1B1, the most extensively studied AKR (Barski et al., 2008), catalyzes the reduction of a wide range of aldehydes and their glutathione conjugates, including lipid peroxidation products 4-hydroxy-trans-2-nonenal (HNE) and acrolein (Vander Jagt et al., 1995). Akr1b3 is induced by Nrf2 *in vitro* (Nishinaka and Yabe-Nishimura, 2005), and human AKR1B10, AKR1C1 and AKR1C2 are induced by Nrf2 in keratinocytes (MacLeod et al., 2009). However, the mRNA of the mouse orthologs of human AKR1B10 (Akr1b10) and AKR1C1 (Akr1c21) remained unchanged with Nrf2 activation (data not shown). This difference may be due to the model used (cell culture versus whole animal), and/or the species (human versus mouse). The AKR7 family catalyzes the reduction of many toxic aldehydes, such as acrolein, methylglyoxal, and especially aflatoxin B1 dialdehyde (Gardner et al., 2004). Rat Akr7a1 is highly inducible (up to 15-fold) in liver in response to antioxidants

(McLellan et al., 1994), whereas mouse Akr7a5 was not induced by antioxidants (Hinshelwood et al., 2002). Similarly, in the present study, the mRNA of Akr7a5 tended to increase with graded Nrf2 activation, but was not statistically significant (Fig. 5.2).

In addition to the aldo-keto reductases, the 2 isoforms of carbonyl reductases (Cbr1, Cbr3) were highly inducible by Nrf2. CBR1 is the major enzyme that reduces doxorubicin (Kassner et al., 2008) in humans, and is involved in the detoxification of reactive aldehydes, such as 4-oxonon-2-enal and its GSH conjugate (Doorn et al., 2004). Human CBR3 catalyzes similar reactions as CBR1 but with narrower substrate specificity, indicating a minor role in xenobiotic metabolism (Pilka et al., 2009). Keap1-knockdown and then Nrf2 activation resulted in dramatic induction of human CBR3 in cancer cell lines (Ebert et al., 2010). In parallel with the human cell line study, the present study shows that Cbr3 mRNA was increased more than 1000 fold in livers of Keap1-HKO mice. In addition, Cbr1 was also induced markedly with Nrf2 activation (Fig. 5.4A), indicating that Nrf2 is an important regulator of Cbr and carbonyl detoxification.

Aldehyde dehydrogenase (Aldh1a1), epoxide hydrolase (Ephx1), and NAD(P)H quinone oxi-reductase (Nqo1) are a group of enzymes that reduce electrophilic substrates into nucleophilic products. Nrf2 is known to be the central regulator that promotes transcription of antioxidant genes. Thus, it is not surprising that Aldh1a1, Eh1, and Nqo1 were induced by Nrf2 in the present study (Fig. 5.4C and Fig.5. 4D) and many other studies (Yates et al., 2006; Alnouti and Klaassen, 2008; Reisman et al., 2009a). Aldehyde oxidase (Aox1) and xanthine dehydrogenase (Xdh) catalyze the generation of reactive oxygen species during oxidation of their substrates, and flavin monooxygenases (Fmo1) catalyze thiobenzamide into an electrophilic intermediate that

causes tissue damage (Nunoya et al., 1995). In the present study, Aox1, Xhd, and Fmo1 are induced by Nrf2 (Fig.5. 4C and Fig.5.4D), indicating that whereas most of the enzymes that Nrf2 increases result in decreasing electrophiles and oxidative stress, a few of its target genes can increase electrophiles and oxidative stress.

Nrf2 has a major impact on inducing numerous phase-II drug metabolism genes, with induction of most isoforms of glutathione *S*-transferases, and multiple isoforms of UDP-glucuronosyltransferases. Ugp2 and Ugdh synthesize UDP-glucuronic acid, the substrate for UDP-glucuronosyltransferases catalyzed conjugation, from glucose in the cytosol. Slc35d1 is the transporter that imports UDP-glucuronic acid into the endoplasmic reticulum (ER) and provides the co-substrates for UGT catalyzed conjugation (Muraoka et al., 2001). Nrf2 increases the mRNA of Ugdh and Slc35d1, and tended to increase the mRNA of Ugp2 (Fig. 5.5B), suggesting that Nrf2 increases the availability of UDP-glucuronic acid in the ER as well as the amount of enzyme for UDP-glucuronic acid conjugation.

In addition to Nrf2, multiple nuclear receptors and other transcription factors, such as AhR, CAR, PXR, PPARα, and FXR, are known to play an important role in regulating the expression of phase-I and -II drug metabolizing enzymes, as well as uptake and efflux transporters (Klaassen and Aleksunes, 2010). In addition, there are known interactions between Nrf2 and other drug metabolism-related nuclear receptors and transcription factors. For example, a number of AhR target genes are induced by the activation of Nrf2 (Yeager et al., 2009). The mRNA of Nrf2 is increased in livers of HNF-4α knockout mice (Lu et al., 2010). The present study indicates that the mRNA of

CAR is almost absent in Nrf2-null mice, and markedly increased in Nrf2 enhanced mice (Fig. 5.6A), indicating that Nrf2 regulates CAR expression at the mRNA level.

Using *in silico* analyses to search for putative ARE binding sites showed that 44 out of 47 genes induced by Nrf2 in the present study have at least one ARE core sequence (5'-TGACnnnGC-3') within 10kb upstream from their transcription start sites. The total number of AREs is larger in the set of genes induced by Nrf2 than in the set of genes where mRNAs are not changed or suppressed with Nrf2 activation (Table 5.1), suggesting that genes are induced in Nrf2 activated mice through direct binding of Nrf2 to promote their transcription. However, it should be noted that 18 out of 47 genes that are induced by Nrf2 do not contain ARE up to 2kb upstream of the TSS, and three genes (Gsta2, Bcrp, and Abcg8) Nrf2 do not contain ARE up to 2kb upstream of the TSS. Thus, more experiments (e.g. ChiP-Seq) are needed to confirm the binding of Nrf2 to these putative AREs, and thus whether these genes are direct Nrf2 target genes. In addition to the enrichment of Nrf2 binding sites in the genes responsive to Nrf2 activation, transcription factor over-representation analyses revealed co-existence of ARE and binding sites for other transcription factors, including C/EBPα, NFkB, Arnt:AhR, and PPARγ:RXRα (Table 5.2), indicating the potential cross-talk between Nrf2 and these transcription-factor signal pathways.

For some of the drug processing genes (example: Nqo1), the mRNA abundance is positively correlated to the enzyme activity (Reisman et al., 2009e). A battery of drug processing genes (example: Cyp2e1) are regulated mainly at post-translational level (Novak and Woodcroft, 2000). However, the mRNA abundance - enzyme activity

correlation of most drug processing genes is unknown. Thus, it is not plausible to extrapolate the protein expression or enzyme activity level by comparing mRNA abundance of the genes. Due to the limitations of antibody specificity and availability of *in vivo* enzyme activity assays, the present study only provides the systemic comparison of mRNA abundance of the drug metabolism genes. Western blot and activity assays should be performed to further study the effect of Nrf2 on protein abundance and activity of a specific drug processing enzyme or transporter.

In conclusion, the present study demonstrates that Nrf2, the key transcription factor in protecting against oxidative and electrophilic stress, is also important in regulating hepatic mRNA of phase-I and -II drug metabolizing enzymes as well as uptake and efflux transporters (Fig. 5.8). Activation of Nrf2 has a minor effect on uptake transporters and P450 phase-I enzymes that activate xenobiotics into toxicants, markedly increased mRNA of other phase-I enzymes and phase-II enzymes that detoxify toxicants, and also increased mRNA of efflux transporters that facilitate the elimination of toxicants.
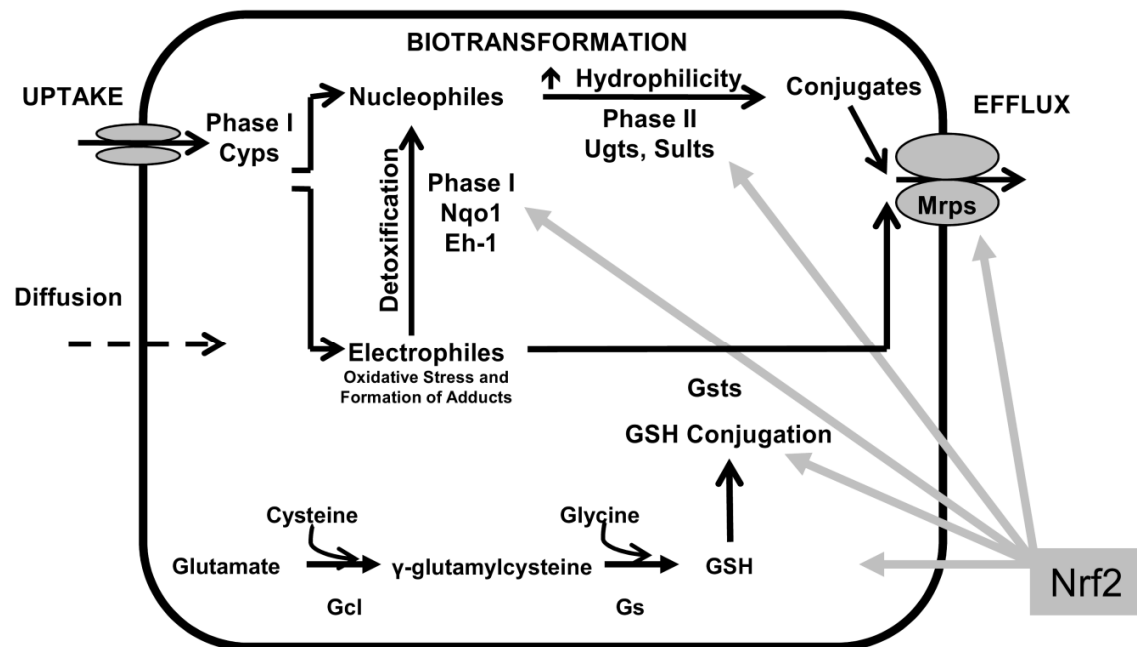
Figure 5.8. Proposed regulatory model for the role of Nrf2 on drug metabolizing genes in liver. Activation of Nrf2 had a minor effect on uptake transporters and P450 phase-I enzymes that activate xenobiotics into toxicants, markedly induces genes encoding other phase-I enzymes and phase-II enzymes that detoxify toxicants, and also induces efflux transporters that facilitate the elimination of toxicants.

Chapter 6 : ROLE OF NRF2 IN PREVENTING ETHANOL-INDUCED OXIDATIVE STRESS AND LIPID ACCUMULATION

Abstract

Oxidative stress and lipid accumulation play important roles in alcohol-induced liver injury. Previous reports showed that, in livers of nuclear factor erythroid 2-related factor 2 (Nrf2)-activated mice, genes involved in antioxidant defense are induced, whereas genes involved in lipid biosynthesis are suppressed. To investigate the role of Nrf2 in ethanol-induced hepatic alterations, Nrf2-null mice, wild-type mice, kelch-like ECH-associated protein 1-knockdown (Keap1-KD) mice with enhanced Nrf2, and Keap1-hepatocyte knockout (Keap1-HKO) mice with maximum Nrf2 activation, were treated with ethanol (5 g/kg, po). Blood and liver samples were collected 6 h thereafter. Ethanol increased alanine aminotransferase and lactate dehydrogenase activities as well as thiobarbituric acid reactive substances in serum of Nrf2-null and wild-type mice, but not in Nrf2-enhanced mice. After ethanol administration, mitochondrial glutathione concentrations decreased markedly in Nrf2-null mice but not in Nrf2-enhanced mice. H_2DCFDA staining of primary hepatocytes isolated from the four genotypes of mice indicate that oxidative stress was higher in Nrf2-null cells, and lower in Nrf2-enhanced cells than in wild-type cells. Ethanol increased serum triglycerides and hepatic free fatty acids in Nrf2-null mice, and these increases were blunted in Nrf2-enhanced mice. In addition, the basal mRNA and nuclear protein levels of sterol regulatory element-binding protein 1(Srebp-1) were decreased with graded Nrf2 activation. Ethanol further induced Srebp-1 mRNA in Nrf2-null mice but not in Nrf2-enhanced mice. In conclusion, Nrf2 activation prevented alcohol-induced oxidative stress and accumulation of free fatty acids in liver by increasing genes involved in antioxidant defense and decreasing genes involved in lipogenesis.

Introduction

Ethanol in fermented drinks is consumed widely across the world, and causes global health problems. Alcohol consumption is related to more than 60 medical conditions, and has been suggested to be responsible for 25% of liver cancer as well as 32% of liver cirrhosis worldwide (Room *et al.*, 2005).

The predominant factor causing ethanol-associated liver damage is the generation of oxidative stress. Liver is the major organ responsible for metabolizing ethanol in the body, mainly through alcohol dehydrogenase in the cytosol, cytochrome P450 2E1 (CYP2E1) in the endoplasmic reticulum, and catalase in peroxisomes (Zakhari, 2006). More specifically, alcohol dehydrogenase serves as the primary pathway to metabolize alcohol in liver, producing acetaldehyde as the major product. Acetaldehyde is highly reactive, and interacts with proteins to form acetaldehyde adducts. In addition, acetaldehyde interacts with endogenous antioxidants (cytosolic and mitochondrial glutathione), induces mitochondrial dysfunction, and sensitizes hepatocytes to oxidative damage (Farfan Labonne *et al.*, 2009). Another enzyme that metabolizes ethanol is CYP2E1. CYP2E1 also oxidizes ethanol to acetaldehyde, and generates reactive oxygen species by transferring electrons to oxygen (Jimenez-Lopez and Cederbaum, 2005). Although catalase reduces hydrogen peroxide into water, the role of catalase in ethanol metabolism is minor (Handler and Thurman, 1990). Thus, an overall consequence of ethanol metabolism in liver is oxidative stress.

Another consequence of ethanol metabolism is lipid accumulation in liver. During ethanol metabolism, large amounts of nicotinamide adenine dinucleotide (NAD+) are reduced into NADH by alcohol dehydrogenase and aldehyde dehydrogenase. The

increased NADH/NAD+ ratio promotes lipid accumulation by stimulating fatty acid synthesis and opposing degradation (Lieber, 2004). In addition, inflammation provoked by oxidative stress promotes the production of proinflammatory cytokine tumor necrosis factor-alpha (TNF-α) in Kupffer cells and hepatocytes, leading to stimulation of collagen synthesis by hepatic stellate cells (Enomoto *et al.*, 2007). Collectively, imbalanced lipid homeostasis, together with generation of oxidative stress, promotes alcohol-induced fatty liver into inflammation, fibrosis, and finally cirrhosis.

Several compounds have been studied to prevent the development of alcoholic liver disease, and the proposed mechanisms of the protective effects of some of these chemicals are focused on ameliorating oxidative stress. For example, *S*-adenosyl-L-methionine (SAMe), a precursor in glutathione biosynthesis, was shown to attenuate alcohol-induced liver injury in both animal models and human studies (Lu and Mato, 2005). The protective effect of poly-enyl-phosphatidylcholine on alcohol-induced toxicity is partially due to inhibition of CYP2E1 (Lieber, 2000). Other direct antioxidants, such as vitamin C and vitamin E, have also been used to treat ethanol-induced liver injury. However, the therapeutic results are not consistent (Yanardag *et al.*, 2007; Chung *et al.*, 2009).

Nuclear factor erythroid 2-related factor 2 (Nrf2) is a transcription factor that induces a battery of cytoprotective genes in response to oxidative/electrophilic insults (Klaassen and Reisman, 2010). Transcription profiling in the Nrf2 "gene dose-response" model by microarray analysis revealed that genes involved in lipid biosynthesis are suppressed with Nrf2 activation in a "gene dose-response" manner (Wu et al., 2011b), indicating that Nrf2 may play a role in preventing lipid accumulation.

The antioxidant and anti-lipogenesis activities of Nrf2 make it a promising target for therapy of alcoholic liver disease. It was reported that loss of Nrf2 results in aggravated steatosis, inflammation, and mortality in Nrf2-null mice exposed to ethanol (Lamle *et al.*, 2008). It is more important to know whether Nrf2 activation protects against ethanol-induced liver toxicity. In the present study, the Nrf2 "gene dose-response" model was used to characterize the role of the Keap1-Nrf2 pathway in liver in maintaining redox as well as lipid homeostasis in response to ethanol administration.

Results

Serum LDH and ALT

By 6h after ethanol administration, ethanol-induced acute hepatotoxicity was indicated by serum lactate dehydrogenase (LDH) and alanine aminotransaminase (ALT). Ethanol increased serum LDH activity in Nrf2-null and wild-type mice, but not in Keap1-KD or Keap1-HKO mice (Fig. 6.1A). After ethanol administration, serum ALT activities were increased in Nrf2-null, wild-type, and Keap1-KD mice, and the increase was similar in Nrf2-null mice but 40% lower in Keap1-KD mice than wild-type mice (Fig. 6.1B). Ethanol did not increase serum ALT activities in Keap1-HKO mice. Histological analysis indicated that livers of wild-type, Nrf2-null, Keap1-KD, and Keap1-HKO mice appeared normal in both control and ethanol-administrated groups (data not shown).
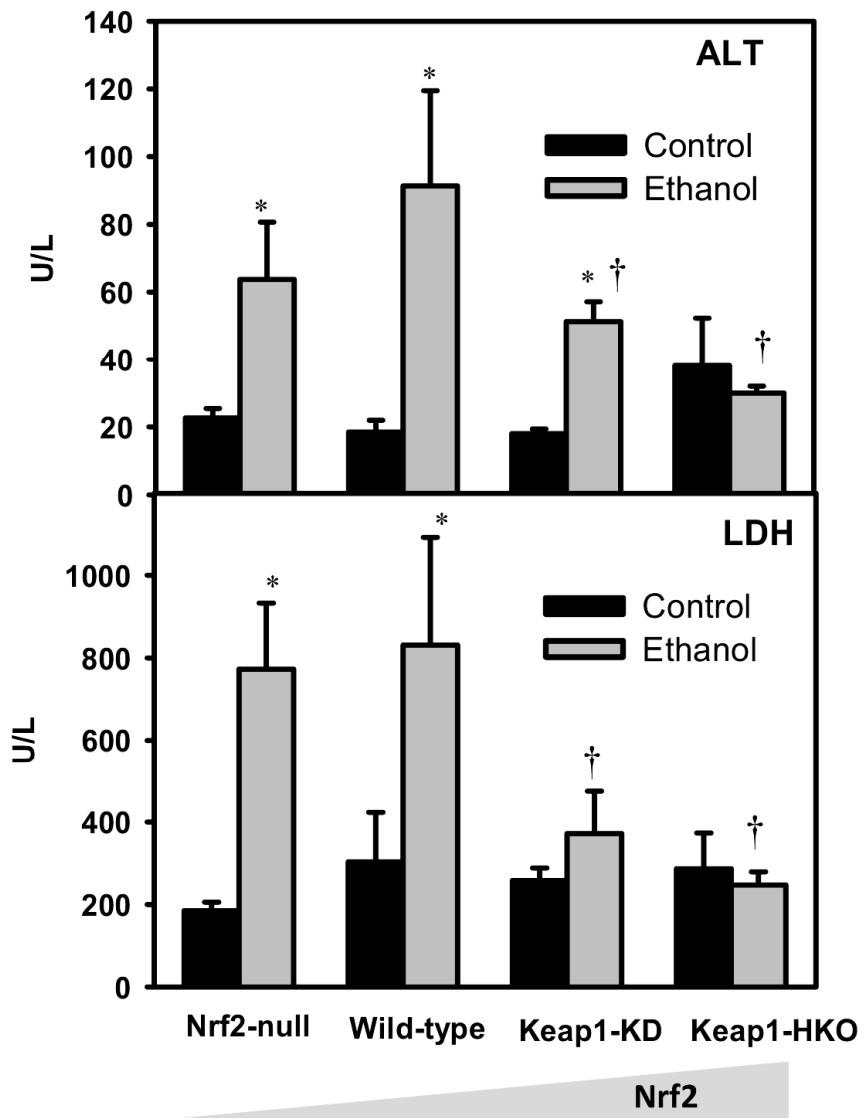
Figure 6.1. Blood biochemistry. Serum lactate dehydrogenase and serum alanine transaminase (ALT) levels in wild-type, Nrf2-null, Keap1-KD and Keap1-HKO mice 6 h after ethanol administration (5 g/kg, p.o.). Units are in International Units/Liter (IU/L) expressed as mean ± S.E.M of 5 mice per group. Asterisks (*) indicate statistically significant differences from control mice of the same genotype ($p < 0.05$). Daggers (†) indicate statistically significant differences from wild-type mice after ethanol administration ($p < 0.05$).

Lipid peroxidation

To determine the effect of ethanol on inducing oxidative stress, and whether Nrf2 activation protects against ethanol-induced oxidative stress, lipid peroxidation products were quantified in serum samples of mice using the TBARS assay. In wild-type mice, TBARS concentrations in the serum increased 65% after ethanol administration. In Nrf2-null mice, the basal TBARS concentration tended to be higher than wild-type mice, and increased after ethanol administration. Ethanol did not have any effect on TBARS concentrations in Keap1-KD and Keap1-HKO mice (Fig. 6.2A).

Cytosolic and mitochondrial GSH concentrations in liver

In an attempt to determine the mechanism of how Keap1-Nrf2 signaling pathway prevents ethanol-induced oxidative stress, cytosolic and mitochondrial GSH concentrations were quantified in livers. Basal cytosolic GSH concentrations were 7% lower in Nrf2-null mice, and 15% higher in Keap1-HKO than wild-type mice. After ethanol administration, GSH concentrations decreased 31% in Nrf2-null mice, 21% in wild-type mice, 11% in Keap1-KD mice, and remained unchanged in Keap1-HKO mice (Fig. 6.2B). Basal mitochondrial GSH concentrations were 12% lower in Nrf2-null mice, and 39% higher in Keap1-HKO mice than in wild-type mice. After ethanol administration, GSH concentrations decreased 52% in Nrf2-null mice, 39% in wild-type mice, unchanged in Keap1-KD mice, and decreased 27% in Keap1-HKO mice (Fig. 6.2C).
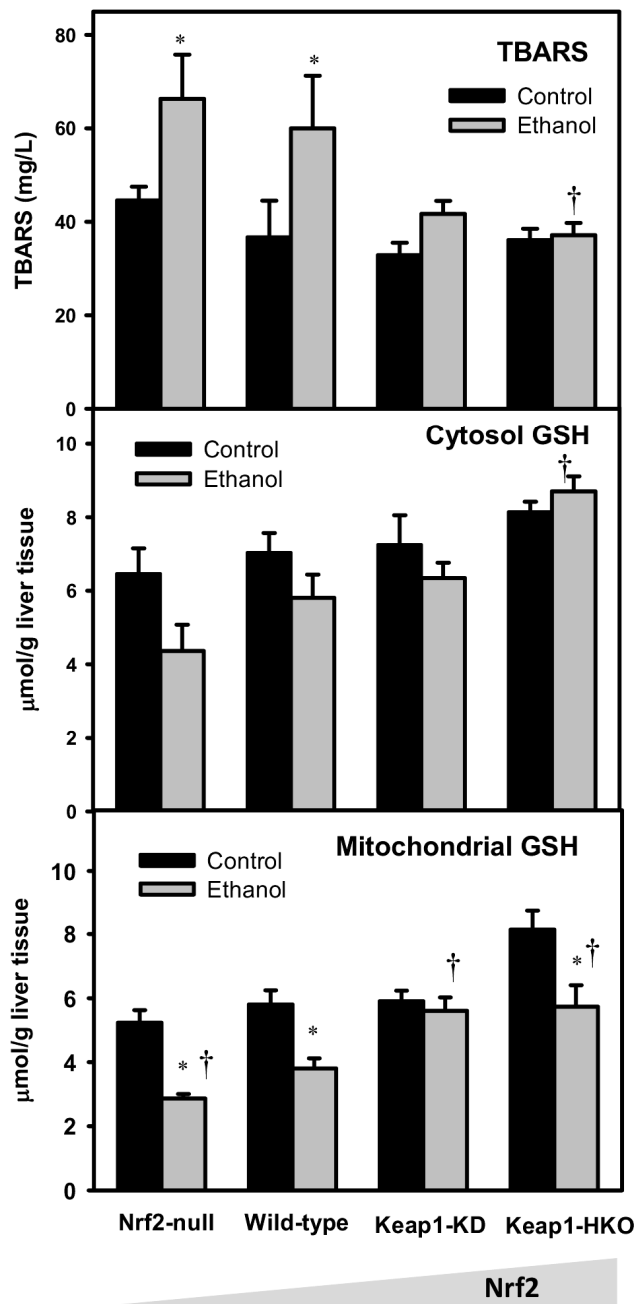
Figure 6.2. Ethanol-induced oxidative stress *in vivo*. Serum thiobarbituric acid reactive substances (TBARS), cytosolic glutathione (GSH) in livers, and mitochondrial GSH in livers of Nrf2-null, wild-type, Keap1-KD, and Keap1-HKO mice 6 h after ethanol administration (5 g/kg, p.o.). Data are expressed as mean ± S.E.M of 5 mice per group. Asterisks (*) indicate statistically significant differences from control mice of the same genotype (p < 0.05). Daggers (†) indicate statistically significant differences from wild-type mice after ethanol administration (p < 0.05).

Gclc and Nqo1 mRNA and protein concentrations in liver

Compared with the wild-type mice, the basal mRNA of Nqo1 was 72% lower in Nrf2-null mice, 120% higher in Keap1-KD mice, and 820% higher in Keap1-HKO mice. Six hrs after ethanol administration, mRNA of Nqo1 decreased in Keap1-HKO mice (Fig. 6.3A). The protein levels of Nqo1 were consistent with the mRNA, which was increased with graded Nrf2 activation in a gene dose-response manner, and decreased after ethanol administration in Keap1-HKO mice (Fig. 6.3B). Compared with the wild-type mice, the basal level of Gclc mRNA was 55% lower in Nrf2-null mice, 28% higher in Keap1-KD mice, and 148% higher in Keap1-HKO mice. Six hours after ethanol administration, mRNA of Gclc decreased in wild-type, Keap1-KD, and Keap1-HKO mice (Fig. 6.3C). Consistent with the mRNA data, Gclc protein was increased with graded Nrf2 activation in a "gene dose-response" manner, and decreased after ethanol administration in wild-type, Keap1-KD, and Keap1-HKO mice (Fig. 6.3D).

Dose-response and time course of ROS generation

To characterize ethanol-induced oxidative stress in vitro, primary hepatocytes from Nrf2-null, wild-type, Keap1-KD, and Keap1-HKO mice were isolated and stained with H_2DCFDA, a general ROS indicator, as described in the Methods. The basal ROS were 83% higher in Nrf2-null cells, and 37 and 44% lower in Keap1-KD and Keap1-HKO cells than wild-type mice, respectively. After the addition of ethanol, ROS increased moderately in wild-type mice, and increased markedly in Nrf2-null mice. In contrast, ROS in Keap1-KD and Keap1-HKO slightly increased at 3 h, and decreased below basal levels at later time points. Ethanol increased ROS in wild-type and Nrf2-null cells
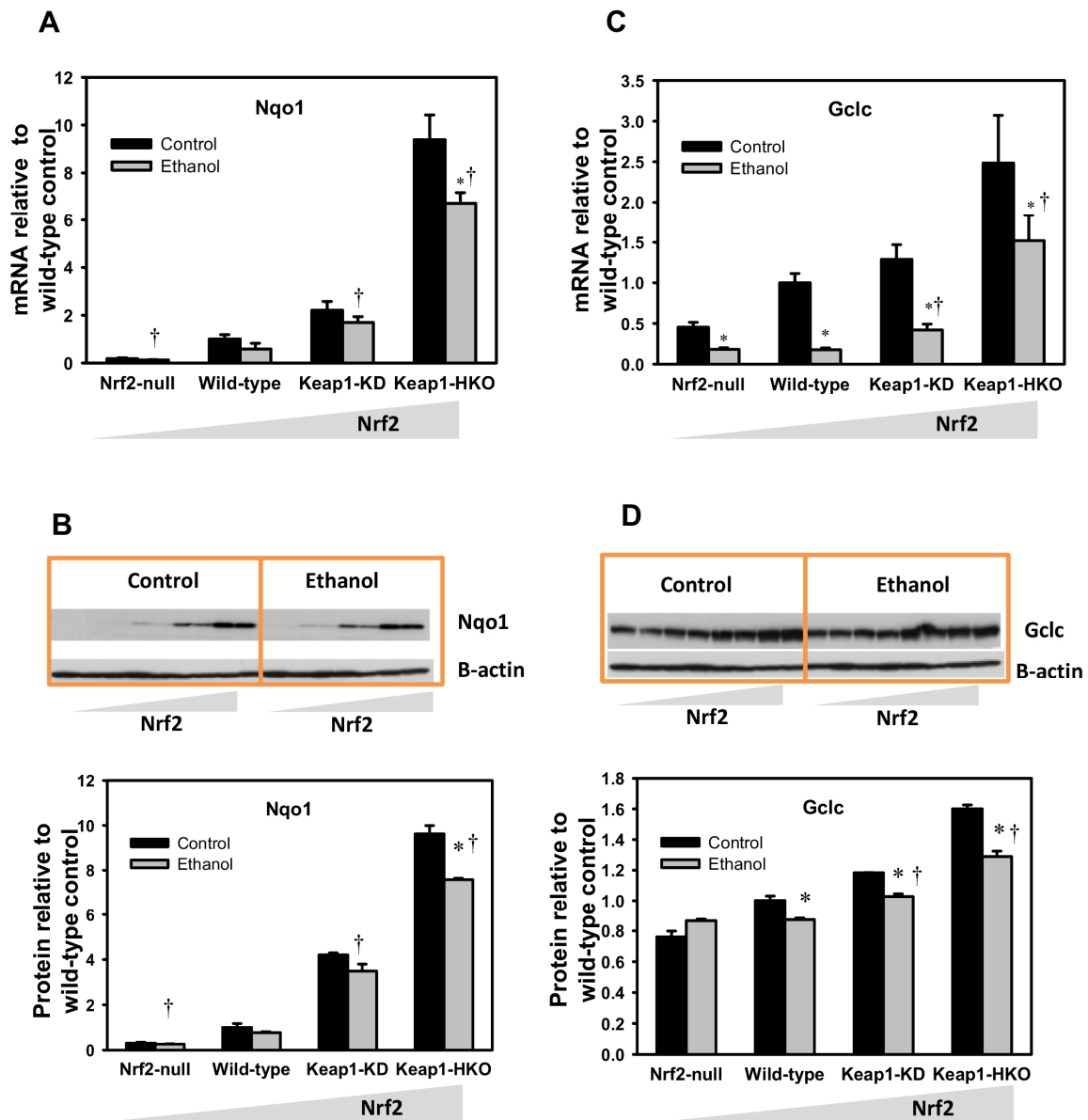
Figure 6.3. Effects of ethanol on the mRNA and protein of prototypical Nrf2-target genes. (A) mRNA of Nqo1, (B) protein of Nqo1, (C) mRNA of Gclc, and (D) protein of Gclc in livers of Nrf2-null, wild-type, Keap1-KD, and Keap1-HKO mice 6 h after ethanol administration (5 g/kg, p.o.). Data are expressed as mean ± S.E.M of 5 animals per group. Asterisks (*) indicate statistically significant differences from control mice of the same genotype (p < 0.05). Daggers (†) indicate statistically significant differences from wild-type mice after ethanol administration (p < 0.05).
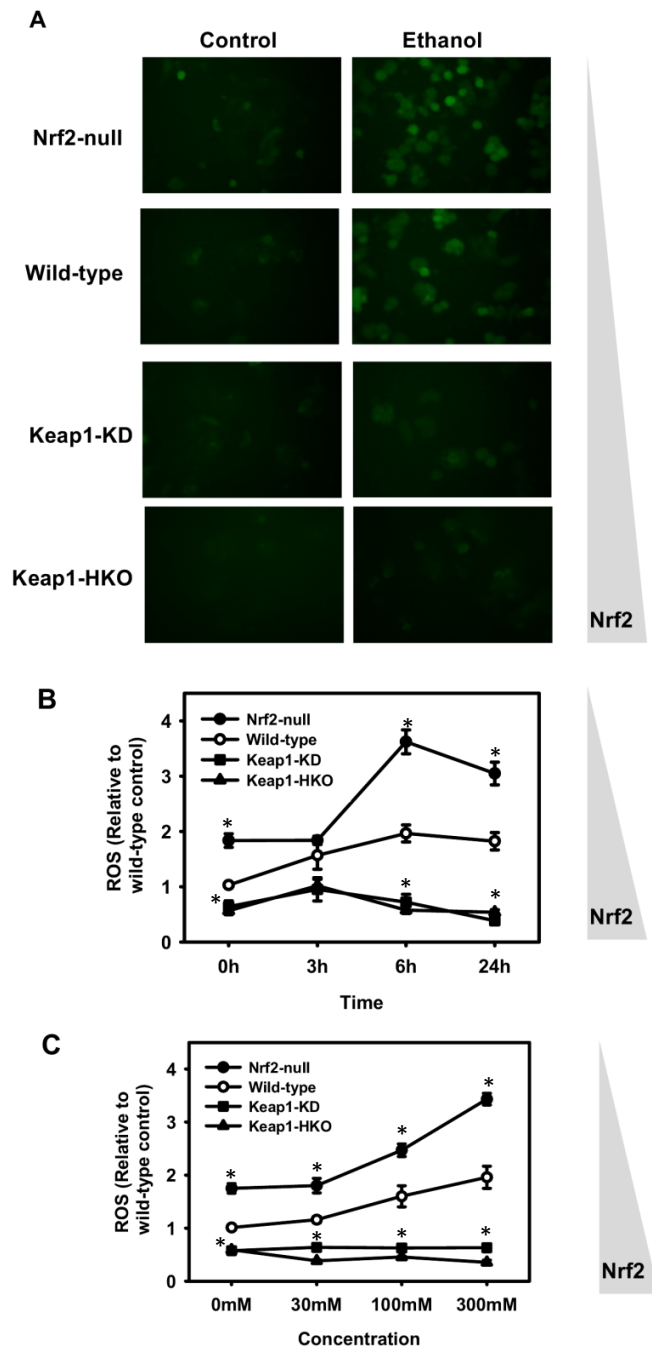
Figure 6.4. Ethanol-induced oxidative stress *in vitro*. (A) DCFDA fluorescence in primary hepatocytes 6 h after ethanol exposure. Primary hepatocytes were isolated and treated with ethanol for 24 h and subjected to live cell imaging. (B) Time-response and (C) dose-response of ROS production after ethanol administration of primary hepatocytes from Nrf2-null, wild-type, Keap1-KD, and Keap1-HKO mice. Data are presented as Mean ± S.E.M. of 3 mice per group in Fig 4B and Fig 4C. Asterisks (*) indicate statistically significant differences from wild-type cells of the same time point ($p < 0.05$).

in a dose-dependent manner. However, ethanol did not increase ROS in Keap1-KD or Keap1-HKO mice even at high concentrations (Fig. 6.4).

Triglyceride and free fatty acid concentrations in serum and liver

To determine the effect of ethanol on increasing lipid accumulation in serum and liver, and whether Nrf2 activation attenuates ethanol-induced lipid accumulation, triglycerides and free fatty acid concentrations were quantified. Ethanol increased triglyceride contents in serum of only in Nrf2-null mice but not in wild-type, Keap1-KD, or Keap1-HKO mice (Fig. 6.5A). In contrast, ethanol increased triglyceride contents livers of in all groups of mice, with no difference among genotypes (Fig. 6.5B). Ethanol also increased free fatty acid contents serum of wild-type and Keapq-KD mice, but not in Nrf2-null or Keap1-HKO mice (Fig. 6.5C). Ethanol After ethanol administration, free fatty acid concentrations in livers were increased markedly in Nrf2-null mice, moderately in wild-type mice, slightly in Keap1-HKO mice, and remained unchanged in Keap1-KD mice (Fig. 6.5D).

Figure 6.5. Ethanol administration induced lipid accumulation. (A) Serum triglyceride, (B) hepatic triglyceride, (C) serum free fatty acid, and (D) hepatic free fatty acid concentrations in Nrf2-null, wild-type, Keap1-KD, and Keap1-HKO mice after ethanol administration (5 g/kg, p.o.). Data are expressed as mean ± S.E.M of 5 mice per group. Asterisks (*) indicate statistically significant differences from control mice of the same genotype (p < 0.05). Daggers (†) indicated statistically significant differences from wild-type mice after ethanol administration.

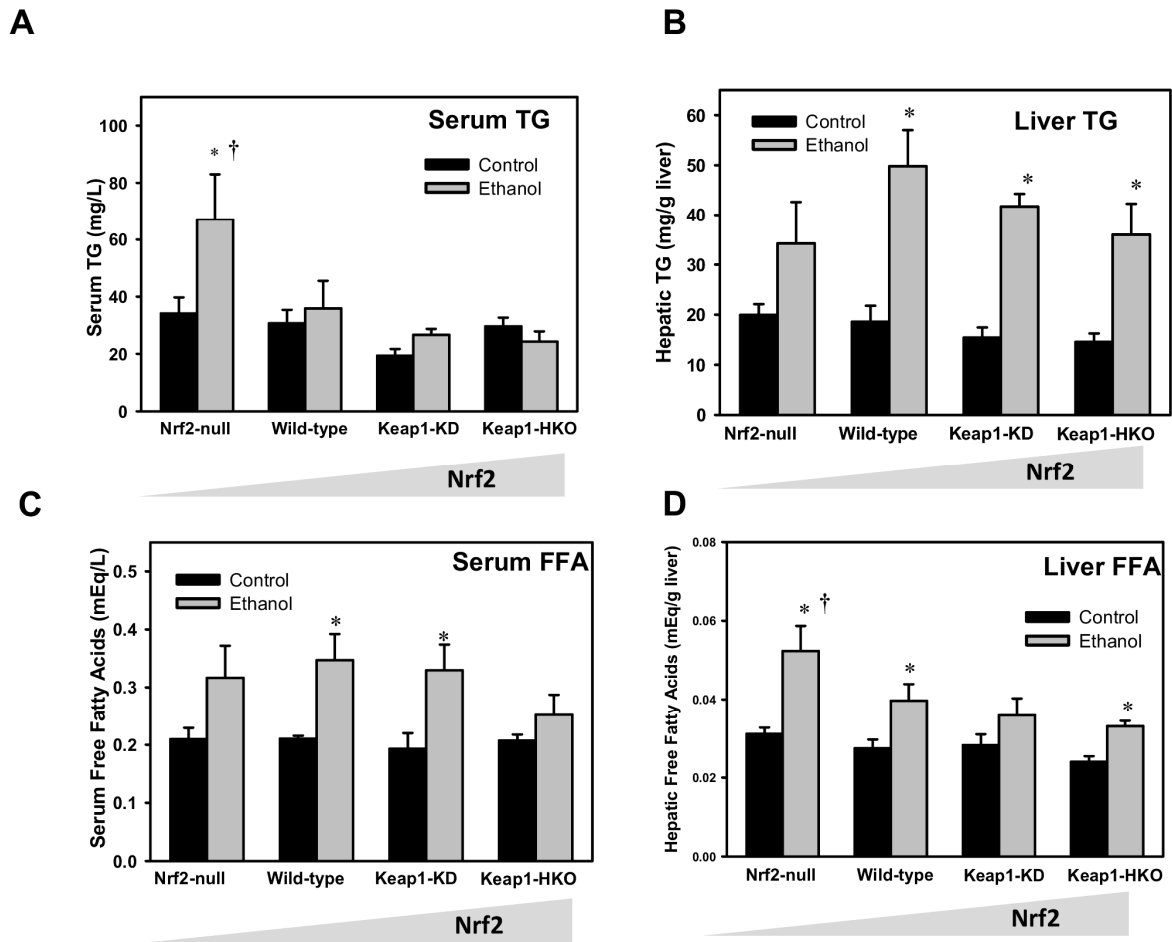**Srebp1 and its target gene expression in liver**

   To determine the mechanism of how Keap1-Nrf2 signaling pathway is protective against ethanol-induced lipid accumulation, the mRNA and protein of Srebp1, the transcription factor that induces genes involved in lipid biosynthesis, were quantified. Compared to wild-type mice, basal Srebp1 mRNA was 41% higher in Nrf2-null mice, 8% lower in Keap1-KD mice, and 59% lower in Keap1-HKO mice. After ethanol administration, Srebp1 mRNA increased 135% in Nrf2-null mice, 160% in wild-type mice, 28% in Keap1-KD mice, and 115% in Keap1-HKO mice. Compared to wild-type mice, the basal level of Srebp1 protein was 28% higher in Nrf2-null mice, 48% lower in Keap1-KD mice, and 51% lower in Keap1-HKO mice. Ethanol did not have any effect on nuclear Srebp1 protein levels in the four genotypes of mice, and Srebp1 protein was maintained in a gene dose-response manner after ethanol administration. To further evaluate the role of Nrf2 in Srebp1 activation, the mRNA of Scd1, a Srebp1-target gene, was quantified in the gene dose-response model. Compared to wild-type mice, the basal level of Scd1 mRNA was 17% higher in Nrf2-null mice, 9% lower in Keap1-KD mice, and 52% lower in Keap1-HKO mice. After ethanol administration, Scd1 mRNA increased 70% in Nrf2-null mice, 37% in wild-type mice, decreased 20% in Keap1-KD mice, and remained unchanged in Keap1-HKO mice (Fig. 6.6).
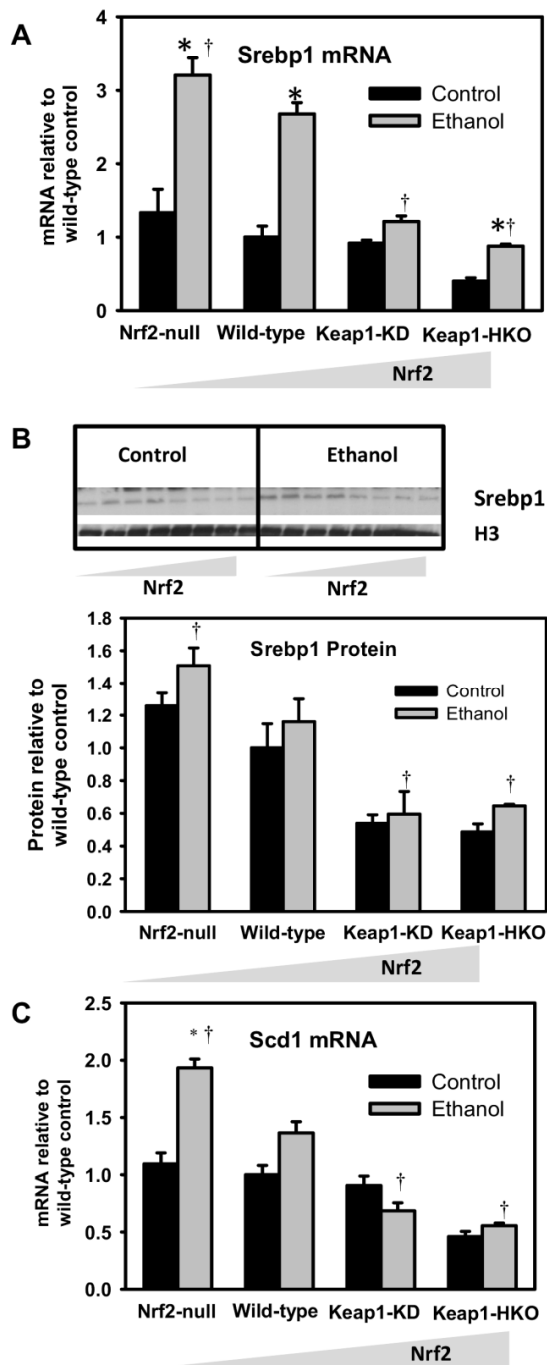
Figure 6.6. Effects of ethanol on the mRNA and protein of the Srebp1 signal pathway. (A) mRNA of Srebp1, (B) protein of Srebp1, and (C) mRNA of Scd1 in livers of Nrf2-null, wild-type, Keap1-KD, and Keap1-HKO mice 6 h after ethanol administration (5 g/kg, p.o.). Data are expressed as mean ± S.E.M of 5 mice per group. Asterisks (*) indicate statistically significant differences from control mice of the same genotype (p < 0.05). Daggers (†) indicate statistically significant differences from wild-type mice after ethanol administration.

Discussion

It is well established that acute and chronic ethanol intoxication causes lipid peroxidation, as evidenced by increased lipid peroxidation products in liver and serum of laboratory animals and humans. For example, chronic feeding of an ethanol-containing diet resulted in production of 4-hydroxynonenal (4-HNE), a product generated in the oxidation of polyunsaturated lipids, and subsequently production of 4-HNE modified proteins in rats and mice (Smathers *et al.*, 2011). A reduction in alcohol consumption in humans was associated with reduced plasma F_2-isoprostanes, a product from non-enzymatic oxidation of arachidonic acid (Barden *et al.*, 2007). Malondialdehyde (MDA), another product generated from oxidation of polyunsaturated fatty acids, was increased after acute (Kim *et al.*, 2009) and chronic (Khanal *et al.*, 2009) ethanol feeding to mice. Consistent with these previous studies, the present study using the TBARS assay, illustrate that acute ethanol intoxication resulted in increased lipid peroxidation products in serum of wild-type mice. TBARS were increased more in Nrf2-null mice, an indication of exaggerated oxidative stress in the absence of Nrf2. In addition, ethanol had no effect on thiobarbituric acid reactive substances in Keap1-KD and Keap1-HKO mice (Fig. 6.2), which indicates that Nrf2 activation blunted the ethanol-induced oxidative stress.

Ethanol enhanced ROS in a dose-dependent manner in primary hepatocytes of Nrf2-null mice and wild-type mice, but not in Nrf2-enhanced mice. This indicates that ethanol induces oxidative stress, and the absence of Nrf2 increases ethanol-induced oxidative stress, whereas Nrf2 activation decreases oxidative stress *in vitro*. Under physiological conditions, reactive oxygen species (ROS) are generated from multiple

sources, including the electron transport chain in mitochondria (Droge, 2002). The basal level of ROS was higher in primary hepatocytes from Nrf2-null mice, and lower in primary hepatocytes from Nrf2-enhanced mice, indicating that Nrf2 decreases oxidative stress even in the absence of an exogenous challenge. In primary hepatocytes of Keap1-KD and Keap1-HKO mice, ROS increased rapidly (3 h) after ethanol exposure (Fig. 6.4B). The increase in ROS may be due to higher CYP2E1 activities in Keap1-KD and Keap1-HKO mice (data not shown). However, ROS in Keap1-KD and Keap1-HKO hepatocytes were low, and remained low after ethanol exposure, indicating that Nrf2 activation-induced antioxidants are efficient in scavenging the ROS generated.

In addition to the formation of lipid peroxidation products, acute and chronic ethanol intoxication also results in a decrease in endogenous antioxidants (GSH in particular) in liver. For example, after a single dose of ethanol to mice, hepatic GSH content was decreased the most 6 h after administration (Vogt and Richie, 2007). In the present study, ethanol tended to decrease GSH in wild-type mice at 6 h. However, the decrease was not statistically significant. The different observations in the two studies may be due to the difference in nutrient status (fasted versus feed) or age difference of the animals (6-month old versus 3-month old). In the present study, cytosolic GSH concentrations in Nrf2-null mice were the most sensitive to ethanol, which indicates that Nrf2 is critical for maintenance of cellular GSH following ethanol consumption. Mitochondria, through the electron transport chain, is the major cellular organelle that generates ROS (Droge, 2002), and the redox status of mitochondria is crucial in ethanol-induced oxidative stress. GSH in mitochondria is a key regulator in the cell survival/death decision (Mari *et al.*, 2009). In livers of wild-type mice, ethanol slightly

114

decreased cytosolic GSH concentrations, but depleted 52% of the mitochondrial GSH (Fig.6. 2). After ethanol administration, the GSH concentrations in mitochondria were lower in Nrf2-null mice than wild-type mice, indicating a role of Nrf2 in maintaining redox homeostasis in mitochondria.

In contrast with the consistent observation of oxidative stress by ethanol, the pattern of transcriptional activation of Nrf2 battery genes has not always been consistent between acute and chronic ethanol intoxication models. For example, chronic feeding of ethanol induced the mRNAs of heme oxygenase 1 (Ho-1) and NAD(P)H quinone dehydrogenase 1 (Nqo1) in rat livers (Yeligar *et al.*, 2010). In another study, chronic feeding of ethanol also induced mRNA of sulfiredoxin (Sxn) and peroxiredoxin 1 (Prx1) in livers of mice (Bae *et al.*, 2011). In contrast, acute ethanol intoxication decreases mRNA and activity of proteins involved in antioxidant defense. For example, acute ethanol decreased markedly the enzyme activities of catalase, glutathione reductase, glutathione peroxidase, and glutathione-*S*-transferase in livers of rats (Khan *et al.*, 2011). Acute ethanol exposure inhibits Nrf2 activation in the cerebellum of rats (Kumar et al., 2011a), and acute ethanol administration decreased mRNA and protein levels of thioredoxin 1(Trx1) (Cohen *et al.*, 2009) and peroxiredoxin 6 (Prx6) (Roede *et al.,* 2008) in livers of mice. Consistent with the previous observations, the present study shows that Gclc mRNA and protein are decreased after ethanol administration. However, it should be noted that after ethanol administration, mRNA and protein concentrations of Nqo1 and Gclc increased with Nrf2 activation in a gene dose-response manner (Fig. 6.3).

In the present study, ethanol had minor effects on increasing serum triglyceride and hepatic free fatty acid concentrations in wild-type mice. Ethanol treatment resulted in more profound increases in free fatty acid concentrations in livers of Nrf2-null mice, whereas Nrf2 activation blunted such an increase in livers of ethanol-treated Keap1-KD and Keap1-HKO mice (Fig. 6.5). However, activation of Nrf2 did not prevent ethanol-induced increase in triglyceride concentrations in liver, which were increased in all genotypes of mice. Sterol regulatory element binding protein 1 (Srebp1) is an endoplasmic reticulum (ER) membrane-bound transcription factor that translocates into the nucleus to promote transcription of genes involved in cholesterol and fatty acid synthesis (Horton *et al.*, 2002). Srebp1 mRNA and protein were decreased with graded Nrf2 activation before and after ethanol administration. The basal mRNA level of Scd1, an Srebp1-target gene, was also decreased with graded Nrf2 activation, and increased markedly after ethanol administration in Nrf2-null mice, but not in Nrf2-enhanced mice (Fig. 6.6). These observations indicate that Srebp1 expression and activity are suppressed by Nrf2 activation. Srebp1 is regulated by multiple nuclear receptors and endogenous signaling molecules, including Liver X receptor (Yoshikawa *et al.*, 2001), insulin, and glucagon (Raghow *et al.*, 2008). Recently, oxidative stress was shown to facilitate Srebp1 activation (Waris *et al.*, 2007). Thus, increased Scd1 mRNA as well as increased fatty acid concentrations in livers of Nrf2-null mice were partially due to ethanol-induced oxidative stress.

In summary, the present study shows that Keap1-Nrf2 signaling pathway plays an important role in protecting against ethanol-induced hepatic alterations *in vitro* and *in*

vivo, and this protective effect may result from Nrf2-regulated elevation of cellular GSH concentrations and suppression of the Srebp1 signaling pathway.

Chapter 7 : NRF2 ACTIVATION PREVENTS CADMIUM-INDUCED ACUTE LIVER INJURY

Abstract

Oxidative stress plays an important role in cadmium-induced liver injury. Nuclear factor erythroid 2-related factor 2 (Nrf2) is a transcription factor that up-regulates cytoprotective genes in response to oxidative stress. To investigate the role of Nrf2 in cadmium-induced hepatotoxicity, Nrf2-null mice, wild-type mice, kelch-like ECH-associated protein 1-knockdown (Keap1-KD) mice with enhanced Nrf2, and Keap1-hepatocyte knockout (Keap1-HKO) mice with maximum Nrf2 activation were treated with cadmium (3.5 mg/kg, i.p.). Blood and liver samples were collected 8 h thereafter. Cadmium increased serum alanine aminotransferase (ALT) and lactate dehydrogenase (LDH) activities, and caused extensive hepatic hemorrhage and necrosis in the Nrf2-null mice. In contrast, Nrf2-enhanced mice had lower serum ALT and LDH activities and less morphological alternations in the livers than wild-type mice. H_2DCFDA (2′,7′-dichlorodihydrofluoresein diacetate) staining of primary hepatocytes isolated from the four genotypes of mice indicated that oxidative stress was higher in Nrf2-null cells, and lower in Nrf2-enhanced cells than in wild-type cells. To further investigate the mechanism of the protective effect of Nrf2, mRNA of metallothionein (MT) and other cytoprotective genes were determined. Cadmium markedly induced MT-1 and MT-2 in livers of all four genotypes of mice. In contrast, genes involved in glutathione synthesis and reducing reactive oxygen species, including glutamate-cysteine ligase (Gclc), glutathione peroxidase-2 (Gpx2), and sulfiredoxin-1 (Srxn-1) were only induced in Nrf2-enhanced mice, but not in Nrf2-null mice. In conclusion, the present study shows that Nrf2 activation prevents cadmium-induced oxidative stress and liver injury through induction of genes involved in antioxidant defense rather than genes that scavenge Cd.

Introduction

Cadmium (Cd) is a heavy metal that causes dose- and route-dependent toxicity in multiple organs in humans and laboratory animals. Acute Cd exposure via inhalation causes pneumonitis, bronchitis, and pulmonary edema (Liu et al., 2007). Chronic Cd exposure through inhalation or by oral ingestion results in renal dysfunction, anemia, osteoporosis, and bone fractures (Liu et al., 2009). Cd is identified as a category-I human carcinogen, due to its potential to induce pulmonary tumors (Waalkes, 2003).

In animal studies, liver injury is the major toxic effect after an acute dose of Cd. The mechanisms of Cd-induced acute hepatotoxicity have been studied and appear to be a biphasic process (Rikans and Yamano, 2000). The first phase of damage is initiated by the binding of Cd to sulfhydryls of glutathione (GSH) and proteins, resulting in the generation of reactive oxygen species (ROS) and protein inactivation. Cd-induced ROS in turn produces lipid peroxidation, and results in DNA damage (Hassoun and Stohs, 1996). Damage to the vascular endothelium also disrupts the microcirculation, causing ischemia and subsequent liver injury (Liu et al., 1992). The second phase of damage is initiated by the activation of Kupffer cells in response to endothelial and parenchymal cell injury. The activated Kupffer cells release inflammatory mediators such as cytokines, chemokines, and adhesion molecules to recruit neutrophils to the sites of injury. Kupffer cells, together with neutrophils, release cytotoxic mediators, such as ROS, reactive nitrogen species (RNS), bioactive lipids, and hydrolytic enzymes to cause further liver injury (Yamano et al., 2000).

The mechanism of Cd detoxification in cells is dependent mainly on the induction of metallothionein (MT). MT is a family of cysteine-rich, low-molecular-weight proteins. MT has a high capacity to bind both physiological (such as zinc, copper, selenium) as well as xenobiotic (such as cadmium, mercury, silver, arsenic) heavy metals through the thiol group of the cysteine residues of MT, and it is highly inducible by metals (Klaassen and Liu, 1998; Klaassen et al., 1999). MT-null mice are more susceptible to Cd-induced hepatotoxicity than wild-type mice, whereas MT-transgenic mice are protected from Cd-induced hepatotoxicity (Liu et al., 1995b). Antioxidants, such as quercetin, α-tocopherol (Prabu et al., 2010), and diallyl tetrasulfide (Ponnusamy and Pari, 2011) also decrease Cd-induced oxidative stress and subsequent tissue injury in rats.

Nuclear factor erythroid 2-related factor 2 (Nrf2) is a transcription factor that promotes transcription of a battery of cytoprotective genes in response to oxidative/electrophilic stress. Recently, a Nrf2 "gene dose-response" model was generated using Nrf2-null mice, wild-type mice, Keap1-knockdown (Keap1-KD) mice with enhanced Nrf2 activation, and Keap1-hepatocyte knockout (Keap1-HKO) mice with maximum Nrf2 activation. Transcription profiling in the Nrf2 "gene dose-response" model by microarray analysis showed that mRNA of MT-1 and MT-2 were induced by Nrf2 activation in a "gene dose-response" manner (Wu et al., 2011a), indicating that Nrf2 may play a role in preventing Cd-induced acute liver injury.

The antioxidant properties of Nrf2 target genes make Nrf2 a promising target in preventing Cd-induced toxicity. Suppression of Nrf2 resulted in greater sensitivity, whereas over-expression of Nrf2 results in resistance to Cd-induced apoptosis in rat kidney cells (Chen and Shaikh, 2009). However, it is not known whether Nrf2 activation

protects against Cd-induced toxicity *in vivo*. In the present study, the Nrf2 "gene dose-response" model was used to characterize the protective effect of Nrf2 in maintaining redox equilibrium in response to Cd exposure.

Results

Serum ALT and LDH

Cd-induced acute hepatotoxicity was indicated by enzyme activities of alanine transaminase (ALT) and lactate dehydrogenase (LDH) in serum. In saline-treated mice, serum ALT activities in Nrf2-null, wild-type, Keap1-KD, and Keap1-HKO mice were low and with no differences between genotypes. Cd increased serum ALT activities 24-fold in Nrf2-null mice, 16-fold in wild-type mice, 4-fold in Keap1-KD mice, but not in Keap1-HKO mice (Fig. 1A). Serum LDH activities of Nrf2-null, wild-type, Keap1-KD, and Keap1-HKO mice were also low, and with no differences among the four genotypes of mice. Cd increased serum ALT activities 16-fold in Nrf2-null mice, 3-fold in wild-type mice, but not in Keap1-KD and Keap1-HKO mice (Fig. 7.1B).

Liver histopathology

There were no observable abnormalities in the livers of Nrf2-null, wild-type, Keap1-KD, and Keap1-HKO mice (data not shown). However, Cd produced severe hemorrhage and necrosis in Nrf2-null mice (under low magnification), and extensive nuclear condensation (under high magnification). Cd produced severe hemorrhage and moderate necrosis in wild-type mice, but mild hemorrhage and no necrosis in Keap1-KD and Keap1-HKO mice (Fig. 7.2).
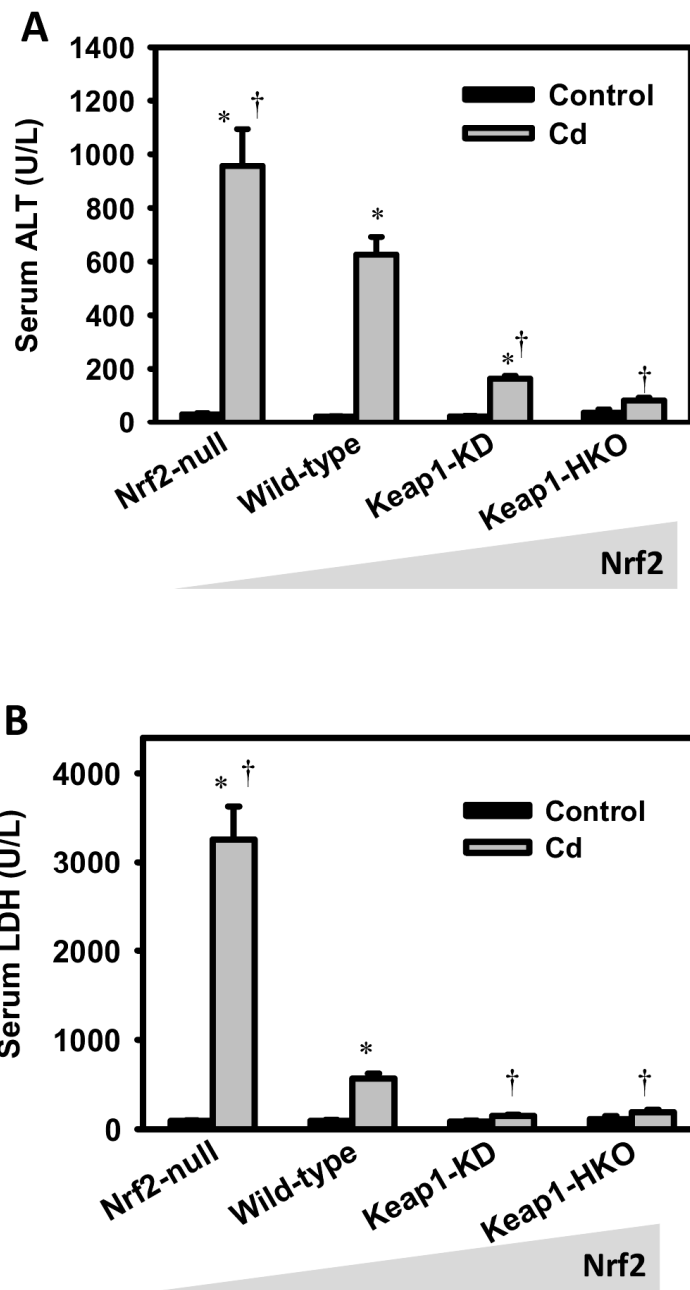
Figure 7.1. (A) Serum alanine transaminase (ALT) and (B) lactate dehydrogenase (LDH) activities in Nrf2-null, wild-type, Keap1-KD, and Keap1-HKO mice (n=5) administered saline (10 mL/kg, i.p.) or Cd (3.5 mg/kg, i.p.). ALT and LDH activities are expressed as International Units/Liter. Values are expressed as mean ± S.E.M. Asterisks (*) indicate a statistically significant difference from saline pretreated mice of the same genotype ($p \leq 0.05$). Daggers (†) indicate a statistically significant difference from wild-type mice treated with Cd ($p \leq 0.05$).
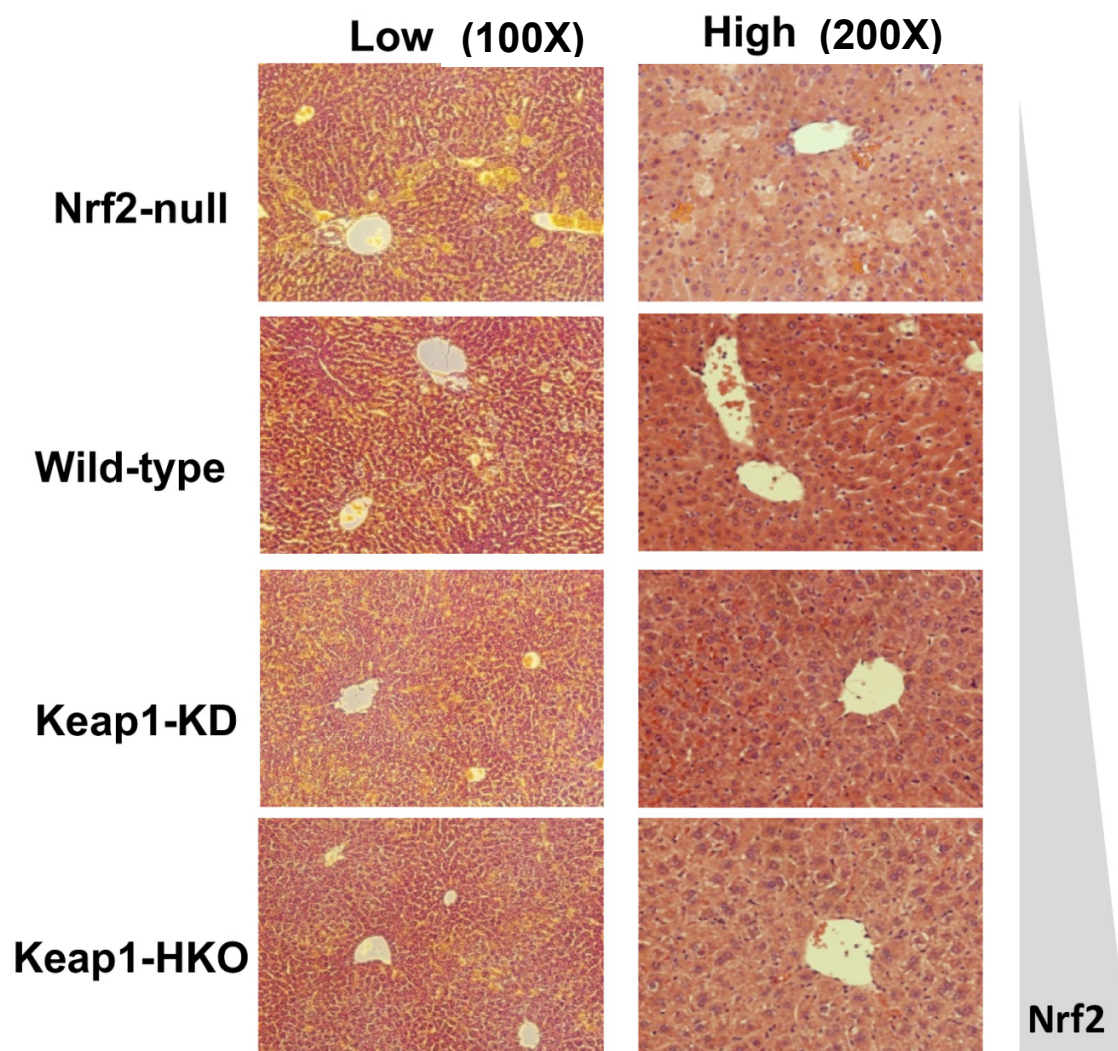
Figure 7.2. Histological analysis of livers from Nrf2-null, wild-type, Keap1-KD, and Keap1-HKO mice treated with Cd (3.5 mg/kg, i.p.). Left panel, low magnification (20×). Right panel, high magnification (40×).

Dose-response and time course of ROS generation

To characterize Cd-induced oxidative stress, primary hepatocytes from Nrf2-null, wild-type, Keap1-KD, and Keap1-HKO mice were isolated and stained with H_2DCFDA, an general indicator of ROS. H_2DCFDA enters cells by simple diffusion, then is deacetylated by cellular esterase and trapped within the cells. It is further oxidized by ROS into DCF to emit a green fluorescence. Without Cd, there was slight green fluorescent staining in the Nrf2-null cells but not in wild-type or Nrf2-activated cells, indicating more ROS were in Nrf2-null cells than wild-type and Nrf2 activated cells. After the addition of Cd, ROS staining was most evident in Nrf2-null cells, but not in Nrf2-activated cells (Fig. 7.3A). Quantitatively, without Cd, the basal levels of ROS were 68% higher in Nrf2-null cells, and 41 and 53% lower in Keap1-KD and Keap1-HKO cells than wild-type cells, respectively. After the addition of Cd, ROS increased 3-fold in Nrf2-null cells and 2.8-fold in wild-type cells. In contrast, ROS in Keap1-HKO cells remained low at all time points (Fig. 7.3B). Cd increased ROS in wild-type and Nrf2-null cells in a concentration-dependent manner, but had no effect on ROS in Keap1-HKO cells (Fig. 7.3C).

mRNA of MT-1, MT-2, and Ho-1 in liver

To determine the mechanism of how Nrf2 protects against Cd-induced toxicity, MT-1 and MT-2 mRNA were quantified in livers of Nrf2-null, wild-type, Keap1-KD, and Keap1-HKO mice (Fig. 7.4). Without Cd, the basal level of MT-1 was 66% higher in Nrf2-null mice, 43% higher in Keap1-KD mice, and 490% higher in Keap1-HKO mice than wild-type mice. Eight h after Cd administration, mRNA of MT-1 increased more

than 200-fold in the four genotypes of mice, with no statistical significance among the genotypes (Fig. 7.4A). Similarly, without the addition of Cd, the basal level of MT-2 was 41% higher in Nrf2-null mice, 65% higher in Keap1-KD mice, and 12-fold higher in Keap1-HKO mice than wild-type mice. Eight h after injection of Cd, mRNA of MT-2 increased more than 500-fold in the four genotypes of mice, with no statistical significance among the genotypes (Fig. 7.4B). The basal level of Ho-1 was 72 and 55% higher in Keap1-KD and Keap1-HKO mice than wild-type mice, respectively. At 8 h of Cd exposure, the mRNA of Ho-1 increased more than 15-fold in Nrf2-null, wild-type, and Keap1-KD mice, and 60-fold in Keap1-HKO (Fig. 7.4C).

mRNA of genes involved in antioxidant defense

The mRNA of certain genes involved in antioxidant defense, including Gpx2, Prdx1, Gclc, Txnrd1, Srxn1, and Txn1 were lowly expressed in Nrf2-null mice, but were induced with graded Nrf2 activation in wild-type, Keap1-KD, and Keap1-HKO mice (Fig. 5). Specifically, the mRNA of Gpx2 was 160-fold more abundant in Keap1-HKO mice than wild-type mice. After Cd administration, Gpx2 mRNA was increased in wild-type and Keap1-KD mice but not in Keap1-HKO mice. However, the abundance of Gpx2 mRNA was 24-fold higher than in Nrf2-null mice, 14-fold higher than in wild-type mice, and 8-fold higher than in Keap1-KD mice. Cd increased Gclc and Srxn-1 mRNA in wild-type mice and Nrf2-activated mice, but not in Nrf2-null mice. In contrast, Cd markedly increased mRNA of Prdx1, Txnrd1, and Txn1 in both Nrf2-null and Nrf2-activated mice (Fig. 7.5).
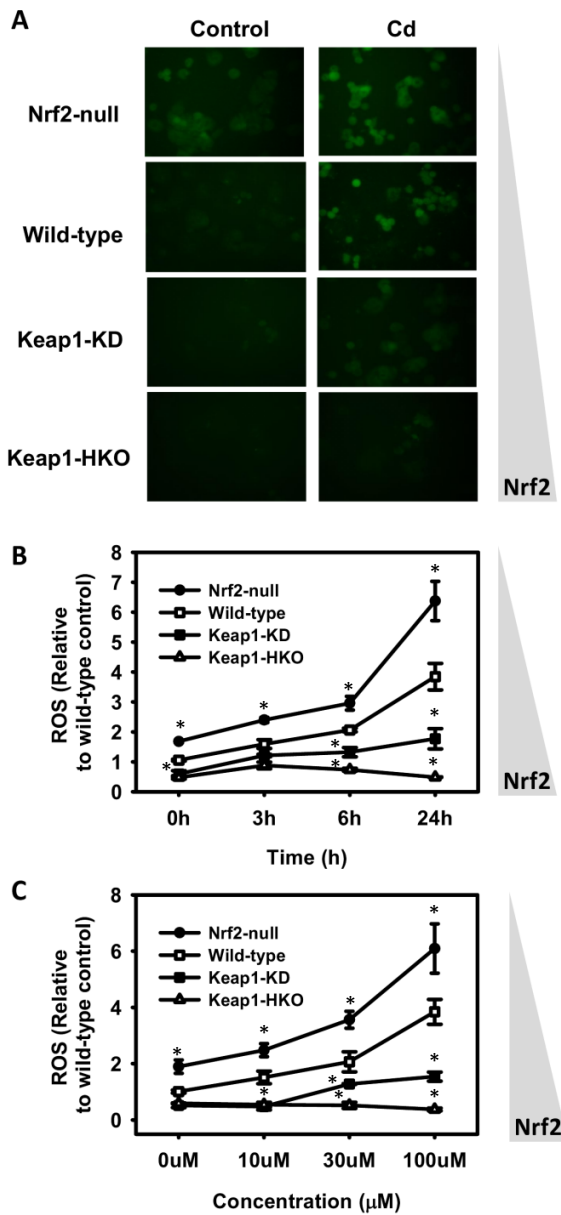
Figure 7.3. Figure 7.4. Cd-induced oxidative stress *in vitro*. (A) DCFDA fluorescence in primary hepatocytes 6 h after ethanol exposure. Primary hepatocytes were isolated and treated with ethanol for 24 h and subjected to live cell imaging. (B) Time-response and (C) dose-response of ROS production after ethanol administration of primary hepatocytes from Nrf2-null, wild-type, Keap1-KD, and Keap1-HKO mice. Data are presented as Mean ± S.E.M. of 3 mice per group in Fig 4B and Fig 4C. Asterisks (*) indicate statistically significant differences from wild-type cells of the same time point ($p < 0.05$).
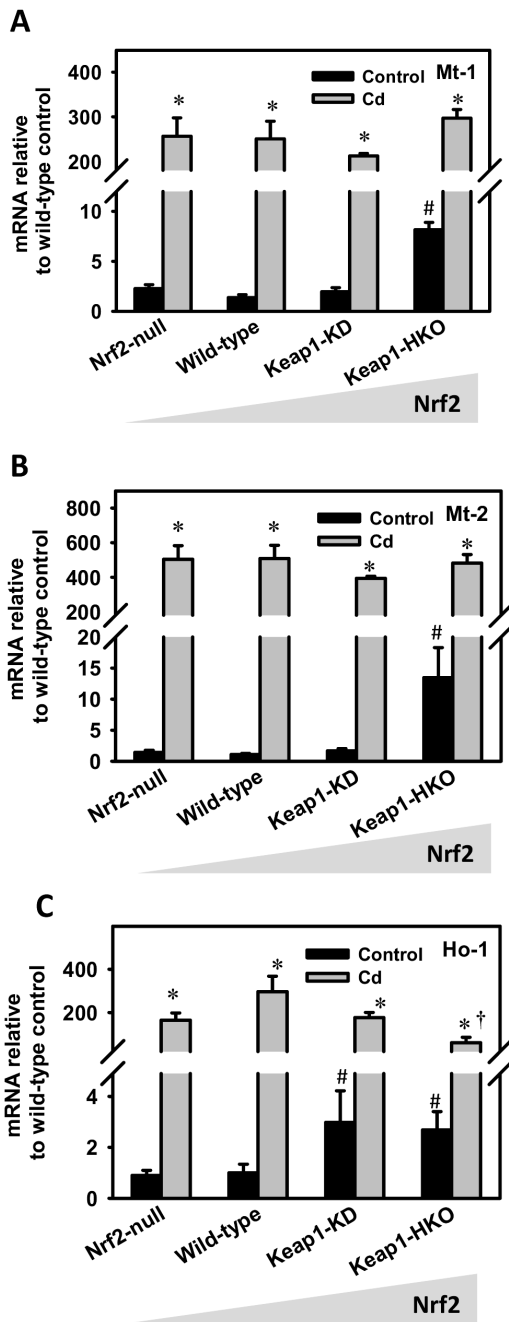
Figure 7.5. (A) MT-1, (B) MT-2, and (C) Ho-1 mRNA in livers of Nrf2-null, wild-type, Keap1-KD, and Keap1-HKO mice after Cd treatment (3.5 mg/kg, i.p.). Livers were removed 8 h after dosing and mRNA quantified by the RT-PCR. Asterisks (*) indicate a statistically significant difference from saline pretreated mice of the same genotype ($p \leq$ 0.05). Number signs (#) indicate a statistically significant difference from wild-type mice treated with saline ($p \leq 0.05$). Daggers (†) indicate a statistically significant difference from wild-type mice treated with Cd ($p \leq 0.05$).
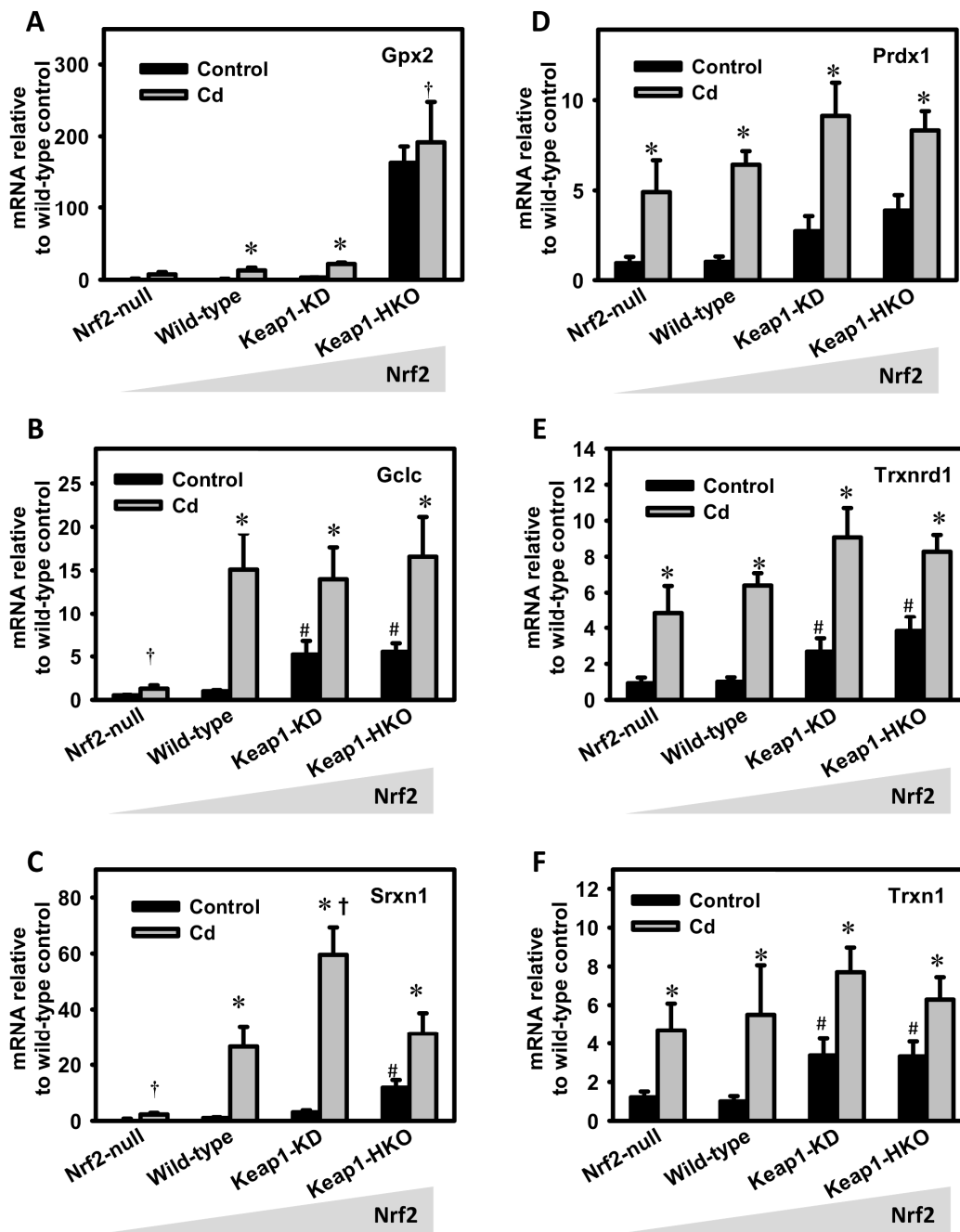
Figure 7.6. (A) Gpx2, (B) Gclc, (C) Srxn, (D) Prdx1, (E) Trxnrd1, and (F) Trxn1 mRNA in livers of Nrf2-null, wild-type, Keap1-KD, and Keap1-HKO mice after Cd treatment (3.5 mg/kg, i.p.). Livers were removed 8 h after dosing and mRNA quantified by RT-PCR. Asterisks (*) indicate a statistically significant difference from saline pretreated mice of the same genotype ($p \leq 0.05$). Number signs (#) indicate a statistically significant difference from wild-type mice before Cd treatment ($p \leq 0.05$). Daggers (†) indicate a statistically significant difference from wild-type mice after Cd treatment ($p \leq 0.05$).

DISCUSSION

In the present study, liver injury was the primary toxic effect observed after an acute dose of Cd (3.5 mg/kg). After administration, Cd is distributed via the blood, where it is bound to red blood cells and plasma proteins, mainly albumin. Albumin-bound Cd is readily distributed to various organs, with the majority going to the liver, where Cd is primarily bound to MT (Liu et al., 2001). After a single injection of Cd to rats, the highest concentration of Cd is in the liver, followed by kidney, spleen, and heart (Goering and Klaassen, 1983). The distribution of Cd changes with time; the concentration of Cd in the liver decreases as it redistributes to the kidney, resulting in nephrotoxicity after chronic Cd exposure (Klaassen and Liu, 1997).

The present study, together with other reports, indicates excessive generation of ROS after Cd exposure. For example, a concentration-response study of Cd (50 -100 µM) in mouse embryonic fibroblasts (MEF) demonstrated the presence of ROS 5 h after incubation using dihydroethidium, a staining technique used to quantify ROS. In addition, MEF derived from Nrf2-null mice showed elevated basal and Cd-induced ROS generation (He et al., 2008). Similarly, the present study demonstrates increases in ROS in mouse primary hepatocytes by Cd in a concentration- (10-100 µM) and time-dependent (3-24 h) manner. The Nrf2-null hepatocytes also have higher basal ROS as well as Cd-induced ROS generation. In addition, the present study further shows that Keap1-HKO hepatocytes not only have the maximum activation of Nrf2, but also a lower basal level of ROS, and protect against Cd-induced generation of ROS at all tested concentrations (Fig. 7.3).

Cd activates the Keap1-Nrf2 pathway through multiple mechanisms. For example, Cd delays the ubiquitin-proteasome mediated degradation of Nrf2, and increase its half-life from 13 to 100 min in mouse hepatoma (Hepa) cells (Stewart et al., 2003). Cd also enhances the nuclear export of BTB and CNC homology 1 (Bach1), which competes with Nrf2 for DNA binding, to promote Nrf2 target gene transcription (Suzuki et al., 2003). The most extensively studied Nrf2 target gene that is induced by Cd is heme oxygenase-1 (Ho-1). For example, Ho-1 is induced by Cd in mouse MCF-7 mammary epithelial cells (Alam et al., 2000), mouse Hepa cells (Stewart et al., 2003), and HeLa cells (Andoh et al., 2006). However, the present study shows that cadmium produces a marked (over 180-fold) increase of Ho-1 mRNA in livers of Nrf2-null mice, which indicates that additional transcription factors or signaling pathways are involved in the induction of Ho-1 by Cd. Thioredoxin reductase (Trxnrd1) is induced by Cd in bovine arterial endothelial cells (BAEC) through Nrf2 activation (Sakurai et al., 2005), and in the present study, both thioredoxin (Trxn1) and Trxnrd1 are induced by Cd in livers of Nrf2-null mice. The mRNA of Trxn1 and Trxnrd1 tended to be higher in Nrf2-activated mice, but was not statistically different (Fig. 7.5).

The critical roles of MT in Cd detoxification are well-established (Klaassen et al., 2009), and there is increasing knowledge about the protective role of Nrf2 against Cd toxicity. However, little is known about whether Nrf2 protects against Cd-induced toxicity through inducing MT. Four major MT isoforms have been identified (MT-1 to MT-4). MT-1 and MT-2 are expressed in all organs, especially in liver, intestine, pancreas, and kidney. MT-3 is mainly expressed in brain and kidney, and MT-4 is most abundant in stratified epithelium (Vesey, 2010). It is estimated that one molecule of MT can bind to

seven molecules of Cd, and MT-bound Cd is generally considered non-toxic (Liu et al., 1996). The present study showed that the mRNA of MT-1 and MT-2 are higher in Keap1-HKO mice than in wild-type mice (5-fold and 11-fold, respectively), indicating MT-1 and MT-2 are potential Nrf2 target genes *in vivo*. However, following Cd treatment, MT-1 and MT-2 in Nrf2-null mice were markedly increased (more than 200-fold), and there was no difference in the quantities of MT-1 or MT-2 mRNA among the four genotypes of mice. This finding indicates that induction of MT-1 and MT-2 mRNA by Cd is through Nrf2-independent mechanism.

In contrast to MT-1, MT-2, and Ho-1, the present study shows that Cd increased the mRNA of Gpx2, Gclc, and Srxn1 in wild-type and Nrf2-activated mice, but not in Nrf2-null mice (Fig. 7.5). Glutathione peroxidase is a family of enzymes that reduces hydrogen peroxide to H_2O and oxidizes glutathione (GSH) to GSSG. There are five isoforms in the Gpx family: cytosolic Gpx (Gpx1), gastrointestinal Gpx (Gpx2), plasma Gpx (Gpx3), phospholipid hydroperoxide Gpx (Gpx4), and olfactory epithelium-specific Gpx (Gpx5) (Margis et al., 2008). Gpx2 is localized in the cytosol and was originally detected in the rodent gastrointestinal tract. In humans, Gpx2 is expressed in the liver and large intestine (Chu et al., 1993). The present study shows that Gpx2 mRNA is almost absent in livers of Nrf2-null mice, and Cd increased 160-fold more Gpx2 mRNA in Keap1-HKO mice than wild-type mice (Fig. 7.5). This observation indicates that Gpx2 is present and highly inducible in mouse liver, and its induction is highly dependent on Nrf2. Gclc is the rate limiting enzyme that synthesizes GSH, the essential substrate for Gpx2 to reduce hydrogen peroxide (Yang et al., 2011). The basal level of Gclc mRNA increased with graded Nrf2 activation, and Cd exposure further induced Gclc in Nrf2-

containing mice but not in Nrf2-null mice (Fig. 7.5). Collectively, the present study shows that Nrf2-Gclc-Gpx2 serves as a novel mechanism to protect against Cd-induced oxidative stress and tissue injury. In addition to Gpx, peroxiredoxin (Prx-SH) is another family of enzymes that directly reduces hydrogen peroxide. Oxidized peroxiredoxin (Prx-SO_2H) under excessive oxidative stress, can only be reduced by surfiredoxin (Srxn) (Lowther and Haynes, 2011). The present study shows that Nrf2 is essential for both the basal and Cd-induced adaptive response of Srxn1 transcription.

In conclusion, the present study shows that Nrf2 activation prevents cadmium-induced oxidative stress and liver injury. The protective effect of Nrf2 is dependent on induction of genes involved in antioxidant defense rather than genes that scavenge Cd.

Chapter 8 : NRF2 ACTIVATION PROTECTS AGAINST DIQUAT-INDUCED LIVER

AND LUNG INJURY

Abstract

Diquat is a herbicide that generates superoxide anions through redox cycling. Nuclear factor (erythroid-derived 2)-like 2 (Nrf2) is a transcription factor that up-regulates cytoprotective genes in response to oxidative stress. To investigate the protective effect of Nrf2 against diquat-induced toxicity, wild-type, Nrf2-null, and Kelch-like ECH-associated protein 1-knockdown (Keap1-KD) mice with enhanced Nrf2 activity were treated with diquat dibromide (125 mg/kg, i.p.). Blood and tissues were collected at 1, 2, 4, and 6 h after treatment. Administration of diquat resulted in lipid peroxidation and lethality in wild-type mice, which were more in Nrf2-null mice and less in Keap1-KD mice. Diquat produced liver injury in Nrf2-null mice, as evidenced by increased serum ALT activity and extensive hepatic necrosis, but not in wild-type and Keap1-KD mice. Diquat produced more severe lung injury in Nrf2-null than in wild-type mice, as evidenced by increased lung weight and alveolar collapse. In contrast, Keap1-KD mice had attenuated lung edema and no histopathological alterations. To further investigate the mechanism of the protective effects of Nrf2, lung and liver glutathione (GSH) concentrations were quantified. Diquat decreased GSH in lung and liver in wild-type mice, and the decrease was more in Nrf2-null mice, and less in Keap1-KD mice. After diquat treatment, the mRNA of the GSH synthesis enzyme Gclc was increased in Keap1-KD, but not in Nrf2-null mice. Collectively, Nrf2 plays an important role in preventing diquat-induced liver and lung injury, and this protective effect results from Nrf2-regulated elevation of cellular GSH and expression of GSH synthetic genes.

Introduction

One of the major challenges in a biological system is to maintain redox cellular homeostasis through balancing the rate and magnitude of oxidant generation and oxidant detoxification. An imbalanced ratio between reactive oxygen species (ROS) production and adaptive antioxidant capacity will result in oxidative stress, a pathogenic state that is both a cause and consequence of numerous acute toxicity and chronic diseases. ROS are free radicals with one or more unpaired electrons, which make them highly reactive. Most common cellular oxidative stress are generated from oxygen metabolism, such as the superoxide radical (O^-) and the hydroxyl radical ($OH^.$) as well as reactive nitrogen species, such as nitric oxide (NO) and the peroxynitrite radical ($ONOO^.$).

The immediate outcomes of oxidative stress include DNA damage (Bertram and Hass, 2008), protein adduction (Filippin et al., 2008), and lipid peroxidation (Cejas et al., 2004), leading to nuclear damage, mitochondrial damage, proteasome inhibition, and endoplasmic reticulum (ER) stress. ROS can damage the enzymes that maintain low intracellular Ca^{2+} (Malhotra and Kaufman, 2007). In addition, mitochondrial damage results in both ROS leakage from the electron transport system and Ca^{2+} release, and impaired ATP generation further disrupts ion homeostasis (Lemasters et al., 2009). Nuclear damage induces p53 activation, Bax activation, and Bcl-2 inhibition, followed by a release of cytochrome c into the cytosol that initiates the caspase signal pathway and apoptosis (Bursch et al., 2008). Oxidative stress also sensitizes cells to pro-inflammatory cytokines, recruits immune cells, and subsequent inflammatory response leads to further injury (Filippin et al., 2008). Thus, oxidative stress and ROS play an integral role in ageing, xenobiotic-induced toxicity, and numerous diseases.

Diquat is a contact herbicide that undergoes oxidation/reduction cycling, resulting in the generation of superoxide (Smith, 1987). It is a pure redox cycler that is minimally metabolized, thus diquat-induced injury serves as a typical model to study ROS generation and oxidative stress. A cell line based study revealed that mouse embryonic fibroblasts derived from Nrf2-deficient mice were more sensitive to diquat-induced toxicity, with impaired capacity to restore endogenous antioxidants (Osburn et al., 2006). However, there is no information on the importance of the Nrf2 in protecting the intact animal from diquat toxicity. In the present study, Nrf2-null, wild-type, and Keap-KD mice were used to characterize the role of the Keap1-Nrf2 signaling pathway on maintaining redox homeostasis after diquat treatment, and whether Nrf2 activation protects against diquat-induced toxicity.

Results

Survival

Wild-type mice treated with diquat dibromide (125 mg/kg, i.p.) began to die 3 h after injection, and 40% died by 6 h (Fig.8.1). Nrf2-null mice began to die at 2 h, and 40 and 60% died by 4 h and 6 h after diquat injection, respectively. In contrast, constitutive Nrf2 activation in the Keap1-KD mice resulted in 100% survival during the 6 h-observation period.
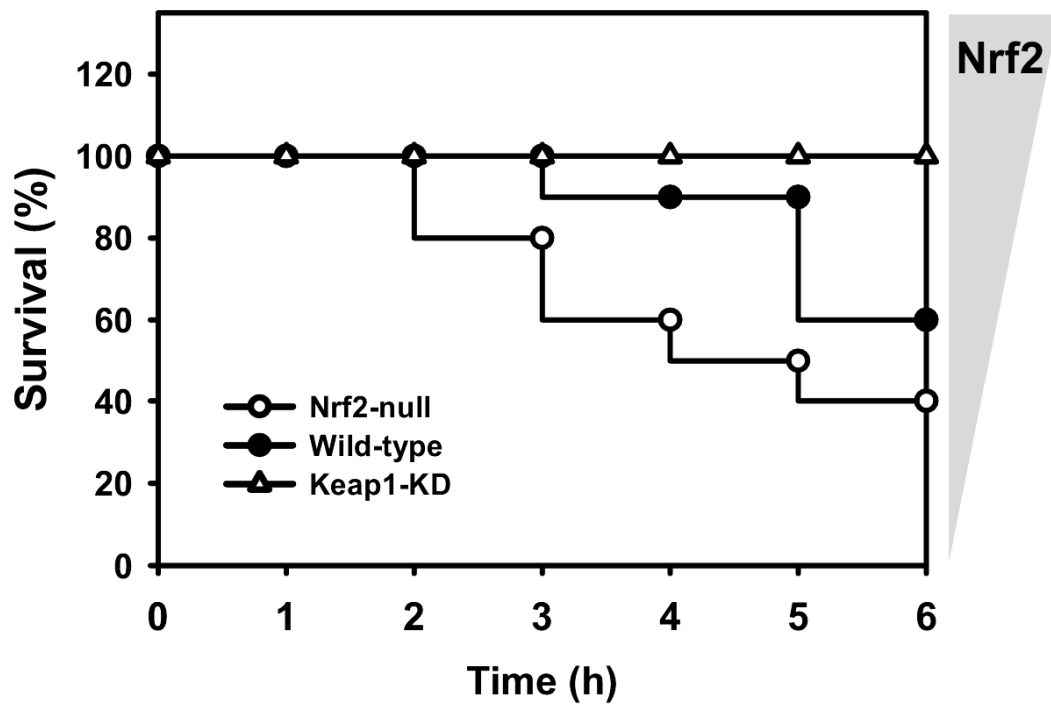
Figure 8.1. Survival rates of wild-type, Nrf2-null, and Keap1-KD mice after treatment with diquat dibromide (125 mg/kg, i.p.).

TBARS

To determine the effect of diquat on oxidative stress and whether Nrf2 activation protects against diquat-induced oxidative stress, lipid peroxidation products were quantified in serum samples of wild-type, Nrf2-null, and Keap1-KD mice using the TBARS method. In wild-type mice, TBARS increased after diquat treatment, and peaked at 4 h, which was 140% higher than before diquat administration. In Nrf2-null mice treated with diquat, TBARS also increased slightly more than wild-type mice during the 6 h-observation period. TBARS in Keap1-KD mice treated with diquat was much lower than in wild-type and Nrf2-null mice (Fig. 8.2).

Serum ALT and liver histology

Diquat-induced hepatotoxicity was detected by serum alanine transaminase (ALT) and histopathology. Diquat increased serum ALT in all genotypes of mice throughout the 6 h-observation period. In the Nrf2-null mice, diquat produced higher serum ALT at all time intervals than in the wild-type mice. Keap1-KD mice tended to have lower ALT after diquat administration, and ALT was statistically lower at 6 h (Fig. 8.3A). Histological analysis showed that livers of wild-type, Nrf2-null, and Keap1-KD mice treated with saline appeared normal. There were no morphological changes in livers of wild-type and Keap1-KD mice after diquat administration. However, in the Nrf2-null mice administered diquat, extensive areas of necrosis were concentrated around the central veins (Fig.8. 3B).
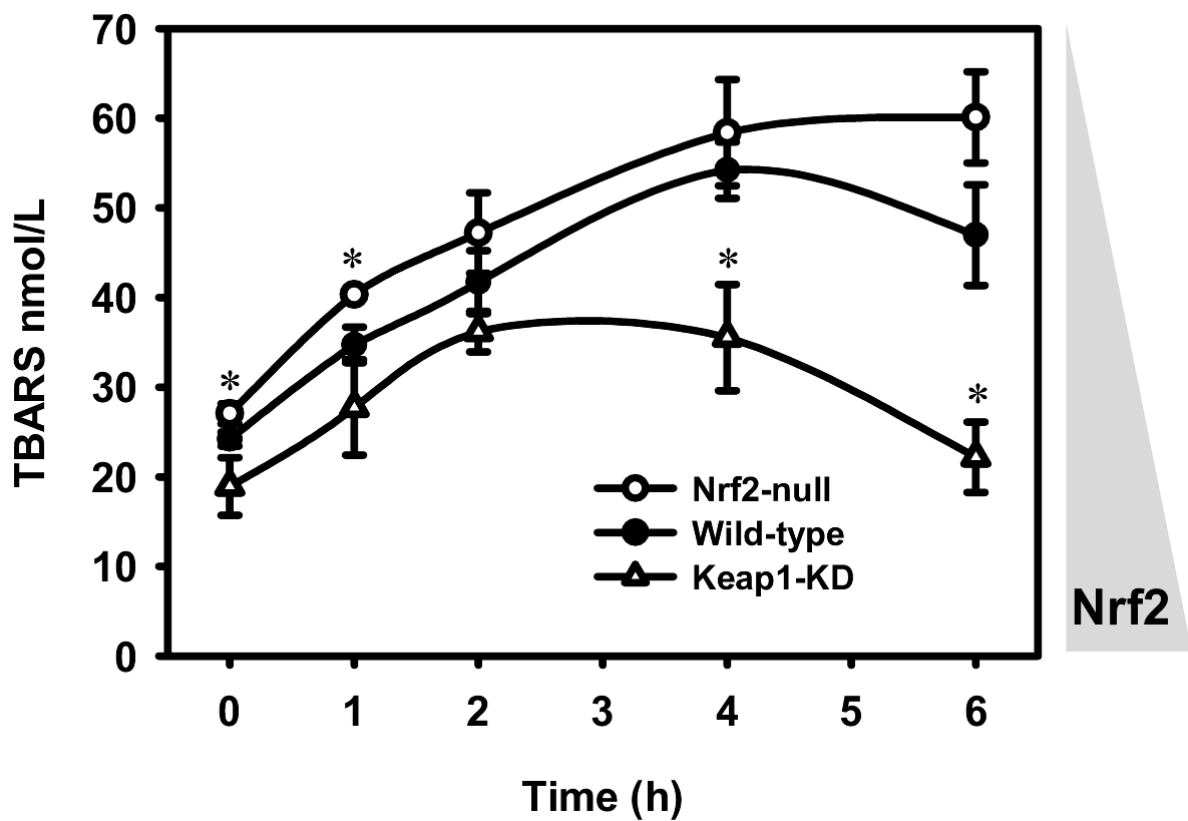
Figure 8.2. Time course of serum thiobarbituric acid-reactive substances (TBARS) in wild-type, Nrf2-null, and Keap1-KD mice after treatment with diquat dibromide (125 mg/kg, i.p.). Data are presented as malondialdehyde equivalences (nmol/L) ± S.E.M. Asterisks (*) indicate statistically significant differences from wild-type mice of the same time point ($p < 0.05$).
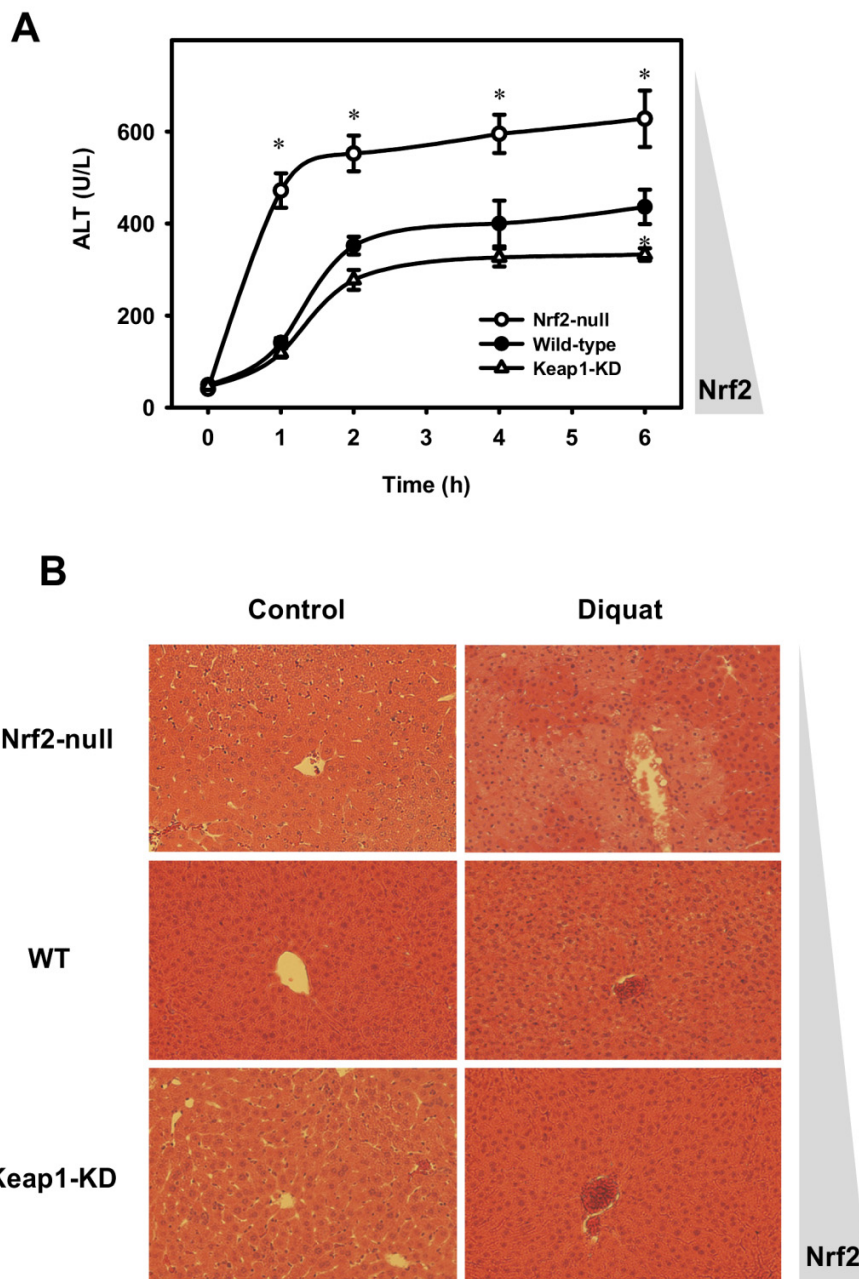
Figure 8.3. (A) Time course of serum alanine transaminase (ALT) levels in wild-type, Nrf2-null, and Keap1-KD mice after treatment with diquat dibromide (125 mg/kg, i.p.). Units are in International Units/Liter (IU/L) expressed as mean ± S.E.M. Asterisks (*) indicate statistically significant differences from wild-type mice of the same time point ($p < 0.05$). (B) Histopathological analysis of liver stained with hematoxylin and eosin in wild-type, Nrf2-null, Keap1-KD mice treated with saline (left panel) and diquat dibromide (125 mg/kg, i.p., right panel).

Glutathione and GSSG concentrations in liver

In an attempt to determine the mechanism of how the Keap1-Nrf2 signaling pathway protects against diquat-induced toxicity, GSH and GSSG concentrations were quantified in livers. The basal concentration of GSH in Nrf2-null mice was 26% lower, and in Keap1-KD mice was 20% higher than in wild-type mice. After diquat injection to wild-type mice, GSH concentrations decreased gradually to 64% of the basal level at 6 h. After diquat injection to Nrf2-null mice, GSH concentrations tended to be lower than in wild-type mice given diquat. In Keap1-KD mice, diquat did not markedly alter GSH concentrations in liver (Fig. 8.4A). The basal GSSG concentrations in livers of wild-type, Nrf2-null, and Keap1-KD mice were similar, but after diquat administration, GSSG increased in wild-type mice, but not in Nrf2-null or Keap1-KD mice (Fig. 8.4B).

Gclc mRNA expression in liver

To study the role of the Keap1-Nrf2 pathway in GSH synthesis after diquat, mRNA expression of Gclc, the rate limiting enzyme in GSH synthesis, was quantified in livers of wild-type, Nrf2-null, and Keap1-KD mice at the 6 h time point. After diquat administration, Gclc mRNA increased in both wild-type and Keap1-KD mice (52 and 75%, respectively), but not in Nrf2-null mice (Fig. 8.5).
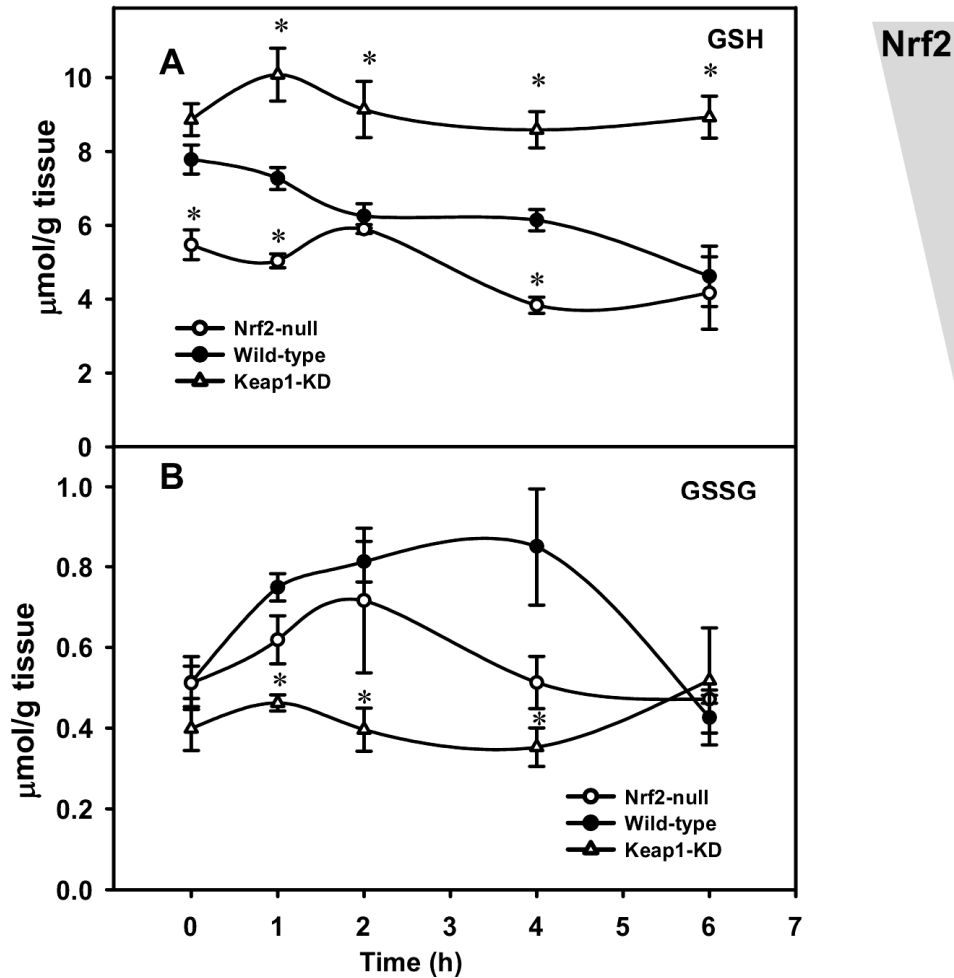
Figure 8.4. (A) Glutathione and (B) GSSG concentrations in livers of wild-type, Nrf2-null, and Keap1-KD mice after treatment with diquat dibromide (125 mg/kg, i.p.). Data are presented as µmol/g tissue or concentrations relative to wild-type controls as mean ± S.E.M. Asterisks (*) indicate statistically significant differences from wild-type mice of the same time point ($p < 0.05$).
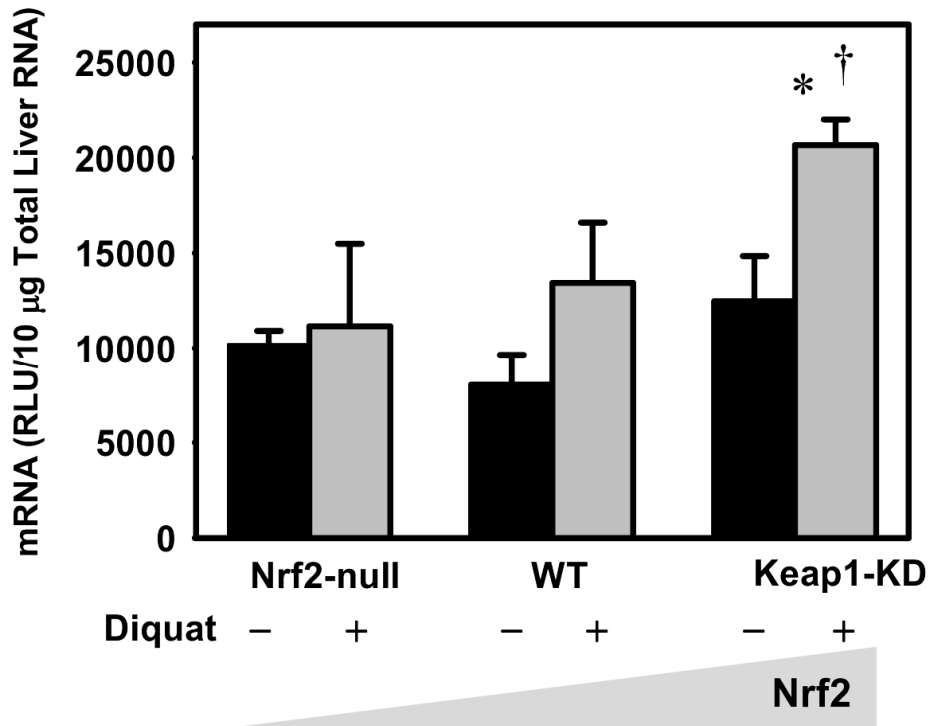
Figure 8.5. Messenger RNA expression of Gclc in livers of wild-type, Nrf2-null, and Keap1-KD mice 6h after treatment with diquat dibromide (125 mg/kg, i.p.). Data are presented as RLU ± S.E.M. Asterisks (*) indicate statistically significant differences from wild-type controls (p < 0.05).

Concentration-response and time course of ROS generation by diquat *in vitro*

To characterize diquat-induced oxidative stress in vitro, primary hepatocytes from Nrf2-null, wild-type, and Keap1-KD mice were isolated and stained with H_2DCFDA, a general indicator of ROS. Basal ROS were 58% higher in Nrf2-null hepatocytes, and 53% lower in Keap1-KD cells than wild-type hepatocytes. After administration of diquat, ROS moderately increased in wild-type cells, but markedly increased in Nrf2-null hepatocytes. In contrast, ROS in Keap1-KD cells remained at basal levels after the addition of diquat. Diquat increased ROS in hepatocytes from wild-type and Nrf2-null mice in a concentration-dependent manner. However, diquat did not increase ROS in Keap1-KD cells, even at the highest concentration of diquat (Fig.8. 6).

Lung histology

Typical photomicrographs of lung parenchyma from wild-type, Nrf2-null, and Keap1-KD mice treated with saline or diquat dibromide are shown in Fig 8.7. Lungs from wild-type and Keap1-KD mice treated with saline appeared normal, whereas lungs of Nrf2-null mice treated with saline appeared to have slight enlargement of the alveolar walls. By 6 h after diquat injection, there are structural alterations of lung parenchyma in wild-type mice, including moderate alveolar edema, intra-alveolar hemorrhage, and interstitial infiltrates; in Nrf2-null mice, severe perivascular and interstitial infiltrates, marked alveolar collapse and enlargement of alveolar walls were evident; however, there was no apparent pathology in Keap1-KD mice (Fig. 8.7).
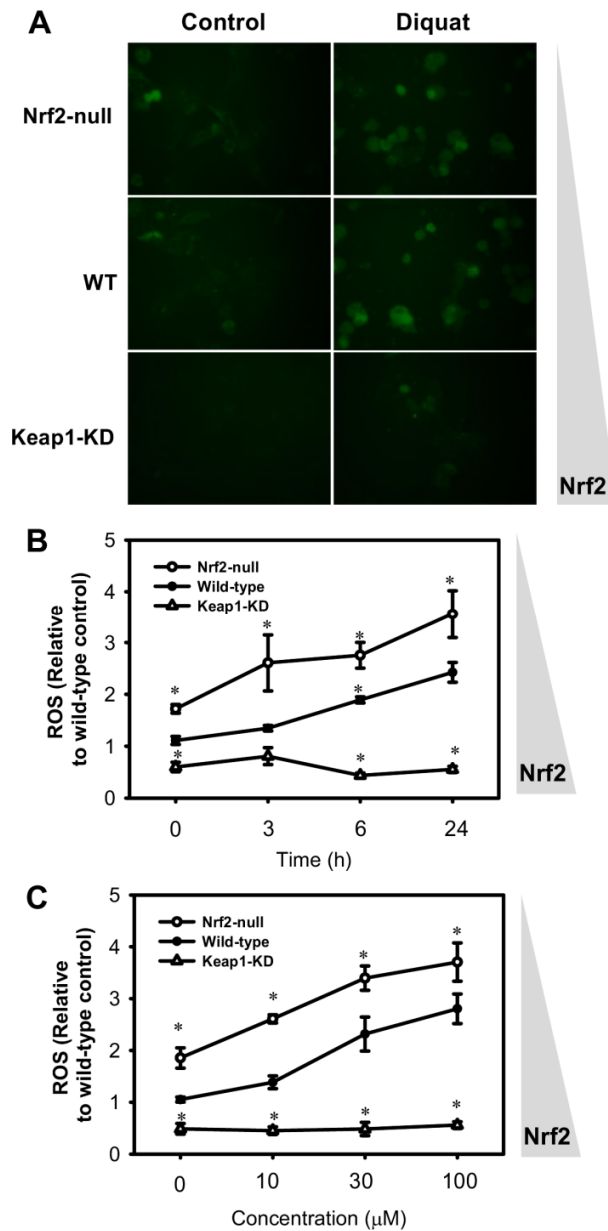
Figure 8.6. Diquat-induced oxidative stress *in vitro*. (A) DCFDA fluorescence in primary hepatocytes after diquat exposure. Primary mouse hepatocytes were isolated and treated with diquat for 24h and subjected to live cell imaging. (B) Time-response and (C) dose response of ROS production after diquat exposure in primary hepatocytes from Nrf2-null, wild-type, and Keap1-KD mice. Data are presented as Mean ± S.E.M. 3 animals per group for Fig 4B and Fig 4C. Asterisks (*) indicate statistically significant differences from wild-type cells in the same time point or concentration ($p < 0.05$).
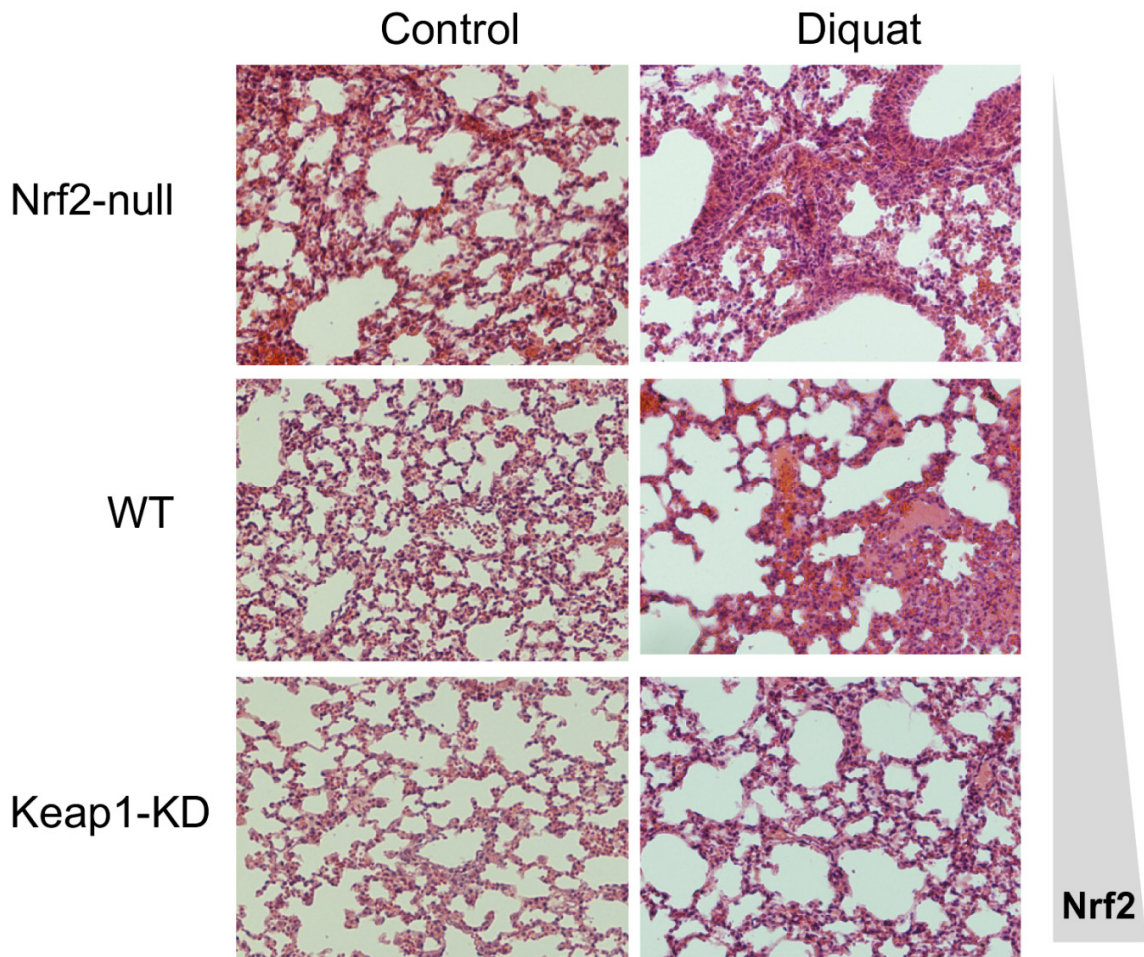
Figure 8.7. Histopathological analysis of lung parenchyma stained with hematoxylin and eosin in wild-type, Nrf2-null, Keap1-KD mice treated with saline (left panel) and diquat dibromide (125 mg/kg, i.p., right panel).

Glutathione and GSSG concentrations in lung

The basal concentration of GSH in lungs of Nrf2-null mice tended to be lower than in wild-type and Keap1-KD mice. Within 1 h of diquat exposure, GSH in lungs was decreased 40% in wild-type mice, and decreased 50% in Nrf2-null mice. In Keap1-KD mice, GSH concentrations in lungs increased 17% during the first h after diquat administration, and decreased gradually thereafter (Fig. 8.8A). GSSG concentrations in lungs of wild-type mice were higher than in Nrf2-null and Keap1-KD mice before diquat administration, and even higher 1 h after administration, and decreased 67% at the end of 6 h. GSSG concentrations in Keap1-KD mice remained unchanged at all time points (Fig.8.8B).
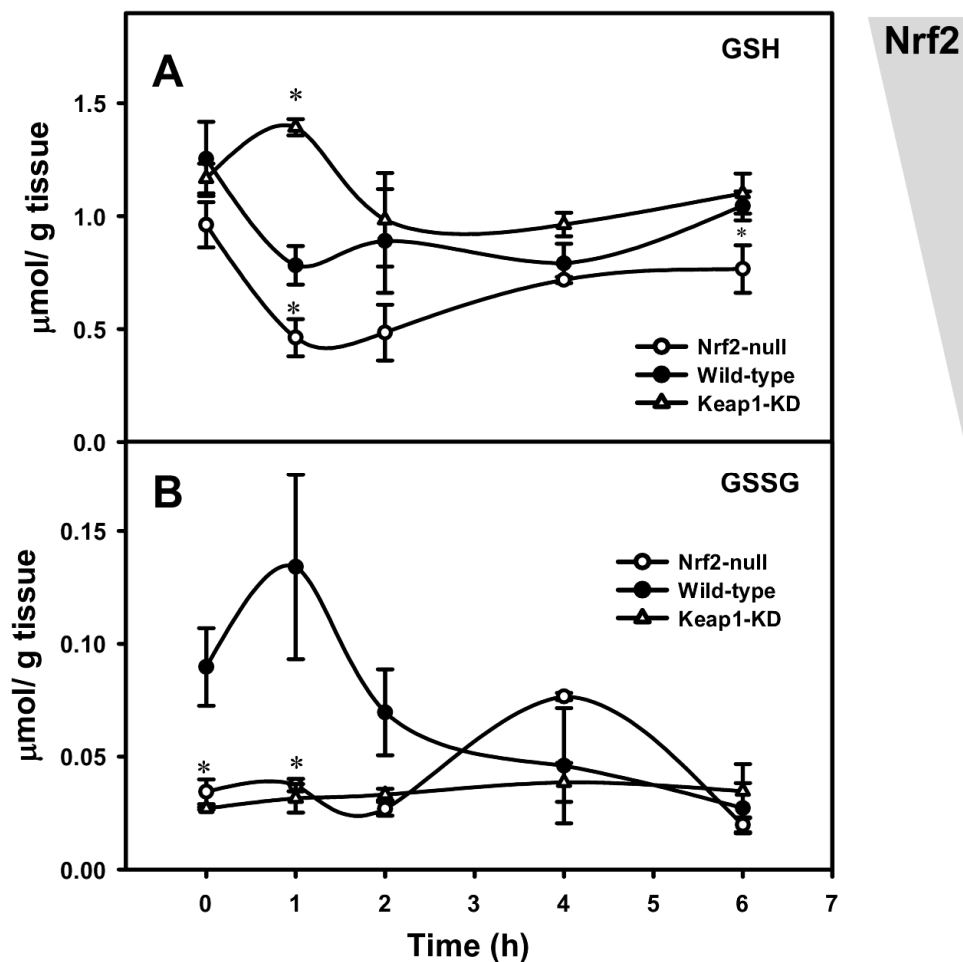
Figure 8.8. (A) Glutathione and (B) GSSG concentrations in lungs of wild-type, Nrf2-null, and Keap1-KD mice after treatment with diquat dibromide (125 mg/kg, i.p.). Data are presented as µmol/g tissue or concentrations relative to wild-type controls as mean ± S.E.M. Asterisks (*) indicate statistically significant differences from wild-type mice of the same time point ($p < 0.05$).

Discussion

In the present study, the protective role of Nrf2 against oxidative stress was investigated using diquat-induced injury as a model of excess ROS. Diquat receives a single electron from NADPH by cytochrome P450 reductase. The diquat radical formed in this step is highly unstable and transfers an electron to molecular oxygen to form a superoxide anion radical. By this mechanism, a small amount of diquat is cycled in a continuous process of receiving electrons from NADPH and donating electrons to oxygen to form large amounts of superoxide anion radicals (Fu et al., 1999). The superoxide anion radicals react with each other, forming hydrogen peroxide and molecular oxygen, either spontaneously or via the enzyme superoxide dismutase. Once protective mechanisms, such as catalase, the glutathione peroxidase system, and the thioredoxin system that detoxify hydrogen peroxide become overwhelmed, oxidative stress results, leading to cellular dysfunction and injury. Consistent with previous reports, the present study shows that diquat induces oxidative stress in *vitro and in vivo*, as demonstrated by increased lipid peroxidation products in serum (Fig. 8.2), decreased GSH content in livers and lungs (Fig. 8.4 and Fig. 8.8), and increased ROS staining in primary hepatocytes (Fig. 8.5).

Diquat produced more mortality in Nrf2-null mice than in wild-type mice, and no mortality in Keap1-KD mice (Fig.8.1). Enhanced susceptibility to diquat-induced toxicity in Nrf2-deficient cells has been reported previously (Osburn et al., 2006). Specifically, Nrf2-deficiency in embryonic fibroblasts resulted in a 5-fold increase in cell death

caused by diquat. The present study indicates that Nrf2 also protects from diquat toxicity in intact mice.

The bipyridyl herbicides, paraquat and diquat, both generate ROS *in vivo*, but they produce different target-organ toxicity as a result of a difference in tissue distribution. Paraquat distributes mainly to the lung by an active transport process (Waddell and Marlowe, 1980; Dinis-Oliveira et al., 2006), whereas diquat distributes mainly to the liver, but also to other organs (Spalding et al., 1989). The present study indicates that diquat is hepatotoxic, as indicated by increased serum ALT and histopathology of mouse liver. In addition, the presence of interstitial edema from pathological analysis confirmed acute lung injury produced by diquat.

One of the earliest targets of oxidative stress are the lipids in biological membranes. Lipid peroxidation by ROS is initiated at the polyunsaturated fatty acid side-chains, which are present in cellular membrane phospholipids (Porter et al., 1995), forming lipid hydroperoxides and resulting in reduced membrane fluidity and disturbed functions of membrane proteins. Lipid hydroperoxides can undergo iron-mediated reduction to form alkoxy radicals and iron-mediated oxidation to form peroxyl radicals, which triggers further lipid peroxidation to form cytotoxic aldehydes (Girotti, 1998). Aldehydes attack proteins and DNA, thereby propagating the initial damage in cellular membranes to other macromolecules (Dargel, 1992). Therefore, inhibiting lipid peroxidation is crucial for cells to survive from oxidative stress. In the present study, diquat-induced oxidative stress increased TBARS, a biomarker of lipid peroxidation, at

early time points in all three genotypes of mice. However, the increase of TBARS was less in Keap-KD mice, indicating Nrf2 protects against diquat-induced lipid peroxidation.

To further understand the mechanism of how Nrf2 activation reduces diquat-induced mortality and lipid oxidation, GSH and GSSG concentrations were quantified in the three genotypes of mice. GSH is the most abundant cellular thiol and provides direct protection from hydrogen peroxide. In the presence of glutathione peroxidase (Gpx), hydrogen peroxide is reduced to water at the expense of oxidizing GSH to its disulfide (GSSG). GSSG is reduced to GSH by glutathione reductase, using NADPH. The Gpx-GSH pathway is also a major intracellular antioxidative mechanism that reduces lipid peroxidation (Imai and Nakagawa, 2003), DNA fragmentation (Higuchi, 2004), and protein adduction (Filippin et al., 2008). Accordingly, free radical reactions, which can cause apoptosis and necrosis, accelerate as a consequence of GSH depletion. In addition, GSH also decreases inflammation at the site of injury (Biswas and Rahman, 2009). In the present study, diquat reduced hepatic GSH concentrations in wild-type mice, and even more in Nrf2-null mice, but not in Keap1-KD mice, indicating a strong correlation between Nrf2 activation and cellular GSH concentrations. The major organ that synthesizes GSH is the liver, which has the highest enzyme activity for GSH synthesis and the most abundant substrates for GSH biosynthesis (Meister and Anderson, 1983). After diquat administration, the GSH concentrations in livers of Keap1-KD mice are higher than in wild-type and Nrf2-null mice, indicating that Nrf2 activation is important to maintain intracellular GSH concentrations. GSH concentrations were decreased more in lung than liver in all genotypes of mice, and failed to recover to

basal levels during the observation period. However, GSH concentrations in lung did correlate with the activity of Nrf2 in the three genotypes of mice.

It is well-documented that Nrf2-null mice are more susceptible to many oxidative stress- and electrophile-induced toxicity models, such as acetaminophen- (Enomoto et al., 2001), pentachlorophenol- (Umemura et al., 2006), and carbon tetrachloride- (Xu et al., 2008) induced hepatotoxicity, as well as bleomycin- (Cho et al., 2004) and tobacco smoke- (Rangasamy et al., 2004) induced lung toxicity. However, there is conflicting data on the role of the Keap1-Nrf2 pathway on basal expression of anti-oxidative genes and redox state in animal models without a chemical challenge. Microarray analyses showed that constitutive expression of some of the genes that provide direct anti-oxidative protection, such as Cat, Txn2, Txnrd1, and Sod1, are similar in wild-type and Nrf2-null mice (Thimmulappa et al., 2002). Additionally, oxidative stress biomarkers, such as aconitase activity and TBARS, as well as GSH concentrations in embryonic fibroblasts derived from Nrf2-null mice were similar to embryonic fibroblasts derived from wild-type mice (Osburn et al., 2006). In contrast, expression of other anti-oxidative genes, such as Gpx, Gst, and Nqo1, as well as genes involved in GSH synthesis were higher in livers of wild-type mice than Nrf2-null mice (Reisman et al., 2009e). In the present study, the basal ROS of primary hepatocytes *in vitro* as well as serum TBARS concentrations *in vivo* were highest in Nrf2-null mice, and lowest in Keap1-KD mice. In addition, the basal levels of hepatic GSH were lowest in Nrf2-null mice and highest in Keap1-KD mice, indicating that Nrf2 is not only essential for the adaptive response under oxidative stress, but also critical in maintaining redox homeostasis under basal conditions.

In conclusion, the present study shows that the Keap1-Nrf2 signaling pathway plays an important role in protecting against oxidative stress-induced liver and lung injury *in vivo*, and this protective effect appears to result from Nrf2-regulated elevation of basal cellular GSH concentration and constitutive expression of GSH synthetic genes.

Chapter 9 : IMPLEMENTATION OF HIGH-THROUGHPUT SCREEN FOR INDENTIFYING SMALL MOLECULES TO ACTIVATE THE KEAP1-NRF2-ARE PATHWAY

Abstract

Nuclear factor erythroid 2–related factor 2 (Nrf2) is a transcription factor that induces a battery of cytoprotective genes involved in antioxidant defense through binding to Antioxidant Response Elements (ARE) located in the promoter regions of these genes. To identify Nrf2 activators for the treatment of oxidative/electrophilic stress-induced diseases, the present study developed a high-throughput assay to evaluate Nrf2 activation using AREc32 cells that contain a luciferase gene under the control of ARE promoters. Of the 47,000 compounds screened, 238 (top 0.5% hits) of the chemicals increased the luminescent signal more than 14.4-fold and were retested at eleven concentrations in a range of 0.01-30 µM. Of these 238 compounds, 231 (96%) increased the luminescence signal in a concentration-dependent manner. Chemical structure relationship analysis of these 231 compounds indicated enrichment of four chemical scaffolds (diaryl amides and diaryl ureas, oxazoles and thiazoles, pyranones and thiapyranones, and pyridinones and pyridazinones). In addition, 30 of these 231 compounds were extremely effective and/or potent in activating Nrf2, with more than a 80-fold increase in luminescence, or an EC_{50} lower than 1.6 µM. These top 30 compounds were also screened in Hepa1c1c7 cells for an increase in Nqo1 mRNA, the prototypical Nrf2-target gene. Of these 30 compounds, 17 increased Nqo1 mRNA in a concentration-dependent manner. In conclusion, the present study documents the development, implementation, and validation of a high-throughput screen to identify activators of the Keap1-Nrf2-ARE pathway. Results from this screening identified Nrf2 activators, and provide novel insights in chemical scaffolds that might prevent oxidative/electrophilic stress-induced toxicity and carcinogenesis.

Introduction

Oxidative stress is the consequence of imbalanced production of reactive oxygen species (ROS) and the ability of cells to detoxify these ROS, which can result in ROS-induced tissue damage. In humans, oxidative stress is involved in the pathogenesis of numerous clinical conditions, including atherosclerosis (Sugamura and Keaney, 2011), Alzheimer's disease (Axelsen et al., 2011), and rheumatoid arthritis (Filippin et al., 2008). In addition, ROS, together with other electrophiles, are capable of attacking DNA in the nucleus and become carcinogens (Jeffrey, 1985).

Data from the previous Chapters suggest potential therapeutic applications of the Keap1-Nrf2 pathway, and thus Nrf2 activators are promising drug candidates in the treatment of oxidative/electrophilic stress-induced diseases. A quantitative bioassay evaluating the induction of NAD(P)H:quinone oxidoreductase 1 (NQO1), the prototypical Nrf2 target gene, in Hepa1c1c7 murine hepatoma cells was developed and still remains a major screening tool for potential activators of the Keap1-Nrf2 pathway (Baird and Dinkova-Kostova, 2011). To date, a number of compounds with diverse chemical structures have been shown to activate Keap1-Nrf2, including oxidizable diphenols (tBHQ), dithiolethiones (oltipraz), isothiocyanates (sulforaphane), and Michael acceptors (curcumin, cinnamates, and chalcones) (Copple et al., 2010). In an effort to develop more potent and effective activators of the Keap1-Nrf2 pathway, chemical derivatives of known active compounds were synthesized and screened. The most potent known Nrf2 activator, 2-cyano-3,12-dioxoolean-1,9-bien-28-oic acid imidazole (CDDO-Im), is a semisynthetic triterpenoid derived from oleanolic acid (Dinkova-Kostova et al., 2005). Based on the structure-activity relationship analyses of the oleanolic triterpenoids, (±)-

(4bS,8aR,10aS)-10a-ethynyl-4b,8,8-trimethyl-3,7-dioxo-3,4b,7,8,8a,9,10,10a-octahydrophenanthrene-2,6-dicarbonitrile (TBE-31), was synthesized. Both CDDO-Im and TBE-31 have been shown to activate Keap1-Nrf2 pathway at nano-molar concentrations *in vitro and in vivo* (Dinkova-Kostova et al., 2010).

Despite the discovery of a few potent Nrf2 activators (CDDO compounds and TBE-31), there is limited information about the chemical scaffolds that can potentially activate Nrf2. Recently, AREc32 cells were engineered, which are MCF7 human breast cancer cells stably transfected with a luciferase reporter gene construct under the control of eight copies of rat Gsta2 AREs in the promoter region (Natsch and Emter, 2008). The ARE-promoted luciferase reporter method provides a rapid and convenient quantification of Nrf2-ARE induction by chemicals, and made large scale-screening of Nrf2 activators possible.

The aim of the present study was to develop a high-throughput assay to evaluate Nrf2 activation using the AREc32 cells, screen a library of 47,000 compounds, and to find compounds that are potent and effective activators of Nrf2. In addition, through structural activity relationship analyses, the present study also aimed to discover novel chemical scaffolds that are highly likely to activate the Keap1-Nrf2-ARE pathway. Results from this screening identified extremely strong Nrf2 activators, and provide novel insights into chemical scaffolds that might detoxify oxidative/electrophilic stress and prevent oxidative/electrophilic stress-induced toxicity and carcinogenesis.

Results

Luciferase assay signal stability

Batch processing of 384-well plates for the HTS library screen requires the readout signal to be steady for 30 min, and preferably one hr to minimize timing effects. To test the luciferase assay signal stability of AREc32 cells, they were seeded at 3000 cells/well in a 384-well plate, and tBHQ, the typical Nrf2 activator, was added to cells to make final concentrations of 0, 10, 20, or 80 μM. All wells had a final DMSO concentration of 0.5%. Twenty-four hrs after treatment, luciferase activity was assessed using the Steady-Glo luciferase assay with luminescence readout. The luminescence signal was recorded 30 min after cell lysis, and was quantified repeatedly every 30 min for six hrs. As shown in Fig 9.1A, the luminescent signal was strong and stable for over one and a half hrs after adding the luciferase reagent.

Optimization of AREc32 cells seeding density

To determine the optimal seeding density of AREc32 cells under screening conditions, cells were seeded at a range of 1,000-10,000 cells/well in a 384-well plate, and were treated with tBHQ or DMSO vehicle (0-50μM tBHQ, 0.5% DMSO). Twenty-four hrs after treatment, luciferase activity was assessed with luminescence readout. The luminescent signal was quantified 30 min after adding the luciferase reagent to the cells. Data are presented as fold increase in luminescence by tBHQ over vehicle control. As shown in Fig 9.1B, 3000-3500 cells/well provided optimal activation of the ARE-luciferase construct by tBHQ.

The effect of DMSO on cell viability and assay sensitivity

Because the compounds are maintained in 100% DMSO, the effect of DMSO on viability and assay sensitivity of AREc32 cells was investigated. Cell viability was

159

unaffected by DMSO below 0.75% (data not shown). To test the effect of DMSO on assay sensitivity, cells were seeded at 3000 cells/well in a 384-well plate and a mixture of media and DMSO was added to each well to achieve a final DMSO content of 0%-10%. Additionally, 5 µL of media with or without tBHQ was added immediately following addition of DMSO. Twenty-four hrs after treatment, luciferase activity was assessed with the luminescence readout. As shown in Fig 9.1C, the ability of tBHQ to activate the luciferase reporter construct was hindered by DMSO concentrations above 1%. To avoid cell stress that may activate undesired molecular pathways, 0.5% DMSO was selected as the maximum tolerable concentration of DMSO in the cell culture medium.

Dose-response activation of ARE-luciferase reporter construct in AREc32 cells by known Nrf2 activators

To validate the ARE-luciferase reporter assay, tBHQ and CDDO-Im, two prototypical Nrf2 activators were tested in the AREc32 cells. Cells were seeded at 3000 cells/well in a 384-well plate and treated with DMSO vehicle or compound (0-100 µM for tBHQ and 0-2 µM for CDDO-Im). Twenty-four hrs after treatment, luciferase activity was assessed by quantifying the luminescent intensity. As shown in Fig 9.2A, both tBHQ and CDDO-Im increased the luminescence signal in a dose-dependent manner, with over a 70-fold increase in luminescence at 100 µM (tBHQ) or 300 nM (CDDO-Im).

Other known Nrf2 activators, namely curcumin, sulfuraphene, and genistein, also increased the luminescence signal in AREc32 cells in a concentration-dependent manner (data not shown).
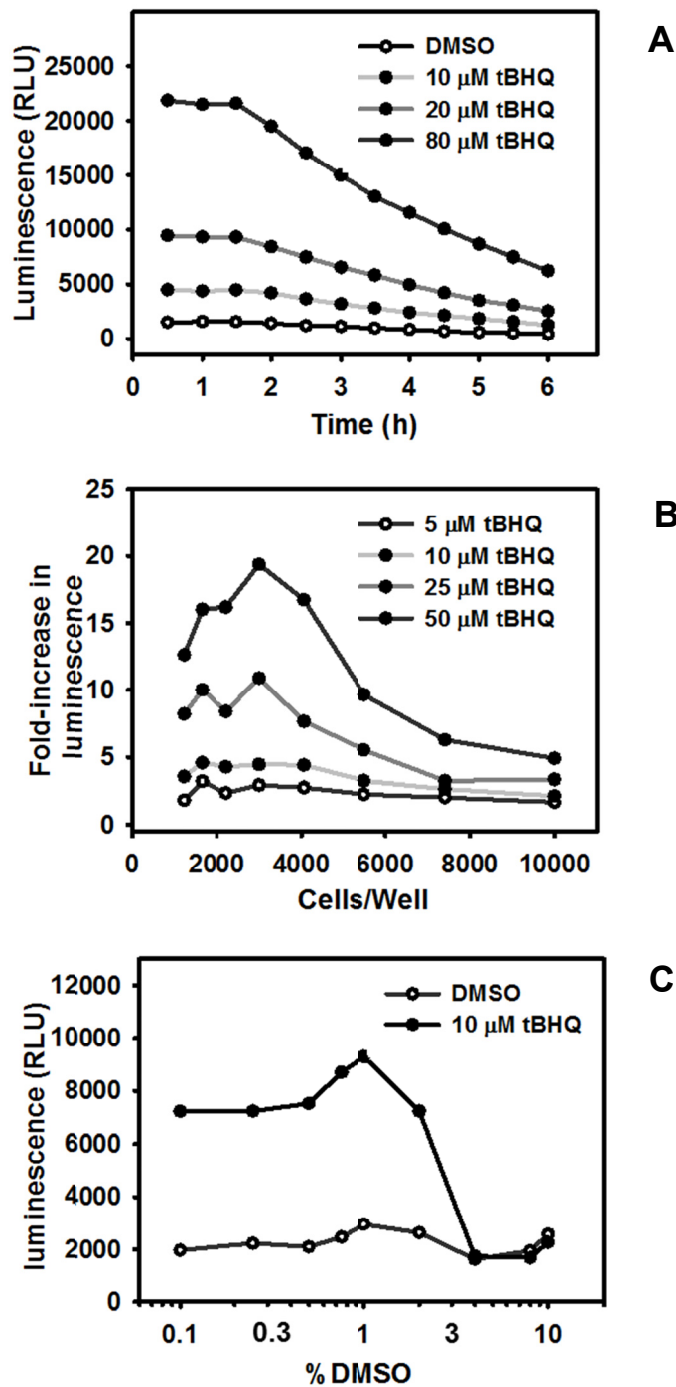
Figure 9.1. Development and optimization of an ARE induction assay in AREc32 Cells. (A) The luciferase assay signal stability in the presence of 0, 10, 20, or 80 µM tBHQ.(B) The effect of AREc32 cells seeding density on the luciferase assay sensitivity in the presence of 0, 10, 20, or 80 µM. (C) The effect of DMSO concentration on the luciferase assay sensitivity using a range of 0%-10% DMSO in the presence or absence of 0 or 10 µM tBHQ.

Pilot screening of 5040 compounds from the Microsource, Prestwick, and CMLD libraries

To further validate the ARE-luciferase reporter assay in a high-throughput manner, Prestwick library containing 1120 compounds was screened in the AREc32 cells at seven concentrations and within a range of 0.25-16 µM. Twenty-one compounds (top 1.9%) increased the luminescence signal in a concentration-dependent manner, with the maximum fold-induction value higher or comparable to tBHQ (data not shown). Microsource library containing 2000 compounds, and CMLD library containing 1920 compounds were screened at a final concentration of 10 µM. The fold-induction of the luminescent signals of the tested compounds are shown in Fig. 9.2B, with the fold-induction values of positive controls for comparison. Specifically, the fold-induction values of compounds in Microsource and CMLD libraries were tested in a final concentration of 10 µM, and compounds in the Prestwick library were treated at 8 µM.

The Z' factor measure of assay robustness and variability was plotted for the 16 validation library plates (Fig. 9.2C). Z' score of each plate was greater than 0.6, confirming the quality of the assay methodology.
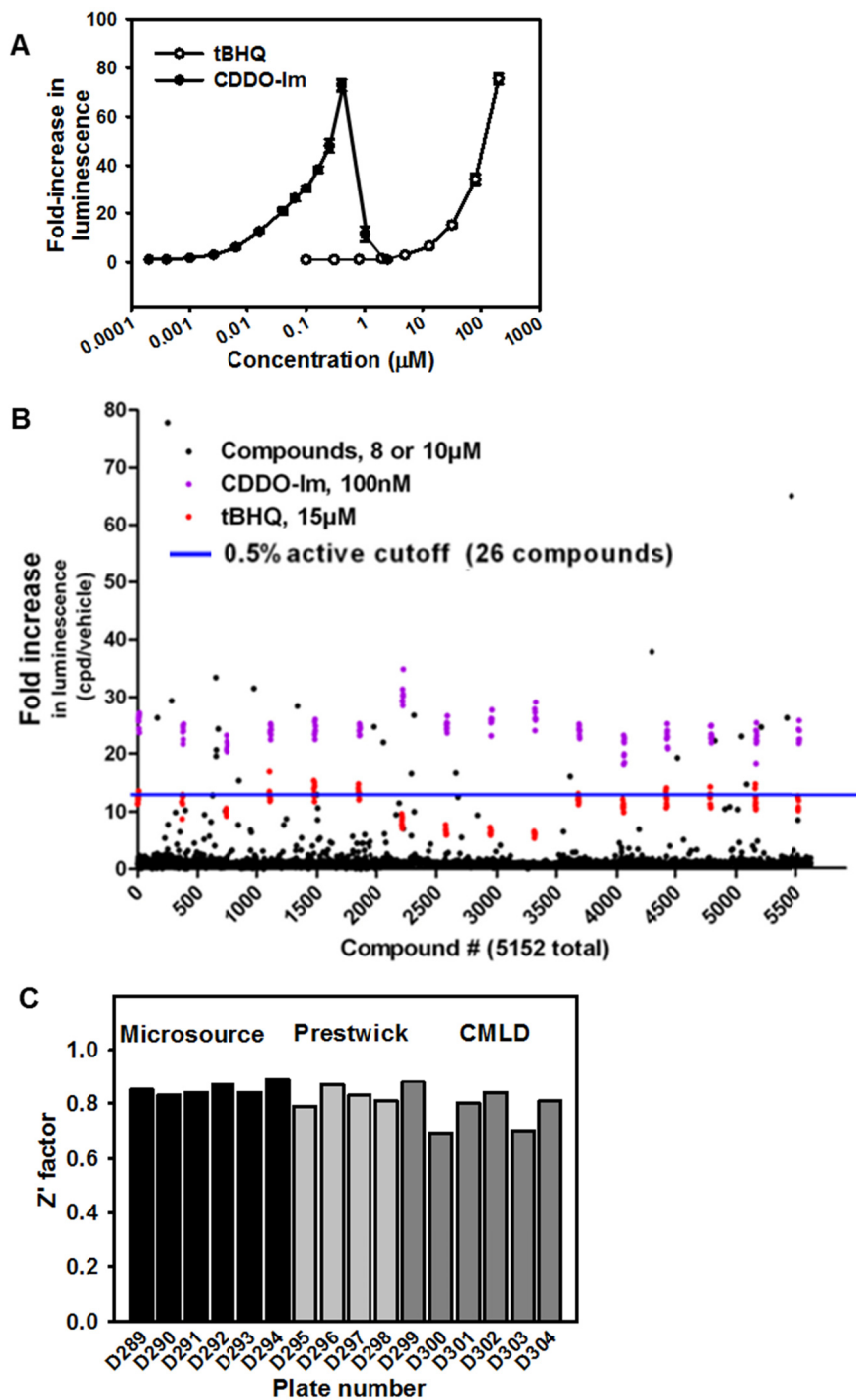
Figure 9.2. Validation of the ARE induction assay using known Nrf2 activators and through pilot screening. (A) Concentration-response curves of tBHQ and CDDO-Im to increase the luminescent signal in AREc32 cells. (B) Activity spread of compounds in Microsource, Prestwick, and CMLD libraries together with positive controls. Compounds in Microsource and CMLD libraries were tested at 10 μM, and compounds in Prestwick library were tested at 8 μM. (C) Z' scores for 16 pilot screening plates.

Full screening of 47,000 compounds from the Microsource, Prestwick, and Chembridge Libraries

After the luciferase-based reporter assay was validated in a high-throughput system, the full library containing 47,000 compounds was screened using this assay. The fold increase in luminescence, indicative of Nrf2 activation by compounds in AREc32 cells, was plotted against each individual well of the libraries (Fig. 9.3A). The majority of compounds did not activate Nrf2, and were densely packed at the bottom of the scatterplot. Only the top 0.5% hits (238 compounds) increased the luminescence more than 14.4-fold. A histogram summarizing the frequency distribution of the ability of the compounds to increase luminescence over the DMSO control was shown in Fig 9.3B. The majority of the compounds did not activate Nrf2. The top 1% hits (485 compounds) increased the luminescence more than 9-fold, the top 0.5% hits (238 compounds) increased the luminescence more than 14.4-fold, the top 0.25% hits (119 compounds) increased the luminescence more than 20-fold, and the top 0.1% hits (48 compounds) increased the luminescent signal more than 28-fold.

Dose-response curves for the 4 compounds with the highest maximal ARE activation

The most active 238 compounds (top 0.5% hit) from the full library screening were retested at multiple concentrations, and 91% of them (216 compounds) activated the Nrf2 pathway in a concentration-dependent manner. Among those 216 validated hits, 18 compounds were shown to be extremely effective and each produced a maximum fold-activation higher than did CDDO-Im. The concentration-response curves of the top
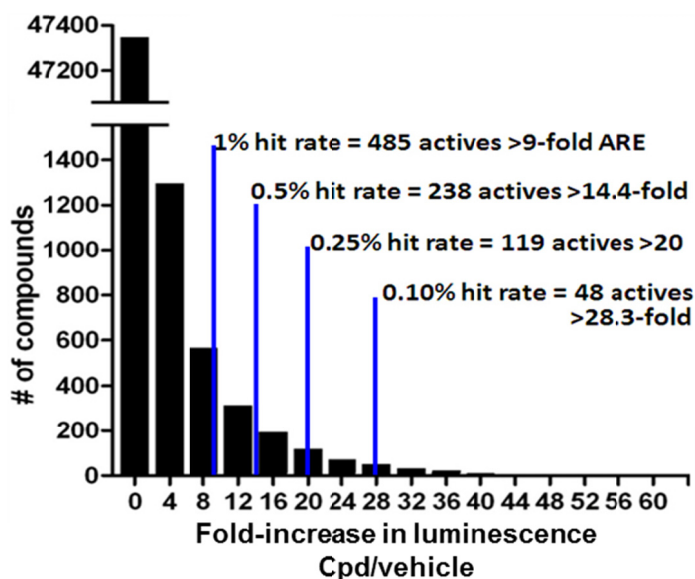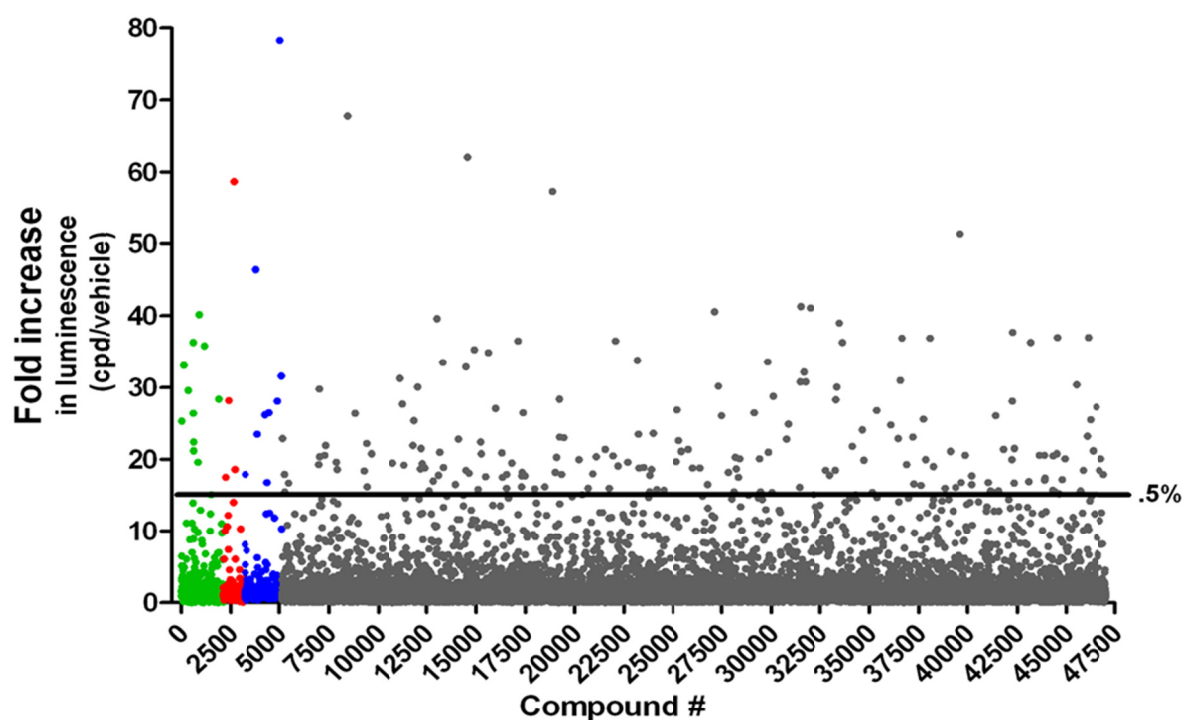
Figure 9.3. Full library screening for Nrf2 activators through ARE induction assay in AREc32 cells. (A) The scatterplot distribution of the screening actives from the ARE library screen was calculated using data from the Chembridge, Prestwick, Microsource, and CMLD library compounds. The fold increase in luminescence, indicative of ARE activation by compounds in AREc32 cells, is plotted against each individual well of the libraries. (B) Frequency distribution of the Chembridge, Prestwick, Microsource, and CMLD library compounds to increase the luminescent signal in AREc32 cells.

165

4 compounds were shown in Fig 9.4A. Compound KU0006807 increased the luminescence signal 125-fold at 18 µM, KU 0105510 increased the luminescence signal 119-fold at 18 µM, KU0103737 increased the luminescence signal 115-fold at 3.9 µM, and KU0017619 increased the luminescence signal 111-fold at 18 µM. The chemical structure of KU0006807, KU 0105510, KU0103737, and KU0017619 are shown in Fig 9.4B.

Dose-response curves for the 4 compounds with the lowest EC$_{50}$ for Nrf2-ARE activation.

Among those 247 validated hits from screening the full library, 6 compounds were shown to be extremely potent and had EC$_{50}$ values lower than 1 µM. However, none of the compounds tested had an EC$_{50}$ value lower than CDDO-Im. The concentration-response curves of the top 4 compounds are shown in Fig 9.4C. KU0009102 had an EC$_{50}$ value of 0.7 µM, and the highest Nrf2 activation was 74-fold; KU0008241 had an EC$_{50}$ value of 0.9 µM, and the highest Nrf2 activation was 46-fold; KU0025955 had an EC$_{50}$ value of 0.9 µM, and the highest Nrf2 activation was 72-fold; and KU0012935 had an EC$_{50}$ value of 1 µM, with the highest Nrf2 activation was 47-fold. The chemical structure of KU0009102, KU0008241, KU0025955, and KU0012935 are shown in Fig 9.4D.

Structure clusters of hits from the primary screening

The chemical structures of the top 238 hits fall into four clusters. The chemical scaffolds of the clusters, as well as the compound numbers were noted in Fig. 9.5. Cluster 1 contains 80 structures that were related diaryl amides and diaryl ureas, and 10 of them were very potent with EC$_{50}$ values lower than 2 µM. Cluster 2 contains 22
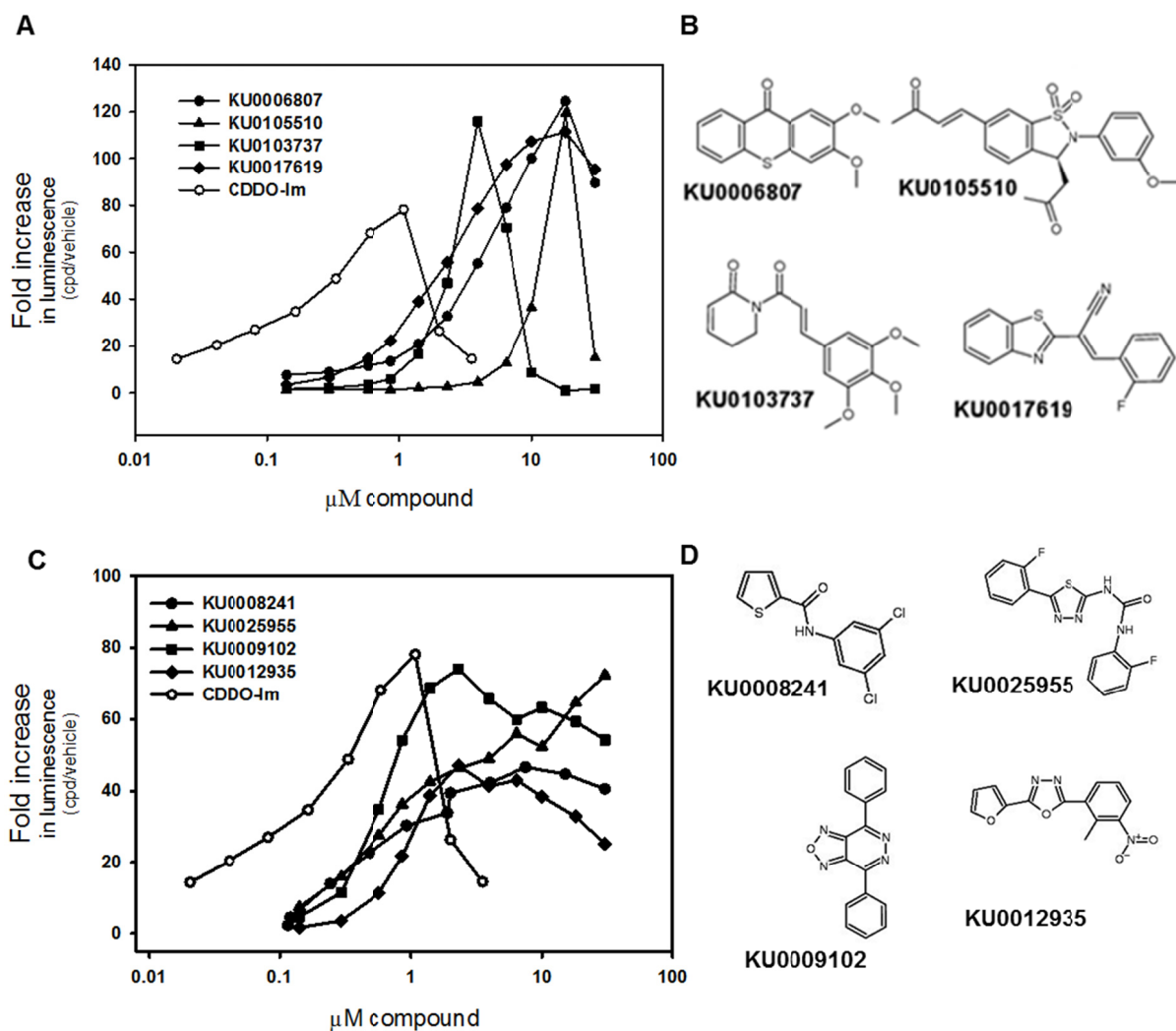
Figure 9.4. Concentration-response curves of the most effective and potent compounds. Concentration-response curves of (A) top four compounds with greatest maximum fold-increase in luminescent signal and (B) top four compounds with lowest EC50. AREc32 cells were treated with compound (0.01-30 µM) or DMSO vehicle. 24 hours after treatment, luciferase activity was assessed using the Steady-Glo luciferase assay with luminescence readout. The luminescence of each well was divided by the median luminescence of the DMSO vehicle control wells to generate the fold ARE activation.

structure-related oxazoles and thiazoles, and eight of them were highly potent with EC_{50} values lower than 2 µM. Cluster 3 contains 23 structure-related pyranones and thiapyranones, including one highly potent compound with an EC_{50} lower than 2 µM. Cluster 4 contains 22 structure-related pyridinones, pyridazinones, and pyrimidones, but none had EC_{50} values lower than 2 µM.

Induction of Nqo1 by the top 30 hits from the primary screening in Hepa1c1c7 cells

To validate the active compounds using a different technique than the ARE-luciferase assay, and to determine the ability of active compounds to induce cytoprotective genes, a secondary screen assay was developed to quantify Nqo1 mRNA in Hepa1c1c7 cells. As shown in Fig 9.6A, both tBHQ and CDDO-Im increased Nqo1 mRNA in a concentration-dependent manner, with over a 7-fold increase in Nqo1 mRNA with 30 µM tBHQ or 100 nM CDDO-Im.

Nineteen compounds with the lowest EC_{50} values and 14 compounds with the highest maximum increase of luminescence signal from the primary screen were selected for the secondary screen. Three compounds (KU0002640, KU0003452, and KU0013654) were shown to activate Nrf2 at both the lowest EC_{50} concentrations and the highest maximum increase of luminescence. Thus, 30 compounds were screened in Hepa1c1c7 cells at six concentrations (0-3 µM). Among those 30 compounds, 17 of them increased Nqo1 mRNA in a concentration-dependent manner, and the concentration-response curves of the most effective four compounds are shown in Fig 9.6B. Specifically, KU002640, which has both lowest EC_{50} and highest Nrf2 activation in the primary screen, also increased Nqo1 mRNA the most in the secondary screen.
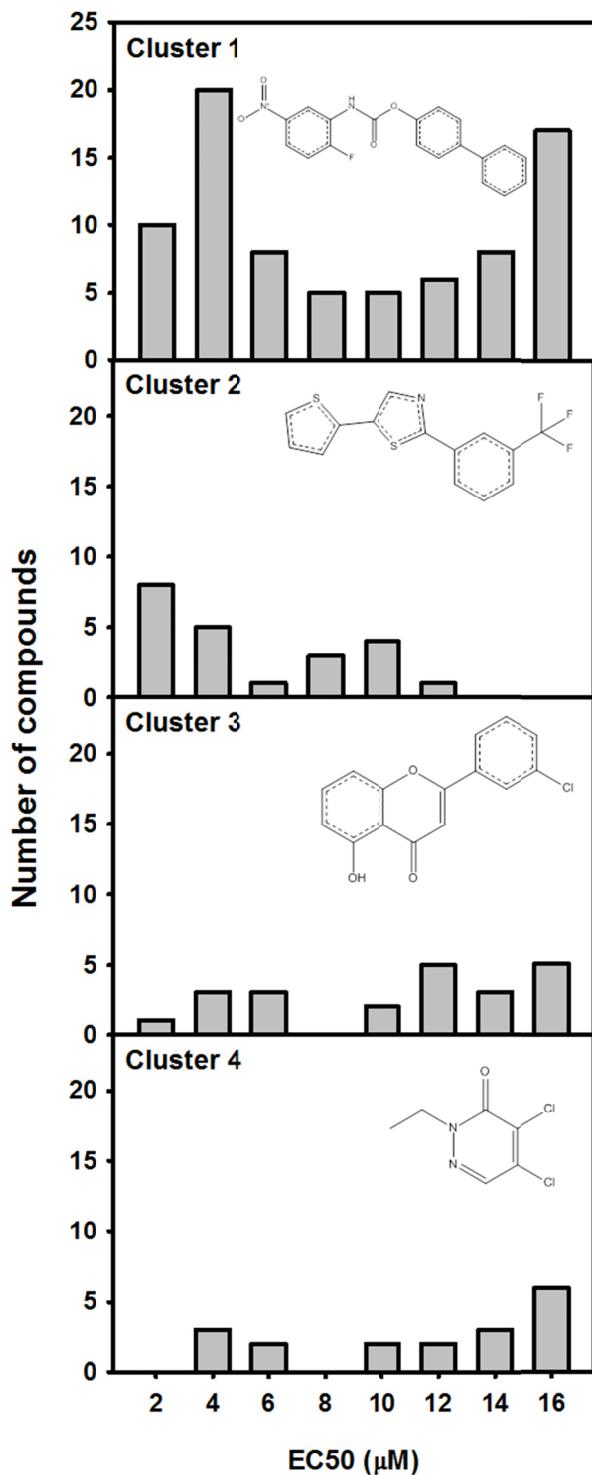
Figure 9.5. Chemical scaffolds clustered in the top 247 validated hits from the primary screening. Preliminary hit clustering was based on the EC_{50} value from the concentration-response curves of the top 240 compounds, and accomplished via the Selector program from Tripos via the Jarvis Patrick routine, using default parameters.
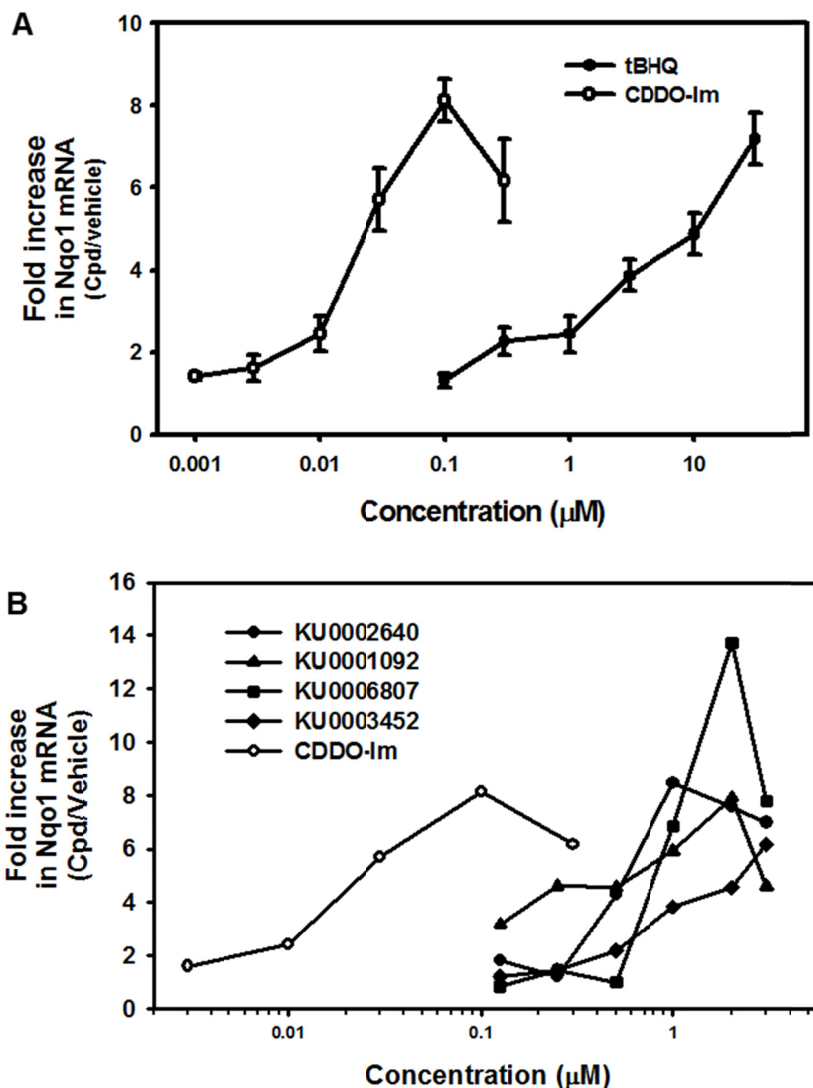
Figure 9.6. Concentration-response curves of known Nrf2 activators and most active compounds from the secondary screening. Concentration-response curves of (A) tBHQ and CDDO-Im, and (B) top 4 compounds from the secondary screening. Hepa1c1c7 cells were treated with compound (0.01-3 µM) or DMSO vehicle. 24 hours after treatment, mRNA of Nqo1 was quantified using reverse transcription q-PCR analysis. Fold-increase in Nqo1 mRNA was normalized by cells treated with DMSO vehicle.

DISCUSSION

The present study describes the development, implementation, and validation of a high-throughput screen to identify activators of the Keap1-Nrf2-ARE pathway. Using a luciferase-based assay driven by AREs in the promoter region of the luciferase gene, the AREc32 cells provided a rapid and convenient quantification of Nrf2-ARE induction by small molecules, and made the large scale-screening for Nrf2 activators possible.

In contrast to many focused-screenings for Nrf2 activators in previous reports, which compared the efficacy and potency of potential Nrf2 activators that were derived from a single chemical scaffold (Lee et al., 2010a; Tanaka et al., 2010; Kumar et al., 2011b), the present study screened 47,000 chemicals with diverse sources and chemical structures. This increased the chances of identifying novel chemical scaffolds for analogs to further improve potency, efficacy, and pharmacokinetics. The present study summarized four novel chemical scaffolds that clustered in the top 0.5% hits: (1) diaryl amides and diaryl ureas, (2) oxazoles and thiazoles, (3) pyranones and thiapyranones, and (4) pyridinones and pyridazinones. Among these four chemical clusters, cluster 1 contains the largest number of the top 0.5% hits (80 hits in cluster 1, 22 hits in cluster 2, 23 hits in cluster 3, and 22 hits in cluster 4), and contains the most number of hits with EC_{50} values less than 1.4 µM (5 hits in cluster 1, 4 hits in cluster 2, and no hits in cluster 3 or cluster 4). Thus, the chemical scaffold of cluster 1 may have the greatest potential for designing chemical analogs and to develop strong Nrf2 activators.

The present study validates the top 0.5% hits (238 compounds) with eleven concentrations in a wide range of concentrations. Thus, the EC_{50} value for activating

Nrf2 of each compound is available, which makes the comparison of the potency of the compounds possible. In addition, the concentration-response assay also generates the highest maximum fold-increase in luminescence data, and the ranking of the top hits was modified accordingly. For example, KU0105510 was shown to increase the luminescence 26-fold at 10 µM. However, the concentration-response assay shows that KU0105510 can increase the luminescence 119-fold at 18 µM, which makes it the second most effective hit in the full library (Fig. 9.4A). Some extremely potent compounds activated Nrf2 at low concentrations, and the activity decreased at higher concentrations. For example, KU0103737 increased the luminescent signal by 18-fold at 10 µM. However, the concentration-response assay shows that KU0103737 induced the luminescent signal most at 3.9 µM (116-fold), and the induction was blunted at higher concentrations (Fig. 9.4). Collectively, the concentration-response assay identified extremely effective and potent compounds among the top 0.5% hits.

The concentration-response studies also revealed two distinct patterns in Nrf2-ARE induction. The first battery of hits (example: KU0103737 and KU0105510) increased the luminescent signal markedly (over 110-fold), but the increase was blunted at higher concentrations after reaching the maximum fold-increase. The second battery of hits (example: KU0009102 and KU0003004) increased the luminescence moderately (70-fold), reached a plateau, but also increased the luminescence moderately (60-70 fold) at higher concentrations (6-30 µM). Compared with the first battery of hits, the second battery of hits may be more plausible for drug development to have a steady effect over a wide range of drug concentrations.

For luciferase reporter-based assays, one major concern is identifying false active compounds that increase the luminescent signal not through activation of the target, but through stabilization of the luciferase enzyme. Therefore, a counter screen was performed to rule out such false positive hits. The 196 hits from the primary screen were randomly selected and tested for the capability of stabilizing purified firefly luciferase. Among these 196 hits, only 11 hits tested stabilized luciferase enzyme, and thus could be false positives (data not shown).

To investigate whether the validated hits from the primary screen can also induce Nrf2 target genes, a secondary screen was designed to test the ability of the hit compounds to induce Nqo1, the prototypical Nrf2 target gene, in Hepa1c1c7 cells. The result shows that 17 of the 30 compounds increase Nqo1 mRNA in a concentration-dependent manner. The relatively low validation rate may result from four reasons. First, once Nrf2 translocates into the nucleus upon activation, Nrf2 heterodimerizes with other transcription factors (example: small Mafs, c-Jun, and c-Fos) and Nrf2-ARE signaling is affected by these Nrf2-binding transcription factors. Second, ERα was shown to bind Nrf2 in the nucleus and facilitates Nrf2-dependent gene transcription (Ansell et al., 2005). Thus, the different responses of AREc32 cells and Hepa1c1c7 cells to Nrf2-ARE activation may result from distinct estrogen signaling in these two cell lines (human breast cancer cells versus mouse hepatoma cells). Thirdly, the luciferase gene in the AREc32 cells contains eight AREs in the promoter region (Wang et al., 2006). However, the mouse Nqo1 gene is induced through one functional ARE (Malhotra et al., 2010). Thus, the secondary assay may be less sensitive to Nrf2 activators than the primary

assay. Lastly, the AREc32 and Hepa1c1c7 cells may have distinct expression of uptake transporters, resulting in different bioavailability of the test compounds.

As for all transcription activation-based assays, neither the primary nor the secondary screening assay provide information about how active compounds activate the Keap1-Nrf2-ARE pathway. However, previous reports suggest that these active compounds may activate Keap1-Nrf2-ARE pathway through multiple mechanisms (Giudice et al., 2010), as shown in Fig. 9.7. Some active compounds may disrupt binding of Keap1 to Nrf2, leading to the release of Nrf2, and allowing Nrf2 to translocate to the nucleus (Dinkova-Kostova et al., 2002). Some active compounds may lead to ubiquitination of Keap1 instead of Nrf2, and facilitate Nrf2 accumulation (Zhang et al., 2005). Some active compounds may cause an inactivation of the Nrf2 export signal, increasing Nrf2 accumulation in the nucleus (Li et al., 2006). Some active compounds may increase nuclear export of Bach1, which competes with Nrf2 for small Maf binding (Suzuki et al., 2003). Lastly, some active compounds may activate protein kinase cascades (example: MAPK and PI3K) (Eggler et al., 2008), causing enhanced Nrf2 phosphorylation.

In conclusion, the present study documents the development, implementation, and validation of a high-throughput screen to identify activators of the Keap1-Nrf2-ARE pathway. Eight compounds which are extremely potent and effective in activating Nrf2 were uncovered. In addition, the present study also summarized four novel chemical scaffolds that may be have great potential to activate Nrf2, and thus could be used in the therapy of oxidative/electrophilic stress-induced diseases.
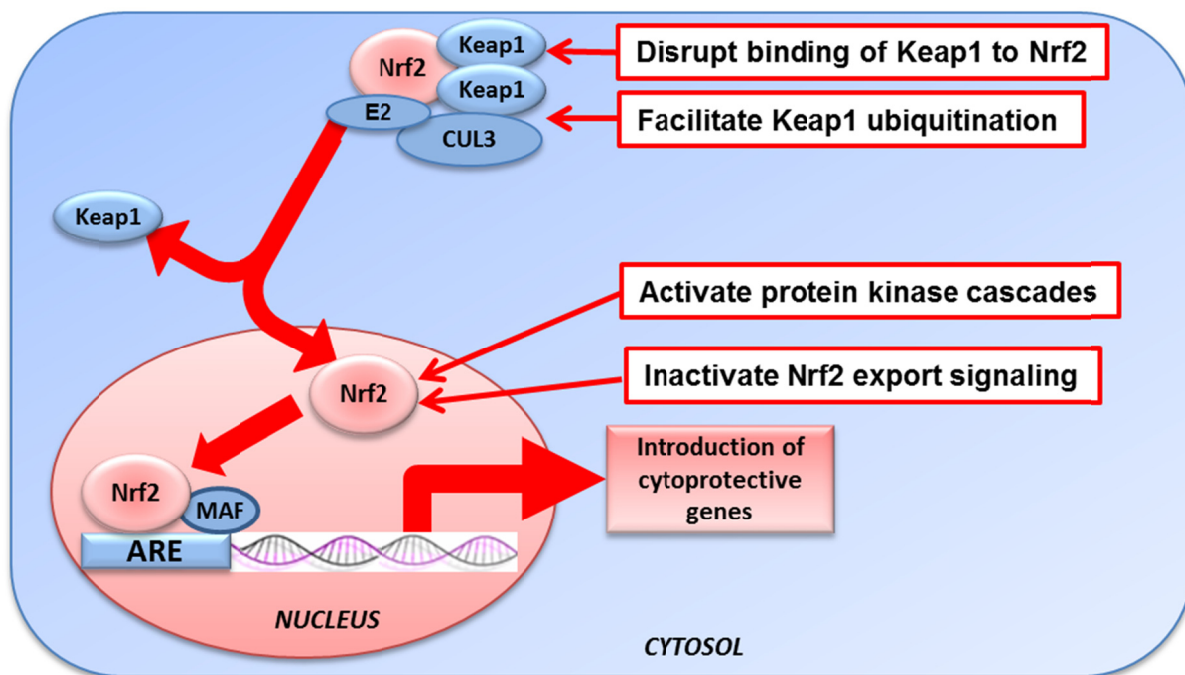
Figure 9.7. Hypothetical modes of action of actives compounds. Four potential mechanisms of action for hit compounds to activate Keap1-Nrf2-ARE pathway. Hit compounds can disrupt binding of Keap1 to Nrf2, facilitate Keap1 ubiquitination, inactivate Nrf2 export signaling, or activate protein kinase cascades for Nrf2 phosphorylation.

Chapter 10 : SCREENING OF NATURAL COMPOUNDS AS ACTIVATORS OF THE KEAP1-NRF2-ARE PATHWAY

Abstract

Nuclear factor erythroid 2-related factor 2 (Nrf2) is a master regulator that promotes transcription of cytoprotective genes in response to oxidative/electrophilic stress. A large number of natural dietary compounds have been reported to induce genes involved in antioxidant defense and phase-II drug metabolism through activating Nrf2. To select natural compounds as Nrf2 activators and compare their efficacy and potency to activate Nrf2, a library of 54 natural compounds were collected and screened using AREc32 cells that contain a luciferase gene under the control of ARE promoters. Each natural compound was tested at 13 concentrations: 0.02, 0.04, 0.08, 0.16, 0.32, 0.59, 1, 2, 3.5, 6.5, 10.7, 18, and 30 µM. Known Nrf2 activators, *tert*-butylhydroquinone (*t*BHQ) and 2-cyano-3,12-dioxooleana-1,9-diene-28-imidazolide (CDDO-Im), were tested as positive controls in parallel with the natural compounds. Among the 54 tested natural compounds, andrographolide had the highest efficacy, followed by *trans*-chalcone, sulforaphane, curcumin, flavone, kahweol, and carnosol, all which had better efficacy than *t*BHQ. Among the compounds tested, CDDO-Im was the most potent, with an EC50 at 0.41 µM. Seven of the natural compounds, namely andrographolide, *trans*-chalcone, sulforaphane, curcumin, flavone, kahweol, and cafestol had higher EC50 values than CDDO-Im, but lower than *t*BHQ. The present study provides insights in which natural compounds activate the Keap1-Nrf2 pathway and thus might be useful for detoxifying oxidative/electrophilic stress.

Introduction

A number of natural compounds are known to be antioxidants. Some of these natural compounds have been shown to exhibit antioxidant effects through activating the Nrf2 pathway. For example, oleanolic acid is known to protect against the toxicity of multiple hepatotoxicants (Liu et al., 1995a) by unknown mechanisms. Recently, it was reported that oleanolic acid stimulates the nuclear translocation of Nrf2 and induces Nrf2-dependent genes, which contributes to protection from acetaminophen hepatotoxicity (Reisman et al., 2009a). Carnosol and curcumin, purified natural compounds, as well as extracts from coffee, thyme, broccoli, rosemary, turmeric, and red onion have been shown to activate the Keap1-Nrf2 pathway *in vitro* and *in vivo* (Balstad et al., 2011). Other numerous natural compounds, including sulforaphane, allyl sulfides, resveratrol, and a battery of dietary flavonoids have been shown to activate the Keap1-Nrf2 pathway and have chemopreventive effect in various cell lines and tissues (Surh et al., 2008).

In addition to descriptive studies showing protective effects of natural compounds against oxidative/electrophilic stress through activating Nrf2, studies revealing molecular mechanisms of how natural compounds activate the Keap1-Nrf2 pathway have provided further knowledge to develop Nrf2 activators as potential therapeutic drugs. For example, quercetin was shown to increase Nrf2 mRNA and protein synthesis, and reduce Keap1 protein through post-translational modification in HepG2 cells (Tanigawa et al., 2007). Carnosol activates the PI3K-Akt pathway to induce phosphorylation and translocation of Nrf2 into the nucleus of P12 cells (Martin et al., 2004). Sulforaphane causes Nrf2 to escape from Keap1-mediated degradation in NIH3T3 cells (Zhang and

Hannink, 2003), as well as ubiquitination and degradation of Keap1 to facilitate Nrf2 activation in COS-1 cells (Zhang et al., 2005).

Collectively, various natural chemicals act as antioxidants and are used for chemoprevention and therapy of oxidative/electrophilic stress-induced tissue damage. However, given the fact that Nrf2 activation also leads to induction of certain phase-I and phase-II drug metabolism genes as well as efflux transporters, Nrf2 activators may be involved in drug-drug interactions and chemotherapeutic resistance. Despite studies that investigated the effect and mechanisms of individual natural compounds on the Keap1-Nrf2 pathway, there are no data comparing the efficacy and potency of natural compounds to activate Nrf2. In the present study, 54 natural compounds were tested as potential Nrf2 activators, and their efficacy and potency to activate Nrf2 was examined using AREc32 cells, which contain a luciferase gene under the control of eight copies of the rat ARE in the promoter region. Results from this screening provide novel insights in which natural compounds might detoxify oxidative/electrophilic stress.

Results

Induction of ARE-regulated luciferase activity by known Nrf2 activators

To validate the AREc32 cell line model for screening Nrf2 activators from a natural compound library, *t*BHQ, a prototypical Nrf2 activator, and CDDO-Im, an extremely potent Nrf2 activator, were tested in the assay. Both tBHQ and CDDO-Im increased the luminescence signal in a concentration-dependent manner. *t*BHQ increased the luciferase activity at concentrations higher than 2 μM, and the luciferase activity was increased 14-fold at 30 μM (Fig. 10.1A). In contrast, CDDO-Im increased
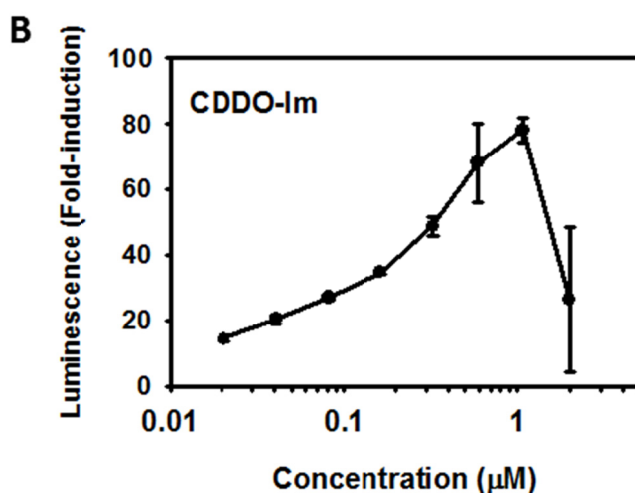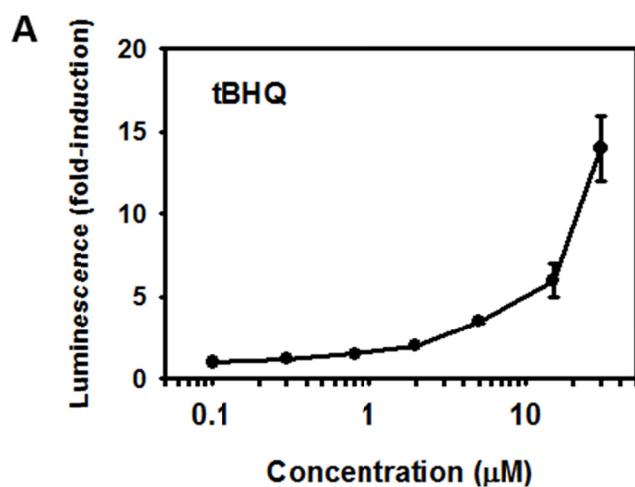
Figure 10.1. Dose response activation of ARE luciferase reporter construct in AREc32 cells by (A) tBHQ and (B) CDDO-Im. AREc32 cells were seeded at 3,500 cells/well in a 384-well plate, 46μL/well. 24 h after seeding, cells were treated with compound (tBHQ or CDDO-Im, 0.5% DMSO) or DMSO vehicle. 24 h after treatment, luciferase activity was assessed using the Steady-Glo luciferase assay with a luminescence readout. The luminescence of each well was divided by the median luminescence of the DMSO vehicle control wells to generate the fold Nrf2 activation.

the luciferase activity 13-fold at 0.02 µM, had maximum induction at 1 µM (77-fold), but the induction of luciferase activity was blunted at higher concentrations (Fig. 10.1B).

Induction of ARE-regulated luciferase activity by natural compounds

Fifty-three natural compounds, as potential Nrf2 activators, were screened using the AREc32 cell line. The maximum-fold induction and EC_{50} concentration of each individual compound are summarized in Table 10.1, and the maximum fold-induction value as well as EC_{50} concentrations for tBHQ and CDDO-Im are listed as positive controls. As shown in Fig. 10.2, andrographolide produced the highest maximum-fold induction over vehicle controls, with an 88-fold increase in luminescence at 30 µM. Six natural compounds had a lower induction of luminescence signal than CDDO-Im but higher than tBHQ: *trans*-chalcone (50-fold), sulforaphane (46-fold), curcumin (39-fold), flavone (35-fold), kahweol (30-fold), and carnosol (15-fold). Six additional natural compounds, namely cafestol, caffeic acid, chlorgenic acid, allyl disulfide, chrysin, and myricetin were less effective than tBHQ, but still produced moderate induction of the luminescence signal (5-13 fold).

EC_{50} values of tBHQ, CDDO-Im, and the natural compounds to activate the Nrf2 pathway are summarized in Fig. 10.3. The concentration-response curve of each compound was fitted to a log-linear extrapolation model and EC_{50} values were calculated as constrained to a 100-fold induction. Among all the compounds tested, CDDO-Im was the most potent, with an EC_{50} of 0.41 µM. There were seven compounds that had higher EC_{50} values than CDDO-Im, but lower EC_{50} values than tBHQ: andrographolide (17 µM), *trans*-chalcone (18 µM), sulforaphane (33 µM),

Table 10.1. Chemical names, EC_{50} (constrained to 100-fold), and maximum fold-induction of all the test natural chemicals.

Compound	EC_{50} (µM)	Maximum fold-induction
CDDO-Im	0.41	78
Andrographolide	17	89
Trans-chalcone	18	52
Sulforaphane	33	47
Curcumin	36	40
Flavone	42	36
Kahweol	41	31
tBHQ	61.6	20
Cafestol	51	14
Carnosol	>100	17
Caffeic acid	>100	13
Caffeic acid phenethyl ester	>100	8
Chlorgenic acid	>100	8
Allyl disulfide	>100	6
Chrysin	>100	5
Myricetin	>100	5
Apigenin	>100	5
(s,s)-(+)-Tetrandrine	>100	5
Quercetin	>100	4
Luteolin	>100	4
Berberine	>100	4
Fisetin	>100	4
Resveratrol	>100	3
Baicalin	>100	3
Kaempferol	>100	3
Galangin	>100	3
(-)-Epicatechin	>100	3
Hesperetin	>100	3
Genistein	>100	2
Indole-3-carbinol	>100	2
Chlorophyllin	>100	2
Daidzein	>100	2
Lupeol	>100	2
Glycitein	>100	2
Daidzin	>100	2
Evodiamine	>100	2
Quercitrin	>100	2
Zebularine	>100	2
Naringenin	>100	2
Silymarin	>100	1

Table 10.1-Con'd

Matrine	>100	1
Oleanolic acid	>100	1
Sennoside B	>100	1
Crocin	>100	1
Morin	>100	1
Oxymatrine	>100	1
Chrysophanic acid	>100	1
Icariin	>100	1
Silibinin	>100	1
Glycyrrhetinic acid	>100	1
Synephrine	>100	1
Rutin	>100	1
Epigallocatechin 3-gallate	>100	1
Naringin	>100	1
(+)-Catechin	>100	1
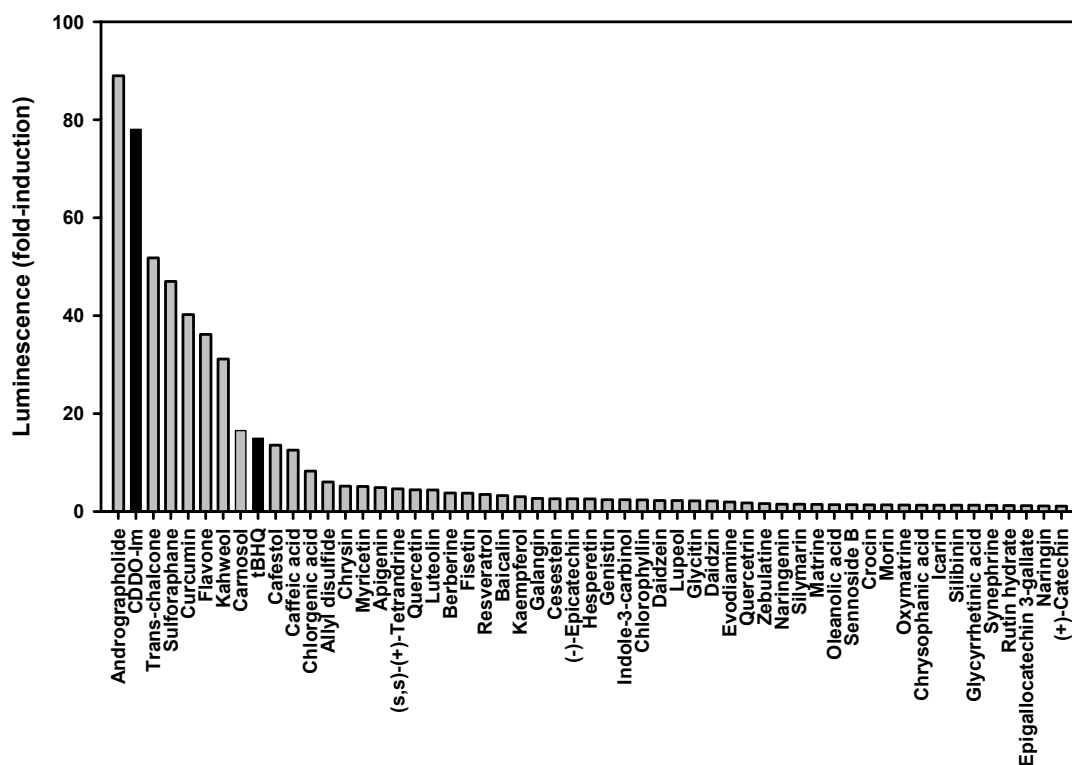
Figure 10.2. Maximum fold-induction of the ARE luciferase reporter by tBHQ, CDDO-Im, and natural compounds. AREc32 cells were seeded at 3,500 cells/well in a 384-well plate, 46 µL/well. 24 h after seeding, cells were treated with compound (0.02-30 µM in 0.5% DMSO) or DMSO vehicle. 24 h after treatment, luciferase activity was assessed using the Steady-Glo luciferase assay with a luminescence readout. The luminescence of each well was divided by the median luminescence of the DMSO vehicle control wells to generate the fold Nrf2 activation.

curcumin (36 µM), flavone (42 µM), kahweol (42 µM), and cafestol (51 µM). All other

natural compounds had EC_{50} values higher than 100 µM for activating the Nrf2 pathway.

Concentration-response of top 10 hits

Figure 10.4 depicts concentration-response curves of the top 10 natural

compounds as well as *t*BHQ and CDDO-Im as positive controls. CDDO-Im induced

luminescence signal 13-fold at the lowest concentration tested (20 nM), with a

continued increase in luminescence signal as the concentration increased, reaching a

maximum fold-induction at 1 µM. The luminescence decreased to basal levels at higher

concentrations of CDDO-Im. *Trans*-chalcone increased the luminescence signal at

concentrations higher than 3.5 µM, reached a maximum fold-induction at 18 µM, but the

induction decreased to basal levels at 30 µM. In contrast, tBHQ and the other nine

natural compounds did not increase the luminescence at concentrations lower than 3.5

µM, and reached the maximum fold-induction at the highest concentration tested (30

µM).
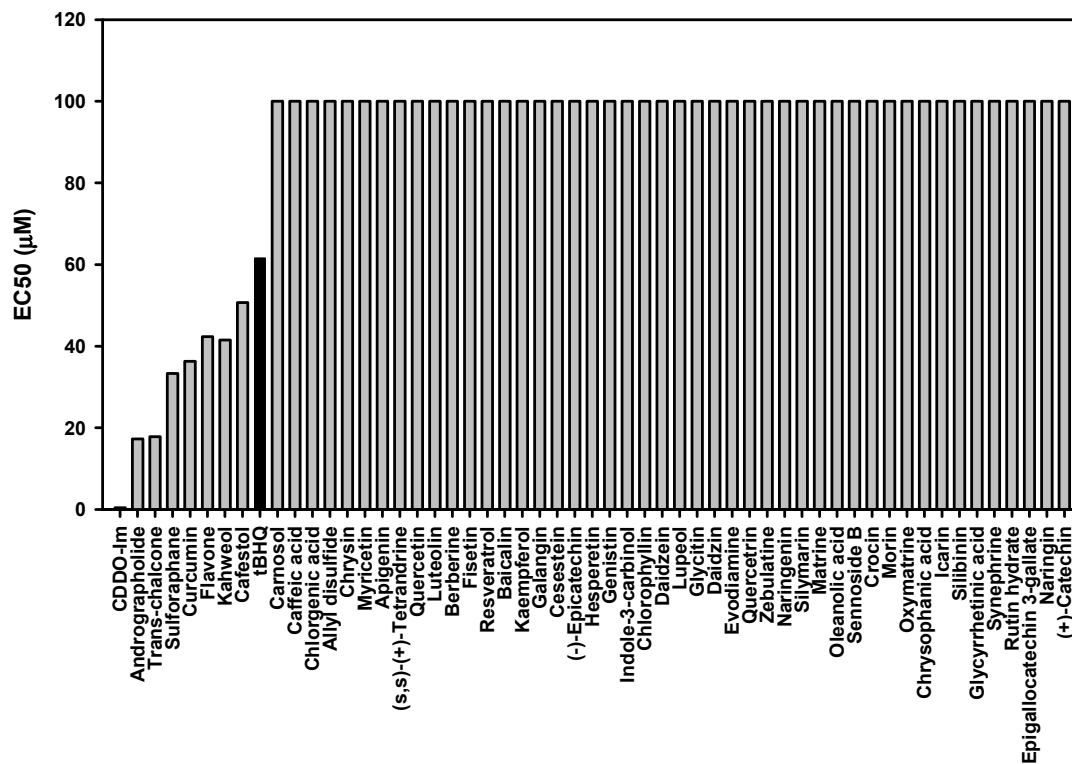
Figure 10.3. EC_{50} of tBHQ, CDDO-Im, and natural compounds to activate Nrf2. AREc32 cells were cultured and treated as described in figure 2. The EC50s were calculated based on the data from concentration-response curve of each individual compound and contrained to 100-fold induction.
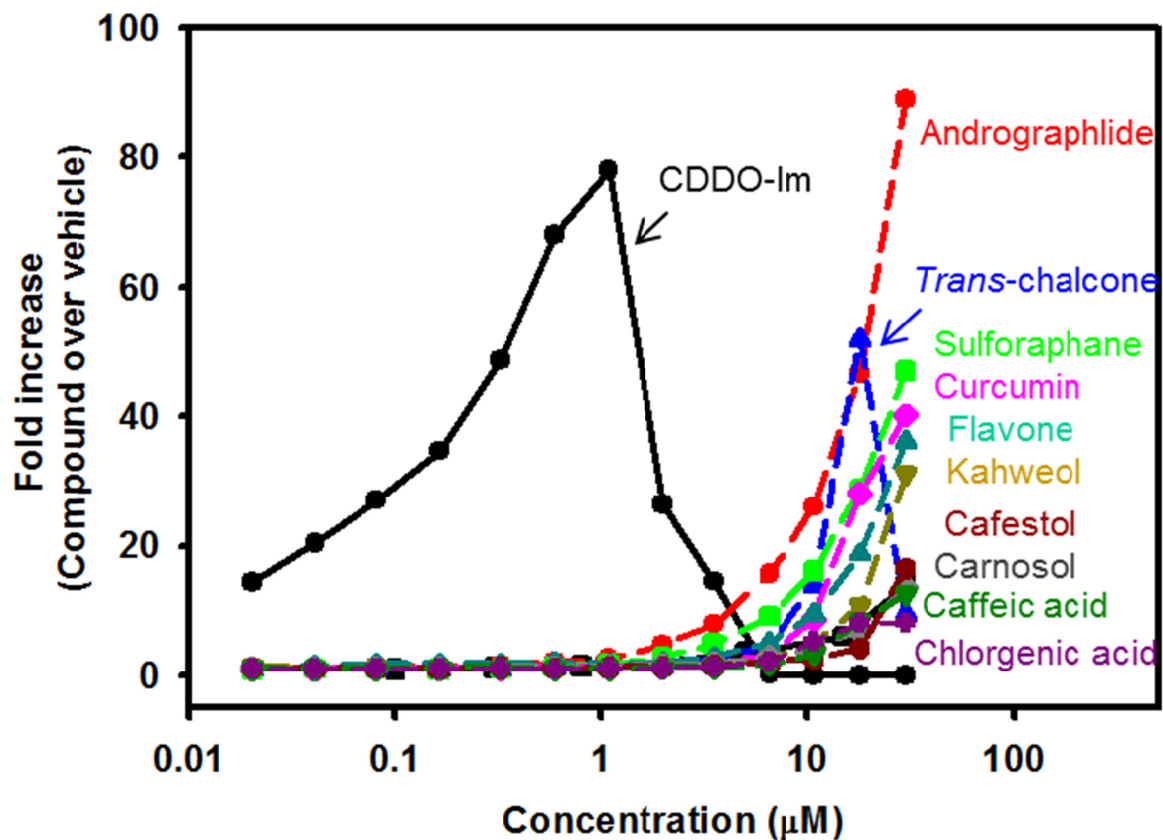
Figure 10.4. Concentration-response activation ARE luciferase reporter construct in AREc32 cells by tBHQ, CDDO-Im, and the best 10 natural compounds. AREc32 cells were cultured and treated as described in Figure 10.2. The luminescence of each well was divided by the median luminescence of the DMSO vehicle control wells to generate the fold Nrf2 activation.

Discussion

The present study compared the efficacy and potency of two synthetic Nrf2 activators as well as 54 natural compounds to activate the Keap1-Nrf2 pathway using the AREc32 cell line system. Results showed that seven natural compounds, namely andrographolide, trans-chalcone, sulforaphane, curcumin, flavone, kahweol, and carnosol were more effective than the classic Nrf2 activator tBHQ, but none of the natural compounds were more potent than CDDO-Im, the potent synthetic Nrf2 activator.

*t*BHQ is a prototypical Nrf2 activator, and has been shown to activate Nrf2 and protect against oxidative stress-induced toxicity *in vitro* and *in vivo*. For example, *t*BHQ has been shown to activate the Keap1-Nrf2 pathway and prevent ethanol-induced apoptosis in cranial neural crest cells *in vitro* (Yan et al., 2010). *t*BHQ has also been shown to inhibit LPS-induced microglial activation through Nrf2 activation in microglial cells (Koh et al., 2009). In addition, *t*BHQ protects against mitochondrial stress through induction of the Nrf2-driven antioxidant response in mice (Shih et al., 2005). CDDO-Im has emerged in recent years as a protective compound against oxidative stress. CDDO-Im activates the Nrf2-Keap1 pathway (Liby et al., 2005), and leads to a cytoprotective response through the up-regulation of gene expression. CDDO-Im has been shown to protect against acetaminophen-induced hepatotoxicity in mice (Reisman et al., 2009b). In addition to the known synthetic Nrf2 activators, two well-established natural Nrf2 activators, namely sulforaphane and curcumin, were also active in the screening system of the present study. Sulforaphane has been used in a pharmacological model to study protein-protein interactions between Keap1 and Nrf2 (Zhang and Hannink, 2003), as well as to identify Nrf2 downstream target genes (Thimmulappa et al., 2002). The

present study shows both synthetic and natural compounds increase the luminescence signal in the AREc32 cell line in a concentration-dependent manner, indicating that this system is excellent for determining the efficacy and potency of potential Nrf2 activators.

Among the 54 natural compounds tested in the AREc32 cell line system, compounds with a diterpene structure, including andrographolide, kahweol, cafestol, and carnosol, were shown to be the most active compounds. Andrographolide was even more effective than CDDO-Im, a triterpenoid known to be an extremely strong activator of the Keap1-Nrf2 pathway. Andrographolide is a diterpene lactone that exists in leaves and stems of *Andrographis paniculata*, which is a plant used for medicinal purposes in India (Mishra et al., 2011). Andrographolide has been shown to have strong anti-inflammatory effects through inactivation of NFκB (Lu et al., 2011), and anti-cancer effects by inhibition of androgen receptor signaling (Liu et al., 2011). Recently, andrographolide was shown to induce heme oxygenase-1 (HO-1) by activating Nrf2 in human endothelial cells, and the Nrf2-HO1 pathway was suggested to be involved in the andrographolide-induced suppression of inflammation (Yu et al., 2010). Kahweol and cafestol are coffee specific diterpenes that produce chemoprevention to a broad range of carcinogens, including 7,12-dimethylbenz[a]anthracene, aflatoxin B1, benzo[a]pyrene, and 2-amino-1-methyl-6-phenylimidazo[4,5-b]pyridine, at least partially through induction of phase-II drug metabolism genes, as well as genes involved in cellular antioxidant defense (Cavin et al., 2002). Recently, it was reported that kahweol and cafestol induce cytoprotective genes primarily by Nrf2 (Higgins et al., 2008). Similarly, carnosol also activates phase-II drug metabolism genes and antioxidant genes through activating Nrf2 *in vitro* (Takahashi et al., 2009) and *in vivo* (Balstad et al.,

2011). In parallel with the previous observations, results from the present study indicate that these diterpenes (andrographolide, kahweol, cafestol, and carnosol) are highly effective activators of the Nrf2 pathway.

In addition to andrographolide, kahweol, cafestol, and carnosol, *trans*-chalcone was reported to activate Nrf2 in certain cell lines or animal models, and also activate Nrf2 in the present study. *Trans*-chalcone was the top hit of 43 potential chemopreventive chemicals to increase glutathione content in rat liver cells (White et al., 1998). Recently, a series of chalcone derivatives were synthesized, and 2-trifluoromethyl-2'-methoxychalone was shown to be a potent Nrf2 activator in human lung epithelial cells and in mice (Kumar et al., 2011b). The present study further confirms the efficacy of *trans*-chalcone to activate the Keap1-Nrf2 pathway, and provides further mechanistic information on the induction of Nrf2 target genes by those natural compounds.

In the present study, both caffeic acid and its derivative caffeic acid phenethyl ester (CAPE) were shown to activate Nrf2, with caffeic acid more effective than CAPE (13-fold versus 8-fold maximum increase of luminescence signal). In previous reports, CAPE was shown to activate Nrf2 in multiple cell lines. However, whether caffeic acid activates the Keap1-Nrf2 pathway was unknown. For example, CAPE was shown to induce Nrf2 target genes in porcine renal epithelial proximal tubule cells and rat kidney epithelial cells (Balogun et al., 2003), rat liver tissue macrophages (Hess et al., 2003), and human colon carcinoma cells (Lee et al., 2010b). The present study indicates that caffeic acid has the potential to be a novel Nrf2 activator, and more *in vivo* studies are necessary to test the antioxidative activity of caffeic acid in whole animals.

Dietary flavonoids are a family of natural compounds that have been shown to have cancer preventive effects through inducing phase-II drug metabolism genes (Saracino and Lampe, 2007), and antioxidative effects against ultraviolet radiation (Dinkova-Kostova, 2008). In addition, a large number of dietary flavonoids, including luteolin (Wruck et al., 2007), epigallocatechin-3-gallate (Tsai et al., 2011), and quercetin (Miyamoto et al., 2011) induce Nrf2 target genes in various cell lines and animal models. Thus, 27 dietary flavonoids were screened in the present study to test whether these dietary flavonoids activate the Nrf2 pathway. Surprisingly, only flavone was highly effective (33-fold increase in luminescence) to activate Nrf2, and the remaining flavonoids tested exhibited slight or no increase in Nrf2 activation. Similarly, several natural compounds, including resveratrol, xanthohumol, isoliquiritigenin, and oleanolic acid have been reported to activate Nrf2, but were inactive in the present study. For example, resveratrol was shown to protect against oxidative/electrophilic stress via inducing Nrf2 target genes in human lung epithelial cells (Kode et al., 2008), rat primary hepatocytes (Rubiolo et al., 2008), coronary arterial endothelial cells, and branches of the femoral artery in mice (Ungvari et al., 2010). Xanthohumol and isoliquiritigenin alkylate cysteine 151 on Keap1 protein, leading to Nrf2 activation *in vitro* and *in vivo* (Luo et al., 2007). Oleanolic acid has been shown to activate Nrf2 in mouse liver (Reisman et al., 2009a) and rat vascular smooth muscle cells (Feng et al., 2011). However, resveratrol, xanthohumol, isoliquiritigenin, and oleanolic acid did not activate Nrf2 in the present study, indicating that activation of Nrf2 by those natural chemicals may be cell line specific. In addition, oleanolic acid was recently shown to inhibit estradiol-17β-glucuronide uptake by OATP1B1, an uptake transporter, suggesting that

oleanolic acid is an OATP1B1 substrate (Roth et al., 2011), and uptake transport maybe required to increase the bioavailability of oleanolic acid. Collectively, oleanolic acid, together with other natural compounds may require transport and/or bio-transformation to activate the Keap1-Nrf2 pathway.

In conclusion, the present study compared the efficacy and potency of 54 natural compounds to activate the Keap1-Nrf2 pathway. Andrographolide, *trans*-chalcone, sulforaphane, curcumin, flavone, kahweol, and carnosol were more effective than classic Nrf2 activator tBHQ, but none of the natural compounds were more potent than CDDO-Im, the most potent synthetic Nrf2 activator.

Chapter 11 : GENERAL SUMMARY AND CONCLUSIONS

The present dissertation has characterized the global target genes of the transcription factor Nrf2 in mouse liver, and investigated the protective role of Nrf2 against chemical-induced oxidative stress and subsequent liver injury in mice. In addition, the present dissertation identified effective and potent activators of Nrf2 from a library of 47,000 compounds, and compared the efficacy and potency of natural existing antioxidants to activate the Nrf2 pathway.

Oxidative stress and electrophilic stress are major mechanisms of pathogenesis of various disease conditions including carcinogenesis, inflammation, and aging. Nrf2 is considered as the master regulator to protect cells from oxidative/electrophilic stress via induction of its target genes. Liver is the most important organ in regard to xenobiotic detoxification as well as many other physiological functions. As a transcription factor, the direct effect of Nrf2 activation or deficiency is alteration of gene transcription profiles. Although the antioxidative role of Nrf2 was proposed and studied for over ten years, the global Nrf2 target genes in liver remain unknown. The present dissertation utilized a Nrf2 "gene dose-response" model to genetically modulate the amount of Nrf2 in mouse liver, and compared the transcription profiles in this Nrf2 "gene dose-response" model. Thus, the Nrf2-target genes in mouse liver were investigated systemically.

Chapter 4 summarizes the genes that were either induced or suppressed with graded Nrf2 activation. Pathway analyses indicate that genes induced by Nrf2 are involved in glutathione synthesis, oxidation/reduction using NADPH as the co-factor, and xenobiotic metabolism. In addition, mRNA of genes involved in pentose phosphate pathways as well as malic enzyme are decreased without Nrf2, and/or increased with Nrf2 activation, indicating that Nrf2 promotes NADPH generation. Surprisingly, in

addition to the 115 genes that are induced by Nrf2, I also found 80 genes that are suppressed with graded Nrf2 activation. Among these genes that are suppressed by Nrf2, the majority of them is involved in lipid synthesis and fatty acid desaturation. Thus, observations in Chapter 2 suggests that Nrf2 protects against environmental insults by promoting the generation of NADPH, which is preferentially consumed by pathways that protect against of oxidative stress rather than by fatty acid synthesis and desaturation.

In addition to being a transcription factor that increases the production of proteins that protect against oxidative stress, Nrf2 also plays a role in xenobiotic detoxification. Chapter 5 summarizes the mRNA abundance of 124 drug processing genes in the Nrf2 "gene dose-response" model. With graded Nrf2 activation, 47 genes are induced, 74 genes are not altered, and 5 genes are suppressed. Specifically, Nrf2 did not have a marked effect on the mRNA of uptake transporters, except for Oatp1a1, NTCP decreased with Nrf2 activation. The effect of Nrf2 on cytochrome P450 (Cyp) genes was minimal, with only Cyp2a5, Cyp2c50, Cyp2c54, and Cyp2g1 being increased, but Cyp2u1 being decreased with enhanced Nrf2 activation. However, Nrf2 increased mRNA of many non P-450 phase-I enzymes, such as aldo-keto reductases, carbonyl reductases, and aldehyde dehydrogenase 1. Many genes involved in phase-II drug metabolism were induced by Nrf2, including most isoforms of the Gst gene family. A number of efflux transporters, such as Mrps, Bcrp, as well as Abcg5 and Abcg8 were induced by Nrf2. Thus, Chapter 5 suggests that Nrf2 has a minor role in regulating uptake transporters and P-450 phase-I enzymes that are involved in xenobiotic activation, but facilitates electrophile detoxification through inducing non P-450 phase-I

enzymes that reduce electrophiles, Gsts that conjugates electrophiles, and Mrp efflux transporters that excrete electrophile-GSH conjugates out of cells.

After the effect of Nrf2 on the global gene transcription profile of mouse liver had been determined, Chapter 6 to Chapter 8 report the function of Nrf2 *in vivo*, by testing whether Nrf2 activation protects against chemical-induced oxidative stress and subsequent liver injury in mice. Oxidative stress and lipid accumulation play important roles in ethanol-induced liver injury. Chapter 6 shows that genes involved in antioxidant defense are induced, whereas genes involved in lipid biosynthesis are suppressed in livers of Nrf2 activated mice. Thus, I investigated whether Nrf2 protects against ethanol-induced liver injury using the Nrf2 "gene dose-response model". Binge administration of ethanol (5g/kg, oral gavage) increased serum ALT and LDH activities in Nrf2-null mice and wild-type mice, but not in Nrf2-enhanced mice, indicating that Nrf2-enhanced mice are more resistant to ethanol toxicity. Ethanol increased serum triglycerides and free fatty acids in livers of Nrf2-null mice, and these increases were blunted in Nrf2-enhanced mice. After ethanol exposure, reactive oxygen species were increased in livers and primary hepatoctyes in Nrf2-null mice but not in Nrf2-enhanced mice. Mechanistic studies show that Nrf2 prevents ethanol-induced oxidative stress through inducing cytoprotective genes including Nqo1 and Gclc, and prevents accumulation of free fatty acids in liver by suppressing the Srebp1 pathway.

Chapter 7 demonstrates the protective effect of Nrf2 against cadmium-induced acute liver injury. The mechanisms of Cd-induced acute hepatotoxicity involve a biphasic process, which is initiated by the binding of Cd to the sulfhydryls of glutathione and proteins, resulting in the generation of reactive oxygen species (ROS) and protein

inactivation. The second phase is initiated by the activation of kupffer cells and followed by ROS release by kupffer cells and neutrophils. In the present study, I found that Nrf2-null mice are more susceptible, whereas Nrf2-enhanced mice are more resistant to cadmium-induced acute liver injury. Multiple genes involved in antioxidant defense, namely Gclc, Gpx2, and Srxn-1 were only induced in Nrf2-enhanced mice, but not in Nrf2-null mice, indicating that Nrf2 protects against cadmium induced oxidative stress and subsequent acute liver injury at least partially through the induction of these cytoprotective genes. Surprisingly, metallothioneins (Mt-1 and Mt-2), a family of cysteine-rich proteins that scavenge cadmium to prevent toxicity, were induced markedly in both Nrf2-null and Nrf2-enhanced mice. Thus, the date in Chapter 7 shows that there are distinct pathways to protect cadmium-induced toxicity: Nrf2-dependent induction of antioxidative genes and Nrf2-independent induction of metallothioneins.

Chapter 8 demonstrates the protective effect of Nrf2 against diquat-induced lung and liver injury. Diquat is a contact herbicide that is minimally metabolized, and undergoes oxidation/reduction cycling, resulting in the generation of superoxide. Diquat-induced tissue injury serves as a model to study ROS generation and oxidative stress. Thus, it is not surprising that Nrf2 activation prevents diquat-induced lethality, alveolar collapse in lungs, and necrosis in livers of mice. Nrf2 activation also prevents glutathione depletion in mouse lung and liver tissues, and increased ROS staining in primary hepatocytes.

Data in the previous Chapters (Chapters 6 to 8) suggest potential therapeutic applications of the Keap1-Nrf2 pathway, and thus Nrf2 is a promising drug target for in the treatment of oxidative/electrophilic stress-induced diseases. To develop effective

and potent Nrf2 activators, a library of synthetic (Chapter 9) and natural existing (Chapter 10) compounds were screened to test their efficacy and potency to activate Nrf2.

Chapter 9 documents the development, implementation, and validation of a high-throughput screen to identify activators of the Keap1-Nrf2-ARE pathway using AREc32 cells, which contain a luciferase gene under the control of eight copies of rat Gsta2 ARE in the promoter region. By screening 47,000 compounds, we found 238 compounds (0.5%) that had comparable or better efficacy to activate Nrf2 than tBHQ, the prototypical Nrf2 activator. Among these 238 compounds, 19 compounds had better efficacy than CDDO-Im, the most effective and potent Nrf2 activator that has been discovered. However, none of the compounds screened had better potency than CDDO-Im. In addition, chemical structure relationship analysis of these 238 compounds showed enrichment of four chemical scaffolds (diaryl amides and diaryl ureas, oxazoles and thiazoles, pyranones and thiapyranones, and pyridinones and pyridazinones). The top 30 compounds were also screened in Hepa1c1c7 cells for increase in Nqo1 mRNA, the prototypical Nrf2 target gene. The results show that 17 of the 30 most active hits increased Nqo1 mRNA in a concentration-dependent manner. Results from this screening identified Nrf2 activators, and provide novel insights in chemical scaffolds that might prevent oxidative/electrophilic stress-induced toxicity and carcinogenesis.

In addition to synthetic compounds, a number of natural compounds are known to be antioxidants, and some of these natural compounds have been shown to exhibit antioxidant effects through activating the Nrf2 pathway. Utilizing the same screening system (AREc32 cells), Chapter 10 evaluates the capability of 54 natural existing

compounds to activate Nrf2. Among the 54 tested natural compounds, andrographolide had the highest efficacy, followed by *trans*-chalcone, sulforaphane, curcumin, flavone, kahweol, and carnosol, which were all more efficient than tBHQ. Among the compounds tested, CDDO-Im was still the most potent. Seven of the natural compounds, namely andrographolide, trans-chalcone, sulforaphane, curcumin, flavone, kahweol, and cafestol had higher EC_{50} values than CDDO-Im, but lower than *t*BHQ.

In addition to the extension of the current knowledge on the Keap1-Nrf2-ARE pathway, the present dissertation provides hints and clues for more hypotheses that could be future directions of this area. For example, Nrf2 is known to heterodimerize with its transcription partners (MafG, c-Jun, and c-Fos) to promote its target gene transcription (Baird and Dinkova-Kostova, 2011). However, the transcription partners of Nrf2 were investigated under *in vitro* systems in various cell lines. It is still unknown which transcription factors act as Nrf2 partners *in vivo*, especially in liver. Transcription factor binding site over-representation analysis shows that putative binding sites of certain transcription factors, including PPARγ, IRF2, and HNF4α are also enriched in promoter region of genes induced by Nrf2 (Chapter 5). The transcription factor binding site co-enrichment indicates potential Nrf2 partners *in vivo*. However, more specific experiments (for example, ChiP-Seq) are needed to study the Nrf2 binding site in mouse liver, and to better predict co-enrichment of other transcription factors as potential Nrf2 partners in the nucleus. Furthermore, mice deficient in the predicted transcription factor should be used to confirm whether Nrf2 promotes certain target gene expression in a predicted partner-dependent manner.

As described in Chapter 4, there are 80 genes suppressed with graded Nrf2 activation. Recently, it was published that Nrf2 binds to the promoter regions of certain genes to inhibit their transcription (Thangasamy et al., 2011). Thus, it is possible that genes suppressed with Nrf2 activation may be a direct target of Nrf2, and their transcription may be inhibited through binding of Nrf2 in the promoter region. ChiP-Seq experiments as well as site-directed mutagenesis studies of the promoters are needed to further confirm if Nrf2 acts as a transcription "repressor" of these genes.

As described in Chapters 6, 7 and 8, Nrf2 protects chemical-induced oxidative stress and liver injury through induction of a battery of cytoprotective genes (Nqo1, Gclc, Gpx2, Srxn, and Txnrd1). However, it is unknown which downstream Nrf2 target genes are essential for the protective function of Nrf2. To address this question, Nrf2-target gene-knockout mice (for example, Nqo1 knockout) are needed to investigate the protective capacity of Nrf2 in the absence of a certain downstream target genes.

As described in Chapters 9 and 10, a number of synthetic and natural existing compounds were shown to be effective in activating Nrf2. However, it is also important to know whether these compounds protect against oxidative stress-induced pathogenesis *in vivo*, and whether the protective effect of these compounds is Nrf2-dependent. To demonstrate the specificity of these compounds, one can do a microarray analysis to compare the transcription profiles in livers of compound-treated wild-type mice and Nrf2-null mice, and test which genes are still altered by these compounds in Nrf2-null mice. To demonstrate the activity of these compounds *in vivo*, one can test whether these compounds protect against ethanol-, cadmium-, and diquat-induced liver oxidative stress and liver injury in mice.

In conclusion, the Nrf2 target genes are involved in NADPH generation, NADPH-facilitated oxidative stress reduction, and detoxification and excretion of electrophiles. Nrf2 activation protects ethanol-, cadmium-, and diquat-induced liver oxidative stress and liver injury in mice. Lastly, a few synthetic and natural existing compounds have been shown to be potent and effective in activating the Keap1-Nrf2-ARE pathway.

Chapter 12 : REFERENCES

Abu-Bakar A, Lamsa V, Arpiainen S, Moore MR, Lang MA, and Hakkola J (2007) Regulation of CYP2A5 gene by the transcription factor nuclear factor (erythroid-derived 2)-like 2. *Drug Metab Dispos* **35:**787-794.

Alam J, Wicks C, Stewart D, Gong P, Touchard C, Otterbein S, Choi AM, Burow ME, and Tou J (2000) Mechanism of heme oxygenase-1 gene activation by cadmium in MCF-7 mammary epithelial cells. Role of p38 kinase and Nrf2 transcription factor. *J Biol Chem* **275:**27694-27702.

Aleksunes LM and Manautou JE (2007) Emerging role of Nrf2 in protecting against hepatic and gastrointestinal disease. *Toxicol Pathol* **35:**459-473.

Alnouti Y and Klaassen CD (2008) Tissue distribution, ontogeny, and regulation of aldehyde dehydrogenase (Aldh) enzymes mRNA by prototypical microsomal enzyme inducers in mice. *Toxicol Sci* **101:**51-64.

Anand P, Sundaram C, Jhurani S, Kunnumakkara AB, and Aggarwal BB (2008) Curcumin and cancer: an "old-age" disease with an "age-old" solution. *Cancer Lett* **267:**133-164.

Anbar M and Neta P (1967) A compilation of specific bimolecular rate constants for the reactions of hydrated electrons, hydrogen atoms and hydroxyl radicals with inorganic and organic compounds in aqueous solution. *The International Journal of Applied Radiation and Isotopes* **18:**493-531.

Andoh Y, Mizutani A, Ohashi T, Kojo S, Ishii T, Adachi Y, Ikehara S, and Taketani S (2006) The antioxidant role of a reagent, 2',7'-dichlorodihydrofluorescin diacetate, detecting reactive-oxygen species and blocking the induction of heme oxygenase-1 and preventing cytotoxicity. *J Biochem* **140:**483-489.

Ansell PJ, Lo SC, Newton LG, Espinosa-Nicholas C, Zhang DD, Liu JH, Hannink M, and Lubahn DB (2005) Repression of cancer protective genes by 17beta-estradiol: ligand-dependent interaction between human Nrf2 and estrogen receptor alpha. *Mol Cell Endocrinol* **243:**27-34.

Arosio P and Levi S (2010) Cytosolic and mitochondrial ferritins in the regulation of cellular iron homeostasis and oxidative damage. *Biochim Biophys Acta* **1800:**783-792.

Axelsen PH, Komatsu H, and Murray IV (2011) Oxidative stress and cell membranes in the pathogenesis of Alzheimer's disease. *Physiology (Bethesda)* **26:**54-69.

Bae SH, Sung SH, Cho EJ, Lee SK, Lee HE, Woo HA, Yu DY, Kil IS, and Rhee SG (2011) Concerted action of sulfiredoxin and peroxiredoxin I protects against alcohol-induced oxidative injury in mouse liver. *Hepatology* **53:**945-953.

Baird L and Dinkova-Kostova AT (2011) The cytoprotective role of the Keap1-Nrf2 pathway. *Arch Toxicol* **85:**241-272.

Balogun E, Hoque M, Gong P, Killeen E, Green CJ, Foresti R, Alam J, and Motterlini R (2003) Curcumin activates the haem oxygenase-1 gene via regulation of Nrf2 and the antioxidant-responsive element. *Biochem J* **371:**887-895.

Balstad TR, Carlsen H, Myhrstad MC, Kolberg M, Reiersen H, Gilen L, Ebihara K, Paur I, and Blomhoff R (2011) Coffee, broccoli and spices are strong inducers of electrophile response element-dependent transcription in vitro and in vivo - studies in electrophile response element transgenic mice. *Mol Nutr Food Res* **55:**185-197.

Barden A, Zilkens RR, Croft K, Mori T, Burke V, Beilin LJ, and Puddey IB (2007) A reduction in alcohol consumption is associated with reduced plasma F2-isoprostanes and urinary 20-HETE excretion in men. *Free Radic Biol Med* **42:**1730-1735.

Barski OA, Tipparaju SM, and Bhatnagar A (2008) The aldo-keto reductase superfamily and its role in drug metabolism and detoxification. *Drug Metab Rev* **40:**553-624.

Barve A, Khor TO, Nair S, Lin W, Yu S, Jain MR, Chan JY, and Kong AN (2008) Pharmacogenomic profile of soy isoflavone concentrate in the prostate of Nrf2 deficient and wild-type mice. *J Pharm Sci* **97:**4528-4545.

Baur JA (2010) Biochemical effects of SIRT1 activators. *Biochim Biophys Acta* **1804:**1626-1634.

Bergheim I, Guo L, Davis MA, Lambert JC, Beier JI, Duveau I, Luyendyk JP, Roth RA, and Arteel GE (2006) Metformin prevents alcohol-induced liver injury in the mouse: Critical role of plasminogen activator inhibitor-1. *Gastroenterology* **130:**2099-2112.

Bertram C and Hass R (2008) Cellular responses to reactive oxygen species-induced DNA damage and aging. *Biol Chem* **389:**211-220.

Biswas SK and Rahman I (2009) Environmental toxicity, redox signaling and lung inflammation: the role of glutathione. *Mol Aspects Med* **30:**60-76.

Blake DJ, Singh A, Kombairaju P, Malhotra D, Mariani TJ, Tuder RM, Gabrielson E, and Biswal S (2010) Deletion of Keap1 in the lung attenuates acute cigarette smoke-induced oxidative stress and inflammation. *Am J Respir Cell Mol Biol* **42:**524-536.

Brigelius-Flohe R and Traber MG (1999) Vitamin E: function and metabolism. *FASEB J* **13:**1145-1155.

Bursch W, Karwan A, Mayer M, Dornetshuber J, Frohwein U, Schulte-Hermann R, Fazi B, Di Sano F, Piredda L, Piacentini M, Petrovski G, Fesus L, and Gerner C (2008) Cell death and autophagy: cytokines, drugs, and nutritional factors. *Toxicology* **254:**147-157.

Cavin C, Holzhaeuser D, Scharf G, Constable A, Huber WW, and Schilter B (2002) Cafestol and kahweol, two coffee specific diterpenes with anticarcinogenic activity. *Food Chem Toxicol* **40:**1155-1163.

Cejas P, Casado E, Belda-Iniesta C, De Castro J, Espinosa E, Redondo A, Sereno M, Garcia-Cabezas MA, Vara JA, Dominguez-Caceres A, Perona R, and Gonzalez-Baron M (2004) Implications of oxidative stress and cell membrane lipid peroxidation in human cancer (Spain). *Cancer Causes Control* **15:**707-719.

Chae HZ, Kim HJ, Kang SW, and Rhee SG (1999) Characterization of three isoforms of mammalian peroxiredoxin that reduce peroxides in the presence of thioredoxin. *Diabetes Res Clin Pract* **45:**101-112.

Chan K, Han XD, and Kan YW (2001) An important function of Nrf2 in combating oxidative stress: detoxification of acetaminophen. *Proc Natl Acad Sci U S A* **98:**4611-4616.

Chan K, Lu R, Chang JC, and Kan YW (1996) NRF2, a member of the NFE2 family of transcription factors, is not essential for murine erythropoiesis, growth, and development. *Proc Natl Acad Sci U S A* **93:**13943-13948.

Chavan H, Oruganti M, and Krishnamurthy P (2011) The ATP-binding cassette transporter ABCB6 is induced by arsenic and protects against arsenic cytotoxicity. *Toxicol Sci* **120:**519-528.

Chen J and Shaikh ZA (2009) Activation of Nrf2 by cadmium and its role in protection against cadmium-induced apoptosis in rat kidney cells. *Toxicol Appl Pharmacol* **241:**81-89.

Cheng Q, Taguchi K, Aleksunes LM, Manautou JE, Cherrington NJ, Yamamoto M, and Slitt AL (2011) Constitutive activation of nuclear factor-E2-related factor 2 induces biotransformation enzyme and transporter expression in livers of mice with hepatocyte-specific deletion of Kelch-like ECH-associated protein 1. *J Biochem Mol Toxicol* **25:**320-329.

Chiarugi P, Pani G, Giannoni E, Taddei L, Colavitti R, Raugei G, Symons M, Borrello S, Galeotti T, and Ramponi G (2003) Reactive oxygen species as essential mediators of cell adhesion: the oxidative inhibition of a FAK tyrosine phosphatase is required for cell adhesion. *J Cell Biol* **161:**933-944.

Chiba M, Kubo M, Miura T, Sato T, Rezaeian AH, Kiyosawa H, Ohkohchi N, and Yasue H (2008) Localization of sense and antisense transcripts of Prdx2 gene in mouse tissues. *Cytogenet Genome Res* **121:**222-231.

Cho HY, Reddy SP, Yamamoto M, and Kleeberger SR (2004) The transcription factor NRF2 protects against pulmonary fibrosis. *FASEB J* **18:**1258-1260.

Chu FF, Doroshow JH, and Esworthy RS (1993) Expression, characterization, and tissue distribution of a new cellular selenium-dependent glutathione peroxidase, GSHPx-GI. *J Biol Chem* **268:**2571-2576.

Chung J, Veeramachaneni S, Liu C, Mernitz H, Russell RM, and Wang XD (2009) Vitamin E supplementation does not prevent ethanol-reduced hepatic retinoic acid levels in rats. *Nutr Res* **29:**664-670.

Cohen JI, Roychowdhury S, DiBello PM, Jacobsen DW, and Nagy LE (2009) Exogenous thioredoxin prevents ethanol-induced oxidative damage and apoptosis in mouse liver. *Hepatology* **49:**1709-1717.

Comporti M, Signorini C, Leoncini S, Gardi C, Ciccoli L, Giardini A, Vecchio D, and Arezzini B (2010) Ethanol-induced oxidative stress: basic knowledge. *Genes Nutr* **5:**101-109.

Copple IM, Goldring CE, Kitteringham NR, and Park BK (2010) The keap1-nrf2 cellular defense pathway: mechanisms of regulation and role in protection against drug-induced toxicity. *Handb Exp Pharmacol***:**233-266.

Cullinan SB, Gordan JD, Jin J, Harper JW, and Diehl JA (2004) The Keap1-BTB protein is an adaptor that bridges Nrf2 to a Cul3-based E3 ligase: oxidative stress sensing by a Cul3-Keap1 ligase. *Mol Cell Biol* **24:**8477-8486.

Dargel R (1992) Lipid peroxidation--a common pathogenetic mechanism? *Exp Toxicol Pathol* **44:**169-181.

Deroo BJ, Hewitt SC, Peddada SD, and Korach KS (2004) Estradiol regulates the thioredoxin antioxidant system in the mouse uterus. *Endocrinology* **145:**5485-5492.

Dhakshinamoorthy S and Jaiswal AK (2000) Small maf (MafG and MafK) proteins negatively regulate antioxidant response element-mediated expression and antioxidant induction of the NAD(P)H:Quinone oxidoreductase1 gene. *J Biol Chem* **275:**40134-40141.

Ding WX, Li M, Chen X, Ni HM, Lin CW, Gao W, Lu B, Stolz DB, Clemens DL, and Yin XM (2010) Autophagy reduces acute ethanol-induced hepatotoxicity and steatosis in mice. *Gastroenterology* **139:**1740-1752.

Dinis-Oliveira RJ, De Jesus Valle MJ, Bastos ML, Carvalho F, and Sanchez Navarro A (2006) Kinetics of paraquat in the isolated rat lung: Influence of sodium depletion. *Xenobiotica* **36:**724-737.

Dinkova-Kostova AT (2008) Phytochemicals as protectors against ultraviolet radiation: versatility of effects and mechanisms. *Planta Med* **74:**1548-1559.

Dinkova-Kostova AT, Holtzclaw WD, Cole RN, Itoh K, Wakabayashi N, Katoh Y, Yamamoto M, and Talalay P (2002) Direct evidence that sulfhydryl groups of Keap1 are the sensors regulating induction of phase 2 enzymes that protect against carcinogens and oxidants. *Proc Natl Acad Sci U S A* **99:**11908-11913.

Dinkova-Kostova AT, Liby KT, Stephenson KK, Holtzclaw WD, Gao X, Suh N, Williams C, Risingsong R, Honda T, Gribble GW, Sporn MB, and Talalay P (2005) Extremely potent triterpenoid inducers of the phase 2 response: correlations of protection against oxidant and inflammatory stress. *Proc Natl Acad Sci U S A* **102:**4584-4589.

Dinkova-Kostova AT, Talalay P, Sharkey J, Zhang Y, Holtzclaw WD, Wang XJ, David E, Schiavoni KH, Finlayson S, Mierke DF, and Honda T (2010) An exceptionally potent inducer of cytoprotective enzymes: elucidation of the structural features that determine inducer potency and reactivity with Keap1. *J Biol Chem* **285:**33747-33755.

Doorn JA, Maser E, Blum A, Claffey DJ, and Petersen DR (2004) Human carbonyl reductase catalyzes reduction of 4-oxonon-2-enal. *Biochemistry* **43:**13106-13114.

Droge W (2002) Free radicals in the physiological control of cell function. *Physiol Rev* **82:**47-95.

Ebert B, Kisiela M, Malatkova P, El-Hawari Y, and Maser E (2010) Regulation of human carbonyl reductase 3 (CBR3; SDR21C2) expression by Nrf2 in cultured cancer cells. *Biochemistry* **49:**8499-8511.

Eggler AL, Gay KA, and Mesecar AD (2008) Molecular mechanisms of natural products in chemoprevention: induction of cytoprotective enzymes by Nrf2. *Mol Nutr Food Res* **52 Suppl 1:**S84-94.

Eismann T, Huber N, Shin T, Kuboki S, Galloway E, Wyder M, Edwards MJ, Greis KD, Shertzer HG, Fisher AB, and Lentsch AB (2009) Peroxiredoxin-6 protects against mitochondrial dysfunction and liver injury during ischemia-reperfusion in mice. *Am J Physiol Gastrointest Liver Physiol* **296:**G266-274.

Enomoto A, Itoh K, Nagayoshi E, Haruta J, Kimura T, O'Connor T, Harada T, and Yamamoto M (2001) High sensitivity of Nrf2 knockout mice to acetaminophen

hepatotoxicity associated with decreased expression of ARE-regulated drug metabolizing enzymes and antioxidant genes. *Toxicol Sci* **59:**169-177.

Enomoto N, Takei Y, Yamashina S, Ikejima K, Kitamura T, and Sato N (2007) Anti-inflammatory strategies in alcoholic steatohepatitis. *J Gastroenterol Hepatol* **22 Suppl 1:**S59-61.

Farfan Labonne BE, Gutierrez M, Gomez-Quiroz LE, Konigsberg Fainstein M, Bucio L, Souza V, Flores O, Ortiz V, Hernandez E, Kershenobich D, and Gutierrez-Ruiz MC (2009) Acetaldehyde-induced mitochondrial dysfunction sensitizes hepatocytes to oxidative damage. *Cell Biol Toxicol* **25:**599-609.

Feng J, Zhang P, Chen X, and He G (2011) PI3K and ERK/Nrf2 pathways are involved in oleanolic acid-induced heme oxygenase-1 expression in rat vascular smooth muscle cells. *J Cell Biochem* **112:**1524-1531.

Filippin LI, Vercelino R, Marroni NP, and Xavier RM (2008) Redox signalling and the inflammatory response in rheumatoid arthritis. *Clin Exp Immunol* **152:**415-422.

Florczyk UM, Jozkowicz A, and Dulak J (2008) Biliverdin reductase: new features of an old enzyme and its potential therapeutic significance. *Pharmacol Rep* **60:**38-48.

Fu Y, Cheng WH, Porres JM, Ross DA, and Lei XG (1999) Knockout of cellular glutathione peroxidase gene renders mice susceptible to diquat-induced oxidative stress. *Free Radic Biol Med* **27:**605-611.

Gabbay KH, Bohren KM, Morello R, Bertin T, Liu J, and Vogel P (2010) Ascorbate synthesis pathway: dual role of ascorbate in bone homeostasis. *J Biol Chem* **285:**19510-19520.

Gao SS, Choi BM, Chen XY, Zhu RZ, Kim Y, So H, Park R, Sung M, and Kim BR (2010) Kaempferol suppresses cisplatin-induced apoptosis via inductions of heme oxygenase-1 and glutamate-cysteine ligase catalytic subunit in HEI-OC1 cell. *Pharm Res* **27:**235-245.

Gardner R, Kazi S, and Ellis EM (2004) Detoxication of the environmental pollutant acrolein by a rat liver aldo-keto reductase. *Toxicol Lett* **148:**65-72.

Girotti AW (1998) Lipid hydroperoxide generation, turnover, and effector action in biological systems. *J Lipid Res* **39:**1529-1542.

Giudice A, Arra C, and Turco MC (2010) Review of molecular mechanisms involved in the activation of the Nrf2-ARE signaling pathway by chemopreventive agents. *Methods Mol Biol* **647:**37-74.

Gloire G, Legrand-Poels S, and Piette J (2006) NF-kappaB activation by reactive oxygen species: fifteen years later. *Biochem Pharmacol* **72:**1493-1505.

Goering PL and Klaassen CD (1983) Altered subcellular distribution of cadmium following cadmium pretreatment: possible mechanism of tolerance to cadmium-induced lethality. *Toxicol Appl Pharmacol* **70:**195-203.

Goven D, Boutten A, Lecon-Malas V, Marchal-Somme J, Soler P, Boczkowski J, and Bonay M (2010) Induction of heme oxygenase-1, biliverdin reductase and H-ferritin in lung macrophage in smokers with primary spontaneous pneumothorax: role of HIF-1alpha. *PLoS One* **5:**e10886.

Grisham MB (2004) Reactive oxygen species in immune responses. *Free Radic Biol Med* **36:**1479-1480.

Gu J, Zhang QY, Genter MB, Lipinskas TW, Negishi M, Nebert DW, and Ding X (1998) Purification and characterization of heterologously expressed mouse CYP2A5 and CYP2G1: role in metabolic activation of acetaminophen and 2,6-dichlorobenzonitrile in mouse olfactory mucosal microsomes. *J Pharmacol Exp Ther* **285:**1287-1295.

Guan X, Hoffman B, Dwivedi C, and Matthees DP (2003) A simultaneous liquid chromatography/mass spectrometric assay of glutathione, cysteine, homocysteine and their disulfides in biological samples. *J Pharm Biomed Anal* **31:**251-261.

Gutterman DD, Miura H, and Liu Y (2005) Redox modulation of vascular tone: focus of potassium channel mechanisms of dilation. *Arterioscler Thromb Vasc Biol* **25:**671-678.

Handler JA and Thurman RG (1990) Redox interactions between catalase and alcohol dehydrogenase pathways of ethanol metabolism in the perfused rat liver. *J Biol Chem* **265:**1510-1515.

Hassoun EA and Stohs SJ (1996) Cadmium-induced production of superoxide anion and nitric oxide, DNA single strand breaks and lactate dehydrogenase leakage in J774A.1 cell cultures. *Toxicology* **112:**219-226.

He X, Chen MG, and Ma Q (2008) Activation of Nrf2 in defense against cadmium-induced oxidative stress. *Chem Res Toxicol* **21:**1375-1383.

Hensley K, Robinson KA, Gabbita SP, Salsman S, and Floyd RA (2000) Reactive oxygen species, cell signaling, and cell injury. *Free Radic Biol Med* **28:**1456-1462.

Hernandez-Montes E, Pollard SE, Vauzour D, Jofre-Montseny L, Rota C, Rimbach G, Weinberg PD, and Spencer JP (2006) Activation of glutathione peroxidase via

Nrf1 mediates genistein's protection against oxidative endothelial cell injury. *Biochem Biophys Res Commun* **346:**851-859.

Hess A, Wijayanti N, Neuschafer-Rube AP, Katz N, Kietzmann T, and Immenschuh S (2003) Phorbol ester-dependent activation of peroxiredoxin I gene expression via a protein kinase C, Ras, p38 mitogen-activated protein kinase signaling pathway. *J Biol Chem* **278:**45419-45434.

Higgins LG, Cavin C, Itoh K, Yamamoto M, and Hayes JD (2008) Induction of cancer chemopreventive enzymes by coffee is mediated by transcription factor Nrf2. Evidence that the coffee-specific diterpenes cafestol and kahweol confer protection against acrolein. *Toxicol Appl Pharmacol* **226:**328-337.

Higuchi Y (2004) Glutathione depletion-induced chromosomal DNA fragmentation associated with apoptosis and necrosis. *J Cell Mol Med* **8:**455-464.

Hinshelwood A, McGarvie G, and Ellis E (2002) Characterisation of a novel mouse liver aldo-keto reductase AKR7A5. *FEBS Lett* **523:**213-218.

Hong F, Freeman ML, and Liebler DC (2005a) Identification of sensor cysteines in human Keap1 modified by the cancer chemopreventive agent sulforaphane. *Chem Res Toxicol* **18:**1917-1926.

Hong F, Sekhar KR, Freeman ML, and Liebler DC (2005b) Specific patterns of electrophile adduction trigger Keap1 ubiquitination and Nrf2 activation. *J Biol Chem* **280:**31768-31775.

Horton JD, Goldstein JL, and Brown MS (2002) SREBPs: activators of the complete program of cholesterol and fatty acid synthesis in the liver. *J Clin Invest* **109:**1125-1131.

Hoshino Y, Nakamura T, Sato A, Mishima M, Yodoi J, and Nakamura H (2007) Neurotropin demonstrates cytoprotective effects in lung cells through the induction of thioredoxin-1. *Am J Respir Cell Mol Biol* **37:**438-446.

Huo Y, Qiu WY, Pan Q, Yao YF, Xing K, and Lou MF (2009) Reactive oxygen species (ROS) are essential mediators in epidermal growth factor (EGF)-stimulated corneal epithelial cell proliferation, adhesion, migration, and wound healing. *Exp Eye Res* **89:**876-886.

Ichijo H, Nishida E, Irie K, ten Dijke P, Saitoh M, Moriguchi T, Takagi M, Matsumoto K, Miyazono K, and Gotoh Y (1997) Induction of apoptosis by ASK1, a mammalian MAPKKK that activates SAPK/JNK and p38 signaling pathways. *Science* **275:**90-94.

Imai H and Nakagawa Y (2003) Biological significance of phospholipid hydroperoxide glutathione peroxidase (PHGPx, GPx4) in mammalian cells. *Free Radic Biol Med* **34:**145-169.

Irizarry RA, Hobbs B, Collin F, Beazer-Barclay YD, Antonellis KJ, Scherf U, and Speed TP (2003) Exploration, normalization, and summaries of high density oligonucleotide array probe level data. *Biostatistics* **4:**249-264.

Ishii T, Yamada M, Sato H, Matsue M, Taketani S, Nakayama K, Sugita Y, and Bannai S (1993) Cloning and characterization of a 23-kDa stress-induced mouse peritoneal macrophage protein. *J Biol Chem* **268:**18633-18636.

Itoh K, Chiba T, Takahashi S, Ishii T, Igarashi K, Katoh Y, Oyake T, Hayashi N, Satoh K, Hatayama I, Yamamoto M, and Nabeshima Y (1997) An Nrf2/small Maf heterodimer mediates the induction of phase II detoxifying enzyme genes through antioxidant response elements. *Biochem Biophys Res Commun* **236:**313-322.

Itoh K, Wakabayashi N, Katoh Y, Ishii T, Igarashi K, Engel JD, and Yamamoto M (1999) Keap1 represses nuclear activation of antioxidant responsive elements by Nrf2 through binding to the amino-terminal Neh2 domain. *Genes Dev* **13:**76-86.

Iversen PW, Eastwood BJ, Sittampalam GS, and Cox KL (2006) A comparison of assay performance measures in screening assays: signal window, Z' factor, and assay variability ratio. *J Biomol Screen* **11:**247-252.

Jansen PJ, Lutjohann D, Abildayeva K, Vanmierlo T, Plosch T, Plat J, von Bergmann K, Groen AK, Ramaekers FC, Kuipers F, and Mulder M (2006) Dietary plant sterols accumulate in the brain. *Biochim Biophys Acta* **1761:**445-453.

Jeffrey AM (1985) DNA modification by chemical carcinogens. *Pharmacol Ther* **28:**237-272.

Jeyapaul J and Jaiswal AK (2000) Nrf2 and c-Jun regulation of antioxidant response element (ARE)-mediated expression and induction of gamma-glutamylcysteine synthetase heavy subunit gene. *Biochem Pharmacol* **59:**1433-1439.

Ji Y, Lee HJ, Goodman C, Uskokovic M, Liby K, Sporn M, and Suh N (2006) The synthetic triterpenoid CDDO-imidazolide induces monocytic differentiation by activating the Smad and ERK signaling pathways in HL60 leukemia cells. *Mol Cancer Ther* **5:**1452-1458.

Jimenez-Lopez JM and Cederbaum AI (2005) CYP2E1-dependent oxidative stress and toxicity: role in ethanol-induced liver injury. *Expert Opin Drug Metab Toxicol* **1:**671-685.

Jurado J, Prieto-Alamo MJ, Madrid-Risquez J, and Pueyo C (2003) Absolute gene expression patterns of thioredoxin and glutaredoxin redox systems in mouse. *J Biol Chem* **278:**45546-45554.

Kassner N, Huse K, Martin HJ, Godtel-Armbrust U, Metzger A, Meineke I, Brockmoller J, Klein K, Zanger UM, Maser E, and Wojnowski L (2008) Carbonyl reductase 1 is a predominant doxorubicin reductase in the human liver. *Drug Metab Dispos* **36:**2113-2120.

Kensler TW, Wakabayashi N, and Biswal S (2007) Cell survival responses to environmental stresses via the Keap1-Nrf2-ARE pathway. *Annu Rev Pharmacol Toxicol* **47:**89-116.

Khan AQ, Nafees S, and Sultana S (2011) Perillyl alcohol protects against ethanol induced acute liver injury in Wistar rats by inhibiting oxidative stress, NFkappa-B activation and proinflammatory cytokine production. *Toxicology* **279:**108-114.

Khanal T, Choi JH, Hwang YP, Chung YC, and Jeong HG (2009) Saponins isolated from the root of Platycodon grandiflorum protect against acute ethanol-induced hepatotoxicity in mice. *Food Chem Toxicol* **47:**530-535.

Kiermayer C, Michalke B, Schmidt J, and Brielmeier M (2007) Effect of selenium on thioredoxin reductase activity in Txnrd1 or Txnrd2 hemizygous mice. *Biol Chem* **388:**1091-1097.

Kim SJ, Lee JW, Jung YS, Kwon do Y, Park HK, Ryu CS, Kim SK, Oh GT, and Kim YC (2009) Ethanol-induced liver injury and changes in sulfur amino acid metabolomics in glutathione peroxidase and catalase double knockout mice. *J Hepatol* **50:**1184-1191.

Kim YC, Yamaguchi Y, Kondo N, Masutani H, and Yodoi J (2003) Thioredoxin-dependent redox regulation of the antioxidant responsive element (ARE) in electrophile response. *Oncogene* **22:**1860-1865.

Kirby J, Halligan E, Baptista MJ, Allen S, Heath PR, Holden H, Barber SC, Loynes CA, Wood-Allum CA, Lunec J, and Shaw PJ (2005) Mutant SOD1 alters the motor neuronal transcriptome: implications for familial ALS. *Brain* **128:**1686-1706.

Kitteringham NR, Abdullah A, Walsh J, Randle L, Jenkins RE, Sison R, Goldring CE, Powell H, Sanderson C, Williams S, Higgins L, Yamamoto M, Hayes J, and Park BK (2010) Proteomic analysis of Nrf2 deficient transgenic mice reveals cellular defence and lipid metabolism as primary Nrf2-dependent pathways in the liver. *J Proteomics* **73:**1612-1631.

Klaassen CD and Aleksunes LM (2010) Xenobiotic, bile acid, and cholesterol transporters: function and regulation. *Pharmacol Rev* **62:**1-96.

Klaassen CD and Liu J (1997) Role of metallothionein in cadmium-induced hepatotoxicity and nephrotoxicity. *Drug Metab Rev* **29:**79-102.

Klaassen CD and Liu J (1998) Induction of metallothionein as an adaptive mechanism affecting the magnitude and progression of toxicological injury. *Environ Health Perspect* **106 Suppl 1:**297-300.

Klaassen CD, Liu J, and Choudhuri S (1999) Metallothionein: an intracellular protein to protect against cadmium toxicity. *Annu Rev Pharmacol Toxicol* **39:**267-294.

Klaassen CD, Liu J, and Diwan BA (2009) Metallothionein protection of cadmium toxicity. *Toxicol Appl Pharmacol* **238:**215-220.

Klaassen CD and Lu H (2008) Xenobiotic transporters: ascribing function from gene knockout and mutation studies. *Toxicol Sci* **101:**186-196.

Klaassen CD and Reisman SA (2010) Nrf2 the rescue: effects of the antioxidative/electrophilic response on the liver. *Toxicol Appl Pharmacol* **244:**57-65.

Knight JA (1997) Reactive oxygen species and the neurodegenerative disorders. *Ann Clin Lab Sci* **27:**11-25.

Kobayashi A, Kang MI, Okawa H, Ohtsuji M, Zenke Y, Chiba T, Igarashi K, and Yamamoto M (2004) Oxidative stress sensor Keap1 functions as an adaptor for Cul3-based E3 ligase to regulate proteasomal degradation of Nrf2. *Mol Cell Biol* **24:**7130-7139.

Kobayashi M, Itoh K, Suzuki T, Osanai H, Nishikawa K, Katoh Y, Takagi Y, and Yamamoto M (2002) Identification of the interactive interface and phylogenic conservation of the Nrf2-Keap1 system. *Genes Cells* **7:**807-820.

Kobayashi M and Yamamoto M (2006) Nrf2-Keap1 regulation of cellular defense mechanisms against electrophiles and reactive oxygen species. *Adv Enzyme Regul* **46:**113-140.

Kode A, Rajendrasozhan S, Caito S, Yang SR, Megson IL, and Rahman I (2008) Resveratrol induces glutathione synthesis by activation of Nrf2 and protects against cigarette smoke-mediated oxidative stress in human lung epithelial cells. *Am J Physiol Lung Cell Mol Physiol* **294:**L478-488.

Koh K, Cha Y, Kim S, and Kim J (2009) tBHQ inhibits LPS-induced microglial activation via Nrf2-mediated suppression of p38 phosphorylation. *Biochem Biophys Res Commun* **380:**449-453.

Krause KH (2004) Tissue distribution and putative physiological function of NOX family NADPH oxidases. *Jpn J Infect Dis* **57:**S28-29.

Kropotov A, Usmanova N, Serikov V, Zhivotovsky B, and Tomilin N (2007) Mitochondrial targeting of human peroxiredoxin V protein and regulation of PRDX5 gene expression by nuclear transcription factors controlling biogenesis of mitochondria. *FEBS J* **274:**5804-5814.

Kuhajda FP, Jenner K, Wood FD, Hennigar RA, Jacobs LB, Dick JD, and Pasternack GR (1994) Fatty acid synthesis: a potential selective target for antineoplastic therapy. *Proc Natl Acad Sci U S A* **91:**6379-6383.

Kumar A, Singh CK, Lavoie H, Dipette D, and Singh U (2011a) Resveratrol restores Nrf2 level and prevents ethanol-induced toxic effects in the cerebellum of a rodent model of Fetal Alcohol Spectrum Disorders. *Mol Pharmacol*.

Kumar V, Kumar S, Hassan M, Wu H, Thimmulappa RK, Kumar A, Sharma SK, Parmar VS, Biswal S, and Malhotra SV (2011b) Novel chalcone derivatives as potent Nrf2 activators in mice and human lung epithelial cells. *J Med Chem* **54:**4147-4159.

Kwak MK, Wakabayashi N, and Kensler TW (2004) Chemoprevention through the Keap1-Nrf2 signaling pathway by phase 2 enzyme inducers. *Mutat Res* **555:**133-148.

Lamle J, Marhenke S, Borlak J, von Wasielewski R, Eriksson CJ, Geffers R, Manns MP, Yamamoto M, and Vogel A (2008) Nuclear factor-eythroid 2-related factor 2 prevents alcohol-induced fulminant liver injury. *Gastroenterology* **134:**1159-1168.

Lamsa V, Levonen AL, Leinonen H, Yla-Herttuala S, Yamamoto M, and Hakkola J (2010) Cytochrome P450 2A5 constitutive expression and induction by heavy metals is dependent on redox-sensitive transcription factor Nrf2 in liver. *Chem Res Toxicol* **23:**977-985.

Lee CY, Chew EH, and Go ML (2010a) Functionalized aurones as inducers of NAD(P)H:quinone oxidoreductase 1 that activate AhR/XRE and Nrf2/ARE signaling pathways: synthesis, evaluation and SAR. *Eur J Med Chem* **45:**2957-2971.

Lee HC and Wei YH (2007) Oxidative stress, mitochondrial DNA mutation, and apoptosis in aging. *Exp Biol Med (Maywood)* **232:**592-606.

Lee Y, Shin DH, Kim JH, Hong S, Choi D, Kim YJ, Kwak MK, and Jung Y (2010b) Caffeic acid phenethyl ester-mediated Nrf2 activation and IkappaB kinase inhibition are involved in NFkappaB inhibitory effect: structural analysis for NFkappaB inhibition. *Eur J Pharmacol* **643:**21-28.

Lemasters JJ, Theruvath TP, Zhong Z, and Nieminen AL (2009) Mitochondrial calcium and the permeability transition in cell death. *Biochim Biophys Acta* **1787:**1395-1401.

Lenzen S, Drinkgern J, and Tiedge M (1996) Low antioxidant enzyme gene expression in pancreatic islets compared with various other mouse tissues. *Free Radic Biol Med* **20:**463-466.

Li M, Chiu JF, Kelsen A, Lu SC, and Fukagawa NK (2009) Identification and characterization of an Nrf2-mediated ARE upstream of the rat glutamate cysteine ligase catalytic subunit gene (GCLC). *J Cell Biochem* **107:**944-954.

Li W, Yu SW, and Kong AN (2006) Nrf2 possesses a redox-sensitive nuclear exporting signal in the Neh5 transactivation domain. *J Biol Chem* **281:**27251-27263.

Li X, Zhang D, Hannink M, and Beamer LJ (2004) Crystal structure of the Kelch domain of human Keap1. *J Biol Chem* **279:**54750-54758.

Liby K, Hock T, Yore MM, Suh N, Place AE, Risingsong R, Williams CR, Royce DB, Honda T, Honda Y, Gribble GW, Hill-Kapturczak N, Agarwal A, and Sporn MB (2005) The synthetic triterpenoids, CDDO and CDDO-imidazolide, are potent inducers of heme oxygenase-1 and Nrf2/ARE signaling. *Cancer Res* **65:**4789-4798.

Lieber CS (2000) Alcoholic liver disease: new insights in pathogenesis lead to new treatments. *J Hepatol* **32:**113-128.

Lieber CS (2004) Alcoholic fatty liver: its pathogenesis and mechanism of progression to inflammation and fibrosis. *Alcohol* **34:**9-19.

Liu C, Nadiminty N, Tummala R, Chun JY, Lou W, Zhu Y, Sun M, Evans CP, Zhou Q, and Gao AC (2011) Andrographolide targets androgen receptor pathway in castration-resistant prostate cancer. *Genes Cancer* **2:**151-159.

Liu J, Goyer R, and Waalkes MP (2007) Toxic effects of metals, in: *Casarett and Doull's Toxicology - the Basic Science of Poisons* (Klaassen CD ed), pp 931-979, McGraw Hill.

Liu J, Kershaw WC, Liu YP, and Klaassen CD (1992) Cadmium-induced hepatic endothelial cell injury in inbred strains of mice. *Toxicology* **75:**51-62.

Liu J, Liu Y, Michalska AE, Choo KH, and Klaassen CD (1996) Metallothionein plays less of a protective role in cadmium-metallothionein-induced nephrotoxicity than in cadmium chloride-induced hepatotoxicity. *J Pharmacol Exp Ther* **276:**1216-1223.

Liu J, Liu Y, Parkinson A, and Klaassen CD (1995a) Effect of oleanolic acid on hepatic toxicant-activating and detoxifying systems in mice. *J Pharmacol Exp Ther* **275:**768-774.

Liu J, Qu W, and Kadiiska MB (2009) Role of oxidative stress in cadmium toxicity and carcinogenesis. *Toxicol Appl Pharmacol* **238:**209-214.

Liu Y, Liu J, Iszard MB, Andrews GK, Palmiter RD, and Klaassen CD (1995b) Transgenic mice that overexpress metallothionein-I are protected from cadmium lethality and hepatotoxicity. *Toxicol Appl Pharmacol* **135:**222-228.

Liu Y, Liu J, and Klaassen CD (2001) Metallothionein-null and wild-type mice show similar cadmium absorption and tissue distribution following oral cadmium administration. *Toxicol Appl Pharmacol* **175:**253-259.

Loft S and Poulsen HE (1998) Estimation of oxidative DNA damage in man from urinary excretion of repair products. *Acta Biochim Pol* **45:**133-144.

Lowther WT and Haynes AC (2011) Reduction of cysteine sulfinic acid in eukaryotic, typical 2-Cys peroxiredoxins by sulfiredoxin. *Antioxid Redox Signal* **15:**99-109.

Lu H, Gonzalez FJ, and Klaassen C (2010) Alterations in hepatic mRNA expression of phase II enzymes and xenobiotic transporters after targeted disruption of hepatocyte nuclear factor 4 alpha. *Toxicol Sci* **118:**380-390.

Lu SC and Mato JM (2005) Role of methionine adenosyltransferase and S-adenosylmethionine in alcohol-associated liver cancer. *Alcohol* **35:**227-234.

Lu WJ, Lee JJ, Chou DS, Jayakumar T, Fong TH, Hsiao G, and Sheu JR (2011) A novel role of andrographolide, an NF-kappa B inhibitor, on inhibition of platelet activation: the pivotal mechanisms of endothelial nitric oxide synthase/cyclic GMP. *J Mol Med (Berl)* **89:**1261-1273.

Lu Y and Cederbaum AI (2008) CYP2E1 and oxidative liver injury by alcohol. *Free Radic Biol Med* **44:**723-738.

Luo Y, Eggler AL, Liu D, Liu G, Mesecar AD, and van Breemen RB (2007) Sites of alkylation of human Keap1 by natural chemoprevention agents. *J Am Soc Mass Spectrom* **18:**2226-2232.

MacLeod AK, McMahon M, Plummer SM, Higgins LG, Penning TM, Igarashi K, and Hayes JD (2009) Characterization of the cancer chemopreventive NRF2-dependent gene battery in human keratinocytes: demonstration that the KEAP1-NRF2 pathway, and not the BACH1-NRF2 pathway, controls cytoprotection

against electrophiles as well as redox-cycling compounds. *Carcinogenesis* **30:**1571-1580.

Maher JM, Dieter MZ, Aleksunes LM, Slitt AL, Guo G, Tanaka Y, Scheffer GL, Chan JY, Manautou JE, Chen Y, Dalton TP, Yamamoto M, and Klaassen CD (2007) Oxidative and electrophilic stress induces multidrug resistance-associated protein transporters via the nuclear factor-E2-related factor-2 transcriptional pathway. *Hepatology* **46:**1597-1610.

Malhotra D, Portales-Casamar E, Singh A, Srivastava S, Arenillas D, Happel C, Shyr C, Wakabayashi N, Kensler TW, Wasserman WW, and Biswal S (2010) Global mapping of binding sites for Nrf2 identifies novel targets in cell survival response through ChIP-Seq profiling and network analysis. *Nucleic Acids Res* **38:**5718-5734.

Malhotra JD and Kaufman RJ (2007) Endoplasmic reticulum stress and oxidative stress: a vicious cycle or a double-edged sword? *Antioxid Redox Signal* **9:**2277-2293.

Mamede AC, Tavares SD, Abrantes AM, Trindade J, Maia JM, and Botelho MF (2011) The role of vitamins in cancer: a review. *Nutr Cancer* **63:**479-494.

Manea A (2010) NADPH oxidase-derived reactive oxygen species: involvement in vascular physiology and pathology. *Cell Tissue Res* **342:**325-339.

Margis R, Dunand C, Teixeira FK, and Margis-Pinheiro M (2008) Glutathione peroxidase family - an evolutionary overview. *FEBS J* **275:**3959-3970.

Mari M, Morales A, Colell A, Garcia-Ruiz C, and Fernandez-Checa JC (2009) Mitochondrial glutathione, a key survival antioxidant. *Antioxid Redox Signal* **11:**2685-2700.

Marklund SL, Westman NG, Lundgren E, and Roos G (1982) Copper- and zinc-containing superoxide dismutase, manganese-containing superoxide dismutase, catalase, and glutathione peroxidase in normal and neoplastic human cell lines and normal human tissues. *Cancer Res* **42:**1955-1961.

Martin D, Rojo AI, Salinas M, Diaz R, Gallardo G, Alam J, De Galarreta CM, and Cuadrado A (2004) Regulation of heme oxygenase-1 expression through the phosphatidylinositol 3-kinase/Akt pathway and the Nrf2 transcription factor in response to the antioxidant phytochemical carnosol. *J Biol Chem* **279:**8919-8929.

Martinez JA (2006) Mitochondrial oxidative stress and inflammation: an slalom to obesity and insulin resistance. *J Physiol Biochem* **62:**303-306.

McLellan LI, Judah DJ, Neal GE, and Hayes JD (1994) Regulation of aflatoxin B1-metabolizing aldehyde reductase and glutathione S-transferase by chemoprotectors. *Biochem J* **300 (Pt 1):**117-124.

Meister A and Anderson ME (1983) Glutathione. *Annu Rev Biochem* **52:**711-760.

Merrell MD, Jackson JP, Augustine LM, Fisher CD, Slitt AL, Maher JM, Huang W, Moore DD, Zhang Y, Klaassen CD, and Cherrington NJ (2008) The Nrf2 activator oltipraz also activates the constitutive androstane receptor. *Drug Metab Dispos* **36:**1716-1721.

Mishra K, Dash AP, and Dey N (2011) Andrographolide: A Novel Antimalarial Diterpene Lactone Compound from Andrographis paniculata and Its Interaction with Curcumin and Artesunate. *J Trop Med* **2011:**579518.

Miyamoto N, Izumi H, Miyamoto R, Kondo H, Tawara A, Sasaguri Y, and Kohno K (2011) Quercetin induces the expression of peroxiredoxins 3 and 5 via the Nrf2/NRF1 transcription pathway. *Invest Ophthalmol Vis Sci* **52:**1055-1063.

Moinova HR and Mulcahy RT (1999) Up-regulation of the human gamma-glutamylcysteine synthetase regulatory subunit gene involves binding of Nrf-2 to an electrophile responsive element. *Biochem Biophys Res Commun* **261:**661-668.

Muraoka M, Kawakita M, and Ishida N (2001) Molecular characterization of human UDP-glucuronic acid/UDP-N-acetylgalactosamine transporter, a novel nucleotide sugar transporter with dual substrate specificity. *FEBS Lett* **495:**87-93.

Natsch A and Emter R (2008) Skin sensitizers induce antioxidant response element dependent genes: application to the in vitro testing of the sensitization potential of chemicals. *Toxicol Sci* **102:**110-119.

New LS and Chan EC (2008) Evaluation of BEH C18, BEH HILIC, and HSS T3 (C18) column chemistries for the UPLC-MS-MS analysis of glutathione, glutathione disulfide, and ophthalmic acid in mouse liver and human plasma. *J Chromatogr Sci* **46:**209-214.

Nishinaka T and Yabe-Nishimura C (2005) Transcription factor Nrf2 regulates promoter activity of mouse aldose reductase (AKR1B3) gene. *J Pharmacol Sci* **97:**43-51.

Novak RF and Woodcroft KJ (2000) The alcohol-inducible form of cytochrome P450 (CYP 2E1): role in toxicology and regulation of expression. *Arch Pharm Res* **23:**267-282.

Ntambi JM, Buhrow SA, Kaestner KH, Christy RJ, Sibley E, Kelly TJ, Jr., and Lane MD (1988) Differentiation-induced gene expression in 3T3-L1 preadipocytes.

Characterization of a differentially expressed gene encoding stearoyl-CoA desaturase. *J Biol Chem* **263:**17291-17300.

Nunoya K, Yokoi T, Itoh K, Itoh S, Kimura K, and Kamataki T (1995) S-oxidation of (+)-cis-3,5-dimethyl-2-(3-pyridyl)-thiazolidin-4-one hydrochloride by rat hepatic flavin-containing monooxygenase 1 expressed in yeast. *Xenobiotica* **25:**1283-1291.

Okada K, Shoda J, Taguchi K, Maher JM, Ishizaki K, Inoue Y, Ohtsuki M, Goto N, Takeda K, Utsunomiya H, Oda K, Warabi E, Ishii T, Osaka K, Hyodo I, and Yamamoto M (2008) Ursodeoxycholic acid stimulates Nrf2-mediated hepatocellular transport, detoxification, and antioxidative stress systems in mice. *Am J Physiol Gastrointest Liver Physiol* **295:**G735-747.

Okado-Matsumoto A, Matsumoto A, Fujii J, and Taniguchi N (2000) Peroxiredoxin IV is a secretable protein with heparin-binding properties under reduced conditions. *J Biochem* **127:**493-501.

Okawa H, Motohashi H, Kobayashi A, Aburatani H, Kensler TW, and Yamamoto M (2006) Hepatocyte-specific deletion of the keap1 gene activates Nrf2 and confers potent resistance against acute drug toxicity. *Biochem Biophys Res Commun* **339:**79-88.

Osburn WO, Wakabayashi N, Misra V, Nilles T, Biswal S, Trush MA, and Kensler TW (2006) Nrf2 regulates an adaptive response protecting against oxidative damage following diquat-mediated formation of superoxide anion. *Arch Biochem Biophys* **454:**7-15.

Perez VI, Lew CM, Cortez LA, Webb CR, Rodriguez M, Liu Y, Qi W, Li Y, Chaudhuri A, Van Remmen H, Richardson A, and Ikeno Y (2008) Thioredoxin 2 haploinsufficiency in mice results in impaired mitochondrial function and increased oxidative stress. *Free Radic Biol Med* **44:**882-892.

Pi J, Leung L, Xue P, Wang W, Hou Y, Liu D, Yehuda-Shnaidman E, Lee C, Lau J, Kurtz TW, and Chan JY (2010) Deficiency in the nuclear factor E2-related factor-2 transcription factor results in impaired adipogenesis and protects against diet-induced obesity. *J Biol Chem* **285:**9292-9300.

Pilka ES, Niesen FH, Lee WH, El-Hawari Y, Dunford JE, Kochan G, Wsol V, Martin HJ, Maser E, and Oppermann U (2009) Structural basis for substrate specificity in human monomeric carbonyl reductases. *PLoS One* **4:**e7113.

Ponnusamy M and Pari L (2011) Protective role of diallyl tetrasulfide on cadmium-induced testicular damage in adult rats: a biochemical and histological study. *Toxicol Ind Health* **27:**407-416.

Porter NA, Caldwell SE, and Mills KA (1995) Mechanisms of free radical oxidation of unsaturated lipids. *Lipids* **30:**277-290.

Prabu SM, Shagirtha K, and Renugadevi J (2010) Amelioration of cadmium-induced oxidative stress, impairment in lipids and plasma lipoproteins by the combined treatment with quercetin and alpha-tocopherol in rats. *J Food Sci* **75:**T132-140.

Primiano T, Kensler TW, Kuppusamy P, Zweier JL, and Sutter TR (1996) Induction of hepatic heme oxygenase-1 and ferritin in rats by cancer chemopreventive dithiolethiones. *Carcinogenesis* **17:**2291-2296.

Puertollano MA, Puertollano E, de Cienfuegos GA, and de Pablo MA (2011) Dietary antioxidants: immunity and host defense. *Curr Top Med Chem* **11:**1752-1766.

Raghow R, Yellaturu C, Deng X, Park EA, and Elam MB (2008) SREBPs: the crossroads of physiological and pathological lipid homeostasis. *Trends Endocrinol Metab* **19:**65-73.

Rangasamy T, Cho CY, Thimmulappa RK, Zhen L, Srisuma SS, Kensler TW, Yamamoto M, Petrache I, Tuder RM, and Biswal S (2004) Genetic ablation of Nrf2 enhances susceptibility to cigarette smoke-induced emphysema in mice. *J Clin Invest* **114:**1248-1259.

Reisman SA, Aleksunes LM, and Klaassen CD (2009a) Oleanolic acid activates Nrf2 and protects from acetaminophen hepatotoxicity via Nrf2-dependent and Nrf2-independent processes. *Biochem Pharmacol* **77:**1273-1282.

Reisman SA, Buckley DB, Tanaka Y, and Klaassen CD (2009b) CDDO-Im protects from acetaminophen hepatotoxicity through induction of Nrf2-dependent genes. *Toxicol Appl Pharmacol* **236:**109-114.

Reisman SA, Csanaky IL, Aleksunes LM, and Klaassen CD (2009c) Altered disposition of acetaminophen in Nrf2-null and Keap1-knockdown mice. *Toxicol Sci* **109:**31-40.

Reisman SA, Csanaky IL, Yeager RL, and Klaassen CD (2009d) Nrf2 activation enhances biliary excretion of sulfobromophthalein by inducing glutathione-S-transferase activity. *Toxicol Sci* **109:**24-30.

Reisman SA, Yeager RL, Yamamoto M, and Klaassen CD (2009e) Increased Nrf2 activation in livers from Keap1-knockdown mice increases expression of cytoprotective genes that detoxify electrophiles more than those that detoxify reactive oxygen species. *Toxicol Sci* **108:**35-47.

Rikans LE and Yamano T (2000) Mechanisms of cadmium-mediated acute hepatotoxicity. *J Biochem Mol Toxicol* **14:**110-117.

Roede JR, Stewart BJ, and Petersen DR (2008) Decreased expression of peroxiredoxin 6 in a mouse model of ethanol consumption. *Free Radic Biol Med* **45:**1551-1558.

Room R, Babor T, and Rehm J (2005) Alcohol and public health. *Lancet* **365:**519-530.

Roth M, Araya JJ, Timmermann BN, and Hagenbuch B (2011) Isolation of Modulators of the Liver-Specific Organic Anion-Transporting Polypeptides (OATPs) 1B1 and 1B3 from Rollinia emarginata Schlecht (Annonaceae). *J Pharmacol Exp Ther* **339:**624-632.

Rubiolo JA, Mithieux G, and Vega FV (2008) Resveratrol protects primary rat hepatocytes against oxidative stress damage: activation of the Nrf2 transcription factor and augmented activities of antioxidant enzymes. *Eur J Pharmacol* **591:**66-72.

Rushmore TH, Morton MR, and Pickett CB (1991) The antioxidant responsive element. Activation by oxidative stress and identification of the DNA consensus sequence required for functional activity. *J Biol Chem* **266:**11632-11639.

Sakurai A, Nishimoto M, Himeno S, Imura N, Tsujimoto M, Kunimoto M, and Hara S (2005) Transcriptional regulation of thioredoxin reductase 1 expression by cadmium in vascular endothelial cells: role of NF-E2-related factor-2. *J Cell Physiol* **203:**529-537.

Saracino MR and Lampe JW (2007) Phytochemical regulation of UDP-glucuronosyltransferases: implications for cancer prevention. *Nutr Cancer* **59:**121-141.

Shah ZA, Li RC, Thimmulappa RK, Kensler TW, Yamamoto M, Biswal S, and Dore S (2007) Role of reactive oxygen species in modulation of Nrf2 following ischemic reperfusion injury. *Neuroscience* **147:**53-59.

Shih AY, Imbeault S, Barakauskas V, Erb H, Jiang L, Li P, and Murphy TH (2005) Induction of the Nrf2-driven antioxidant response confers neuroprotection during mitochondrial stress in vivo. *J Biol Chem* **280:**22925-22936.

Shimomura I, Shimano H, Korn BS, Bashmakov Y, and Horton JD (1998) Nuclear sterol regulatory element-binding proteins activate genes responsible for the entire program of unsaturated fatty acid biosynthesis in transgenic mouse liver. *J Biol Chem* **273:**35299-35306.

Shin S, Wakabayashi J, Yates MS, Wakabayashi N, Dolan PM, Aja S, Liby KT, Sporn MB, Yamamoto M, and Kensler TW (2009) Role of Nrf2 in prevention of high-fat diet-induced obesity by synthetic triterpenoid CDDO-imidazolide. *Eur J Pharmacol* **620:**138-144.

Short DM, Lyon R, Watson DG, Barski OA, McGarvie G, and Ellis EM (2006) Metabolism of trans, trans-muconaldehyde, a cytotoxic metabolite of benzene, in mouse liver by alcohol dehydrogenase Adh1 and aldehyde reductase AKR1A4. *Toxicol Appl Pharmacol* **210:**163-170.

Singh S, Sreenath K, Pavithra L, Roy S, and Chattopadhyay S (2010) SMAR1 regulates free radical stress through modulation of AKR1a4 enzyme activity. *Int J Biochem Cell Biol* **42:**1105-1114.

Smathers RL, Galligan JJ, Stewart BJ, and Petersen DR (2011) Overview of lipid peroxidation products and hepatic protein modification in alcoholic liver disease. *Chem Biol Interact* **192:**107-112.

Smith CV (1987) Effect of BCNU pretreatment on diquat-induced oxidant stress and hepatotoxicity. *Biochem Biophys Res Commun* **144:**415-421.

Soerensen J, Jakupoglu C, Beck H, Forster H, Schmidt J, Schmahl W, Schweizer U, Conrad M, and Brielmeier M (2008) The role of thioredoxin reductases in brain development. *PLoS One* **3:**e1813.

Spalding DJ, Mitchell JR, Jaeschke H, and Smith CV (1989) Diquat hepatotoxicity in the Fischer-344 rat: the role of covalent binding to tissue proteins and lipids. *Toxicol Appl Pharmacol* **101:**319-327.

Stewart D, Killeen E, Naquin R, Alam S, and Alam J (2003) Degradation of transcription factor Nrf2 via the ubiquitin-proteasome pathway and stabilization by cadmium. *J Biol Chem* **278:**2396-2402.

Stocker R and Keaney JF, Jr. (2004) Role of oxidative modifications in atherosclerosis. *Physiol Rev* **84:**1381-1478.

Stocker R, Yamamoto Y, McDonagh AF, Glazer AN, and Ames BN (1987) Bilirubin is an antioxidant of possible physiological importance. *Science* **235:**1043-1046.

Storz P (2005) Reactive oxygen species in tumor progression. *Front Biosci* **10:**1881-1896.

Sugamura K and Keaney JF, Jr. (2011) Reactive oxygen species in cardiovascular disease. *Free Radic Biol Med* **51:**978-992.

Surh YJ, Kundu JK, and Na HK (2008) Nrf2 as a master redox switch in turning on the cellular signaling involved in the induction of cytoprotective genes by some chemopreventive phytochemicals. *Planta Med* **74:**1526-1539.

Suzuki H, Tashiro S, Sun J, Doi H, Satomi S, and Igarashi K (2003) Cadmium induces nuclear export of Bach1, a transcriptional repressor of heme oxygenase-1 gene. *J Biol Chem* **278:**49246-49253.

Taguchi K, Maher JM, Suzuki T, Kawatani Y, Motohashi H, and Yamamoto M (2010) Genetic analysis of cytoprotective functions supported by graded expression of Keap1. *Mol Cell Biol* **30:**3016-3026.

Takahashi T, Tabuchi T, Tamaki Y, Kosaka K, Takikawa Y, and Satoh T (2009) Carnosic acid and carnosol inhibit adipocyte differentiation in mouse 3T3-L1 cells through induction of phase2 enzymes and activation of glutathione metabolism. *Biochem Biophys Res Commun* **382:**549-554.

Takebe G, Yarimizu J, Saito Y, Hayashi T, Nakamura H, Yodoi J, Nagasawa S, and Takahashi K (2002) A comparative study on the hydroperoxide and thiol specificity of the glutathione peroxidase family and selenoprotein P. *J Biol Chem* **277:**41254-41258.

Takeda K, Noguchi T, Naguro I, and Ichijo H (2008) Apoptosis signal-regulating kinase 1 in stress and immune response. *Annu Rev Pharmacol Toxicol* **48:**199-225.

Tanaka A, Hamada N, Fujita Y, Itoh T, Nozawa Y, Iinuma M, and Ito M (2010) A novel kavalactone derivative protects against H2O2-induced PC12 cell death via Nrf2/ARE activation. *Bioorg Med Chem* **18:**3133-3139.

Tanaka Y, Aleksunes LM, Cui YJ, and Klaassen CD (2009) ANIT-induced intrahepatic cholestasis alters hepatobiliary transporter expression via Nrf2-dependent and independent signaling. *Toxicol Sci* **108:**247-257.

Tanaka Y, Aleksunes LM, Yeager RL, Gyamfi MA, Esterly N, Guo GL, and Klaassen CD (2008) NF-E2-related factor 2 inhibits lipid accumulation and oxidative stress in mice fed a high-fat diet. *J Pharmacol Exp Ther* **325:**655-664.

Tanigawa S, Fujii M, and Hou DX (2007) Action of Nrf2 and Keap1 in ARE-mediated NQO1 expression by quercetin. *Free Radic Biol Med* **42:**1690-1703.

Thangasamy A, Rogge J, Krishnegowda NK, Freeman JW, and Ammanamanchi S (2011) Novel function of transcription factor Nrf2 as an inhibitor of RON tyrosine kinase receptor-mediated cancer cell invasion. *J Biol Chem* **286:**32115-32122.

Thimmulappa RK, Mai KH, Srisuma S, Kensler TW, Yamamoto M, and Biswal S (2002) Identification of Nrf2-regulated genes induced by the chemopreventive agent sulforaphane by oligonucleotide microarray. *Cancer Res* **62:**5196-5203.

Tsai PY, Ka SM, Chang JM, Chen HC, Shui HA, Li CY, Hua KF, Chang WL, Huang JJ, Yang SS, and Chen A (2011) Epigallocatechin-3-gallate prevents lupus nephritis

development in mice via enhancing the Nrf2 antioxidant pathway and inhibiting NLRP3 inflammasome activation. *Free Radic Biol Med* **51:**744-754.

Umemura T, Kuroiwa Y, Kitamura Y, Ishii Y, Kanki K, Kodama Y, Itoh K, Yamamoto M, Nishikawa A, and Hirose M (2006) A crucial role of Nrf2 in in vivo defense against oxidative damage by an environmental pollutant, pentachlorophenol. *Toxicol Sci* **90:**111-119.

Ungvari Z, Bagi Z, Feher A, Recchia FA, Sonntag WE, Pearson K, de Cabo R, and Csiszar A (2010) Resveratrol confers endothelial protection via activation of the antioxidant transcription factor Nrf2. *Am J Physiol Heart Circ Physiol* **299:**H18-24.

Vander Jagt DL, Kolb NS, Vander Jagt TJ, Chino J, Martinez FJ, Hunsaker LA, and Royer RE (1995) Substrate specificity of human aldose reductase: identification of 4-hydroxynonenal as an endogenous substrate. *Biochim Biophys Acta* **1249:**117-126.

Vesey DA (2010) Transport pathways for cadmium in the intestine and kidney proximal tubule: focus on the interaction with essential metals. *Toxicol Lett* **198:**13-19.

Vogt BL and Richie JP, Jr. (2007) Glutathione depletion and recovery after acute ethanol administration in the aging mouse. *Biochem Pharmacol* **73:**1613-1621.

Waalkes MP (2003) Cadmium carcinogenesis. *Mutat Res* **533:**107-120.

Waddell WJ and Marlowe C (1980) Tissue and cellular disposition of paraquat in mice. *Toxicol Appl Pharmacol* **56:**127-140.

Wakabayashi N, Itoh K, Wakabayashi J, Motohashi H, Noda S, Takahashi S, Imakado S, Kotsuji T, Otsuka F, Roop DR, Harada T, Engel JD, and Yamamoto M (2003) Keap1-null mutation leads to postnatal lethality due to constitutive Nrf2 activation. *Nat Genet* **35:**238-245.

Wang XJ, Hayes JD, and Wolf CR (2006) Generation of a stable antioxidant response element-driven reporter gene cell line and its use to show redox-dependent activation of nrf2 by cancer chemotherapeutic agents. *Cancer Res* **66:**10983-10994.

Waris G, Felmlee DJ, Negro F, and Siddiqui A (2007) Hepatitis C virus induces proteolytic cleavage of sterol regulatory element binding proteins and stimulates their phosphorylation via oxidative stress. *J Virol* **81:**8122-8130.

White EL, Ross LJ, Schmid SM, Kelloff GJ, Steele VE, and Hill DL (1998) Screening of potential cancer preventing chemicals for induction of glutathione in rat liver cells. *Oncol Rep* **5:**507-512.

Wiegand H, Wagner AE, Boesch-Saadatmandi C, Kruse HP, Kulling S, and Rimbach G (2009) Effect of dietary genistein on Phase II and antioxidant enzymes in rat liver. *Cancer Genomics Proteomics* **6:**85-92.

Winterbourn CC and Kettle AJ (2004) Reactions of superoxide with myeloperoxidase and its products. *Jpn J Infect Dis* **57:**S31-33.

Woods CG, Fu J, Xue P, Hou Y, Pluta LJ, Yang L, Zhang Q, Thomas RS, Andersen ME, and Pi J (2009) Dose-dependent transitions in Nrf2-mediated adaptive response and related stress responses to hypochlorous acid in mouse macrophages. *Toxicol Appl Pharmacol* **238:**27-36.

Wruck CJ, Claussen M, Fuhrmann G, Romer L, Schulz A, Pufe T, Waetzig V, Peipp M, Herdegen T, and Gotz ME (2007) Luteolin protects rat PC12 and C6 cells against MPP+ induced toxicity via an ERK dependent Keap1-Nrf2-ARE pathway. *J Neural Transm Suppl*:57-67.

Wu KC, Cui JY, and Klaassen CD (2011a) Beneficial role of Nrf2 in regulating NADPH generation and consumption. *Toxicol Sci* **123:**590-600.

Wu KC, Cui JY, and Klaassen CD (2011b) Beneficial Role of Nrf2 in Regulating NADPH Generation and Consumption. *Toxicol Sci*.

Xu W, Hellerbrand C, Kohler UA, Bugnon P, Kan YW, Werner S, and Beyer TA (2008) The Nrf2 transcription factor protects from toxin-induced liver injury and fibrosis. *Lab Invest* **88:**1068-1078.

Yamano T, DeCicco LA, and Rikans LE (2000) Attenuation of cadmium-induced liver injury in senescent male fischer 344 rats: role of Kupffer cells and inflammatory cytokines. *Toxicol Appl Pharmacol* **162:**68-75.

Yan D, Dong J, Sulik KK, and Chen SY (2010) Induction of the Nrf2-driven antioxidant response by tert-butylhydroquinone prevents ethanol-induced apoptosis in cranial neural crest cells. *Biochem Pharmacol* **80:**144-149.

Yanardag R, Ozsoy-Sacan O, Ozdil S, and Bolkent S (2007) Combined effects of vitamin C, vitamin E, and sodium selenate supplementation on absolute ethanol-induced injury in various organs of rats. *Int J Toxicol* **26:**513-523.

Yang C, Zhang X, Fan H, and Liu Y (2009) Curcumin upregulates transcription factor Nrf2, HO-1 expression and protects rat brains against focal ischemia. *Brain Res* **1282:**133-141.

Yang YC, Lii CK, Lin AH, Yeh YW, Yao HT, Li CC, Liu KL, and Chen HW (2011) Induction of glutathione synthesis and heme oxygenase 1 by the flavonoids

butein and phloretin is mediated through the ERK/Nrf2 pathway and protects against oxidative stress. *Free Radic Biol Med* **51:**2073-2081.

Yates MS, Kwak MK, Egner PA, Groopman JD, Bodreddigari S, Sutter TR, Baumgartner KJ, Roebuck BD, Liby KT, Yore MM, Honda T, Gribble GW, Sporn MB, and Kensler TW (2006) Potent protection against aflatoxin-induced tumorigenesis through induction of Nrf2-regulated pathways by the triterpenoid 1-[2-cyano-3-,12-dioxooleana-1,9(11)-dien-28-oyl]imidazole. *Cancer Res* **66:**2488-2494.

Yeager RL, Reisman SA, Aleksunes LM, and Klaassen CD (2009) Introducing the "TCDD-inducible AhR-Nrf2 gene battery". *Toxicol Sci* **111:**238-246.

Yeligar SM, Machida K, and Kalra VK (2010) Ethanol-induced HO-1 and NQO1 are differentially regulated by HIF-1alpha and Nrf2 to attenuate inflammatory cytokine expression. *J Biol Chem* **285:**35359-35373.

Yokota SI, Higashi E, Fukami T, Yokoi T, and Nakajima M (2010) Human CYP2A6 is regulated by nuclear factor-erythroid 2 related factor 2. *Biochem Pharmacol*.

Yoshikawa T, Shimano H, Amemiya-Kudo M, Yahagi N, Hasty AH, Matsuzaka T, Okazaki H, Tamura Y, Iizuka Y, Ohashi K, Osuga J, Harada K, Gotoda T, Kimura S, Ishibashi S, and Yamada N (2001) Identification of liver X receptor-retinoid X receptor as an activator of the sterol regulatory element-binding protein 1c gene promoter. *Mol Cell Biol* **21:**2991-3000.

Yu AL, Lu CY, Wang TS, Tsai CW, Liu KL, Cheng YP, Chang HC, Lii CK, and Chen HW (2010) Induction of heme oxygenase 1 and inhibition of tumor necrosis factor alpha-induced intercellular adhesion molecule expression by andrographolide in EA.hy926 cells. *J Agric Food Chem* **58:**7641-7648.

Zakhari S (2006) Overview: how is alcohol metabolized by the body? *Alcohol Res Health* **29:**245-254.

Zamek-Gliszczynski MJ, Nezasa K, Tian X, Kalvass JC, Patel NJ, Raub TJ, and Brouwer KL (2006) The important role of Bcrp (Abcg2) in the biliary excretion of sulfate and glucuronide metabolites of acetaminophen, 4-methylumbelliferone, and harmol in mice. *Mol Pharmacol* **70:**2127-2133.

Zhang DD and Hannink M (2003) Distinct cysteine residues in Keap1 are required for Keap1-dependent ubiquitination of Nrf2 and for stabilization of Nrf2 by chemopreventive agents and oxidative stress. *Mol Cell Biol* **23:**8137-8151.

Zhang DD, Lo SC, Sun Z, Habib GM, Lieberman MW, and Hannink M (2005) Ubiquitination of Keap1, a BTB-Kelch substrate adaptor protein for Cul3, targets

Keap1 for degradation by a proteasome-independent pathway. *J Biol Chem* **280:**30091-30099.

Zhang H, Shih A, Rinna A, and Forman HJ (2009) Resveratrol and 4-hydroxynonenal act in concert to increase glutamate cysteine ligase expression and glutathione in human bronchial epithelial cells. *Arch Biochem Biophys* **481:**110-115.

Zhang JH, Chung TD, and Oldenburg KR (1999) A Simple Statistical Parameter for Use in Evaluation and Validation of High Throughput Screening Assays. *J Biomol Screen* **4:**67-73.

Zhang YK, Yeager RL, Tanaka Y, and Klaassen CD (2010) Enhanced expression of Nrf2 in mice attenuates the fatty liver produced by a methionine- and choline-deficient diet. *Toxicol Appl Pharmacol* **245:**326-334.

Zhu M and Fahl WE (2001) Functional characterization of transcription regulators that interact with the electrophile response element. *Biochem Biophys Res Commun* **289:**212-219.